DOE/NOAA/OTEC-7

PRELIMINARY DESIGN REPORT FOR OTEC STATIONKEEPING SUBSYSTEMS (SKSS)

December 12, 1979

Work Performed Under Contract No. EG-77-A-29-1078

Lockheed Missiles & Space Company, Inc.
Ocean Systems
Sunnyvale, California

U.S. Department of Energy

Solar Energy

DISCLAIMER

DISCLAIMER

Available from the National Technical Information Service, U. S. Department of Commerce, Springfield, Virginia 22161.

Price: Paper Copy $18.00
Microfiche $3.50

LMSC-D678771

DOE/NOAA/OTEC-7
Distribution Category UC-64

PRELIMINARY DESIGN REPORT FOR OTEC STATIONKEEPING SUBSYSTEMS (SKSS)

12 December 1979

Prepared for
NOAA, Office of Ocean Engineering

by
LOCKHEED OCEAN SYSTEMS
Sunnyvale, California 94086

THIS PAGE

WAS INTENTIONALLY

LEFT BLANK

FOREWORD

Lockheed Ocean Systems is performing the Preliminary Design for OTEC Stationkeeping Subsystems (SKSS) study contract NA-79-SAC-00635 for NOAA, Office of Ocean Engineering, in support of the Department of Energy, Ocean Thermal Energy Conversion (OTEC) program. Participating with Lockheed are IMODCO on design and analysis of mooring systems for the spar, Simplex Wire and Cable Company on SKSS interface with the Electrical Transmission System riser cable, and Eager & Associates on reliability assessment. The results of other tasks in this study were reported as follows:

- Task I, Design Requirements, LMSC-D673832
- Task II, Conceptual Design, LMSC-D676379
- Task IV, Development and Testing Recommendations, LMSC-D677783

The results of Task III, Preliminary Designs, Task V, Cost and Schedule, and Task VI Commercial Plant SKSS Recommendations are presented in this final report. The tension anchor leg (TAL) SKSS for the spar, Section 3, was prepared by IMODCO, and the multiple anchor leg/active tensioning (MAL) SKSS for the barge, Section 2, was prepared by Lockheed. The SKSS designs were also presented in Rockville, Maryland, in a design review for NOAA, DOE, and the OTEC community.

CONTENTS

Section Page

ILLUSTRATIONS

TABLES

GLOSSARY

CWP	cold water pipe
IWRC	independent wire rope core
MAL	multiple anchor leg
MST	motion sensing transducer
NOAA	National Oceanographic and Atmospheric Administration
OTEC	Ocean Thermal Energy Conversion
SALM	single anchor leg moor
SKSS	stationkeeping subsystem
TAL	tension anchor leg
UJ	universal joint

Section 1
INTRODUCTION

Lockheed Ocean Systems with IMODCO prepared these preliminary designs for OTEC Stationkeeping Subsystems (SKSS) under contract to NOAA in support of the Department of Energy OTEC program. The results of Tasks III, V, and VI are presented in this design report. The report consists of five sections: introduction, preliminary designs for the multiple anchor leg (MAL) and tension anchor leg (TAL), costs and schedule, and conclusions. Extensive appendixes provide detailed descriptions of design methodology and include backup calculations and data to support the results contained in this report.

1.1 SCOPE OF TASK

The objective of this effort is to complete the preliminary designs for the barge-MAL and Spar-TAL SKSS. A set of drawings is provided for each which show arrangements, configuration, component details, engineering description, and deployment plan. Loads analysis, performance assessment, and sensitivity to requirements are presented, together with the methodology employed to analyze the systems and to derive the results presented. Life cycle costs and schedule are prepared and compared on a common basis. Finally, recommendations for the Commercial Plant SKSS are presented for both platform types.

1.2 SKSS CONCEPT SELECTION

In Task II, Conceptual Design, a total of eight SKSS concepts were developed and evaluated to identify the most promising candidates for further design development. NOAA selected the MAL with active tensioning for the barge, and the TAL for the spar. This selection provides designs for comparison with MALs for ship and spar prepared by a second contractor. The active tensioning feature is selected to assess the extent of anchor leg tension and barge

heading control. The TAL offers an opportunity for SKSS cost reduction by incorporating the cold water pipe (CWP) in the anchor leg.

1.3 REQUIREMENTS

The design requirements defined in the Task I report are modified in some areas to reflect both concept development in Task II and NOAA direction. Sea state wave height, wind, and current are increased to reflect the DOE standard environmental conditions (Section 1.4). The water depth is reduced from 4,000 to 3,280 ft for the TAL to take advantage of the CWP fixity realizable with this SKSS.

A CWP design is provided by NOAA for purposes of the TAL design development. One objective is to determine if the CWP can function as a tension member in mooring the spar. Platform characteristics are summarized in Table 1-1.

The MAL active tensioning SKSS is to control barge heading, if possible, and to equalize loading, thereby improving the efficiency of a MAL not equipped with active tensioning. Full barge rotation, as may occur with a turret moor, is not required in part because a swivel for the electrical riser cable is not undergoing a parallel development. Barge rotation is restricted to less than 90 deg. Anchor leg disconnect is not allowable.

1.4 ENVIRONMENT

The environmental conditions summarized in Table 1-2 are revised to reflect the hurricane prediction of Bretschneider (Ref. 1-1). Relationships which yield magnitude of wind, wave, and current for a specified average return period were derived to parameterize the enviromental loading on the barge and SKSS. The formulae are given in Appendix A, Subroutine "SITE."

Table 1-1 BARGE AND SPAR CHARACTERISTICS

Characteristics	Barge	Spar
LOA (ft)	381.5	
LWL (ft)	378	35
Beam (ft), maximum	121	200
Draft (ft), excluding discharge pipe	65	215
Depth (ft)	89	290
Displacement (ft)	67,901	54,300
CWP Diameter (ft)	30	32
CWP Length (ft)	2,935	2,825

The wind, wave, and current are assumed to be coplanar for estimation of environmental forces on the barge. The probability of this event is equal to the product of the probabilities of wind, wave, and current acting in the specified heading range. Utilizing the expression derived in Ref. 1-2, the following results are obtained for selected direction ranges. The wave crest is assumed to travel in the direction of wind. This assumption is supported by ship weather observations for seas up to 20-ft significant wave height. The results indicate a highest probability of 23 percent for coplanar wind, wave, and current in the range of 30 to 100 deg, i.e., propagation from the East North East.

Wind, Wave, and Current Direction (deg)	Compass Heading	Probability of Occurrence (%)
65 $\pm$ 35	ENE	23.0
65 $\pm$ 10		3.0
90 $\pm$ 35	E	4.0
90 $\pm$ 10		0.4
135 $\pm$ 10	SE	0.02

Table 1-2 SUMMARY OF ENVIRONMENTAL CONDITIONS, PUNTA TUNA

Property	Condition
Climate	Marine Tropical
Latitude	17° 57' N
Longitude	65° 52' W
Approximate Depth (ft)	4,000(a)
Distance to Shore (miles)	3
Distance along Shore (miles)	± 5
Return Period of Design Operational Sea State (years)	3
Return Period of Design Extreme Sea State (years)	100
Surface Current (knots)	1.8 to 2.4
Bottom Quality	Silt, Clay, Mud, underlain by dense sand
Bottom Slope (deg)	10 to 18
Operational Sea State:	
Maximum Wave Height (ft)	36.2
Significant Wave Height (ft)	20.1
Period of Maximum Energy (sec)	10.3
Wind (knots)	46.5
Surface Current (knots)	1.8
Seafloor Current (knots)	0.18
Current Profile	(b)
Astronomical Tide (Diurnal Range) (ft)	1.0
Astonomical Tide (Annual Max. Range) (ft)	1.8
Extreme Sea State:	
Maximum Wave Height (ft)	64.6
Significant Wave Height (ft)	35.9
Period of Maximum Energy (sec)	13.1
Wind (knots)	85.0
Surface Current (knots)	2.4
Seafloor Current (knots)	0.24
Current Profile	(b)
Astronomical Tide-Storm Surge (ft)	5.5

(a) Depth for TAL is 3,280 ft
(b) See Fig. 2-2, Ref. 1-1

In the case of a hurricane, the wind direction is assumed to act along the hurricane track, which is generally Easterly (Ref. 1-1). The predicted storm center radius of maximum wind (10 nm) and forward speed (10 knots) indicates that the storm acts as a point disturbance traveling slower than the progressive waves generated by the center. In this case the longer waves encountered by the moored plant have a direction of approach equal to the hurricane track. Spectral data measured in the Gulf of Mexico during hurricane Eloise indicate that "long period wave energy propagation direction varies only slightly during the storm even though the azimuth of the storm center with respect to the station varies considerably" (Ref. 1-3). These results indicate extensive spreading of wave energy, with low period waves generally propagating in the direction of the local wind velocity, with the latter at 90 deg or more to the direction of travel of the long period waves. Thus, assumptions of unidirectional wave spectra and coincident wind and wave are evidently not supported by these observations. Wind and wave spectra directionality based on data collected during hurricane Frederick in the Caribbean and near Puerto Rico will, if available, assist in identifying appropriate design conditions. The effect of directionality is further discussed in Section 2.2.1.

1.5 REFERENCES

1-1 U. of Hawaii Look Laboratory, Hurricane Design Winds and Waves and Current Criteria for Potential OTEC Sites, by C. L. Bretschneider, Report No. 45, Apr 1979

1-2 Lockheed Missiles & Space Company, Inc., Preliminary Design for OTEC SKSS, Task I Final Report, LMSC-D673832, Sunnyvale, Calif., 1 Jun 1979

1-3 "Hurricane Eloise Directional Wave Energy Spectra," by J. L. Black, Offshore Technology Conference Paper No. 3594, May 1979

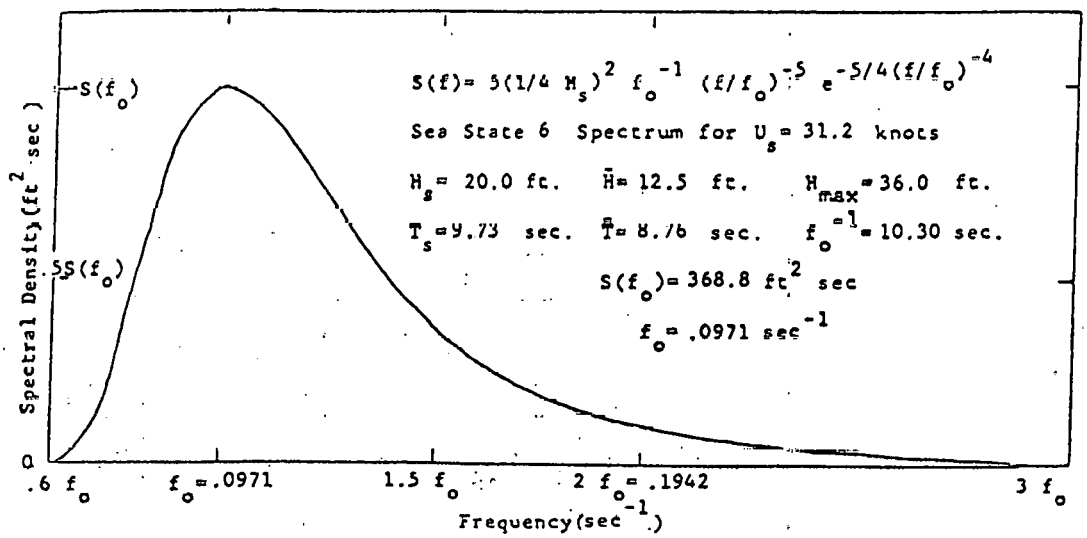

Frequency f= (sec^{-1})	Spectral Density $S(f)$=(ft^2 sec)	Frequency f=(sec^{-1})	Spectral Density $S(f)$=(ft^2-sec)
0.058	1.07186	0.205	28.82007
0.060	2.70023	0.210	25.69676
0.065	18.95708	0.215	22.96211
0.070	64.62093	0.220	20.56244
0.075	139.72730	0.225	18.45215
0.080	224.98690	0.230	16.59224
0.085	297.99950	0.235	14.94948
0.090	345.97330	0.240	13.49546
0.095	367.01580	0.245	12.20575
0.100	365.76730	0.250	11.05949
0.105	348.99530	0.255	10.03864
0.110	323.00850	0.260	9.12772
0.115	292.67130	0.265	8.31331
0.120	261.30950	0.270	7.58385
0.125	230.97880	0.275	6.92928
0.130	202.81790	0.280	6.34085
0.135	177.34920	0.285	5.81100
0.140	154.71370	0.290	5.33306
0.145	134.82780	0.295	4.90125
0.150	117.49160	0.300	4.51051
0.155	102.45260	0.305	4.15636
0.160	89.44426	0.310	3.83491
0.165	78.20984	0.315	3.54271
0.170	68.51167	0.320	3.27670
0.175	60.13739	0.325	3.03422
0.180	52.90005	0.330	2.81287
0.185	46.63707	0.335	2.61056
0.190	41.20891	0.340	2.42540
0.195	36.49556	0.345	2.25573
0.200	32.39500	0.350	2.10007

Fig. 7.9 Sea State 6 Spectrum for U_s = 31.2 knots, H_s = 20.0 feet and f_o^{-1} = 10.30 seconds.

Fig. 1-1 Operational Sea State Spectrum

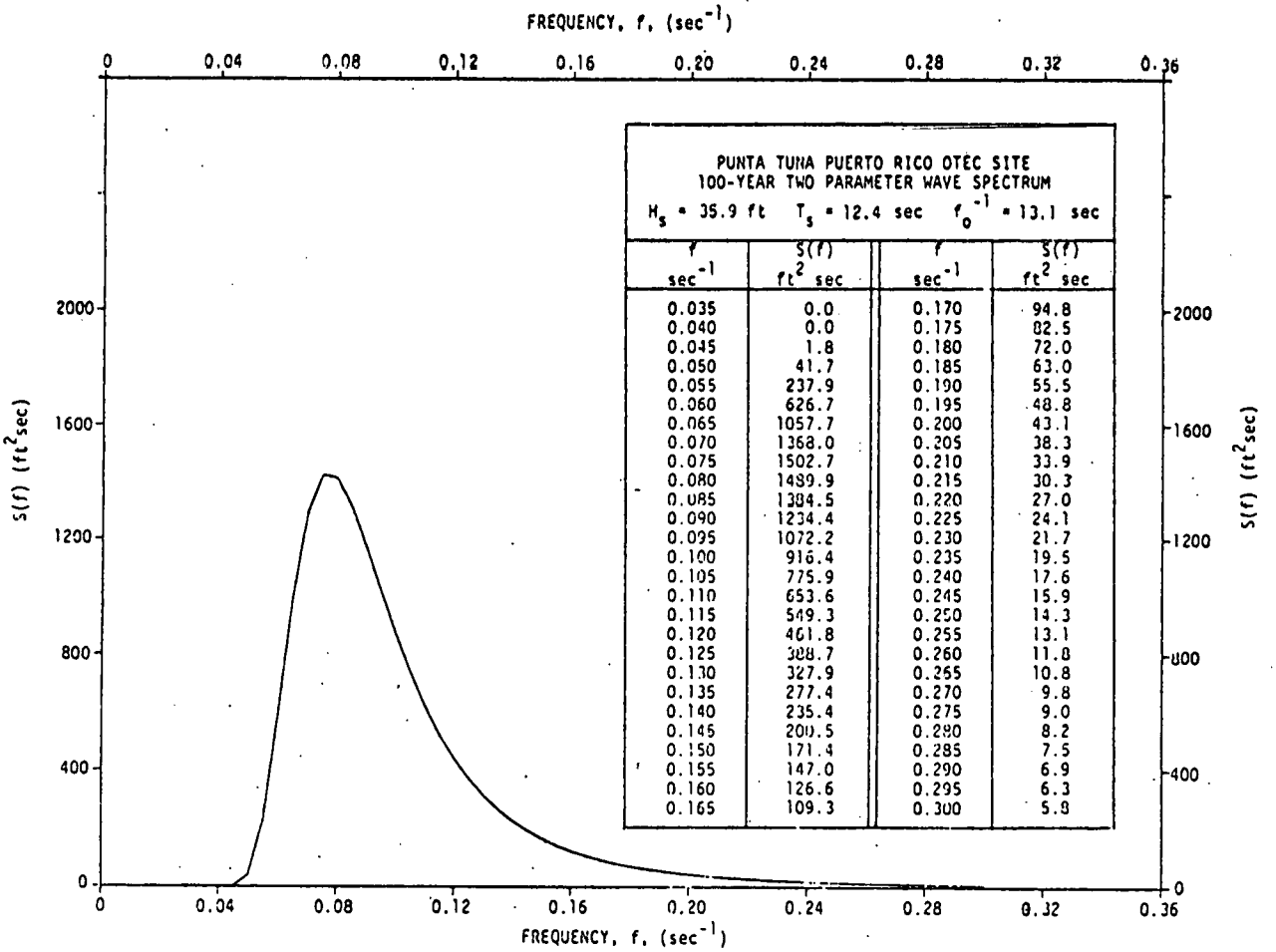

PUNTA TUNA PUERTO RICO OTEC SITE
100-YEAR TWO PARAMETER WAVE SPECTRUM
H_s = 35.9 ft T_s = 12.4 sec f_0^{-1} = 13.1 sec

f sec^{-1}	S(f) ft^2 sec	f sec^{-1}	S(f) ft^2 sec
0.035	0.0	0.170	94.8
0.040	0.0	0.175	82.5
0.045	1.8	0.180	72.0
0.050	41.7	0.185	63.0
0.055	237.9	0.190	55.5
0.060	626.7	0.195	48.8
0.065	1057.7	0.200	43.1
0.070	1368.0	0.205	38.3
0.075	1502.7	0.210	33.9
0.080	1489.9	0.215	30.3
0.085	1384.5	0.220	27.0
0.090	1234.4	0.225	24.1
0.095	1072.2	0.230	21.7
0.100	916.4	0.235	19.5
0.105	775.9	0.240	17.6
0.110	653.6	0.245	15.9
0.115	549.3	0.250	14.3
0.120	461.8	0.255	13.1
0.125	388.7	0.260	11.8
0.130	327.9	0.265	10.8
0.135	277.4	0.270	9.8
0.140	235.4	0.275	9.0
0.145	200.5	0.280	8.2
0.150	171.4	0.285	7.5
0.155	147.0	0.290	6.9
0.160	126.6	0.295	6.3
0.165	109.3	0.300	5.8

Fig. 1-2 Extreme Sea State Spectrum (Ref. 1-1)

Section 2
PRELIMINARY DESIGN OF MULTIPLE ANCHOR LEG SKSS FOR OTEC BARGE

The preliminary design of the multiple anchor leg SKSS with active tensioning for the OTEC barge is presented in this section. An engineering description of the system is followed by system loads analysis, performance evaluation, design development, and sizing. Following the subsection on installation are discussions of inspection, interfaces, requirements sensitivity, and Commercial Plant SKSS. System cost and schedule are presented in Section 4.

2.1 MAL ACTIVE TENSIONING - DESCRIPTION OF THE SKSS

The barge Stationkeeping Subsystem (SKSS) is a catenary multiple anchor leg (MAL) system with active tensioning. The active tensioning feature provides the capability to vary the anchor leg geometry by lengthening or shortening anchor legs and transferring load from each leg to an attached pendant. The latter provides for barge heading control. A description of the MAL is presented, including general arrangement, deck machinery, anchor leg and ground tackle characteristics, and design features.

2.1.1 General Arrangement

The MAL is comprised of eight catenary anchor legs arranged in pairs at each corner of the barge. One leg of each pair lies in a vertical plane at 45 deg to the barge centerline, and the second at 15 deg from the beam, providing fore and aft symmetry with respect to included angle. A general arrangement showing the anchor leg configuration is given in Fig. 2-1, and arrangement characteristics including bearing, range, and water depth are listed in Table 2-1.

The first four anchor legs are oriented seaward, while legs 5 through 8 are landward. Anchors on the longer seaward legs have a 1,000-ft greater range

Table 2-1 ARRANGEMENT CHARACTERISTICS OF MAL

Anchor Leg	Bearing Relative To Bow (deg)	Range to Outer Anchor (ft)	Water Depth At Anchor (ft)	Attachment Angle Off Vertical (deg)
1	45	6,277	5,640	20.0
2	75	6,206	5,680	19.9
3	105	6,206	5,440	20.6
4	135	6,277	4,920	22.8
5	225	5,278	3,458	27.6
6	255	5,206	3,122	30.2
7	285	4,990	3,206	29.4
8	315	5,278	3,710	25.9

and are set at a depth 2,400 ft greater than that on the landward legs. This asymmetry is a direct result of the sloped sea floor at the site. The seaward anchors and chain rest on the sea floor sloping down from the leg; conversely, the landward anchors and chain rest on the up slope.

Each anchor leg consists of chain, wire rope, and a pair of drag embedment anchors. The upper segment chafing chain passes under a fairlead on the barge side to a wildcat on a deck-mounted windlass and down to a chain locker below the main deck. A chain pendant is attached to the anchor leg at the chafing-chain/wire-rope connection and secured at the barge keel. The scantlings of each leg are identical, while wire rope and lower chain segment lengths vary between legs (see Fig. 2-1).

2.1.2 MAL Components

Anchor leg component details are shown in Fig. 2-2, including a parts list of wire rope, chain, shackle, socket, swivel, and anchor. A complete list of components is given in Table 2-2. A brief description of each component follows.

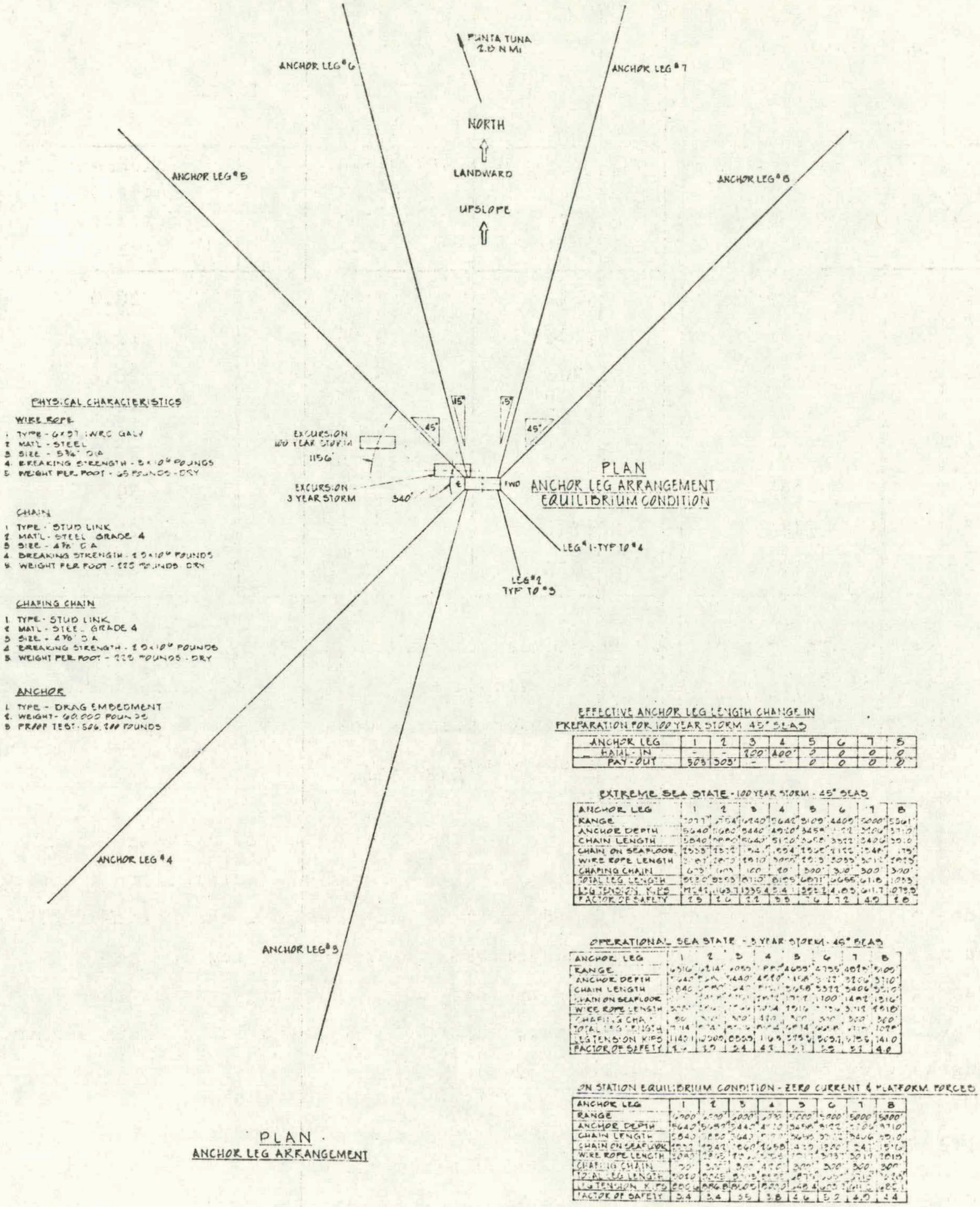

EFFECTIVE ANCHOR LEG LENGTH CHANGE IN PREPARATION FOR 100 YEAR STORM 45' SEAS

ANCHOR LEG	1	2	3	4	5	6	7	8
HAUL-IN	-	-	300'	400'	0	0	0	0
PAY-OUT	303	303'	-	-	0	0	0	0

EXTREME SEA STATE - 100 YEAR STORM - 45' SEAS

ANCHOR LEG	1	2	3	4	5	6	7	8
RANGE	[illegible]	[illegible]	6240'	5642'	5109'	4405'	5000'	5561'
ANCHOR DEPTH	5640'	5680'	5440'	4920'	3458'	[illegible]	3106'	3710'
CHAIN LENGTH	5840'	[illegible]	5643'	5120'	[illegible]	3532	3406'	[illegible]
CHAIN ON SEAFLOOR	2333'	2372'	[illegible]	1554	1356'	2132	1348'	179'
WIRE ROPE LENGTH	[illegible]	2870'	2910	3055'	[illegible]	3033'	[illegible]	2975'
CHAFING CHAIN	603'	603'	100	40'	300'	300'	300	300'
TOTAL LEG LENGTH	9530'	9293	[illegible]	8195	6671'	6655'	61.8	[illegible]
LEG TENSION, KIPS	[illegible]	[illegible]	[illegible]	[illegible]	[illegible]	[illegible]	611.7	[illegible]
FACTOR OF SAFETY	2.5	2.6	2.2	3.5	[illegible]	[illegible]	4.5	2.8

OPERATIONAL SEA STATE - 3 YEAR STORM - 45' SEAS

ANCHOR LEG	1	2	3	4	5	6	7	8
RANGE	6516'	[illegible]	[illegible]	[illegible]	4655'	4755'	[illegible]	5109'
ANCHOR DEPTH	[illegible]	[illegible]	5440'	4920'	[illegible]	[illegible]	3106'	3710'
CHAIN LENGTH	[illegible]	[illegible]	[illegible]	[illegible]	3658'	3532'	3406'	[illegible]
CHAIN ON SEAFLOOR	[illegible]	[illegible]	[illegible]	[illegible]	[illegible]	1100'	1482'	1316'
WIRE ROPE LENGTH	[illegible]	[illegible]	[illegible]	[illegible]	[illegible]	[illegible]	[illegible]	2910'
CHAFING CHAIN	[illegible]	[illegible]	300'	[illegible]	[illegible]	[illegible]	300	300'
TOTAL LEG LENGTH	[illegible]	[illegible]	[illegible]	[illegible]	[illegible]	[illegible]	[illegible]	[illegible]
LEG TENSION KIPS	[illegible]	[illegible]	[illegible]	[illegible]	[illegible]	[illegible]	[illegible]	141.0
FACTOR OF SAFETY	[illegible]	[illegible]	2.4	4.3	[illegible]	[illegible]	[illegible]	4.0

ON STATION EQUILIBRIUM CONDITION - ZERO CURRENT & PLATFORM FORCES

ANCHOR LEG	1	2	3	4	5	6	7	8
RANGE	[illegible]	[illegible]	6000'	[illegible]	5000'	5000'	5000'	5000'
ANCHOR DEPTH	5640'	[illegible]	5440'	[illegible]	3458'	[illegible]	[illegible]	3710'
CHAIN LENGTH	5840	[illegible]	5643	[illegible]	3658	[illegible]	3406	[illegible]
CHAIN ON SEAFLOOR	[illegible]	[illegible]	[illegible]	1658	[illegible]	[illegible]	[illegible]	[illegible]
WIRE ROPE LENGTH	[illegible]	[illegible]	[illegible]	[illegible]	[illegible]	[illegible]	3017	[illegible]
CHAFING CHAIN	[illegible]	[illegible]	[illegible]	[illegible]	300'	300'	300	300'
TOTAL LEG LENGTH	[illegible]	[illegible]	[illegible]	[illegible]	[illegible]	[illegible]	[illegible]	[illegible]
LEG TENSION KIPS	[illegible]	[illegible]	[illegible]	[illegible]	[illegible]	[illegible]	[illegible]	[illegible]
FACTOR OF SAFETY	3.4	3.4	3.5	3.8	4.6	5.2	4.0	4.4

Fig 2-1 General Arrangement

(Continued on next page)

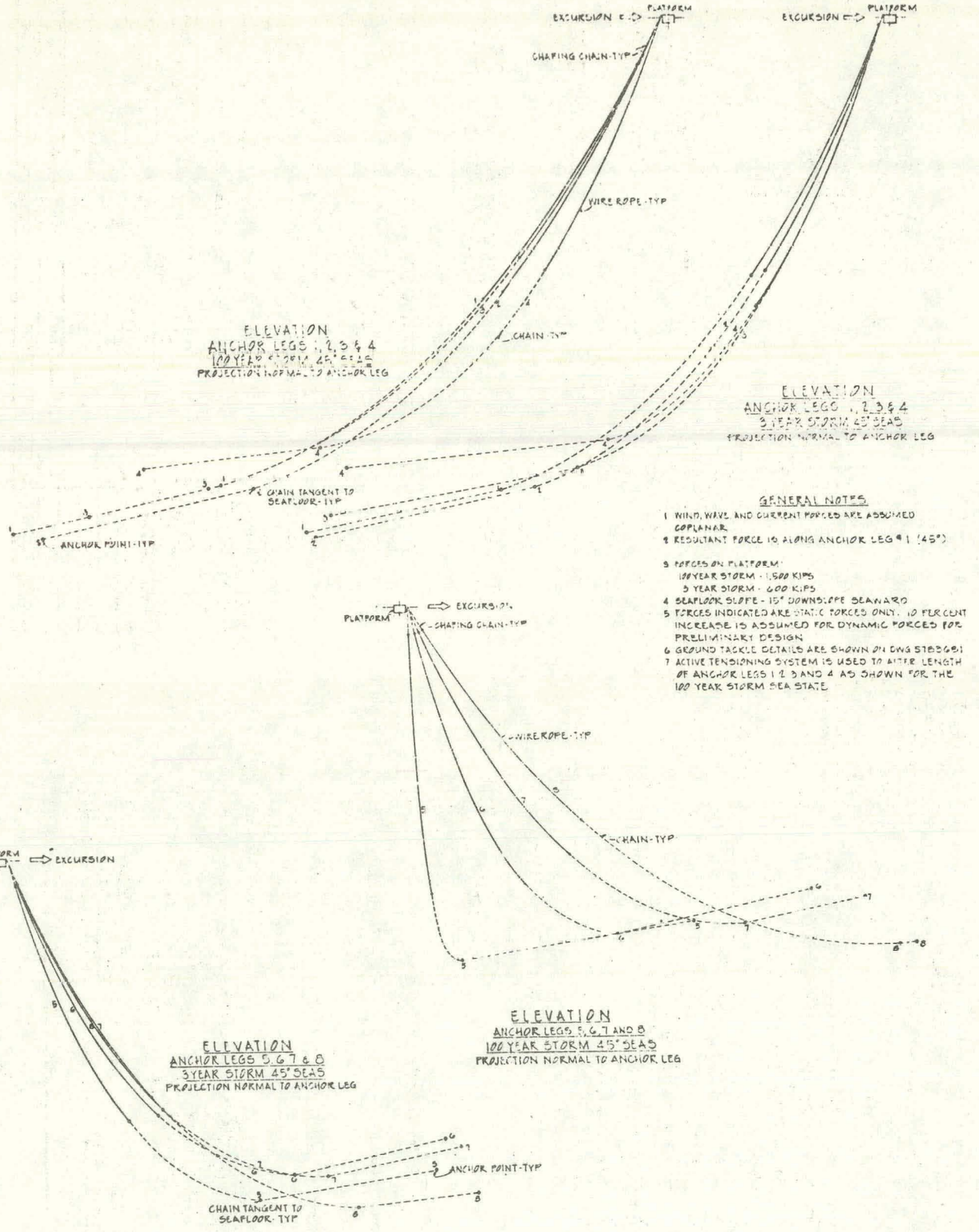

Fig. 2-1 (Continued)

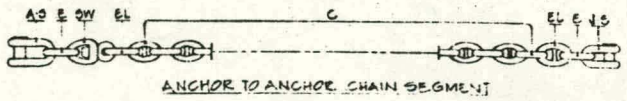

ANCHOR TO ANCHOR CHAIN SEGMENT

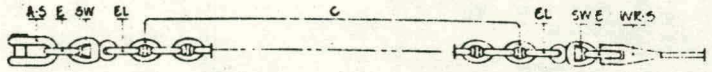

ANCHOR TO WIRE ROPE CHAIN SEGMENT

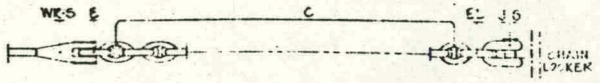

CHAFING CHAIN SEGMENT

	LEGEND	ITEM NO.
A-S	ANCHOR SHACKLE	1
E	END LINK	2
SW	SWIVEL	3
EL	ENLARGED LINK	4
C	COMMON LINKS	5
J-S	JOINING SHACKLE	6
WR-S	WIRE ROPE SOCKET	7
WR	WIRE ROPE	8
A	ANCHOR	9

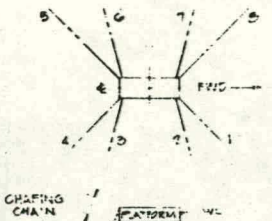

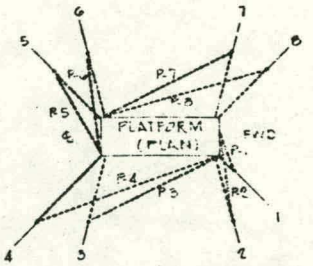

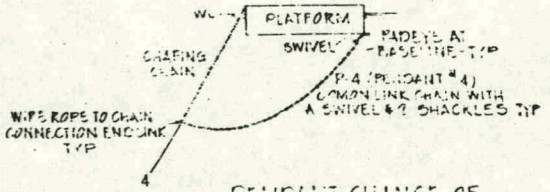

PENDANT CHANGE OF HOOKING ARRANGEMENT

1" = 200'

TABLE OF LENGTHS

PENDANT #	P-1	P-2	P-3	P-4	P-5	P-6	P-7	P-8
LENGTH-FEET	650	650	650	800	650	650	700	850

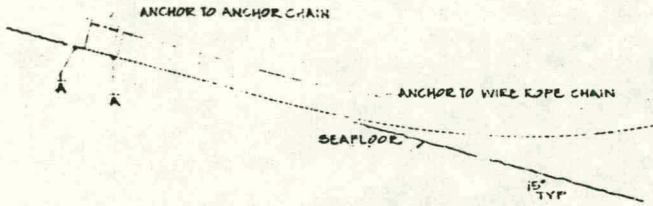

TYPICAL ANCHOR LEG

UPSLOPE SEAFLOOR CATENARY SHOWN

1" = 400'

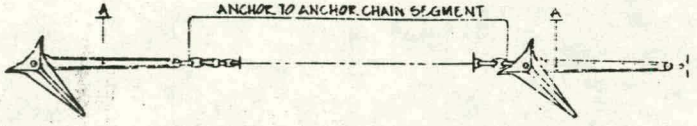

ANCHOR TO ANCHOR ARRANGEMENT

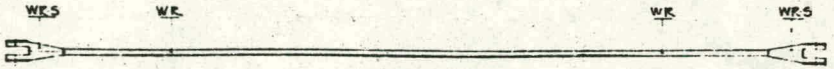

WIRE ROPE SEGMENT

TABLE OF LENGTHS

ANCHOR LEG

SEGMENT	1	2	3	4	5	6	7	8
ANCHOR TO ANCHOR	100'	100'	100'	100'	100'	100'	100'	100'
ANCHOR TO WIRE ROPE	1540'	5880'	5640'	5170'	3558'	3377'	3406'	3919'
CHAFING CHAIN	700'	700'	700'	700'	700'	100'	700'	100'
WIRE ROPE	3870'	2855'	2755'	3045'	2916'	3030'	3001'	2810'

QTY REQD	CODE IDENT	PART OR IDENTIFYING NO	NOMENCLATURE OR DESCRIPTION	MATERIAL DESCRIPTION OR NOTE	MATERIAL SPECIFICATION	ZONE	ITEM NO
16		ANCHOR - 60,000# MOORFAST - 506700# PROOF TEST			STEEL		9
23680		WIRE ROPE - 5¾" DIA - 6 x 37 IWRC - 3.10# LB B.S.			"		8
16		WIRE ROPE SOCKET - 5¾" WIRE ROPE - 6x37 IWRC			"		7
32		JOINING SHACKLE - 4⅛" DIA CHAIN - GR 4			"		6
4800 FEET		COMMON LINKS - 4⅛" DIA - GR 4 - 1932000# B.S.			"		5
40		ENLARGED LINK - 4⅛" DIA - GR 4			"		4
40		SWIVEL - 4⅛" DIA - GR 4			"		3
42		END LINK - 4⅛" DIA - GR 4			"		2
16		ANCHOR SHACKLE			"		1

PARTS LIST

INTERPRET DWG PER		UNLESS OTHERWISE SPECIFIED DIM ARE IN INCHES. TOLERANCES ON: FRACTIONS = ± 1/16 DECIMALS: .X = ± .1, .XX = ± .03, .XXX = ± .010 ANGLES = ± 2 DEG	DATE 12 SEP 1975	LOCKHEED MISSILES & SPACE COMPANY, INC. A SUBSIDIARY OF LOCKHEED AIRCRAFT CORPORATION SUNNYVALE, CALIFORNIA			
			DWN J.T. IWASHITA				
			APVD	OTEC 5KSS STATION KEEPING SUBSYSTEM GROUND TACKLE DETAILS			
			APVD				
			ENGR J.T. IWASHITA				
			CHKR				
			APVD	SIZE D	CODE IDENT 17077	DRAWING NO 5783681	REV -
NEXT ASSY	USED ON	CONTR	APVD	SCALE 1" = 10'		SHEET	
APPLICATION		CCA/C1/F0					

Fig. 2-2 Anchor Leg Component Details

THIS PAGE

WAS INTENTIONALLY

LEFT BLANK

Table 2-2 MAL LIST OF COMPONENTS

Component	Size	Quantity	
		Per Leg	Total
Drag Embedment Anchor	60,000 lb	2	16
Anchor Shackle	4-7/8 in.	2	16
Swivel	4-7/8 in.	5	40
Enlarged Link	4-7/8 in.	5	40
Stud Link Chain (Gr. 4)	4-7/8 in.	5,400 ft (typ.)	48,976 ft
Joining Shackle	4-7/8 in.	2	16
Socket	5-3/4 in.	2	16
Joining Shackle	4-7/8 in.	3	24
Wire Rope (6 x 97 IWRC)	5-3/4 in.	3,000 ft (typ.)	23,680 ft
Anchor Windlass	4-7/8 in.	1	8
Chain Stopper	4-7/8 in.	1	8
Fairleader	4-7/8 in.	1	8
Power Unit	455 hp	-	4
Control Unit	-	1	8
Central Control Unit	-	-	1
Chain Locker	24x10x10 ft	1	8
Windlass Platform	33x34 ft	-	4
Windlass Deckhouse	13x33x34 ft	-	4
Padeye	4-7/8 in.	2	16

Anchor Segment. A pair of drag embedment-type anchors is attached to each anchor leg in series. Fitted to the bottom of the first anchor is a padeye to accept the 100-ft, 4-7/8-in.-diam chain leading from the trailing anchor. Anchor weight is 60,000 lb each with fluke angle dependent on as-measured soil conditions at the site (TBD). Anchor efficiency, holding-power-to-weight ratio, is assumed to be 20 in sand with a penetration angle of 34 deg, a minimum depth of 7 ft, and a scope angle of zero. Anchor length is 19.3 ft, width of 22.6 ft, depth of 5.8 ft, and fluke height of 11.7 ft. The shank on the first anchor is sized to carry the bending moment resulting from the

trailing anchor in the deployed, set condition. An anchor shackle, end link, swivel, and enlarged link are utilized to attach each anchor to the chain. Stock length is sufficient to maintain roll stability of the first anchor. These components are compatible with 4-7/8-in. diam chain, Grade 4.

Anchor Chain. The anchor chain is stud link chain, 4-7/8-in. diam, Grade 4. Proof test load is 2,052,000 lb, and break test load is 2,932,000 lb. The latter is assumed to be the chain breaking strength. The dry weight is 229 lb/ft. The segment consists of a single, continuous length of common links. The total length of each segment varies from 5,900 ft on the seaward legs to 3,300 ft on the landward legs. Ultrasonic testing is recommended to ensure satisfactory service life of 30 years.

Chemical composition of the cast alloy steel is typically as follows:

Element	Percent
C	0.07
Si	0.23
Mn	1.89
P	0.015
S	0.006
Cr	1.82
Ti	0.16
V	0.06
Al	0.04

Typical mechanical properties of the chain steel are (minimum value)

Tensile strength (psi)	128 to 135,000
Elongation (%)	15
Reduction (%)	40

Wire Rope. The anchor chain segment below and the chafing chain segment above are connected by the wire rope segment. The length of each wire rope segment varies from 2,800 to 3,100 ft depending upon anchor leg location, while the diameter is constant for all legs at 5-3/4 in. The wire rope construction is

six strands, right hand regular lay, each strand consisting of 97 steel wires (6 x 97). At the center is an independent wire rope core (IWRC). Wire rope material is extra improved plow steel. Preloading of the wire rope is recommended to extend fatigue life.

Wire rope weight is 65 lb/ft. The designed breaking strength is 3,000,000 lb. The apparent modulus of elasticity is 12,780,000 psi, with a steel area of 61 percent of the enclosed area. The wire is zinc galvanized and blocked with a petrolatum-based grease or synthetic infill to retard the onset of corrosion. Wire rope terminations are the open socket, Crosley-type, filled with zinc or, alternatively, a resin potting compound if appropriate as determined from development testing.

Sheathing of the wire rope can increase wire rope resistance to corrosion. Although not specified in this design, the addition of a 1/4-in.-thick sheathing of polyvinylchloride to the wire rope exterior surface may provide extended service life. To limit sheathing distortion during handling and deployment, compression load may not exceed 2,000 psi. This requirement, however, is not compatible with the linear winch used in deployment as the compressive load on the cable in the linear winch is well in excess of this limit.

Chafing Chain. The upper segment of each anchor leg consists of a 700-ft continuous length of 4-7/8-in.-diam stud link chain. The chain is identical to the anchor chain at the lower position of the leg. The wire rope socket is connected to the chain via an end link, joining shackle and a second end link. The upper end of the chain is terminated in the chain locker below the main deck of the barge by a joining shackle to a padeye on the side of the chain locker. Nominally, 300 ft of chafing chain is located on the anchor leg and 400 ft is stowed in the chain locker.

The deck machinery on the barge dedicated to the MAL consists of a fairleader, windlass, and chain locker for each of eight anchor legs. In addition, a

power unit and control panel for each windlass pair and a central control unit is required (Fig. 2-3).

Fairlead. The fairlead is a large fabricated and cast assembly. The sheave, supported on a horizontal bearing, is a five-whelp wildcat, of 8.7-ft diam, designed for the 4-7/8-in.-diam stud link chain. A vertical axis pivot allows rotation of the fairlead and chain to accomodate relative motion between anchor leg and barge. Allowable rotation is ± 90 deg and +60/-30 deg for the corner and side fairleader, respectively. Fairlead overall dimensions are 11.5 ft (L) x 4 ft (W) x 13 ft (H), and approximate weight is 45,000 lb each. The sheave centerline is located 12.2 ft above the waterline.

Windlass Module. Directly above the fairlead is a windlass module consisting of two anchor windlasses, power unit, and control box mounted on a platform which extends 10 ft beyond the hull.

The windlass wildcat is a standard five-whelp design similar to that on the fairlead. Braking holding power is 1,500,000 lb and delivered minimum horsepower is 455, providing a chain speed of 10 fpm at 1,500,000 lb tension. A chain stopper with minimum capacity of 3,000,000 lb is integral with the windlass frame.

A tension-sensing flexure is mounted in the chain stopper with the signal cabled to the local and central control units. The latter unit is capable of remote control of each windlass module and is located on the bridge. The electric-hydraulic power unit provides for operation of each single drive windlass, one at a time. A control panel provides for local operation of the windlasses. The entire module is enclosed in a deckhouse to prevent water and salt spray on the windlasses, thereby extending service life and reducing frequency of maintenance.

Approximate overall dimensions of each windlass are 18 ft (L), 10 ft (W), 11 ft (H), with a weight of 150,000 lb. The windlass is sandblasted and painted with an organic zinc coating, followed by a urethane coating. This finish may have up to a 20-year life.

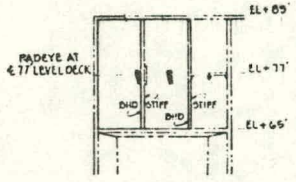

SECTION GG

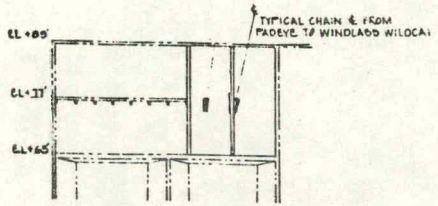

SECTION FF

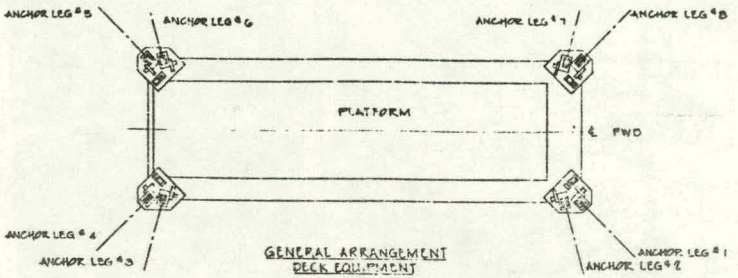

GENERAL ARRANGEMENT
DECK EQUIPMENT
1" = 40'

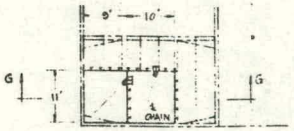

SECTION-FWD

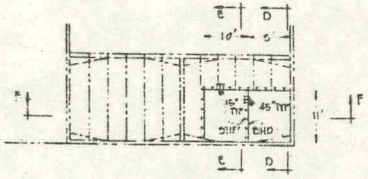

SECTION-AFT

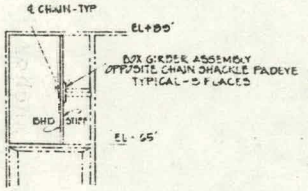

SECTION EE

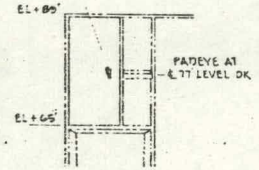

SECTION DD

PLAN - CHAIN LOCKER
1" = 10'

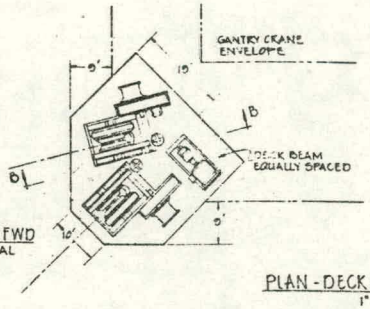

PLAN FWD
TYPICAL

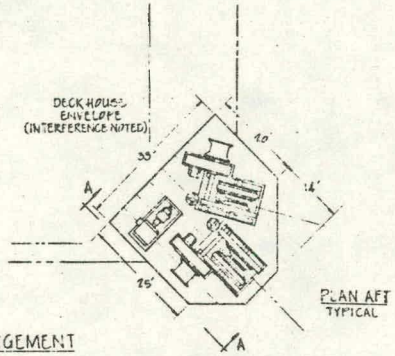

PLAN AFT
TYPICAL

PLAN - DECK ARRANGEMENT
1" = 10'

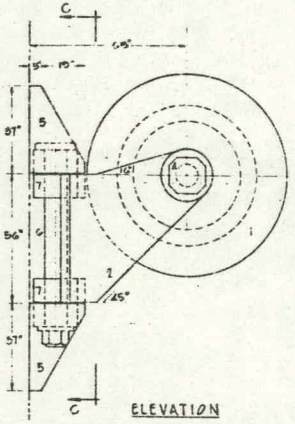

ELEVATION

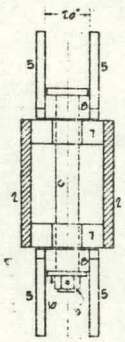

SECTION CC

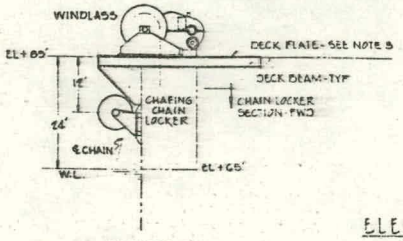

SECTION BB

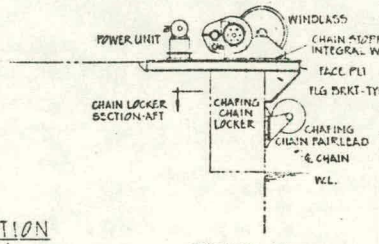

ELEVATION
1" = 10'

SECTION AA

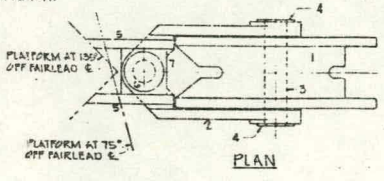

PLAN

CHAFING CHAIN FAIRLEAD 1" = 20"

GENERAL NOTES

1. MAX LINE TENSION 1.6×10^6 POUNDS. THIS IS 50% OF THE ANCHOR LEG WIRE ROPE BREAKING STRENGTH
2. MATERIAL FOR PLATE, SHAPE, ETC - A-36
3. TWO CHAIN PASS-THROUGH HOLES PROVIDED IN DECK PLATE FOR EACH WINDLASS - ONE OVER FAIRLEAD - ONE OVER CHAIN LOCKER
4. WEATHER PROTECTION PROVIDED BY A DECK HOUSE OVER WINDLASSES (NOT SHOWN)
5. CHAIN LOCKER VOLUME - 2277 FT³ TOTAL CHAIN LENGTH - 700 FT.
6. WINDLASS DATA:
   - CHAIN SIZE - 4 7/8" DIA STUD LINK
   - WILDCAT - CAST STEEL WITH STANDARD FIVE WHELP DESIGN
   - WILDCAT BRAKE HOLDING POWER - 1,500,000 POUNDS
   - CHAIN STOPPER - INTEGRAL WITH THE UNIT - 3.1^{06} POUNDS (MIN)
   - EQUIPPED WITH LOAD CELLS FOR ACTUAL CHAIN TENSION READOUT
   - DELIVERED HORSEPOWER - 455
   - WEIGHT - 150,000 POUNDS
   - LINE SPEED - 10 FPM AT 1.6×10^6 POUNDS
7. MOORING PATTERN ARRANGEMENT IS SHOWN ON DWG 5783680
8. GROUND TACKLE DETAILS ARE SHOWN ON DWG 5783681
9. DEPLOYMENT - ARRANGEMENT AND DETAILS ARE SHOWN ON DWG 5783683
10. CHAIN LOCKER BELOW DECK INTERFERENCES:

	AFT		FWD	
	STBD	PORT	STBD	PORT
77' LVL	FUTURE ELECT SP	FUTURE ELECT SP	PLTF EQUIP.	PLTF EQUIP
65' LVL	ELECT. WORKSHOP	ENGRNG WORKSHOP	THRUSTER ACC.	THRUSTER ACC.

LEGEND

1. 5 WHELPS CHAIN SHEAVE - 4 7/8" DIA STUD LINK CHAIN
2. SHEAVE YOKE PLATE - 4" THK W/2" THK BOSS - 75" DIA
3. SHEAVE SHAFT AND BEARING - 10" DIA
4. COVER PLATE W/ MACHINE SCREWS AND WASHERS
5. PIVOT ASSEMBLY SUPPORT PLATE - 4" THK
6. PIVOT ASSEMBLY BOLT - 10" DIA
7. YOKE ASSEMBLY PIVOT BEARING BLOCK
8. STATIONARY PIVOT BEARING BLOCK - 20" x 20" x 10"
9. HEX NUT WITH SET SCREW
10. WASHER

Fig. 2-3
MAL Deck Equipment

SKSS			
STATION KEEPING SUB SYSTEM			
DECK EQUIPMENT AND CHAIN LOCKER			
SIZE	CODE IDENT	DRAWING NO	REV
E		5783682	

THIS PAGE

WAS INTENTIONALLY

LEFT BLANK

The windlass platform consists of an extension of the deck supported by a faceplate and flange brackets below. Two chain pull through holes are provided in the deck above the fairleader and above the chain locker. This platform is located 24 ft above the waterline. Interference is noted with the deckhouse envelope in the aft portion of the barge.

Chain Locker. A chain locker is provided for stowage and termination of the chafing chain on each anchor leg. The volume required for each leg is 1,300 ft^3 minimum. The locker extends between the 65 ft and 89 ft elevation on the barge, and is typically 10 ft square in plan, providing well in excess of the minimum volume. A padeye and foundation are located on a bulkhead in each locker for chain termination. A portion of space required for these lockers is allocated to storage and shop space of the barge.

Pendants. A pendant is attached to each anchor leg, at the chafing chain to wire rope connection. The other end of the pendant is connected to a padeye on the platform keel below the adjacent anchor leg fairlead. These 4-3/8 in. chain pendants provide platform heading control capability for transferring anchor leg load to another point on the platform.

2.2 LOADS ANALYSIS

2.2.1 Barge Loading

Environmental loading on the barge is based on the quasi-static force and moment analysis presented in Ref. 2-1. The following results, revised to reflect changes in the sea state definition, indicate the resultant horizontal-plane force and yaw moments on the barge, assuming coplanar wind, wave, and current. The components induced by wind, current, and wave, respectively, are presented in Appendix A for both barge and spar, together with the computer program listing developed for both spar and barge loading. The force is shown to increase approximately 50 percent as the loading rotates from head to beam (Fig. 2-4). The force in the Extreme Sea State is 130 percent greater than that in the Operational Sea State. The barge orientation is East-West.

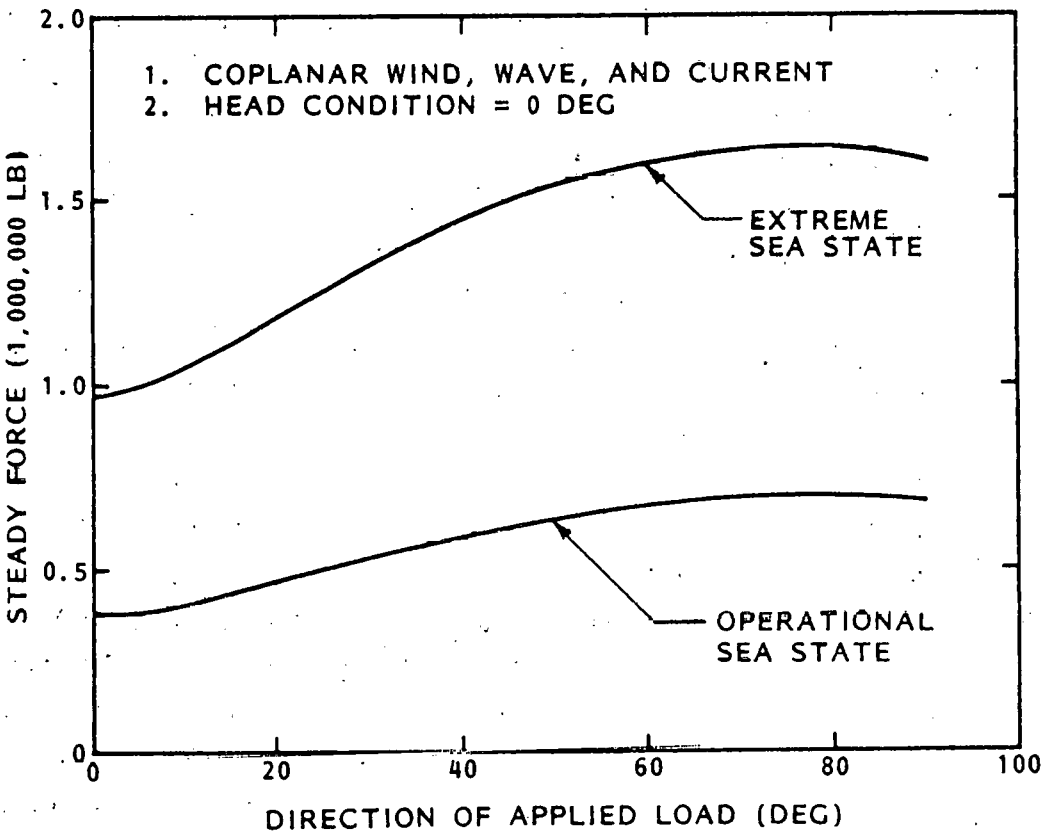

Fig. 2-4 Environmental Loads on Barge
(Steady Force Versus Barge Heading)

The probability of a storm from the South resulting in a beam condition is extremely low (Section 1.4), at least for nonhurricane sea states.

The yaw moment on the barge is sensitive to relative heading between barge and storm (Fig. 2-5). The yaw moment, maximum at 10 deg off the bow, is a restoring moment for headings from 0 to 45 deg.

Noncoincident wind, wave, and current force is found to be lower than the maximum force in beam conditions (see Appendix A). The assumption of coplanar forces is therefore conservative with respect to environmental loads on the platform constrained by the multiple anchor leg SKSS. In the operational sea state, the wind and mean wave drift forces are comparable, whereas in the extreme sea state the wave force exceeds the current force and is 50 percent of the total load (see Table 2-3).

The application of the mean wave drift force as a quasi-static load on the platform and superimposed with wind and current forces to determine platform excursion and anchor leg tension is the most common approach to anchor leg design (Ref. 2-2). Although not capable of treating the time-dependent excitations nor the dynamic response of the SKSS, this is an approach particularly appropriate to preliminary design. Several techniques for dynamic simulation are under development (Refs. 2-2, 2-3, 2-4), with continued research required in frequency differencing, viscous damping, simulation time, and application of time histories in design. Some results of the dynamic simulation indicate that high peaks in the slowly varying wave drift forces do not necessarily produce high peaks in the line tension, although the dynamic method does give about 25 percent higher line tension than the quasi-static method. The significance of an underestimated wave force on line tension using the quasi-static method in this preliminary design is discussed in Section 2.9.

Directionality of Environmental Loading. The directional properties of the high sea states, particularly the Extreme Sea State resulting from a hurricane in the Caribbean, are examined to assess the assumptions of unidirectional

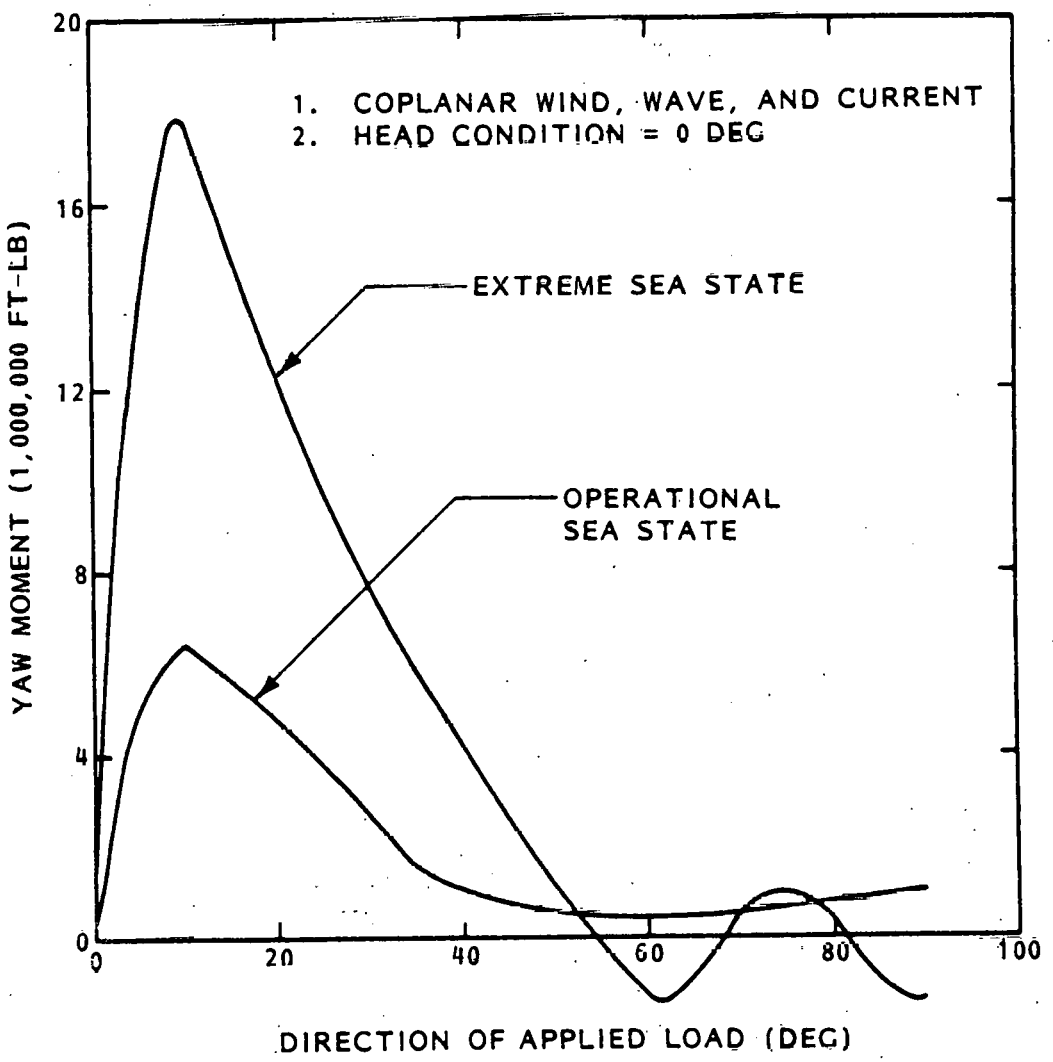

Fig. 2-5 Environmental Loads - Barge (Yaw Moment Versus Heading)

Table 2-3 SUMMARY OF ENVIRONMENTAL LOADS ON BARGE

Item	Operational Sea State		Extreme Sea State	
Storm Return Period (yr)	3	3	100	100
Heading (deg)	0	90	0	90
Wind Force (10^6 lb)	0.05	0.08	0.17	0.26
Current Force (10^6 lb)	0.21	0.30	0.37	0.53
Wave Force (10^6 lb)	0.12	0.31	0.44	0.81
Net Force (10^6 lb)	0.38	0.69	0.98	1.60
Net Moment (10^6 ft-lb)	0.42	-0.98	1.4	-1.4

(a) Coplanar Wind, Wave, Current (0 deg Easterly)

seaway and coplanar wind, wave, and current. Storm directionality is also relevant to the barge heading control requirement of the SKSS; if the seaway is directional and if it can be forecasted, then the barge heading control to maintain head seas is a realistic expectation for the SKSS.

Hurricane seaway direction is illustrated for two cases of a track passing South and North of the OTEC barge (see Fig. 2-6). As the hurricane eye travels West in the Caribbean, most probable for hurricanes passing within 50 miles of Puerto Rico, long waves are generated and propagate outward from the disturbance. These waves of period 10 to 15 sec or greater travel faster than the speed of the disturbance, reaching the barge ahead of the disturbance. The local wind, at right angles to these waves, generates waves of lower period which travel downwind. The seaway is therefore short crested, bidirectional and bi-modal at this stage. As the hurricane eye proceeds West and passes South of the barge, the sea spectrum becomes narrower and single peaked. The wind is Westerly following the counterclockwise flow of the air mass in the hurricane eye, and in the direction of the dominant waves. In the case of the track to the North of the barge, the shorter waves approaching from the North are fetch-limited by Puerto Rico.

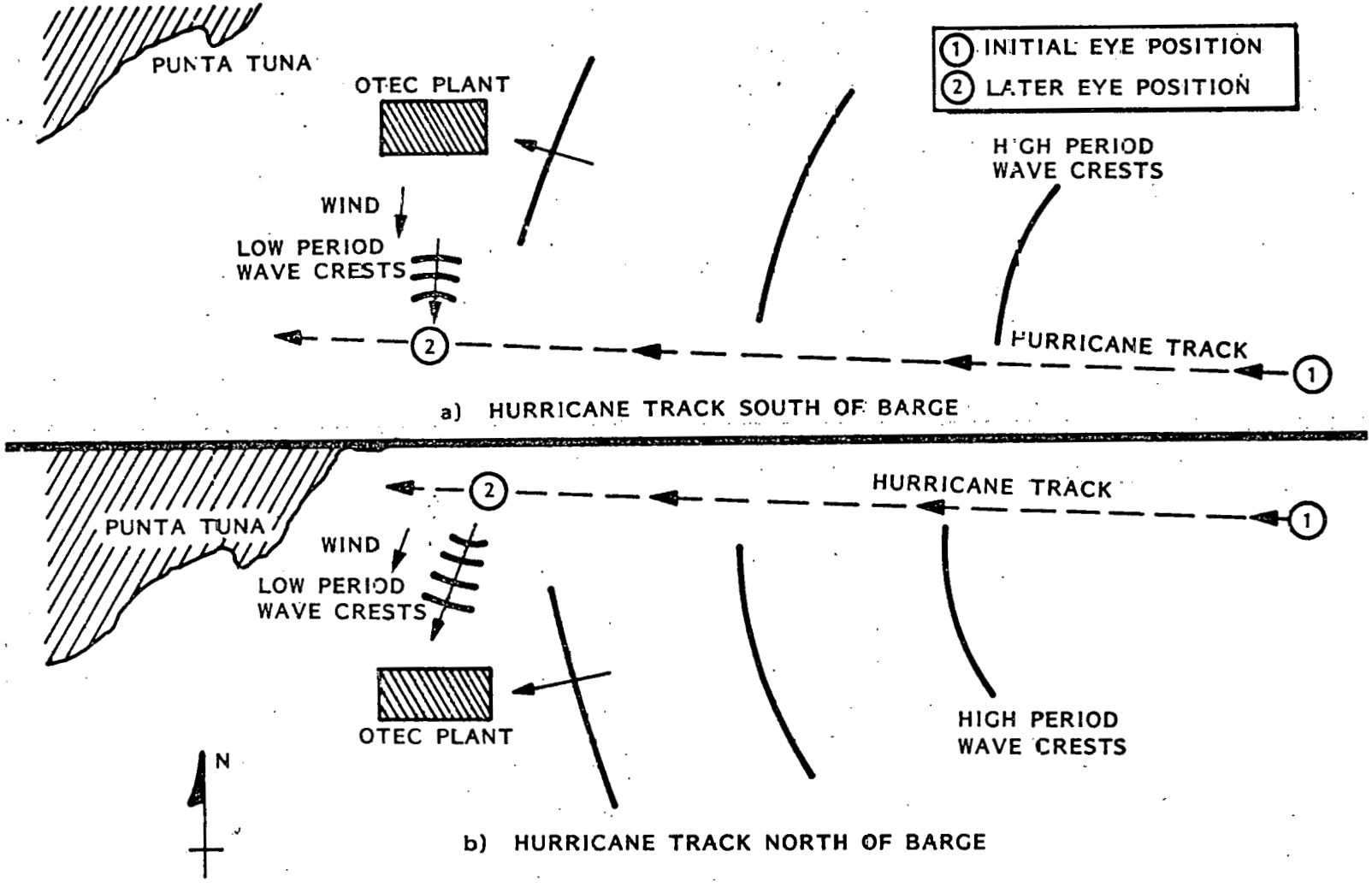

Fig. 2-6 Hurricane Tracks

A similar set of conditions exists for the eye traveling North and passing to the East or West of the barge, respectively (Ref. 1-3).

The assumption of a unidirectional seaway for the computation of wave drift force and barge motions is inconsistent with wind and sea direction in the initial position. The forces and motions are therefore likely to be lower than the predicted values. Waves of approximately 10 sec result in a drift force of greater magnitude than waves of higher or lower period. Instead of a drift force acting in a single direction it is expected that drift forces are spread over a 90-deg arc, the quadrant depending on the relative positions of barge and hurricane track. Forces and platform motions in a short-crested seaway are generally lower than the wave-induced force and motion in a long-crested seaway, so that this assumption is also conservative.

The assumption of a unidirectional, narrow band spectrum and coplanar wind and waves more closely models the conditions when the eye passes the platform. A preferred heading with respect to the waves is more readily identified therefore as the eye passes the platform than in the earlier stages of the hurricane.

The wind, assumed coplanar with the waves, is in the wave direction of the locally generated waves, and at right angles to the long period waves. The current consists of the geostrophic current with components of wind- and wave-driven surface currents. It is difficult to assess the directionality of the current although the probability of all current components being coplanar would appear to be low.

Barge Kinematics. The MAL induces net moments on the barge which result in trim about the transverse axis, heel about the longitudinal axis, and yaw about the vertical axis. The magnitude of these angular changes are examined for the Extreme Sea State.

In the case of heel the maximum heeling moment occurs in the beam condition and is 270×10^6 ft-lb. This moment causes the barge to heel into the oncoming wind, waves, and current, thereby reducing the freeboard on the

weather side. For a displacement of 67,000 LT and GM_T of 12.34 ft, the heel angle is found as follows:

$$\phi = \sin^{-1}\left(\frac{270 \times 10^6}{GM}\right)$$

$$= 8.4 \text{ deg}$$

The resultant loss in freeboard on the weather side is 8.9 ft, leaving a net freeboard of 15.1 ft. The reduced freeboard may result in increased deck wetting and reduced transverse static stability and therefore is an unfavorable impact on the barge.

Barge trim, based on a moment to change trim by 1 in. of 6.45×10^6 ft-lb, is estimated to be 0.7 ft at the bow, for a 45 deg heading. Trim changes of this magnitude are considered to be insignificant to barge stationkeeping.

The MAL provides a restoring moment about the barge vertical axis, or yaw moment, which is balanced by the applied sea state moment. The magnitude of yaw moment and the extent of yaw offset is presented in this section.

Static analysis of the MAL is based on force equilibrium with the barge fixed in yaw, while moment equilibrium is not satisfied. The moment induced by the MAL due to barge excursion, shown in Fig. 2-7, increases with sea state heading to a maximum of -61×10^6 ft-lb at 45 deg in the Extreme Sea State. The effect of excursion and yaw on moment is shown in Fig. 2-8. The barge yaws until the MAL restoring moment is equal and opposite to the sea state-induced moment:

$$M_y = -(a + 7.4\,\beta_1) \times 10^6 \text{ ft-lb}$$

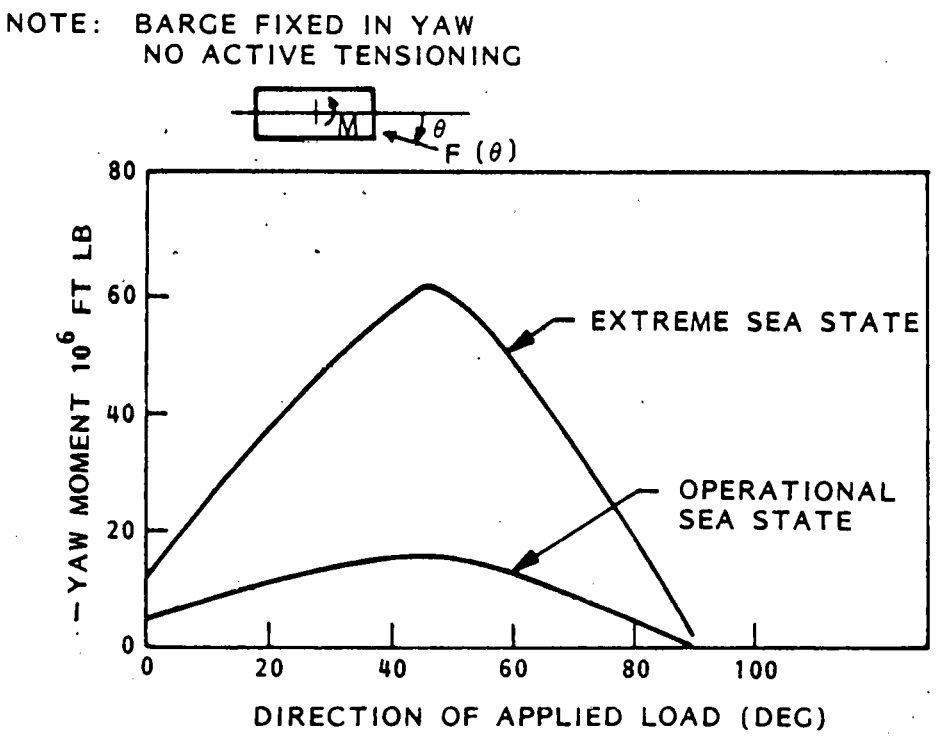

Fig. 2-7 Yaw Moment Induced by SKSS Due to Barge Excursion

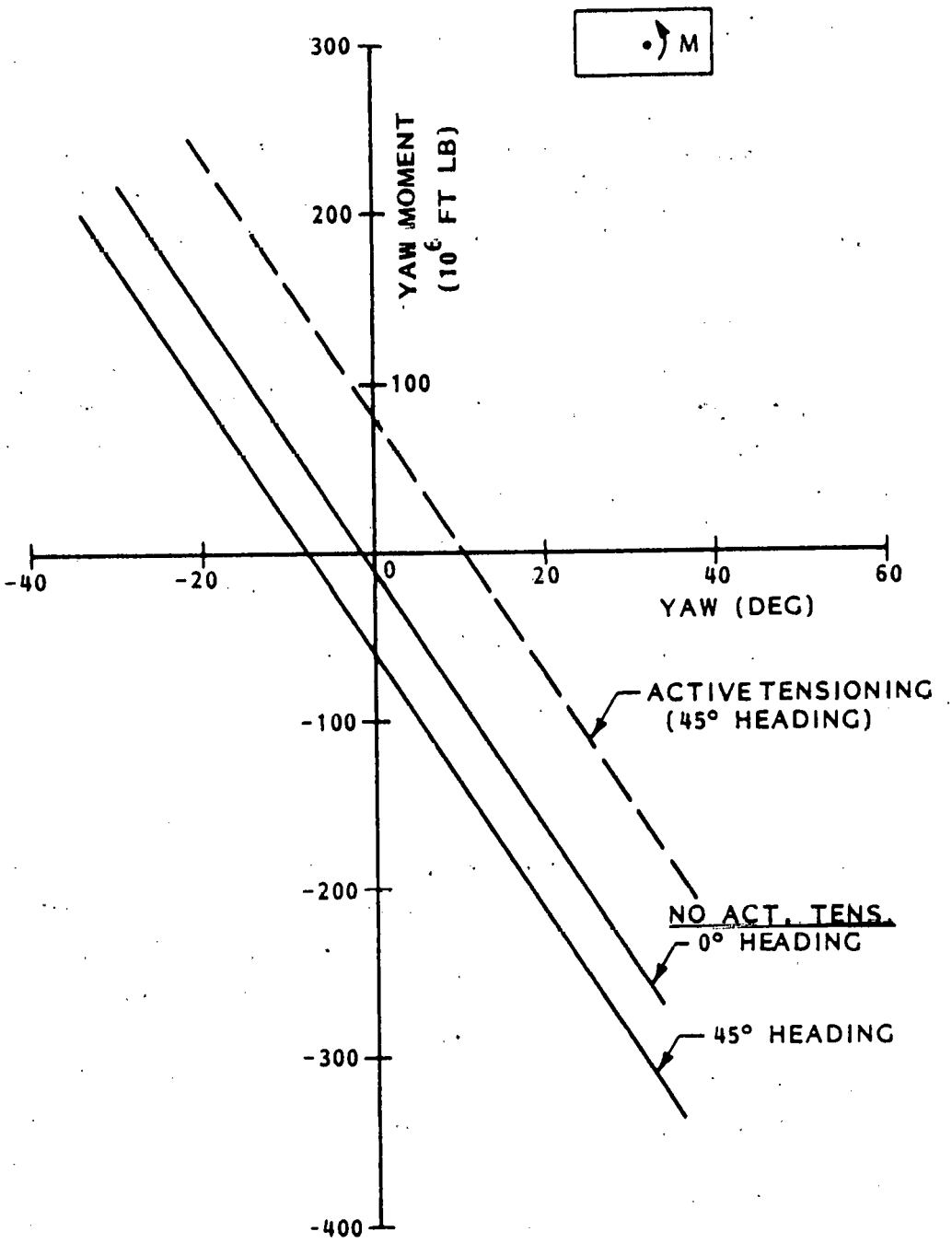

Fig. 2-8 Yaw Moment Induced by SKSS Due to Barge Excursion and Yaw

where

M_y = restoring moment in yaw, ft-lb

β_1 = barge yaw, deg

The intercept, a, is dependent on sea state heading: 12 for zero heading, 62 for 45 deg heading. The yaw offset for quartering seas is -9 deg; the barge rotates into the sea state so that the resultant sea-state heading is 36 deg.

2.2.2 Static Loads Analysis

Objectives of This Analysis. The principal objective of this section is to present methodology and results of static-loads calculations for the MAL SKSS in a variety of environmental conditions, including platform storm loads for return periods of of 3- and 100-year with various angular orientations to the platform.

Actual mooring site anchoring depths and approximate bottom slopes are used in developing the mooring leg configurations. Depths are shown in Fig. 2-9. Calculation techniques are developed in some detail in Appendix D.

The analysis detailed in Appendix D differs from those previously conducted in that it includes the effects of varying depths and bottom slopes. Depths are tabulated and the average slopes from the center out to the anchor locations calculated. Anchor locations are specified in a coordinate system centered at the platform neutral position, with the x-axis parallel to eastern geographical direction. The anchors placed in deeper water in the +z direction are all at a nominal 6,000-ft range from the platform. Inshore anchors are at a range of 5,000 ft. Anchor placement information is contained in Table 2-4.

The platform orientation, coordinate system, and mooring line configuration are shown in Fig. 2-10. Attachment points for the 45-deg mooring legs are at the platform corners $x = \pm 189$ ft, $z = \pm 60.5$ ft. The four additional lines

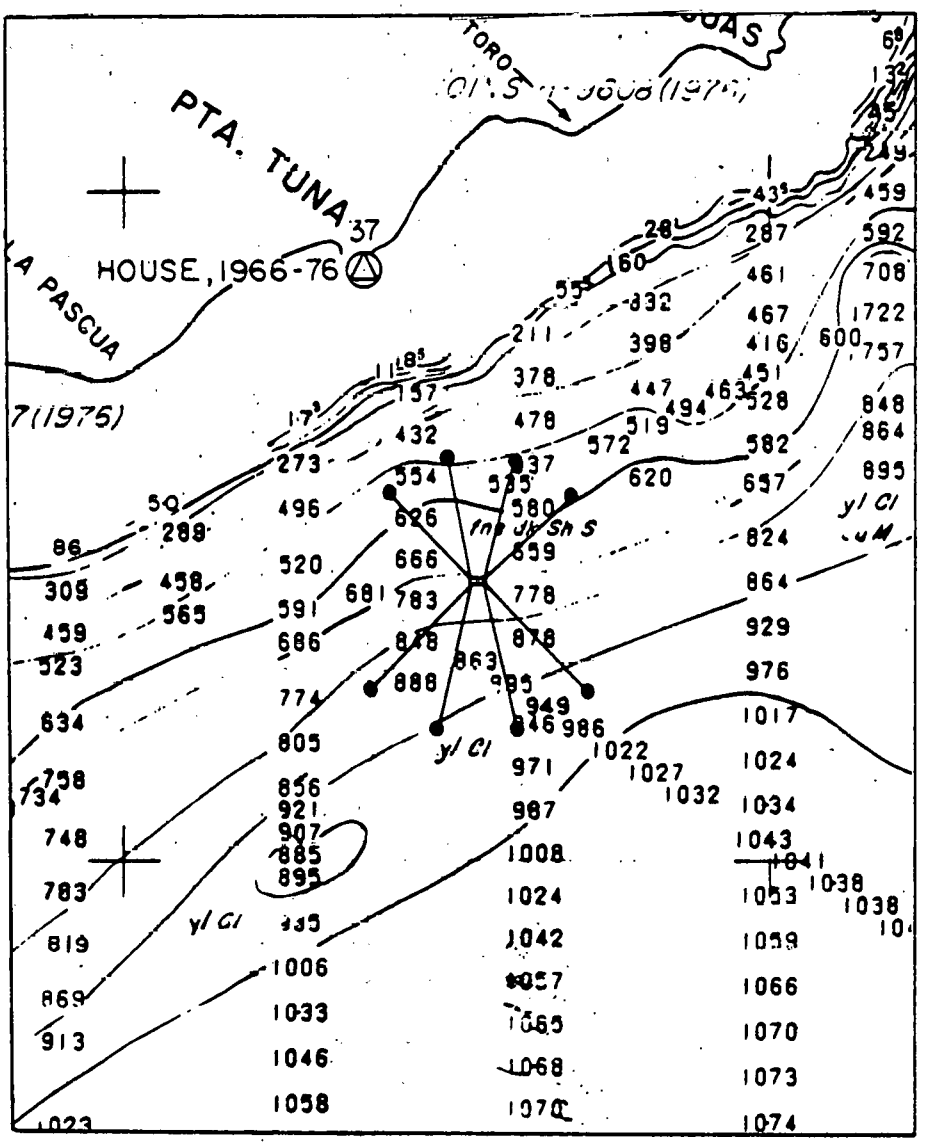

Fig. 2-9 MAL Shown on Pt. Tuna Site Contours (Depth in Fathoms)

Table 2-4 ANCHOR COORDINATES, DEPTHS, BOTTOM SLOPES

Anchor No.	Location (ft)	(ft)	Depth (ft)	Bottom Slope (deg)
1	4432	4303	-5640	-13.0
2	1729	5856	-5680	-13.3
3	-1729	5856	-5440	-11.1
4	-4432	4303	-4920	-6.3
5	-3725	-3597	-3458	9.1
6	-1470	-4890	-3122	12.8
7	1470	-4890	-3206	11.9
8	3725	-3597	-3710	6.3

are 15 deg from the beam fore and aft as shown. Attachment points for these lines are $x = \pm 176$ ft, $z = \pm 60.5$ ft.

The mooring lines are in two sections consisting of a 5-3/4-in. steel-wire rope for the upper section with a weight of 56.5 lb/ft in the water. A section of 4-7/8-in. chain with a wet weight of 199 lb/ft connects the wire rope to the anchor. Lengths of wire and chain for each of the 8 mooring legs are listed in Table 2-5. Length of each section of chain is set at 200 ft greater than the water depth of that particular anchor for maintenance considerations.

The length of each section of wire rope is determined by providing an equal horizontal tension component at the platform for each of the mooring legs. This ensures that the equilibrium position of the platform is at the prescribed center of the chosen site. The horizontal tension components of the undisturbed mooring are set at 300,000 lb to achieve a slightly greater than necessary stiffness for the static deflections. This mooring system deflection stiffness is shown in Fig. 2-11 for a 3-year load at an incidence angle of 45 deg.

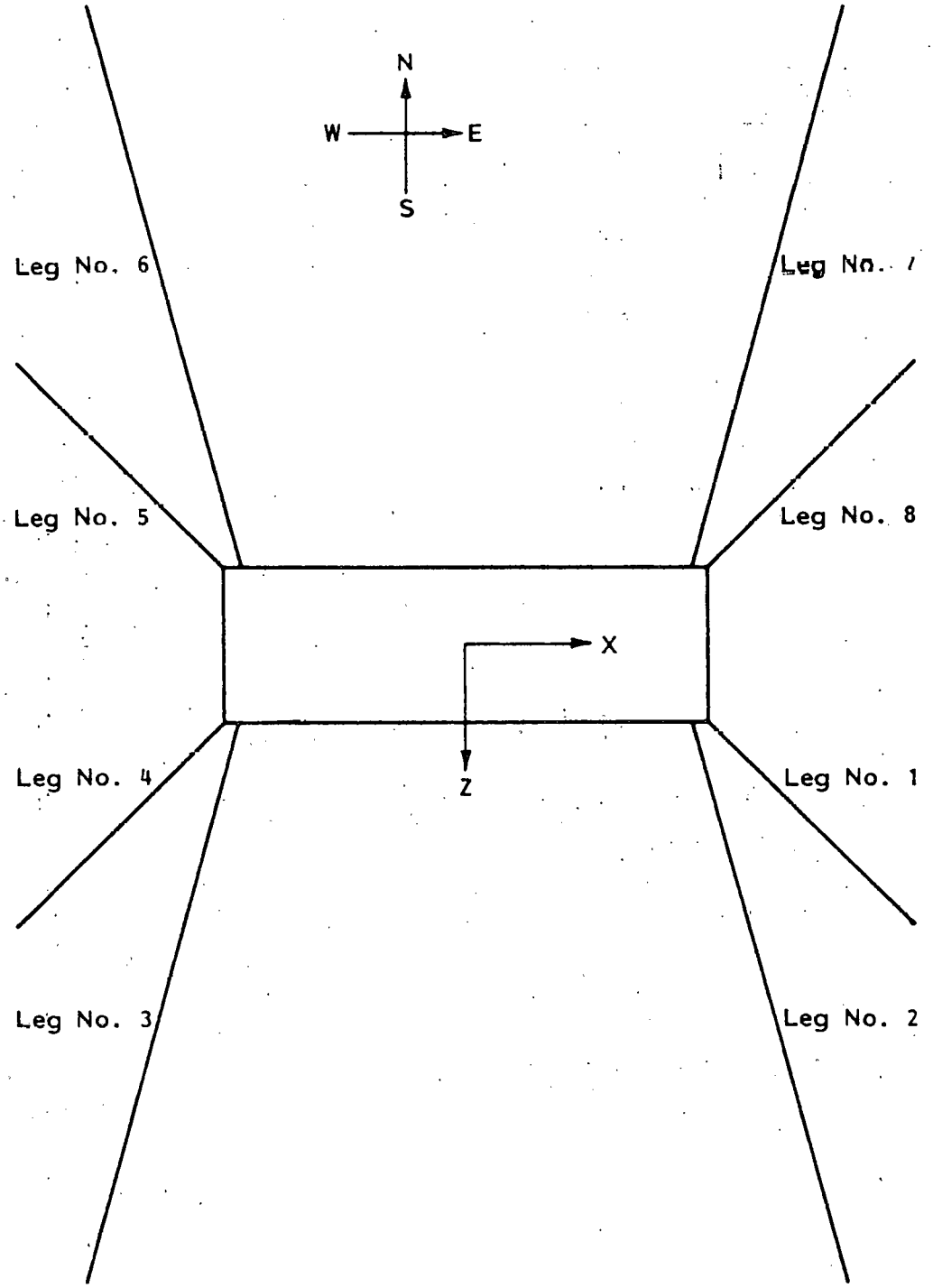

Fig. 2-10 Surface Platform Orientation Coordinate System and Mooring Legs

Table 2-5 COMPOSITE MOORING LEG LENGTHS (FEET)

Leg No.	Chain Length	Wire Rope Length	Total Length
1	5840	3170	9010
2	5880	3155	9035
3	5640	3255	8895
4	5120	3465	8585
5	3658	3210	6868
6	3322	3330	6652
7	3406	3305	6711
8	3910	3110	7020

(Horizontal tensions at the platform are uniform at 300,000 lb)

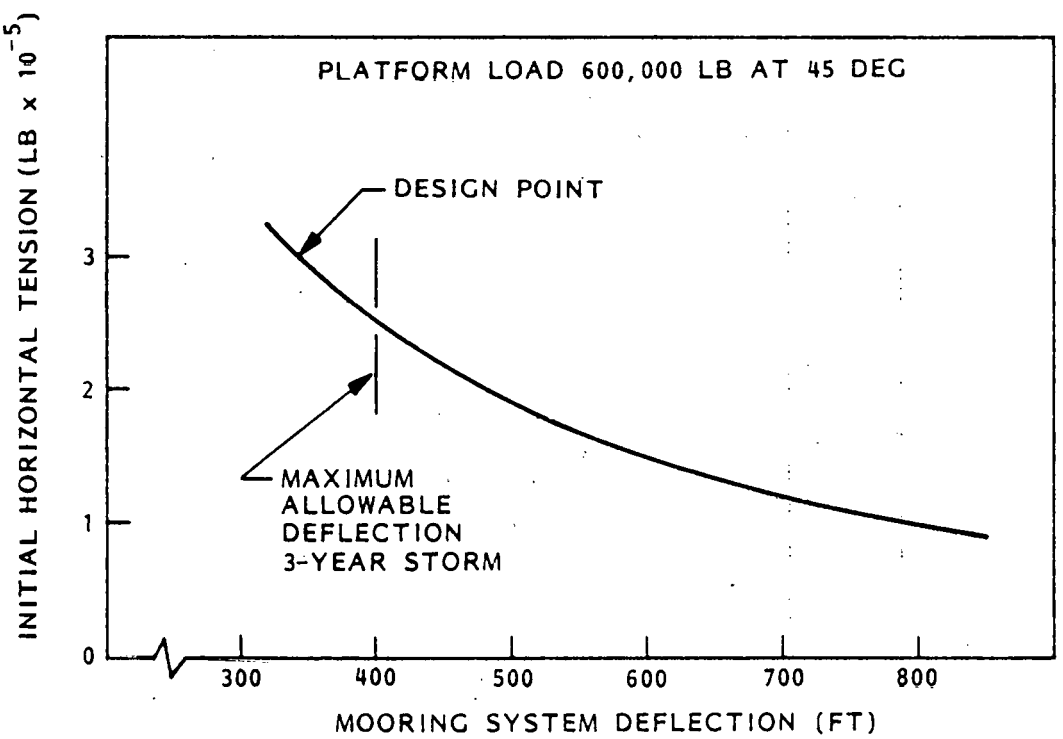

Fig. 2-11 Variation of Mooring Deflection with Initial Horizontal Tension

Comparison of Constant Depth, Flat Bottom Calculations to Sloping Bottoms. A practical measure of mooring system performance is the horizontal restoring force developed with increasing range from the anchor location. The sloping bottom causes a change in the range required to develop a particular restoring force. Figure 2-12 presents the variation of restoring force with range from the anchor for three different bottom slopes ± 15 deg and zero, depth and cable characteristics are held constant. A difference of 1,000 ft exists for slopes from +15 to -15 deg in the region of 250,000 lb of restoring force for this composite line. This difference is the principal reason that the range to the inshore, positive slope anchors is reduced to 5,000 ft from the 6,000-ft range of the deep water anchors.

Effects of varying depth are also shown in Fig. 2-12. Mooring line characteristics are again held constant as is the bottom slope at +15 deg. A change in depth of 1,000 ft shifts the restoring force range increment approximately 700 ft.

Influence of Line Lengths and Initial Tensions on Maximum System Tension Under Loaded Conditions. The chain length of each of the 8 mooring legs is determined by the corresponding anchor depth. Steel wire rope length is a function of the initial horizontal tension. Lengths of wire rope corresponding to various initial horizontal tensions are shown in Fig. 2-13 for each anchor leg. These data are divided into two distinct groups by the slope of the curves. One group comprises all of the deep-water lines and the other contains all of the inshore mooring legs. Vertical tensions for the same grouping are displayed in Fig. 2-14. These curves provide an indication of the tension relief realized by relaxing and tensioning individual legs of the mooring array.

Maximum system tension under load depends partially on the mooring system deflection characteristics. Load sharing between adjacent lines is promoted by allowing greater platform deflections.

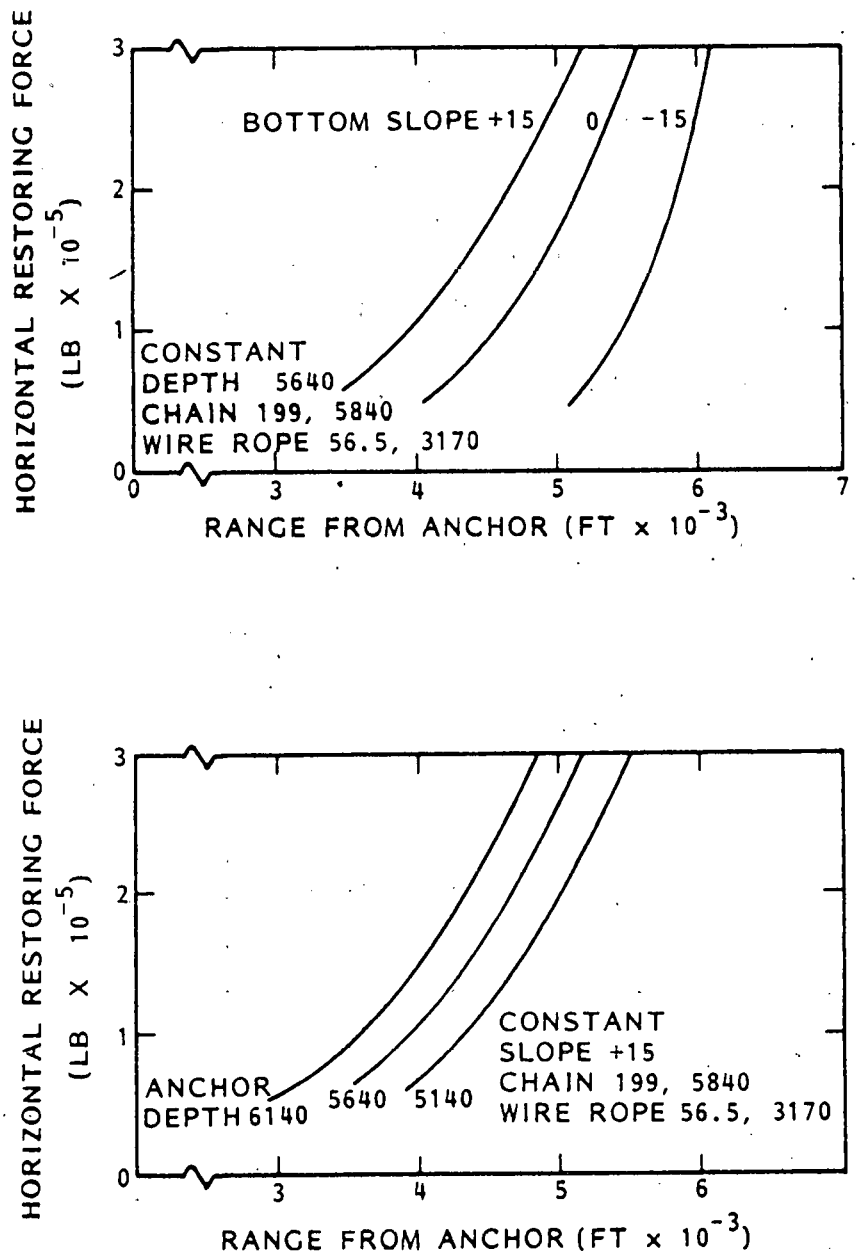

Fig. 2-12 Single Anchor Line Performance

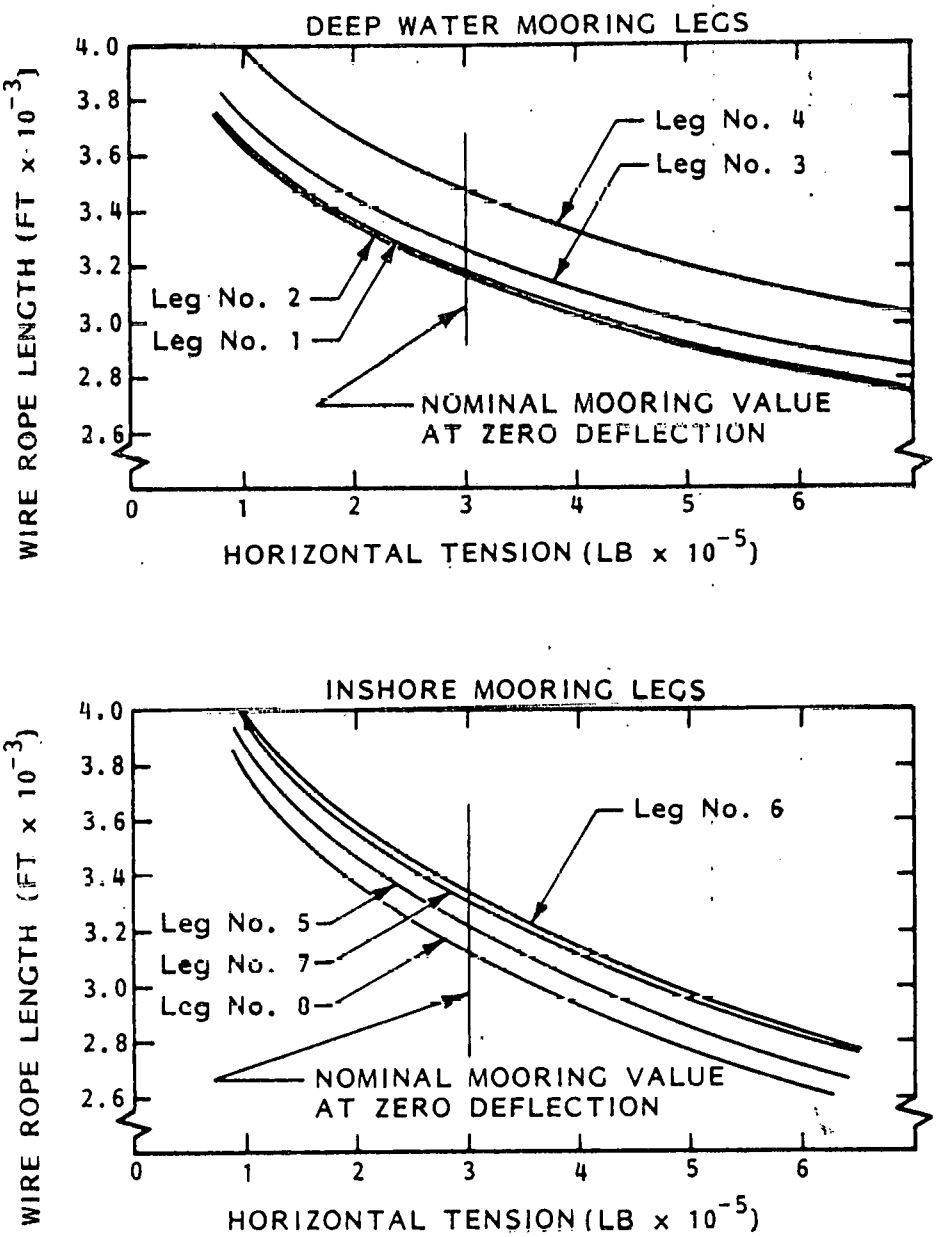

Fig. 2-13 Horizontal Tensions at Platform Attachment Point

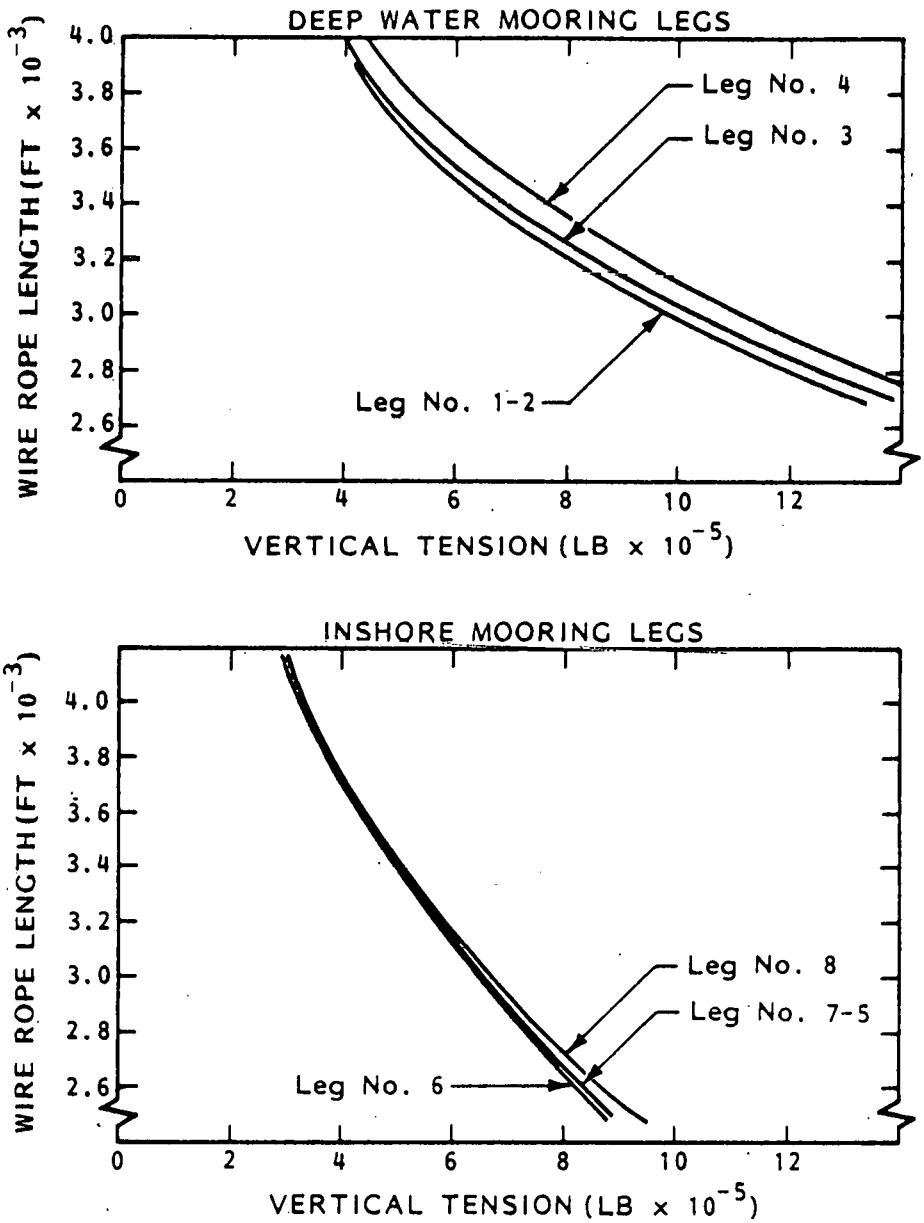

Fig. 2-14 Vertical Tension at Platform Attachment Point

Figure 2-15 indicates the change in maximum system tension with initial horizontal tension for a 3-year storm at 45 deg. Decreasing the initial horizontal tension allows greater mooring system deflection as shown in Fig. 2-11.

The process of lowering maximum system tension by changing the deflection characteristics of the entire mooring system is most effective at the lower tension values associated with 3-year storm loads. An examination of maximum system line tension plotted against platform load in Fig. 2-16 shows that the change in maximum tension at 1.5×10^6 lb of platform load is less than 1/2 of the value at 0.6×10^6 lb.

Decreasing maximum system tension is mandatory in the case of storm loads near 45 deg at 100-year storm levels. This SKSS design has the capability of tensioning or relaxing individual mooring legs. Changing tension levels and lengths of a single mooring leg alters the distribution in tension for all the

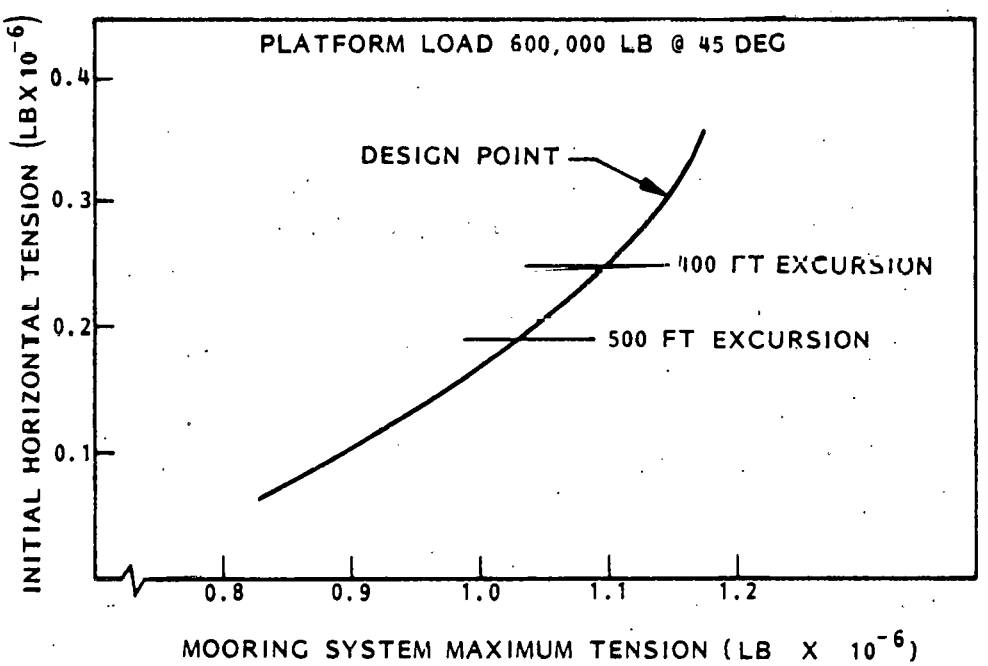

Fig. 2-15 Variation of Maximum Tension with Initial Horizontal Tension

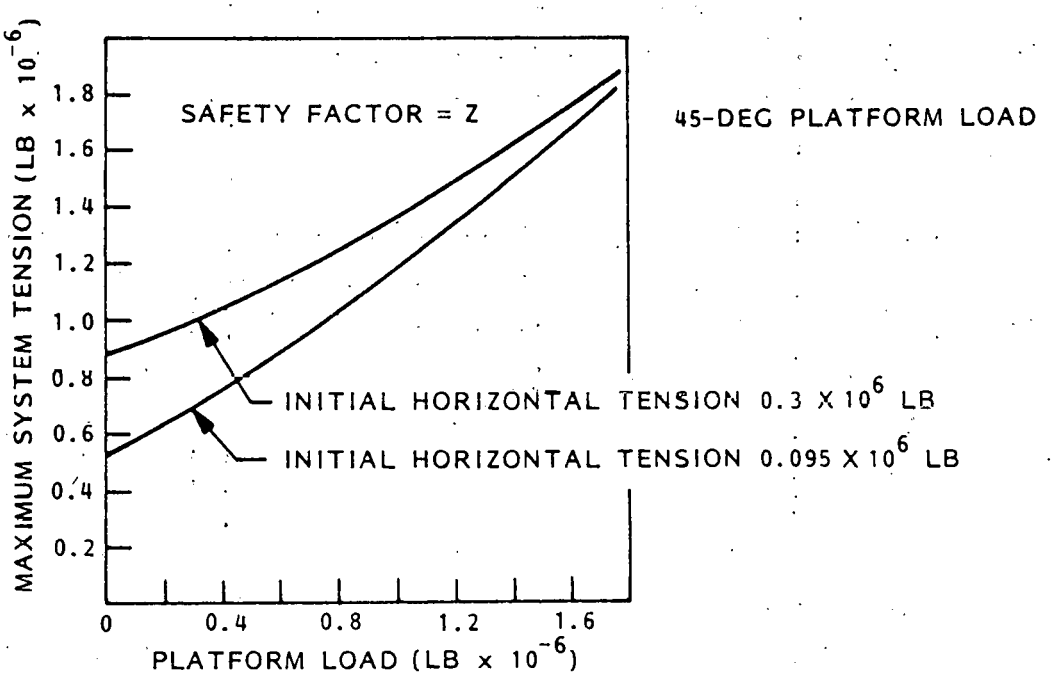

Fig. 2-16 Variation of Maximum Tension with Platform Load

legs. This particular interaction is difficult to solve without knowledge of the magnitudes of the cross coupling effects. The mechanism of load sharing in the mooring is illustrated by examining the horizontal tension vector components acting at the platform. The horizontal tension distribution in a deflected mooring system illustrates the restoring force. Figure 2-17 shows the load distribution in the mooring when the imposed load is 1.5 x 10^{6} lb acting at 45 deg.

The effect of increasing line length 500 to 700 ft for all mooring legs is shown in Fig. 2-17(b). A decrease in horizontal tension for lines 4 to 7 is the most notable feature. The next step in Fig. 2-17(c) is to decrease the length of lines 3 and 4 by approximately 900 ft. This brought about an unacceptable increase in tension for line 3, but promoted load sharing between lines 1 and 8 for the x-component of the platform load. The final change in Fig. 2-17(d) is tensioning line 2 by taking in 200-ft of line and relaxing

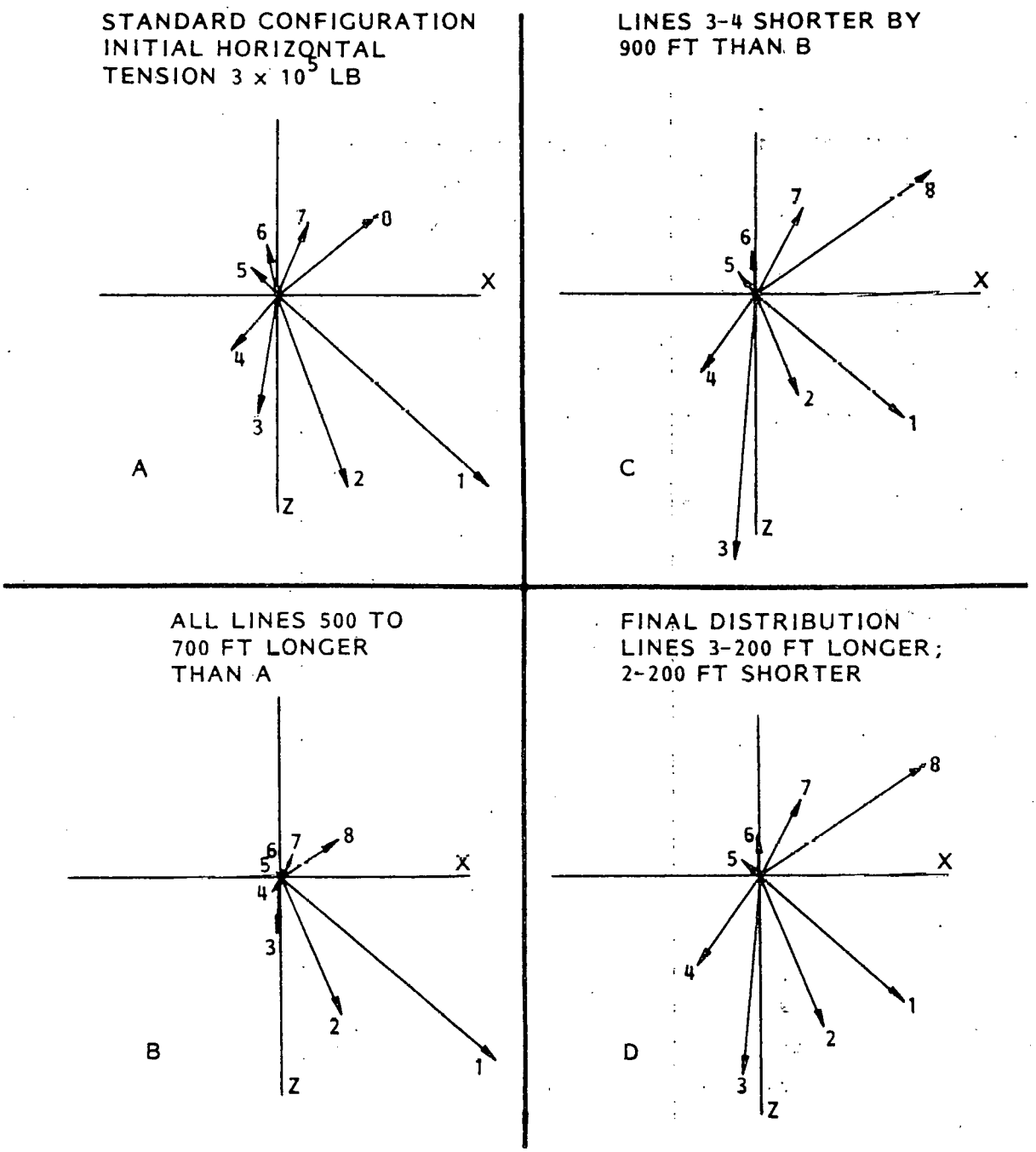

Fig. 2-17 Anchor Leg Horizontal Tension Vectors

line 3 by the same amount. Maximum total tension in this final configuration is 1.33×10^6, within the prescribed safety factor of 2 for the 3.0×10^6 lb breaking strength line under survival conditions.

Tension changes due to line length increases or decreases of 2 to 3 percent of total mooring leg length can be estimated from the data in Figs. 2-13 and 2-14. Changes indicated in Fig. 2-17 (c) and 2-17 (d) involve an increase of 200 ft in the length of leg 3 and a similar decrease in the length of leg 2. Corresponding horizontal and vertical tension changes are 200,000 to 300,000 lb. Utilizing the starting horizontal tension as the first point on Fig. 2-13 indicates the magnitude of the tension change for a 200-ft change in line length. The change in horizontal tension associated with the 200-ft length change is plotted in Fig. 2-18 and compared with the tension change estimated from Fig. 2-13. Figure 2-19 repeats the same relationship for vertical tension. The estimates of change in tension are reasonably accurate for small changes in line length.

An application of this technique shows that an increase in length of 100-ft for line 1 in a 3-year storm at 45 deg decreases the tension in that line to 1.0×10^6 lb. This is an estimated decrease of 0.14×10^6 lb, without increasing the platform displacement more than 50 ft.

These studies indicate that manipulation of the mooring line lengths can control the maximum tensions in the system while maintaining the platform displacement within prescribed boundaries.

Influence of Load Direction on the Mooring. Mooring displacement is very dependent on the platform load direction. The mooring lines are arranged to provide greater stiffness for beam loads, because platform force is greater at this orientation for a given storm level. The displacement of the platform as a function of load direction is shown in Fig. 2-20. Peak displacement occurs at angles of 20 to 30 deg. Maximum system tension variation with load direction is also shown. Tension is maximum where the load is directed down

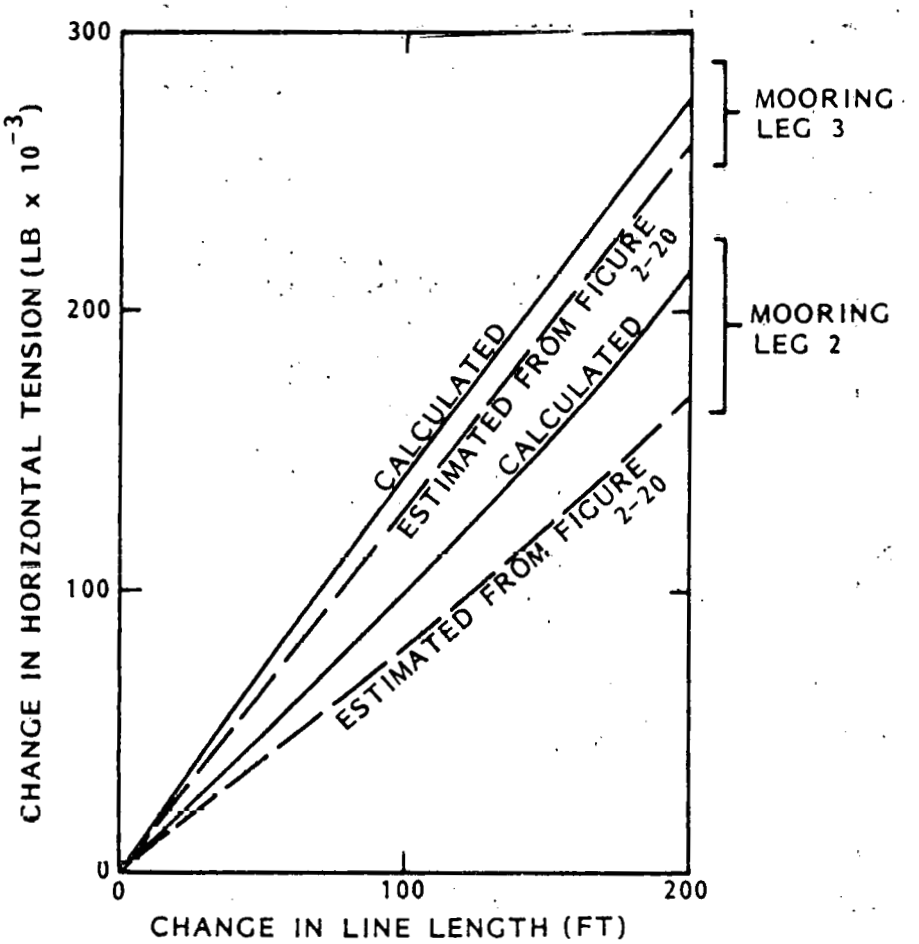

Fig. 2-18 Change in Horizontal Tension with Line Length

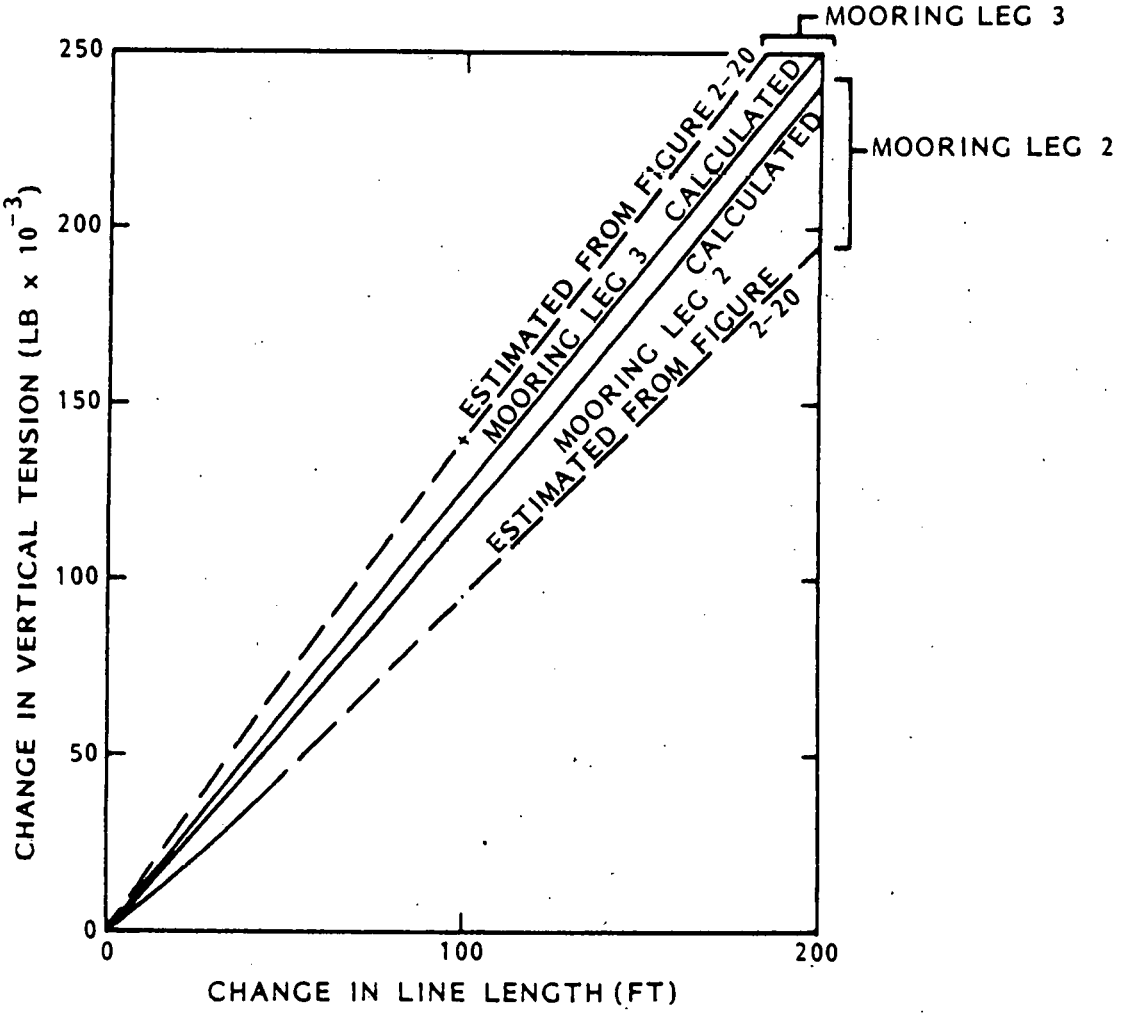

Fig. 2-19 Change in Vertical Tension with Line Length

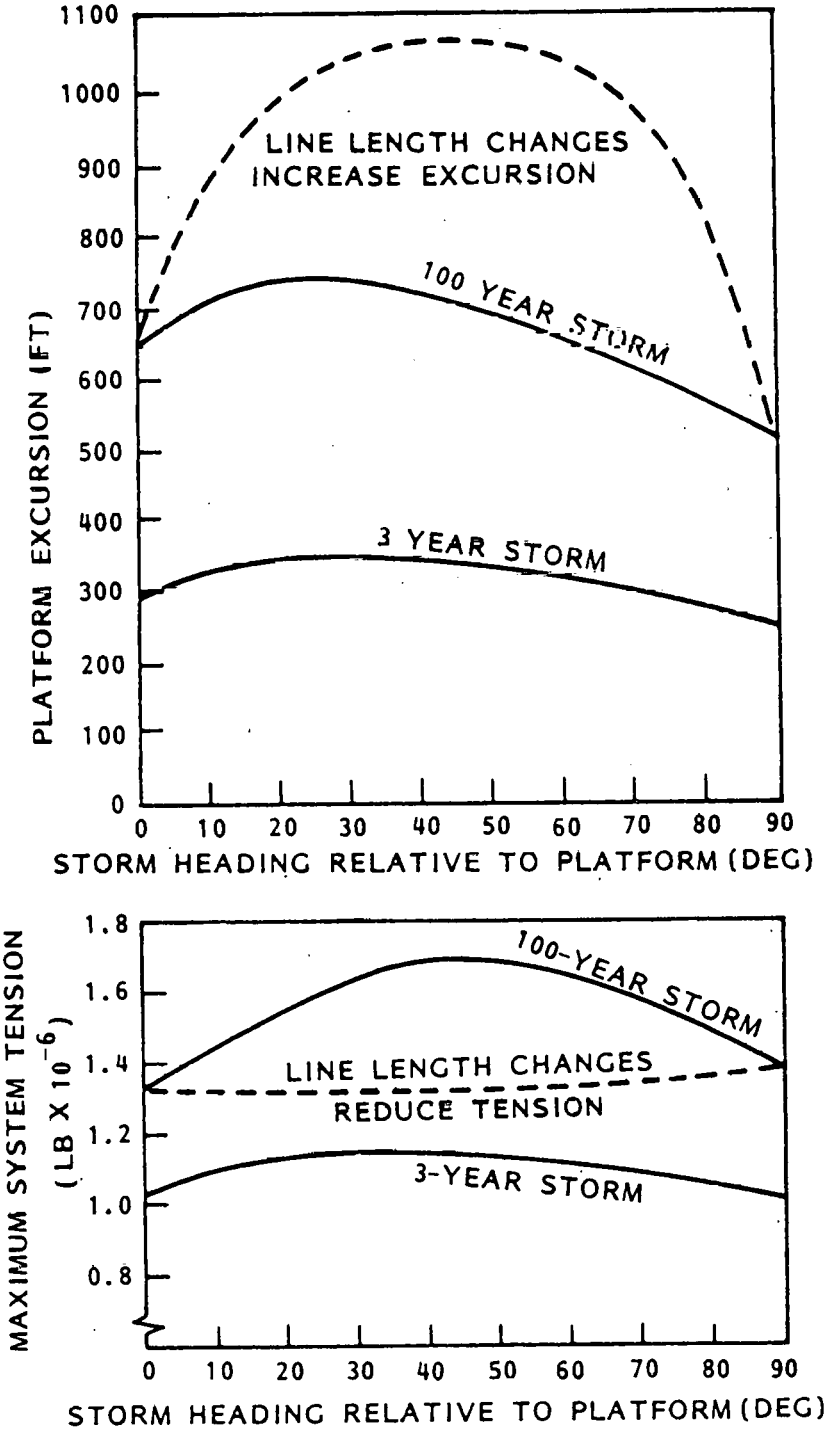

Fig. 2-20 MAL Performance

leg number 1 at a 45-deg angle relative to the platform. Solid lines in both portions of the figure indicate results for the original mooring leg lengths. The dashed lines show what is expected for the system with controlled length lines. These line length changes described in the previous section also increase the platform displacement greatly. The displacement increases from 700 to 1,157 ft in a 100-year storm with an incidence angle of 45 deg.

Active line tensioning capability is an excellent method of controlling maximum tensions in under survival conditions in a 100-year storm.

Loading in Replacement Operation. The tension in the anchor chain is examined for the operation of lifting the wire rope-chain connection to the surface for wire rope replacement. Chain length is adequate to maintain horizontal pull on the anchor, while the minimum safety factor is two.

The shallow leg on the land side and the deep leg seaward are examined for maximum tension in a current of 1.8 knots. It is assumed that changeout will be conducted in calm seas with low winching speed to minimize dynamic loading. The deeper leg, more critical due to greater chain length, has an adequate safety factor to allow for a dynamic load equal to 30 percent of static and for strength reduction due to wear and corrosion.

	Landward Leg	Seaward Leg
Chain Breaking Strength (Grade 4) (10^6 lb)	2.93	2.93
Linear Density (wet, lb/ft)	197	197
Water Depth (ft)	2,736	5,695
Chain Length (ft)	2,800	5,800
B.S./Tension	5.3	2.6
Horiz. Force at Surface (lb)	16,000	27,000

2.2.3 Dynamic Loads Analysis

A study conducted to determine the capability of the mooring lines to withstand the dynamic loads associated with extreme conditions and long term cyclic fatigue loading is presented in this section. An assessment of MAL system dynamics is first presented.

Dynamic Characteristics of MAL. The natural frequencies of the MAL in surge and sway as well as the sources and extent of damping are examined to assess the potential for resonant response in a seaway.

The MAL is assumed to behave as a linear spring mass system in response to external excitation, in this case a slowly varying wave drift force. The natural frequency is

$$f \cong \frac{1}{2\pi}\sqrt{\frac{k}{m}} \quad \text{Hertz}$$

where

k = aggregate surge or sway spring constant (slug/sec^2)

m = sum of barge displaced mass (4.72×10^6 slugs) and added mass

The added mass coefficient for low frequency oscillation is 0.7 in sway or surge, while the spring constant of the MAL is 2,800 lb/ft in sway and 1,400 lb/ft in surge under Extreme Sea State loading.

Motion	Natural Frequency		Natural Period (sec)
	(Hz)	(rad/sec)	
Surge	0.002	0.014	458
Sway	0.003	0.0188	334

Wave groups in the seaway with period in the range of 250 to 500 sec can be expected to result in dynamic amplification of anchor leg tension. The

existence of such wave groups in a hurricane-induced seaway is a subject for further investigation.

In the event that resonance occurs, the system is shown to be sufficiently damped to preclude oscillatory motion. Sources of damping are barge motions as well as barge and anchor leg viscous drag. Assuming a barge damping coefficient of 0.1, the wave damping is 2.4×10^5 lb-sec/ft. The barge drag is a source of nonlinear damping and is found to be 54,000 lb for 50-ft-surge amplitude and a drag coefficient of 1.0. The equivalent linear damping is 9.4×10^4 V lb-sec/ft where V is surge velocity. Damping due to drag on the anchor legs is 2.42×10^4 V lb-sec/ft for a drag coefficient of 1.2. The total damping, assuming 50-ft surge amplitude, is then 3.23×10^5 lb-sec/ft. In comparison, the critical damping is

$$\lambda_c = 2\sqrt{mk}$$

$$= 2.1 \times 10^5 \text{ lb-sec/ft}$$

so that the ratio of total to critical damping is 1.54, indicating that MAL damping is large and motion will decay in less than one cycle of surge.

Dynamic Tension. The dynamic tensions are presented for short term sea state conditions in Fig. 2-21. Significant tension amplitudes are shown versus depth for line 1 with the barge in a beam sea condition. The significant tensions are expressed in terms of actual loading (kips) and also percent of breaking strength.

The tension-fatigue study shows that there is more than adequate fatigue life for the wire rope because the cyclic tension amplitudes that occur are well below the endurance limit associated with the cycles to failure. The analysis assumes that wire corrosion does not occur.

In determining the significant tension and fatigue life, data for the environment, static configuration, barge response characteristics and mooring

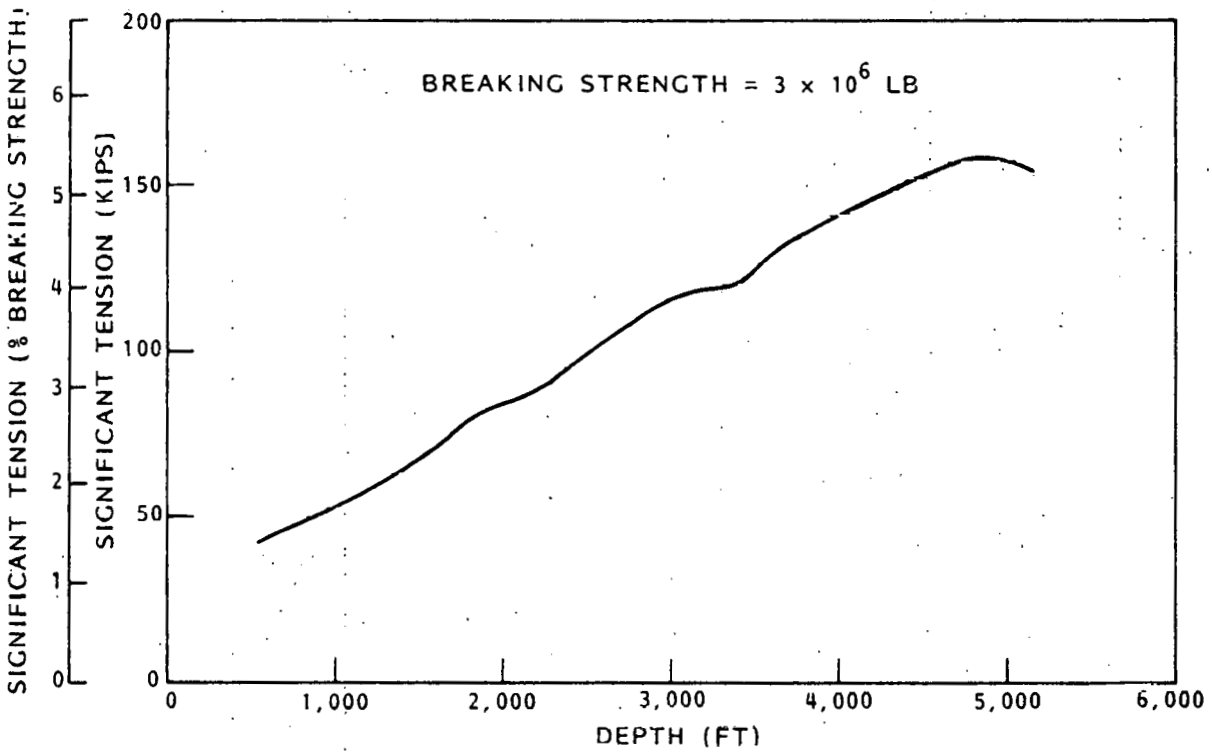

Fig. 2-21 Significant Tension Versus Depth for Anchor Leg No. 1, Beam Seas in Extreme Sea State

line fatigue properties are utilized by computer programs to compute anchor leg tension response and to determine both the fatigue life in all sea states and significant tensions for the Extreme Sea State. The method of analysis, together with intermediate results, are presented in Appendix F.

Short-Term Dynamics. Dynamic tensions in the No. 1 anchor leg induced by barge motion are obtained for the maximum operating and survival conditions in both beam and head seas. Twenty points along the cable are monitored; the largest significant dynamic tensions are presented in Table 2-6.

Table 2-6 ANCHOR LEG DYNAMIC TENSIONS

Sea Condition	Heading	Max. Dynamic Sign. Tension (lb)	Max. Total Tension (lb)
Operational Sea State	Beam	47,966	1,048,000
Operational Sea State	Head	74,454	1,100,000
Extreme Sea State	Beam	158,967	1,255,130
Extreme Sea State	Head	151,352	1,463,500

From these data, we see that, for the two cases investigated, the largest dynamic tension occurs during the survival condition in a beam sea. It is assumed that the anchor line dynamic tension does not exceed 1.86 x 158,967 = 295,678 lb for 1,000 waves (Ref. 2-5). The maximum dynamic tension is then added to the static tension value given in Section 2.2.2 to provide the total maximum tension. Maximum total tension occurs near the top of the anchor leg, while maximum dynamic tension occurs near the bottom.

Intermediate results for the survival condition with a beam sea heading are shown in Table 2-7. There are 20 frequencies ranging from 0.208 to 1.234 rad/sec used to define the Bretschneider spectrum with a significant height of 35.9 ft. The wave-amplitude squared values corresponding to the frequencies show a peak at a period of 14.82 sec. The tension squared distribution also peaks at this frequency and the distribution for the third cable point up from the bottom shows a narrow banded highly peaked shape indicative of a Rayleigh distribution. As discussed previously, the tension

squared distributions are integrated with respect to frequency to obtain the areas under the curves for each of 20 points on the anchor leg. The significant tensions are then obtained with the following formulae: (Ref. 2-5)

For i-th point

$$A_i = \int_0^\infty T_i^2 (w)\, dw$$

and

$$T_{i\ sig} = 2.83 \sqrt{A_i}$$

where A_i is the area under the curve and $T_{i\ sig}$ is the significant dynamic tension.

Long-Term Dynamics - Fatigue. The fatigue life of the anchor legs are shown to be essentially unlimited if not subjected to corrosion, salt water, bending, or physical damage. The fatigue analysis shows the life of anchor leg No. 1 is 130,945 years. This is the worst value of all the cases run and occurs when the barge is continuously oriented in a beam sea direction.

Vortex shedding, not included in the analysis, is not expected to significantly reduce fatigue life, assuming that the oscillatory tension levels are an order of magnitude lower than those experienced by the barge motion induced excitation. Since the tension levels induced by the barge motion are under the endurance limit for the great majority of the wave induced tensile vibrations, then vortex shedding would also be under this limit. The endurance limit is defined as the oscillatory tension level below which the number of cycles to failure approaches infinity.

To illustrate how fatigue life is generated, intermediate results for the beam sea case are presented in a discussion of fatigue analysis methodology in Appendix F. The assumptions and conclusions of this analysis are also included in this apprendix.

Table 2-7 TENSION SPECTRAL DENSITY AND SIGNIFICANT TENSIONS FOR ANCHOR LEG NO. 1 IN EXTREME SEA STATE (POINT 1 IS AT THE LEG BOTTOM)

HEAD OR BEAM_@@@@
BEAM SEA
X,Y,Z LOCATION OF SHEAVE REL TO CENTER 190.750 60.5000 -59.0000 SIGNIFICANT HEIGHT = 35.9 FT

WAVE AMPLITUDE SQUARED SPECTRAL DENSITY FUNCTION

FREQUENCIES (RAD/SEC)

.208000	.262000	.316000	.370000	.424000	.478000	.532000	.586000	.640000	.694000
.748000	.802000	.856000	.910000	.964000	1.01800	1.07200	1.12600	1.18000	1.23400

WAVE AMPLITUDE SQUARED (FT**2)

.308647-04	4.11550	145.585	436.999	544.867	480.719	368.151	266.714	189.958	135.388
97.3585	70.8908	52.3338	39.1749	29.7219	22.8394	17.7619	13.9679	11.0987	8.90392

TENSION SPECTRAL DENSITY FOR 20 CABLE POINTS

CABLE POINT	1								
95.2239	.876249+07	.173125+09	.685669+08	.480036+11	.365033+10	.172719+10	.793297+09	.352588+09	.162468+09
.738411+08	.330381+08	.144073+08	.582632+07	.192958+07	584218.	213082.	72451.1	18954.6	2818.81
CABLE POINT	2								
97.3466	.899204+07	.178150+09	.702816+08	.501277+11	.381029+10	.180360+10	.823899+09	.365130+09	.167843+09
.758023+08	.336176+08	.144138+08	.565651+07	.178341+07	534700.	204639.	71531.9	18930.4	2829.86
CABLE POINT	3								
98.3596	.910425+07	.180467+09	.708534+08	.510030+11	.386052+10	.181961+10	.825927+09	.364055+09	.166527+09
.750086+08	.332394+08	.143903+08	.582597+07	.196938+07	608855.	218032.	72530.1	18677.7	2742.15
CABLE POINT	4								
98.3208	.909613+07	.179813+09	.701668+08	.502622+11	.376722+10	.175605+10	.791434+09	.346058+09	.157222+09
.709790+08	.321445+08	.147358+08	.672417+07	.274396+07	893758.	271659.	78978.6	18845.5	2639.53
CABLE POINT	5								
97.4030	.898245+07	.176478+09	.683797+08	.479645+11	.354005+10	.162159+10	.727411+09	.315859+09	.143239+09
.660432+08	.317872+08	.163398+08	.884820+07	.431564+07	.143972+07	376032.	93798.0	20255.4	2664.59
CABLE POINT	6								
95.8296	.878790+07	.171088+09	.658181+08	.444741+11	.321859+10	.144342+10	.649795+09	.282434+09	.129969+09
.632573+08	.337397+08	.198843+08	.123763+08	.663652+07	.219899+07	519682.	115679.	22977.6	2866.08
CABLE POINT	7								
93.8203	.853944+07	.164374+09	.628625+08	.402746+11	.285187+10	.125265+10	.574748+09	.253869+09	.121554+09
.644077+08	.384639+08	.251666+08	.168442+08	.930546+07	.301876+07	670755.	139408.	26303.5	3180.25
CABLE POINT	8								
91.5630	.826166+07	.157025+09	.598721+08	.358204+11	.248246+10	.107355+10	.512889+09	.234403+09	.119320+09
.693278+08	.451645+08	.312460+08	.214212+08	.118108+08	.373884+07	799046.	159896.	29379.9	3498.92
CABLE POINT	9								
89.2115	.797505+07	.149613+09	.571524+08	.314599+11	.213933+10	.919676+09	.468117+09	.224446+09	.122318+09
.766592+08	.525781+08	.371524+08	.254726+08	.138585+08	.428999+07	893560.	174953.	31664.9	3730.44
CABLE POINT	10								
86.8818	.769601+07	.142590+09	.549522+08	.274208+11	.183792+10	.795298+09	.439556+09	.222301+09	.128818+09
.850490+08	.598515+08	.424734+08	.288994+08	.155033+08	.471463+07	963915.	185639.	33124.8	3847.86
CABLE POINT	11								
86.5772	.755598+07	.136898+09	.512527+08	.234888+11	.150244+10	.654915+09	.409007+09	.220239+09	.139873+09
.996941+08	.726287+08	.515130+08	.342324+08	.176957+08	.518463+07	.104066+07	201988.	36763.0	4331.96
CABLE POINT	12								
86.3861	.740234+07	.130582+09	.472713+08	.198702+11	.120334+10	.539795+09	.379455+09	.217004+09	.150143+09
.113093+09	.837026+08	.586739+08	.377845+08	.186066+08	.514013+07	984592.	188714.	34813.2	4173.04
CABLE POINT	13								
85.5163	.719676+07	.124078+09	.453593+08	.165883+11	.968676+09	.440932+09	.327838+09	.193933+09	.140344+09
.108262+09	.804151+08	.557697+08	.349959+08	.163720+08	.412802+07	701781.	124147.	22871.8	2858.57
CABLE POINT	14								
84.4487	.697814+07	.117534+09	.436130+08	.135520+11	.759527+09	.356725+09	.284727+09	.176791+09	.134548+09

.106025+09	.787323+08	.537948+08	.326991+08	.143835+08	.324428+07	477604.	80702.4	16550.4	2368.93
CABLE POINT	15								
83.1852	.674693+07	.110954+09	.420183+08	.107845+11	.577481+09	.288914+09	.252113+09	.167184+09	.134054+09
.107362+09	.793314+08	.531813+08	.311491+08	.127655+08	.252985+07	322954.	61118.9	16420.0	2772.85
CABLE POINT	16								
81.7336	.650399+07	.104349+09	.405306+08	.831601+10	.424916+09	.239693+09	.232168+09	.166679+09	.139987+09
.113030+09	.826062+08	.542071+08	.305006+08	.115908+08	.200688+07	242482.	66172.1	22559.2	4069.76
CABLE POINT	17								
80.1034	.625002+07	.977114+08	.391005+08	.617517+10	.303983+09	.210830+09	.226472+09	.176330+09	.153010+09
.123408+09	.889891+08	.569611+08	.307937+08	.108756+08	.167786+07	235173.	95107.2	34713.3	6218.07
CABLE POINT	18								
78.3026	.598506+07	.910117+08	.375835+08	.438150+10	.216014+09	.203228+09	.235599+09	.196486+09	.173278+09
.138521+09	.982054+08	.613961+08	.319921+08	.105999+08	.153397+07	297402.	146673.	52565.5	9174.70
CABLE POINT	19								
76.3347	.570821+07	.841871+08	.350177+08	.294071+10	.161432+09	.217031+09	.259111+09	.226837+09	.200554+09
.158178+09	.110193+09	.674167+08	.340392+08	.107362+08	.156507+07	426005.	220008.	75938.2	12920.2
CABLE POINT	20								
74.1972	.541748+07	.771455+08	.335907+08	.184282+10	.140192+09	.252285+09	.295946+09	.266637+09	.234413+09
.182138+09	.124821+09	.749567+08	.369026+08	.112694+08	.176637+07	620183.	315124.	104886.	17468.2

SIGNIFICANT TENSIONS	154326.	157678.	158967.	157651.	153801.	147906.	140621.	132594.	124360.
116324.	107846.	99438.4	90975.6	82458.6	73967.3	65648.7	57714.3	50442.8	44185.1
39355.6									

MAX EXPECTED TOTAL TENSIONS (LBS									
854785.	882896.	915853.	951440.	988579.	.102707+07	.106718+07	.110934+07	.115390+07	586525.
.124937+07	.124899+07	.124859+07	.124816+07	.124786+07	.124796+07	.124883+07	.125101+07	.125513+07	625572.

2.3 PERFORMANCE

MAL performance is summarized and evaluated in this section with respect to design criteria and SKSS requirements. Operation of the active tensioning and heading control features of the MAL are described.

2.3.1 Operational Sea State

The MAL is required to constrain the barge within a watch circle of 400-ft radius in sea states up to and including the Operational Sea State of 3-year return period. The MAL satifies this requirement as indicated by the results in Table 2-8. This design is actually stiffer than required, as the maximum excursion of 340 ft is 60 ft less than the allowable. Accounting for barge sway and surge, which are additive to these static excursions, the MAL stiffness may be reduced at least 15 percent.

Table 2-8 MAL RESPONSE IN OPERATIONAL SEA STATE

Seaway Heading (deg)	Seaway Force (10^6 lb)	Longitudinal Excursion (ft)	Lateral Excursion (ft)	Excursion (ft)	Leg No. 1 Tension (10^6 lb)	Safety Factor
0	0.38	-291	3	291	1.04	2.9
45	0.60	-314	-132	340	1.14	2.6
90	0.69	2	-249	249	1.07	2.8

An anchor leg tension safety factor of 3 is required in this nominal excursion range. A reduction in tension on the most highly loaded leg as well as an increase in excursion is realized by a length increase in this leg. Further iterations in pre-tension and leg length are required to balance stiffness and leg tension. The active tensioning feature is adequate to adjust leg length to raise the safety factor to 3 with a reduction in stiffness.

The locus of barge excursion, shown for the second quadrant in Fig. 2-22, is a maximum of 340 ft at 23 deg with the sea state at 45 deg. MAL stiffness is greater in the longitudinal than transverse directions. Asymmetry is also expected, although not shown in this figure, in the lateral direction arising from the 1,000-ft difference in anchor leg length between the landward and seaward legs. The MAL configuration in this sea state is shown in elevation in Fig. 2-1.

2.3.2 Extreme Sea State

MAL performance in the Extreme Sea State, as in the Operational Sea State, is dependent on sea state heading (see Fig. 2-23). The tension safety factor for beam and head loading exceeds the criteria by 20 percent, allowing for dynamic tension component due to leg oscillations and dynamic amplification of drift response. On the intermediate headings, however, the safety factor is less than the minimum of 2. The lengths are increased on the most highly loaded legs (see Fig. 2-1), realizable by the active tensioning capability, resulting in a safety factor of 2.2 (see Table 2-9). Although platform excursion is greatly increased from 704 to 1,157 ft, there is adequate depth below the CWP inlet to ensure clearance with the seafloor.

In the high excursion of the Extreme Sea State and with active tensioning the unloaded, "down-wind" legs are slack (see Fig. 2-1, leg 5). The vertical portion of this leg poses potential interference problems at the chafing chain on the hull side and with the wire rope segment on the lower portion of the CWP. Horizontal deflection of the CWP in this sea state is required to evaluate the potential for interference between the CWP and anchor leg.

2.3.3 Survivability

Survivability in the Extreme Sea State as measured by SKSS redundancy is examined in the highest loading condition of a 45-deg sea state heading. In

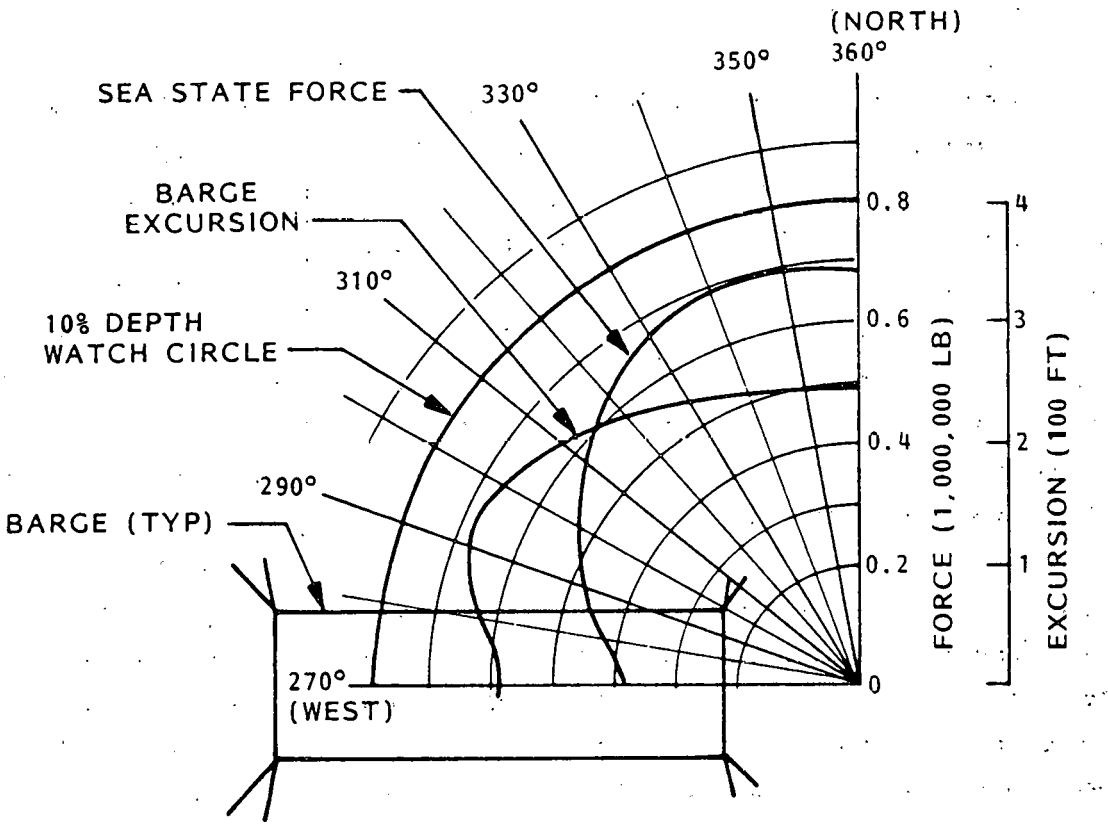

Fig. 2-22 Barge Excursion in Operational Sea State

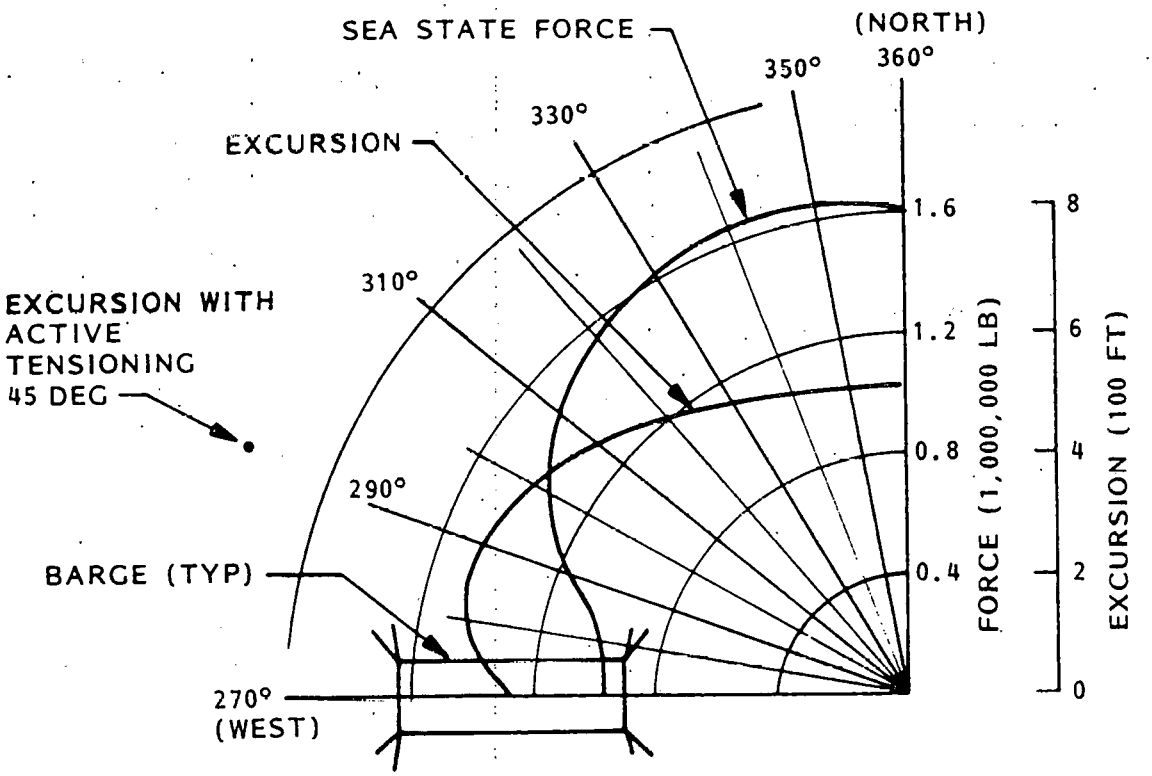

Fig. 2-23 Barge Excursion in Extreme Sea State

Table 2-9 MAL RESPONSE IN EXTREME SEA STATE

Seaway Heading (deg)	Seaway Force (10^6 lb)	Longitudinal Excursion (ft)	Lateral Excursion (ft)	Excursion (ft)	Max Tension (10^6 lb)	Minimum Safety Factor
0	0.97	-656	17	656	1.34	2.2
30	1.33	-714	-182	737	1.64	1.8
45	1.50	-635	-304	704	1.69	1.8
45	1.50	-1,075	-427	1,157	1.34	2.2(a)
90	1.61	6.7	-514	514	1.38	2.2

(a) Active Tensioning

this case the anchor leg lengths are altered by the active tensioning system to equalize the load distribution. The highly loaded leg No. 1 is then assumed lost and response of the resulting seven-leg MAL is determined. Active tensioning capability after the loss is assumed to be unavailable.

As summarized in Table 2-10, platform excursion increases by 50 percent and the minimum safety factor drops 14 percent. The design criteria for the survival condition, safety factor greater than unity, is satisfied by the MAL. Anchor holding power safety factor is 2 on leg No. 1, with tension in the bottom chain of 944,000 lb. Thus, sufficient redundancy is demonstrated, at least for this configuration of loading and leg loss. Loss of this leg in the plane of sea state force is assumed to be the most severe condition for a single leg loss. The number of leg failures that can be sustained by the MAL with retention of stationkeeping capacity is not determined.

2.3.4 Heading Control

Platform heading is controllable to a limited extent by the active tensioning feature of the MAL. By virtue of the windlass, fairleader, and chain on the upper segment of each anchor leg, the leg lengths are variable by approximately $\pm$ 300 ft (landward legs) and +400/-200 ft (seaward legs).

Table 2-10 MAL RESPONSE WITH LOSS OF ANCHOR LEG NO. 1

Condition	Longitudinal Excursion (ft)	Lateral Excursion (ft)	Excursion (ft)	Max. Tension (10^6 lb)	Min Safety Factor
MAL	-1,075	-427	1,157	1.34	2.2
Loss of Leg No. 1	-1,454	-550	1,555	1.62	1.9

The active tensioning operation of paying out and reeling in anchor legs is effective in reducing leg tension. However, as shown below, this operation is ineffective in adjusting barge heading. The applied yaw moment in the Extreme Sea State at 45 deg is 76.4 x 10^6 ft-lb, with a resultant yaw offset of 10 deg (see Fig. 2-8). Thus the barge rotates away from the seaway, with a 55-deg relative heading between barge and seaway. In this case active tensioning results in turning the barge more "beam-to" than "bow-to" the seaway.

Given the high anchor leg tensions, the active tensioning system cannot be effectively utilized to adjust tension and heading simultaneously in the Extreme Sea State. Heading control is achieved by the transfer of anchor leg load to a pendant connected to the anchor leg and to a distant point on the barge.

The heading control system facilitates a zero to ninety deg change of heading of the platform. The change is effected by sharing or completely transferring the anchor leg tension from the anchor leg to a pendant. One end of the pendant is permanently attached to the end link at the wire tope to chafing chain connection. The other end is connected to a padeye on the platform keel below the adjacent anchor leg. Load transfer is accomplished by paying out the chafing chain on each leg until the pendant is taut and the chafing chain is slack. This arrangement permits turning the bow seaward from the initial

Easterly heading in increments to a South Easterly heading as required. This is compatible with hurricane tracks passing to the South of the moored OTEC plant. A counterclockwise rotation is effected by hauling-in on the anchor legs, disconnecting the pendant lines, and reattaching lines on the opposite side of each anchor leg. This change necessitates altering some of the lengths of pendants. The pendant arrangement is shown in Fig. 2-2. Pendants may be supported in midlength on the keel to minimize the catenary swing and potential interference.

2.3.5 Anchoring

The load on the first anchor is assumed to be equal to the tension in the chain at the chain touchdown point on the seafloor. These tensions are summarized for the worst case condition in Table 2-11 for the Extreme Sea State, 45 deg heading, with and without active tensioning (see Fig. 2-1).

Active tensioning reduces the maximum tension from 944,000 lb on leg No. 1 to 680,000 lb on leg No. 3, with 1,341 ft of chain on the seafloor between the touchdown point and the first anchor. The holding power which this length of chain provides is ignored, as is the force component of chain weight along the seafloor, so that the anchor load anchor is conservatively assumed to be 680,000 lb. Chain length is sufficient to prevent chain lift up at the anchor. Anchor holding power safety factor is

$$\frac{60{,}000 \text{ lb} \times 20\ (1 + 0.7)}{680{,}000 \text{ lb}} = 3$$

where the efficiency of the second anchor is assumed to be 70 percent of the first anchor's efficiency. If the seafloor is composed of clay instead of sand, then the safety factor is 1.5. The anchors therefore provide sufficient holding power to prevent slippage in the Extreme Sea State.

Table 2-11 BOTTOM CHAIN LOADS IN EXTREME SEA STATE (45-DEG HEADING)

Anchor Leg	Tension At Touchdown (10^6 lb)		Length of Chain on Seafloor (ft)	
	No Act. Tens.	Act. Tens.	No Act. Tens.	Act. Tens.
1	0.97	0.65	810	2,333
2	0.69	0.57	1,627	2,372
3	0.40	0.68	2,500	1,341
4	0.23	0.37	2,990	1,994
5	0.12	0.07	2,285	2,569
6	0.17	0.14	1,940	2,122
7	0.27	0.31	1,487	1,348
8	0.44	0.67	959	179

2.3.6 Active Tensioning

The MAL is equipped with the capability to alter the anchor leg lengths and thereby the leg tension. This capability is useful in the following areas:

- Equalize anchor leg tension to reduce maximum tension and fatigue loading
- Equalize anchor loading
- Alter heading of barge in the seaway
- Compensate for anchor slippage
- Reposition chain on sheave
- Inspection of upper segment of anchor leg

The first two areas are illustrated in the preceding sections, for the Extreme Sea State, wherein the required safety factors are obtained by length changes in selected legs. The control of heading is then shown to be feasible by pendants which are loaded by paying out all anchor legs, effectively transferring the anchor leg loads to a distant point on the barge, thereby turning the barge within the MAL array.

Operation of the MAL active tensioning SKSS is controlled from the bridge by a central control unit. Active tensioning is initiated when monitoring of the anchor leg tension shows that mean tensions are rising and approaching or exceeding the safety factor for the existing sea state. A prescribed sequence of pay out and reel in steps are followed until the tensions are adjusted. The operation is initiated by starting the windlass, taking the load on the windlass, releasing the chain stopper and powering the windlass for pay out or reel in. A length change of 100 ft is made in 10 minutes, while the sequence of changes is expected to be 1 hour or more in duration. Control stations at each corner of the barge provide for local operation of the windlass pair at the corner. If heading adjustment is required, then all windlasses are activated to pay out the necessary length of chain to achieve the desired rotation. Barge heading is adjusted as required if for example the wave direction shifts during a storm. These operations are expected to be routine in sea states up to and including the Operational Sea State.

Active tensioning and heading control in the Extreme Sea State requires adequate forecasting of the approaching hurricane. As noted in Section 2.1, the long waves progressing from the hurricane eye reach the barge well before the storm itself. Barge heading is adjusted as required to place the barge "head-to" these oncoming waves. If the barge is not abandoned and if the eye passes the barge, the MAL active tensioning system may be engaged to readjust the barge heading as required. Note however that the seaway is then likely to be a multidirectional, confused sea, so that desireable barge heading is less clearcut. If the barge is abandoned, then the system is left in the most favorable condition of heading and leg tension distribution. In trading the benefits of heading and leg tension adjustment, the seaworthiness of the barge and particularly the necessity of maintaining a head seas orientation are compared with the stationkeeping ability of the MAL in the hurricane. Total loss of one leg is shown to be noncatastrophic in this sea state. Anchor slippage is compensated to some extent by reeling in chain.

2.4 MAL DESIGN DEVELOPMENT

2.4.1 Anchor Leg Selection

The selection of anchor leg configuration and scantlings is based on the results of trade studies conducted in the performance of the preliminary design Task III. Consideration is given to acquisition cost, state-of-practice in component manufacturing and deployment operations, and SKSS performance requirements.

Number of Anchor Legs. In the first trade study, four wire and chain sizes are examined to establish the variation of size with number of anchor legs. Assumed conditions include a zero-sloped seafloor, equal included angle between legs, constant length of wire rope (3,600 ft) and chain (4,500 ft), coplanar beam sea forces in plane of first anchor leg, and a 4,000-ft depth. Performance requirements include 400 ft maximum excursion in 3 year storm, safety factor greater than 2, and zero angle of pull at anchor. Results, summarized in Table 2-12, indicate that more than 14 legs are required for 3.5-in. wire rope, more than 10 legs are required for 4.5-in. wire, 8 legs are required for 5-in. wire, and 6 legs for 7-in. wire. The number of legs for the first two cases, based on extrapolation of computed tensions, is 17 and 11, respectively, and these greater number of legs are used in the cost study.

A cost analysis of these designs indicates the relative cost of MAL components as well as a trend of cost with number of anchor legs. The most costly component is the windlass, followed by chain, wire rope, anchor and chain locker. Other components such as fairleaders, connecting links, and chain stoppers are not included and are not expected to affect the conclusions. The results are illustrated in Fig. 2-24, the calculations are included in Appendix B. Costs shown are the cost of each component summed for the number of legs indicated. Wire rope and chain costs are a decreasing function of number of anchor legs, and conversely, an increasing function of wire and chain diameter. Windlass costs, assumed to be proportional to the anchor leg breaking strength, has a local maximum at 11 legs and decrease for MALs with

Table 2-12 FOUR MAL SKSS DESIGNS

Case	Wire Rope		Chain		No. of Legs	Wire B.S. Tension		Excursion (ft)	
	Diam (in.)	$B_6S.$ (10^6 lb)	Diam (in.)	$B_6S.$ (10^6 lb)		(3 yr)	(100 yr)	(3 yr)	(100 yr)
1	3.5	1.1	2.9	1.3	14 (17)	-	1.81	-	631
2	4.5	1.9	3.6	1.9	10 (11)	2.8	1.95	271	657
3	6.0	3.0	5.1	3.3	8	3.6	2.45	327	635
4	7.0	4.2	6.0	4.3	6	3.8	2.51	364	717

fewer legs. Installation cost is derived based on relative total anchor leg weight and length, utilizing the estimate for deployment obtained in Task II for a 10-leg MAL. This cost is generally a decreasing function of number of anchor legs. Although the sum of component cost has a local maximum at 10 legs and no apparent minimum in the range studied, the sum of component and deployment cost indicates lower cost as the number of legs is decreased and component size is increased. On the basis of this study a six-leg MAL is lower cost and therefore favored over an eight-leg MAL. However, the 7-in. wire rope is twice the diameter of the largest wire rope mooring system in use today and is therefore considered to be too great an extension of state-of-practice. Furthermore, a six-leg MAL is not readily arranged on the deck for optimum load distribution. Therefore, the eight-leg MAL with smaller wire rope size and greater arrangement flexibility is selected for further development.

Angular Separation of Anchor Legs. The arrangement of the eight-leg MAL is investigated to identify the most advantageous included angle between adjacent legs. The symmetric, 45-deg included angle arrangement serves as a baseline for this study.

As shown in Table 2-13, the azimuth of each pair of legs located at each corner of the barge is varied, as is the angle between legs in each pair. Symmetry is maintained at each corner of the barge. Environmental

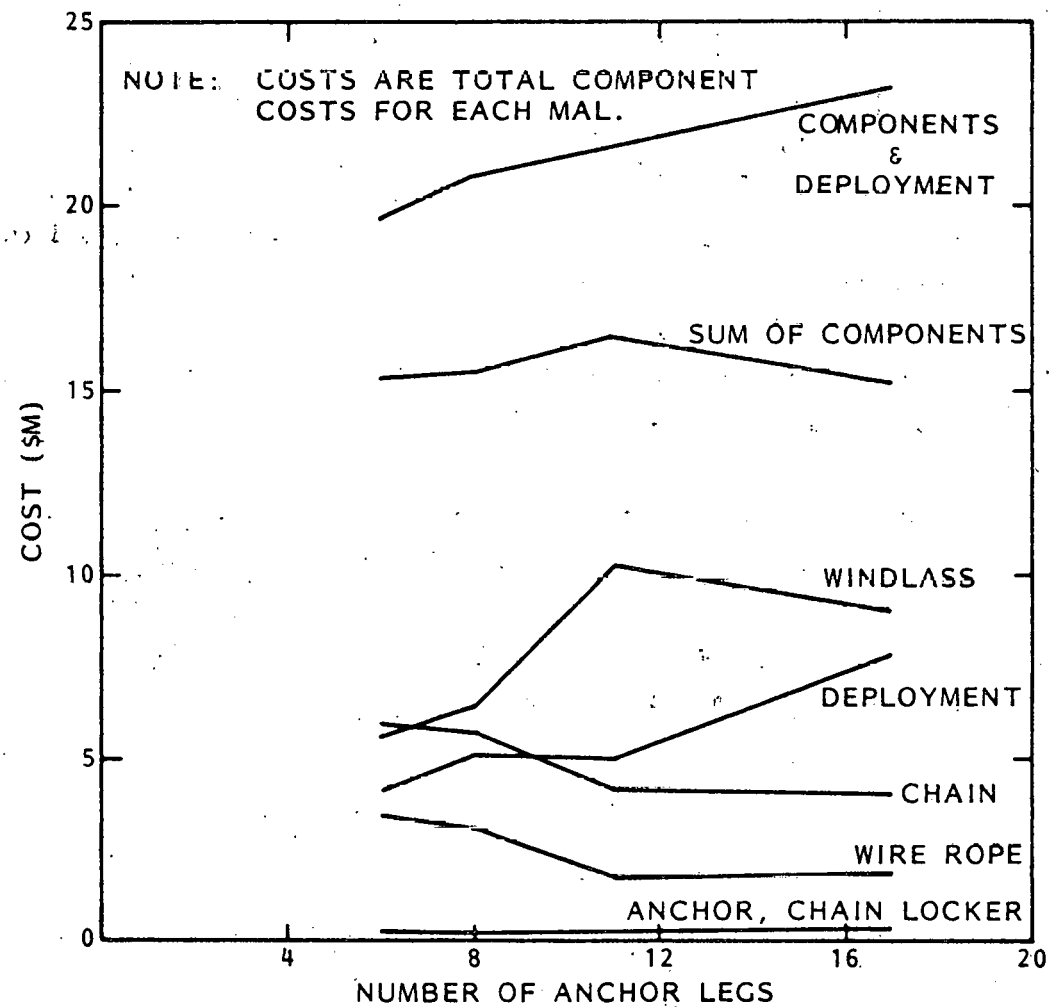

Fig. 2-24 Variation of MAL Component and Deployment Costs With Number of Anchor Legs

Table 2-13 VARIATION OF ANGULAR SEPARATION OF ANCHOR LEGS

1 (deg)	2 (deg)	Maximum Tension (10^6 lb)	
		Head	Beam
0	45	-	1.29
30	45	0.99	1.27
30	30	0.94	1.18
15	30	0.97	1.12

loading on the barge is both head and beam, coplanar wind, wave, and current in the Extreme Sea State of 100 year return period (1.6×10^6 lb). The 15/30 combination reduces the maximum tension in the highest loaded anchor leg by 13 percent in comparison with the symmetrically arranged legs. This configuration is therefore selected for further analysis on a sloped seafloor.

Since the sea heading is predominantly Easterly, it is possible to consider adding forward anchor legs and removing aft legs, resulting in an asymmetric configuration. However, in a Westerly storm (an event with low probability of occurrence) the aft legs will not provide adequate holding power. Therefore, the configuration with fore and aft symmetry is selected.

2.4.2 Deck Machinery

Deck machinery is required to provide the active tensioning feature of the MAL SKSS. Several configurations are presented in this section which illustrate the iterations examined in the design development.

The primary function of the deck machinery is to shorten or lengthen each anchor leg for the purpose of effecting heading change, load distribution, etc. The first two configurations accomodate chafing chain in the upper portion of each anchor leg (see Figs. 2-25 and 2-26). A combination of dedicated windlass and winch, located in mid-deck or at deck edge, is capable

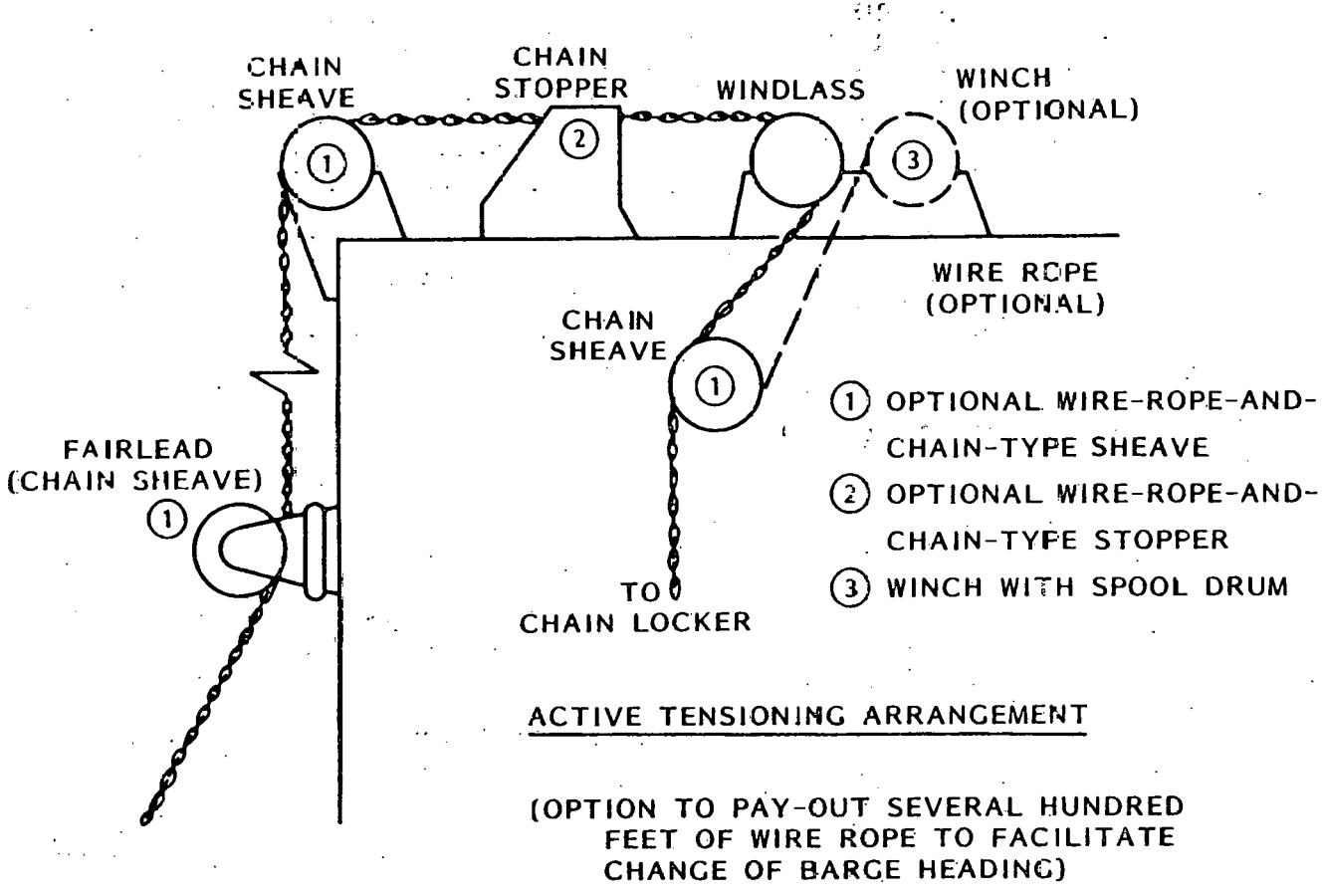

Fig. 2-25 Deck Machinery Configuration No. 1

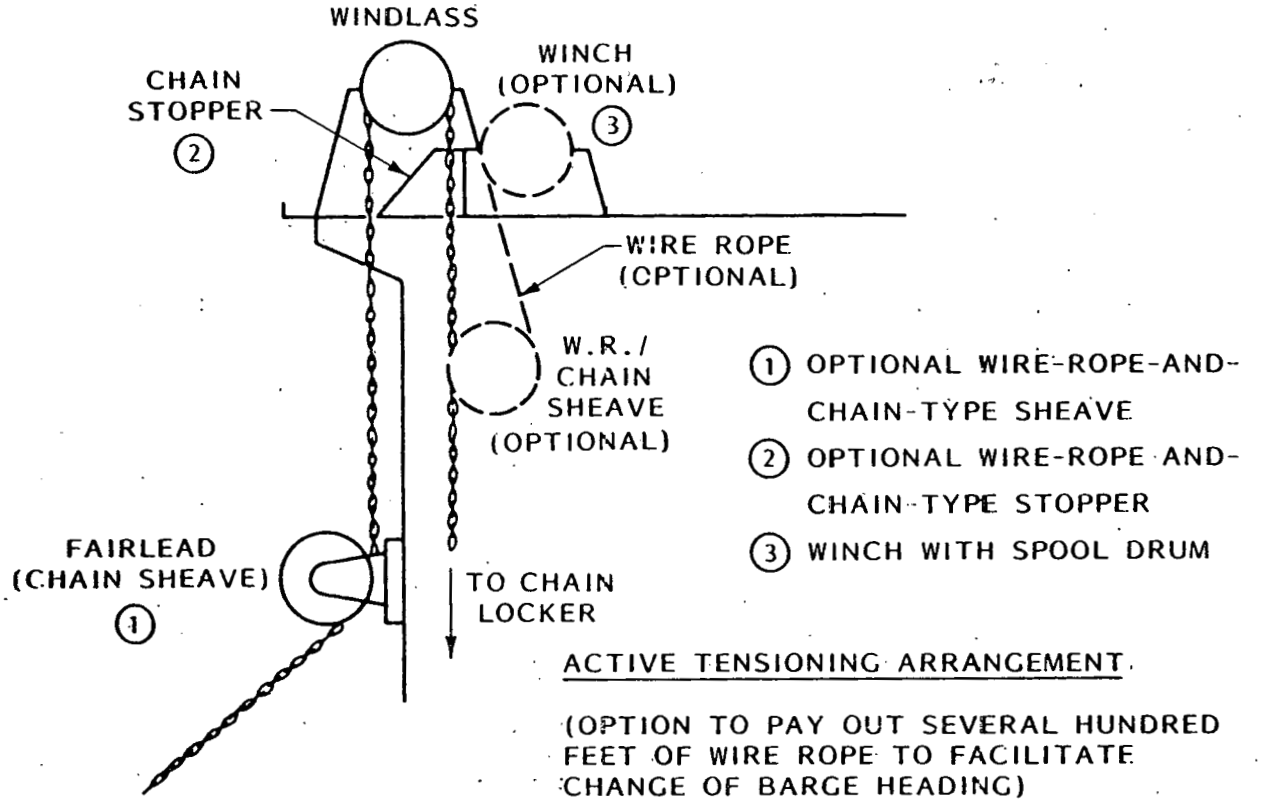

Fig. 2-26 Deck Machinery Configuration No. 2

of hauling in or paying out the chain. The winch located behind the windlass provides for wire rope handling in the event that required anchor leg length change is greater than chain length. In this event the chain-wire connection is opened after lowering all chain into the chain locker, the wire-wire connection completed, and wire hauled in on the winch. This configuration provides chain-wire capability at relatively high cost and undesirable disconnect.

The third configuration, consisting of a winch and a set of three fairleaders, provides for paying out wire rope to lengthen the anchor leg or optionally for load transfer to a secondary pendant chain leading to a fixed point on an adjacent corner of the platform (see Fig. 2-27). In shortening the anchor leg, the chafing chain is hung below decks and disconnected from the wire at both ends, followed by wire-wire connection and haul in on the winch. This design reduces cost by elimination of the windlass but requires a disconnect for haul in.

The selected configuration, shown in Fig. 2-27, consists of a single fairleader and windlass located on an overhanging platform at the deck edge. A chain locker below decks provides storage for 700 ft of chain. This chain is the upper segment of the anchor leg and is long enough so that wire rope handling capability is not required for haul-in during anchor leg length reduction. Wire or chain disconnect is not required and cost is reduced by replacement of the winch by the windlass. Since a disconnect is not required, the active tensioning operation is more reliable and safer, particularly in higher sea states.

An electric-hydraulic drive is selected over an electrically driven windlass. Although single units are selected to provide independence between anchor legs, pairing of two windlasses through a common drive may lead to a reduction in deck machinery cost. A possible alternate to the windlass is a continuous pulling machine for chain. This concept appears to be feasible and may provide a significant reduction in cost. Further investigation is recommended.

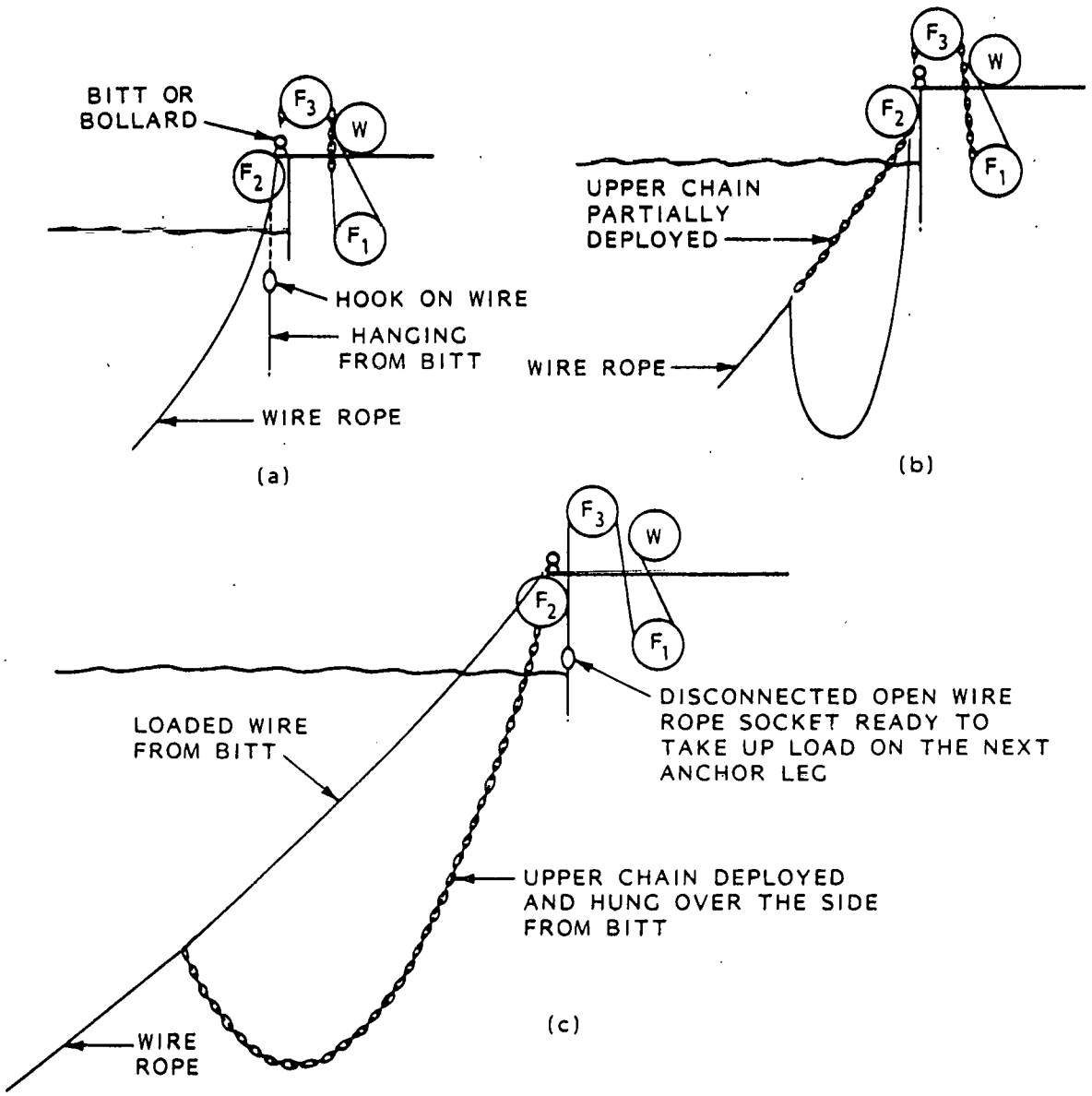

Fig. 2-27 Deck Machinery Configuration No. 3

2.4.3 Wire Rope

Wire rope is selected for the middle segment of the anchor leg. The considerations leading to this selection including strength, weight, construction, service life, cost, and precedent application are discussed in this section.

The evaluation of number of legs versus wire strength indicates that a configuration of few legs of high strength is desirable from overall system cost. The strength requirement, determined from the maximum tension in the Extreme Sea State, is 3.0×10^6 lb for an eight-leg MAL. Wire rope manufacturing is limited to 100 tons for a single length of six-strand rope, and 60 tons for spiral strand. The resulting length limit is 3,360 ft for continuous, six-strand rope of 6-in. diameter. A wire rope socket is necessary if a longer segment is required. By limiting the wire diameter this constraint is accomodated in the design. Small wire diameter leads to smaller sheave and drum diameters. However, the long service life requirement is more readily achieved with larger diameter wire rope due to corrosion protection provided by the larger cross section.

Wire rope corrosion life is less significant than bending fatigue and flexibility in some applications. This conclusion is based on a survey of operational life of large diameter (3-in.) wire rope in ocean anchoring of exploratory drillships and pipe-laying barges. Typical wire rope life in the anchoring of exploration platforms in the North Sea is 2.5 years. These MALs are deployed and redeployed several times a year for relatively short duration operations (24 to 42 days). The wire rope often receives mechanical damage during handling in the rough conditions of the North Sea. Service life in less severe conditions is 3 years. Wire rope lengths running over fairleaders are often replaced in 12 to 14 months due to broken wires, wear, abrasion, and fatiguing. Pipe laying barges deploy and retrieve wire rope anchor legs at high speeds in "walking" the barge forward. This wire rope, bright (ungalvanized) and heavily greased, is overheated on the winch drum leading

to reduced fatigue life. A service life of 0.3 to 2 years is typical in this application. Wire rope in these applications is therefore fatigue limited, not corrosion limited, with service life significantly lower than that required for the OTEC SKSS. Examination of a 3.5-in.-diameter galvanized steel wire rope utilized in the North Sea for 8 years as a mooring leg revealed extensive corrosion of outer wires and core. Tensile tests for residual load indicate a 5 percent reduction in original strength. Wire ropes tested under static load in depths to 6,000 ft retain original breaking strength if the area density of the zinc galvanizing is adequate, 1.50 oz/ft^2 for a 3-year immersion (Ref. 2-6).

To avoid the bending fatigue loads and wire hardening over sheaves and winch drum, as well as high corrosion and potential of mechanical damage above and near the splash zone, the wire segment termination to chain on the barge is located at a depth of 100 ft or greater. This approach is more likely to lead to realization of full service life of the wire rope than leading wire over sheaves to a winch on the barge.

Alternative constructions to the six-strand wire are the spiral and locked-spiral strand ropes. These ropes provide a smaller diameter for a given breaking strength, albeit at a cost of 2 to 3 times six-strand rope. The locked spiral does not unravel from a broken wire, provides sealing of the inner wires and therefore greater corrosion resistance, requires a 24-ft-diameter sheave for a 5.5-in.-diameter wire, and is limited to 60 tons for production of a single, continuous segment. The six-stranded wire is selected because of lower cost, smaller diameter sheave required for deployment, and availability of a single, continuous segment.

Corrosion protection is provided in the six-strand rope by galvanizing of the bright, extra improved plow steel. This material is selected over stainless steel; the latter is approximately four times as costly and experiences stress corrosion in seawater. An extra coating of zinc is optional in post-construction finishing to cover wires abraded during construction. This

option, an alternative to lubricating the rope with grease, requires further investigation. A second option is to attach sacrificial anodes to the wire during deployment. Anode mass and spacing are sized to prolong the wire rope life through reduction of wire corrosion (Ref. 2-7).

Further corrosion protection may be provided by sheathing of the wire rope with a polyethylene jacket. At the present time, maximum sheathing diameter is 5 in., although an increase in capacity is planned. The sheathing seals the wire rope from seawater unless it is damaged during handling, in which case corrosion will occur in the wire adjacent to the damaged sheathing. A comparison of the cost of unsheathed versus sheathed wire indicates that sheathing is cost effective if it provides a service life greater than 13.5 years in comparison to 10 years for the expected service life of unsheathed wire. The potential for extended wire rope service life, possibly to the 30-year SKSS design life, warrants further investigation of sheathing, particularly in the effects of the gripper type deployment winch on sheathing and prevention of and detection of sheathing damage.

2.4.4 MAL Without Active Tensioning

To assess the cost effectiveness of the active tensioning portion of the MAL, the wire rope and chain diameter are increased to provide adequate strength in the Extreme Sea State, assuming no active anchor leg length adjustment.

The loading direction which results in maximum tension is 45 deg. This condition results in a maximum tension of 1.72×10^6 lb in leg No. 1.

Condition:	Extreme Sea State, 45 deg off Starboard Bow
Wire:	6.25 in.
Chain:	5.38 in.
Wire Tension Safety Factor:	2.0
Chain Tension Safety Factor:	2.24

The estimated savings in acquisition cost of this design is 15 percent (~$3M) of the design with active tensioning; half of the savings arising from deleting the windlasses is lost to increases in wire rope and chain scantlings. While the reduced maintenance cost may be added to this savings, additional costs will arise from service such as resetting of anchors after slippage, reduced fatigue life of wire rope, and loss in production due to OTEC plant shutdown during periods of excessive roll motion. With a rate of 50 mills/kWh and a 75-percent availability, the value of electrical production is $1,500/hr, leading to a loss of $3M for 84 days of shutdown beyond the assumed availability. Note that this shutdown period is 0.0003 percent of the 30-year service life. The electrical riser cables are torque loaded by barge yaw, a rotation which may be reduced by active tensioning in the lower sea states if this loading is more significant in terms of availability, than is maintenance of head sea orientation. Although difficult to assess, it is certainly feasible that such costs may exceed the savings in acquisition cost.

2.5 MAL COMPONENT SIZING AND SELECTION

The loads analysis of Section 2.2 and the design requirements of Task I establish the criteria for the selection and sizing of MAL components. The maximum line tension of 133.5 kips in the Extreme Sea State with a dynamic loading of at least 10 percent and a safety factor of 2 yields the design load of 3000 kips. The maximum design operating load is 2,510 kips. The sizing and selection of the MAL components using the above criteria are presented as follows.

Anchor. The maximum pull at the anchor for a 100-year storm is 664 kips. The required anchor holding power including dynamic loading, with a safety factor of 2.0, is 1,460 kips This value satisfies the requirement of being one half of the line breaking strength. Two 60,000 pound anchors in tandem provide a maximum holding power of 2,040 kips with the anchors embedded in sand and a minimum of 918 kips in mud. Subsequent seafloor sediment sampling and shear strength testing is required for final selection and design of the anchors.

The tandem arrangement is selected to provide redundancy and reliability to the system. Under ideal conditions, one anchor alone can provide a maximum holding power of 1,200 kips which is nearly twice the anticipated static pull on the anchor for a 100 year storm. Furthermore, consideration of the selection included the fact that a 60,000-lb anchor is presently manufactured.

Chain. The maximum static chain tension anticipated during a 100 year storm is 1,119 kips. The 4-7/8 in. diameter, Grade 4 chain has a breaking strength of 2,932 kips. This results in a factor of safety of 2.0. The length of chain is established by the depth of the anchor. The wire rope change-out operation requires raising the end of the chain above the water surface to facilitate replacement of wire rope. Lifting the chain above the deepest anchor imposes a load of 1,130 kips. The maximum load on the chain is 1,234 kips when the two 60,000 pound anchors are being deployed at maximum depth. This constitutes a factor of safety of 2.4 excluding dynamic loading.

Wire Rope. The 5-3/4 in. diameter wire rope breaking strength of 3,000 kips is at least twice the maximum 100 year storm static tension of 133.5 kips. A corrosion rate of three to six mils a year at depths below 200 ft is assumed.

Chafing and Pendant Chain. The design load on each of these chains is 3,000 kips. The same as the wire rope. The physical dimensions of the chain are identical to the anchor chain; however, the breaking strength is increased from 2,930 to 3,000 kips by modification to the steel alloy. The length of each of the chains is selected to provide the optimum pay out and haul in to provide the active tensioning and change of heading operation where the barge is rotated as much as 90 deg. For a 100 year storm with the weather at 45 deg from the starboard bow or stern the loads on anchor legs one and two or three and four become excessive. Therefore, in anticipation of the 100 year storm, two anchor legs are payed out as much as 503 and 303 ft and two legs are hauled in as much as 400 and 200 ft. Detailed configurations and loads on the anchor legs are as shown in Fig. 2-1.

Chafing Chain Fairlead. The fairlead design is based on a 1,500 kips chafing chain tension at a maximum of 45 deg from the horizontal. The resultant force on the sheave assembly is 1,148 kips. Material selected for the assembly is A36 steel with a yield strength of 36,000 psi. Allowable stress levels are 60 percent of yield for tensile stresses, 75 percent for compressive and 40 percent for shear. The five whelp wildcat design with a 67-5/8-in. critical pitch diameter is required to preclude chain bending. Details of the design are as shown in Fig. 2-3.

Windlass. The windlass, requires a small extension to the state-of-the-art; however, the responses from the manufacturers indicated that they are equipped to custom design and/or modify their standard equipment for this particular application. The basic specification for the windlass is as follows:

Chain size - 4-7/8 in. diameter
Wildcat - five-whelp design
Wildcat brake holding power - 3,000 kips
Chain stopper (integral to frame) - 3,000 kips
Horsepower - 455
Two-speed gearbox - 10 and 20 fpm
Haul-in characteristics:

- Low speed - 10 fpm at 1,500 kips
- High speed - 20 fpm at 750 kips

Lock pawls release at 3,000 kips controls:

- Complete control from local stand
- Complete control from remote station
- Emergency release from remote station
- Continuous static and dynamic tension readout (recorded) and speed indicators
- All controls are electrohydraulic for high reliability

Chain Locker. The volume of chain locker space to store 600 ft of chain is a function of the stowage factor. Stowage factor is defined as the ratio of the volume remaining over the total volume available when the stowed material occupies a most compacted volume within the available space. 600 ft of chain

occupies approximately 440 cubic ft when neatly arranged. A stowage factor of 80 percent results in a chain locker space of 2,200 cubic ft. This is five times the compacted volume. The chain locker volume is 10 ft x 10 ft x 24 ft.

Deployment Windlass. The requirements for the anchor lowering windlass on the workbarge are identical to that of the platform windlass. The anchor lowering load is 1,234 kips. The design load for the windlass is 1,500 kips.

Deployment Linear Winch. The continuous pulling machine for wire rope on the deployment workbarge requires minor extension to the state-of-practice. The Lucker Manufacturing Company has developed numerous models of continuous wire rope pulling machines. The largest machine to date is capable of pulling a 5-in.-diameter wire rope at 1,000 kips at 10 ft per minute. Increasing the wire rope diameter to 5-3/4 in. and line pull to 1,400 kips at 10 ft per minute requires a slight modification to an existing design. The continuous pull machine pulls the rope with a continuous, steady motion. There is no limit to rope length which can be pulled in this manner because the machine can be adapted to pass coupled ends through the grips. The force of pull and speed are adjustable in ranges from zero to the machine's maximum. A load gauge on the control panel displays the actual pounds being pulled on the rope at all times. At any time during a pull, the rope can be stopped under load and held stationary. With a push of a button the pulling operation can be restarted and continued. The machine can also be stopped and reversed to feed out wire rope and relieve tension.

Storage Reels on the Workbarge. Two 10 horsepower storage reels facilitate pay-out and reel-in of 3,400 ft maximum of 5-3/4-in.-diameter wire rope. The physical characteristics of the storage reel are as follows:

Drum diameter	88 in.
Drum length	152 in.
Line speed	10 and 20 fpm
Line tension	33,000 lb at 10 fpm

Line tension	16,500 lb at 20 fpm
Brake capacity	50,000 lb
Horsepower	10

Workbarge Thrusters. Three workbarge thrusters are capable of maintaining a bollard pull of 226 kips during the deployment of a seaward anchor leg with a range of 6,000 ft between the platform and the deployment workbarge. Two of the thrusters are mounted aft, each capable of 85,000 lb thrust. The third is mounted forward for heading control and contributes 60,000 lb of thrust while operating 45 deg off the line of pull port or starboard. Each thruster is rated at 3,400 horsepower. Speed is variable between 0 and 180 rpm. A fourth thruster is added to provide redundancy and additional thrust underway.

Workbarge Diesel Generator. Power to the workbarge deployment equipment is provided by the 8 megawatt, 440 volt, three-phase diesel generator. The maximum generated output during deployment includes windlass and winch operations, one of the storage reels in operation and the running of the three thrusters. The diesel generator rated at 8 megawatts provides 95 percent of the rated output for the above operations simultaneously. The deployment equipment on the workbarge is rated as follows:

Thrusters (3)	3,400 hp
Linear winch	455 hp
Windlass	455 hp
Supply storage reel	10 hp
Auxiliary storage reel	10 hp

2.6 ANCHOR LEG DEPLOYMENT AND RETRIEVAL

The equipment and procedure for deployment of the anchor legs and subsequent retrieval at the end of the service life are presented in this section.

2.6.1 Deployment Workbarge

The workbarge characteristics, deck equipment, and arrangement are shown in Fig. 2-28. The system meets the requirements to pay out the wire rope segment and to lower the anchors and chain while maintaining a bollard pull of 226 kips. The distance of the anchor drop from the platform is 5,000 ft landward and 6,000 ft seaward. The maximum anchor depth is 5,680 ft. The combined static and dynamic design load on the 500-hp windlass is 1,375 kips. There is a 2.4-deg change of trim when the full chain length and two anchors are supported by the windlass. Two fixed thrusters are mounted aft and two rotatable thrusters are mounted forward for propulsion and heading control. Each thruster is rated at 3,400 hp for 85,000 lb bollard thrust. The continuous pulling machine (Lucker Winch) for wire rope facilitates restraining maximum line tension of 1,400 kips while paying out wire rope at 10 fpm. The machine is reversible, allowing wire rope haul in at the same load and speed. Two 10-hp wire rope reels provide stowage for the anchor leg wire rope and auxiliary wire rope. The latter provides the length to span the range from the platform to anchor location. A 15-ton crawler crane facilitates faking the chain on deck during loading operations and during controlled lowering of anchors and chain.

2.6.2 Deployment Procedure

Loading. The workbarge is moored dockside for loading of a single anchor leg and deployment support material. The loading operation sequence outlined below is repeated after deployment of the first anchor leg and sequentially until the eight legs are deployed.

- Use of dockside crane and 15-ton crawler crane to load and fake the anchor chain (5,880 ft, max) on the workbarge deck.

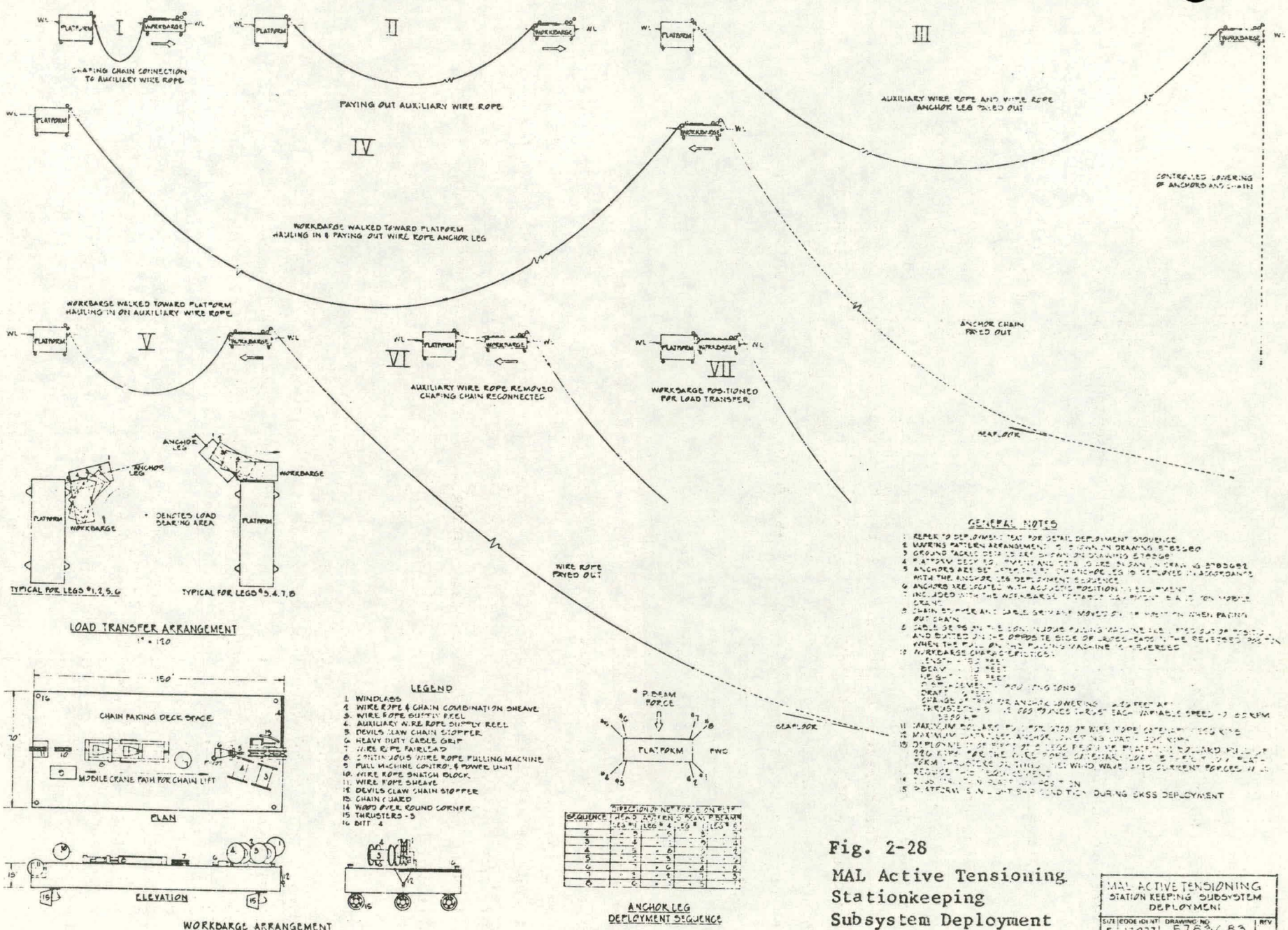

LOAD TRANSFER ARRANGEMENT
1" = 120'

WORKBARGE ARRANGEMENT
1" = 20'

LEGEND

1. WINDLASS
2. WIRE ROPE & CHAIN COMBINATION SHEAVE
3. WIRE ROPE SUPPLY REEL
4. AUXILIARY WIRE ROPE SUPPLY REEL
5. DEVILS CLAW CHAIN STOPPER
6. HEAVY DUTY CABLE GRIP
7. WIRE ROPE FAIRLEAD
8. CONTINUOUS WIRE ROPE PULLING MACHINE
9. PULL MACHINE CONTROL & POWER UNIT
10. WIRE ROPE SNATCH BLOCK
11. WIRE ROPE SHEAVE
12. DEVILS CLAW CHAIN STOPPER
13. CHAIN GUARD
14. WARD OVER ROUND CORNER
15. THRUSTERS - 3
16. BITT 4

SEQUENCE	DIRECTION OF LINE FOR ANCHOR LEG #					
	LEG #1	LEG #2	LEG #3	LEG #4	LEG #5	LEG #6
1						
2						
3						
4						
5						
6						
7						
8						

ANCHOR LEG DEPLOYMENT SEQUENCE

GENERAL NOTES

1. REFER TO DEPLOYMENT TEXT FOR DETAIL DEPLOYMENT SEQUENCE
2. MOORING PATTERN ARRANGEMENT AS SHOWN ON DRAWING ES5582
3. GROUND TACKLE DETAILS ARE SHOWN ON DRAWING ES5582
4. * APPROX DEPTH TO PAYOUT AND DETAILS ARE SHOWN ON DRAWING ES5582
5. ANCHORS ARE SET AT THEIR PREDESIGNATED ANCHOR LEG IS DEPLOYED IN ACCORDANCE WITH THE ANCHOR LEG DEPLOYMENT SEQUENCE
6. ANCHORS ARE LOCATED WITH ACOUSTIC POSITIONING EQUIPMENT
7. INCLUDED WITH THE WORKBARGE PORTABLE SURVEY EQUIPMENT IS A TON MOBILE CRANE
8. CHAIN STOPPER AND CABLE GRIP ARE MOVED OUT OF WAY WHEN PAYING OUT CHAIN
9. CABLE GRIPS ON THE CONTINUOUS PULLING MACHINE ARE USED OUT OF SEQUENCE AND LOCATED ON THE OPPOSITE SIDE OF REEL-LEADS IN THE REVERSED POSITION WHEN THE PULL ON THE PULLING MACHINE IS REVERSED
10. WORKBARGE CHARACTERISTICS:
    LENGTH - 150 FEET
    BEAM - 32 FEET
    DRAFT - 10 FEET
    CRANE LEVERAGE POSITIONS
    DRAFT - 9 FEET
    CRANE LIFT FOR ANCHOR LOWERING - 450 FEET AT
    THRUSTERS - 3 - 10,000 POUNDS FORCE EACH VARIABLE SPEED 0 - 600 RPM
    3000 HP
11. MAXIMUM BOLLARD PULL FOR 3500 FT WIRE ROPE CATENARY - 100 KIPS
12. MAXIMUM UNRELIEVED ANCHOR LEG HOLDING LOAD - 100 KIPS
13. DEPLOYMENT IS BY MEANS OF A SINGLE FAIRLEAD PLACED AT A BOLLARD PULL OF 200 KIPS FOR THE WIRE ROPE CATENARY. USE OF THE 3 - 10,000 POUND FORCE THRUSTERS IN THIS DEPLOYMENT WILL WAVE AND CURRENT FORCES IN ADDITION TO REDUCE THE MOORING EFFORT
14. * DENOTES THE NOMINAL PLATFORM POSITION
15. PLATFORM SHUT-IN SHOULD TICK DURING ES5S DEPLOYMENT

Fig. 2-28
MAL Active Tensioning Stationkeeping Subsystem Deployment

MAL ACTIVE TENSIONING STATION KEEPING SUBSYSTEM DEPLOYMENT			
SIZE	CODE IDENT	DRAWING NO.	REV
E	11077	5763683	

THIS PAGE

WAS INTENTIONALLY

LEFT BLANK

- o Threading the leading end of chain under the wire rope and chain combination sheave and over the windlass wildcat.
- o Loading of two 60,000-lb anchors and the 100 ft of connecting chain.
- o Transfer of wire rope from dockside supply reel to workbarge storage reel.
- o Transfer of auxiliary wire rope from dockside supply reel to workbarge auxiliary wire rope storage reel (one time only).
- o Loading of 170-ft load transferring wire rope (one time only).
- o Loading of 5,000 gal of diesel fuel.

Deployment Sequence. The order in which the eight anchor legs are deployed is dependent on the resultant wind, wave, and current force on the platform. The first leg selected is in line with the resultant vector, directed toward the platform. Accordingly, the second leg deployed is next closest in line to the resultant vector. The third and fourth legs are opposite to the first and second, respectively. The remaining four legs are then deployed and set.

Deployment Procedure. Deployment consists of workbarge loading at dockside, transit to and from the deployment site, anchor leg lowering, and anchor setting. The anchor lowering operation is estimated to require 15 hours and is completed in daylight. The procedure to deploy the first anchor leg is as follows:

1. The loaded workbarge is moored alongside the platform outboard of the anchor leg fairlead.
2. The two anchors with the 100-ft connecting chain is lifted by the platform pedestal crane and hung overboard by the anchor chain on the windlass.
3. A 170-ft length of wire rope is connected to the chain from the platform windlass. The rope is placed in the grips of the linear winch for pay out from the workbarge.
4. Mooring lines are released. The workbarge is headed out to sea under the anchor drop point while the 170-ft wire rope is payed out. Tugs assist moving the platform and barge.

5. Anchor lowering via the windlass commences as soon as the workbarge is headed out to sea.
6. Connection is made between the 170-ft wire rope and the wire on the storage reel with an end link between the wire rope sockets. Pay out of wire rope commences from the storage reel.
7. Pay out of wire rope through the linear winch continues until the storage reel is emptied. The wire rope is then secured while the workbarge is acoustically positioned for anchor lowering.
8. Final acoustic positioning is established before anchors are lowered to the seafloor.
9. Monitoring the load sensor on the windlass, the anchors are landed in sequence while paying out chain and moving toward the platform. The anchors are set subsequent to landing and before entire chain length is on seafloor.
10. The chain stopper is engaged when the wire-rope-to-chain connecting link is above the stopper.
11. The wire-rope-to-chain connection is made, operating the linear winch as necessary to facilitate the connection.
12. The load on the linear winch is relieved and the grips of the winch are reversed for passing wire rope in the opposite direction.
13. The load is transferred from the chain stopper and the windlass to the linear winch.
14. The workbarge is powered toward the platform with the winch and thrusters until the wire rope socket-to-socket joint with the 170-ft wire rope is just below the windlass wildcat. The wire rope is then secured by the linear winch and the wire rope stopper.
15. The workbarge is moored alongside the platform, and the slack chain is disconnected from the wire rope.
16. The chain is payed out from the platform windlass along the workbarge deck and connected to the end link between the wire rope sockets outboard of the windlass.
17. The wire rope stopper is opened. The wire rope is payed out with the linear winch to transfer the load from the wire rope to chain.

18. The chain is hauled in while the workbarge is moved inboard and to port of the anchor leg. When the chain lifts off from the workbarge deck, the chain is hauled in as required to facilitate disconnecting the 170-ft wire rope from the end link.

Deployment of the second up to the eighth leg is identical to the above procedure except for the insertion of the auxiliary wire rope between the 170-ft and the storage reel wire rope segments. This alters the procedural steps between 6 and 7. After each leg is deployed, the workbarge returns to port for dockside loading of the next leg to be deployed. The line tensions in the equilibrium (no environmental load on platform) condition as shown on Fig. 2-1 provide the leg tensions that are realized for proper anchor set. Platform station is maintained by tugs until MAL installation progress is sufficient to permit removal of the tugs. A standby tug is provided throughout the deployment sequence to provide emergency bollard pull in the event of power loss on the workbarge.

Error in Anchor Deployment. This error is dependent on the accuracies of the anchor lowering operation and the predicted anchor setting distance. The error in anchor deployment is determined and minimized through conduct of the development test program recommended in Task IV. Following the test program, the expected tolerance of locating the anchor touchdown point and the maximum predicted anchor set distance are added to determine how much the anchor leg is shortened. The anchor leg is then shortened by 80 percent of this amount. This allows the system to be compensated by taking in 20 percent of the maximum error or paying out 80 percent of the maximum error. The addition of chain is preferable to the shortening of wire rope once the anchor leg is deployed. If the allowable set distance or touchdown location is not achieved, or if the anchors do not set as indicated by low leg tension, then the anchor leg is redeployed. The deployment operation is reversed with the auxiliary wire rope inserted. The procedure is similar to changeout of wire rope except in addition the anchors are lifted off the seafloor and replanted.

2.6.3 Retrieval Operation

The MAL SKSS is to be removed from the seafloor at completion of the 30-year service life. The anchor leg retrieval procedure is a modified version of the changeout procedure combined with a modified reversal of the initial deployment procedure. The workbarge is arranged as for deployment but with the supply storage reel empty.

After the workbarge is over the anchor, the procedure to haul in the anchors, chain, and wire rope is the reverse of the deployment procedure except for breaking out of the anchors. Acoustic positioning is not required in this procedure. The procedure is as follows:

1. The workbarge is moored to the platform in the vicinity of the leg scheduled for retrieval.
2. The platform windlass hauls in on the chafing chain of the leg until the connection between the chafing chain and the anchor wire is clear of the water and above deck height of the workbarge.
3. The workbarge is then maneuvered under the connection and the connection is lowered to the deck alongside the windlass.
4. While paying out 150 ft of chain, the barge is moved outboard in line with the anchor leg. The barge is securely moored to the platform in this orientation.
5. The 170-ft of load transfer wire rope (stored on the workbarge) is then layed in the linear winch, gripped, threaded under the sheave, hung over the wildcat and connected to the end link of the wire rope and chain connection.
6. With the workbarge moored to the platform, the anchor leg chain is payed out to transfer the load to the linear winch. Using the linear winch, the wire rope is hauled in until the connection is outboard of the windlass. The chain is disconnected and hauled in to facilitate reconnection at the other end of the 170-ft wire rope. The chain is reconnected to the wire rope and the slack taken up. Mooring lines are gradually relieved.

7. The anchor leg is hauled in until the wire-rope-to-wire-rope connection is inboard of the forward heavy duty cable grip. The forward and aft heavy duty cable grips are engaged. The linear winch is then unloaded and the 170-ft wire disconnected at the forward cable grip.
8. The grips on the linear winch are reversed to pay out wire rope from the after end. The auxiliary wire rope from the storage reel is connected to the 170-ft wire. The load is then transferred from the aft cable grip to the linear winch.
9. The workbarge proceeds to a point over the anchor as the auxiliary wire rope is passed through the linear winch.
10. When the end of the auxiliary wire is reached, the wire is connected to the wire rope stopped at the forward heavy duty cable grip. Slack is taken up.
11. The workbarge proceeds toward a point over the anchor as the wire is pulled through the linear winch.
12. Thruster power is increased as the workbarge approaches the anchor point.
13. When the connection between the cable and anchor chain is inboard of the chain stopper on deck, the load is transferred to the chain stopper on deck and the windlass.
14. The aft cable grip is engaged on the wire rope.
15. The wire rope is disconnected from the chain and attached to the supply reel drum to facilitate haul in.
16. The chain is hauled in by the windlass and faked on deck, assisted by the crawler crane. The anchors are left hanging over the side until they are hoisted onboard with the platform crane.
17. The wire rope is hauled in and wound on the supply reel. This is done concurrently with Step 16.
18. When the wire rope end is hauled in, the auxiliary wire rope is disconnected from it and wound on the auxiliary wire rope reel.
19. The workbarge moves toward the platform with the winch and thrusters until the wire rope socket-to-chain connection is just upstream of

the wire rope sheave. The wire rope is then secured by the grips of the winch and the wire rope stopper.

20. The workbarge is moored to the platform, the chain is slackened and disconnected from the wire rope. Anchors are lifted onboard.

Retrieval of the second leg up to the seventh leg is identical to the above procedure. The eighth leg does not require the use of the auxiliary wire rope. After each leg is retrieved, the workbarge returns to port for dockside unloading of wire rope and chain.

2.7 INSPECTION, MAINTENANCE, AND REPAIR

2.7.1 Inspection

Above the Waterline. Inspection of elements of the stationkeeping subsystem which are installed on the platform or are situated above the waterline permit simple periodic visual examination of the anchor windlass equipment and the mooring cable running to the waterline. Such inspections are the responsibility of the platform crew and are carried out by the assigned anchor watch and anchor detail. The anchor watch is a continuous watch rotating every 4 hours over a 24-hour period. The watch stander is required to sight and log load cell load readings on each of the eight anchor legs every hour. These readings are displayed on the bridge. If any reading exceeds redlined limits, the anchor detail mans their stations for adjustment of anchor leg tensions. Functional inspection of the anchor windlass equipment is made once each day during the forenoon. This inspection is made by the anchor detail during the morning watch period. The inspection consists of providing power to the anchor windlass of each anchor leg. The wildcat on each leg is loaded sufficiently to take the load from the chain stopper; the load is then returned to the stopper. Once each week the functional inspection additionally requires taking the load successively on each wildcat, tripping the chain stoppers, and walking out each chain a distance of 50 ft. The chains are then returned to their prescribed position and the load is again transferred to the chain stoppers.

Below the Waterline. Inspection of the elements below the waterline is accomplished by divers, or by manned or remotely controlled submersibles. The primary tool for deep underwater inspection is a remotely controlled submersible. A limited diver capability is part of the crew structure in order to accomplish inspection of the underwater portion of the platform. This capability is also used for shallow water inspection of each anchor leg with hand held TV cameras to assist in visualization.

Visual inspection to depths of 6,000 ft by submersibles now in the ocean industries inventory is feasible. Examples of two vehicles with deep ocean capability are the manned Arms Bell (3,000 ft) and the remote controlled MS-6000 (6,000 ft). Although the Arms Bell is currently limited to 3,000-ft depths, it does provide for direct visual inspection (and parallel TV inspection) of the anchor legs to sufficient depth to provide for inspection of representative segments and thus, by extrapolation, a means for evaluating the condition of the entire leg. The MS-6000 provides for remote TV viewing and even some limited work to depths of 6,000 ft. Both of these tools are owned and operated by Oceaneering International, Inc., of Santa Barbara, California. A third tool of particular note is a magnetic inductance vehicle with the capability of providing for an NDT-type inspection. This tool gives an indication of wire strand failures in the wire portion of the legs, not detectable by the human eye or TV viewing, thereby providing warning of wire degradation. The tool can readily be attached to the anchor cable and by use of a simple control line it is lowered down the leg and retrieved while providing readouts of the wire's condition. This tool is under development by Noranda of South Yorkshire, England.

The capability to conduct the foregoing inspection is provided outside of the platform crew structure. Contractural arrangements are established on a routine and on a call basis. The recommended schedule for such services is:

a. Immediate post deployment inspection. This provides:
   - o Continuation of compliance with the mooring plan
   - o Signature or base information for subsequent inspections

- o Initial training and determination of adequacy of the inspection plan

b. Two years after initial deployment
c. Five years after initial deployment
d. Eight years after initial deployment
e. Interim inspections may be required if the SKSS is subjected to unusual stress such as heavy storms.

2.7.2 Maintenance

Above the Waterline. SKSS equipment installed on the platform is maintained in the manner prescribed by the manufacturer. The schedule for such maintenance is also in accordance with the manufacturer's instructions. The machinery controlling each anchor leg is, except for the exceptionally high load requirements, common to the marine industry and thus introduces no new or extraordinary maintenance tasks.

The elements of the anchor legs above the waterline are blasted and recoated every 6 months to arrest corrosion. Portions of the chain that are immediately below the waterline and subject to air exposure due to heave receive similar treatment. These latter portions are made accessible during the period of functional inspection checks requiring movement of the anchor chafing chain. Care is also taken to ensure that the point of contact between the chafing chain and the platform is changed during the weekly functional inspections. Color coding contact points will facilitate this operation. These tasks are within the scope of shipboard maintenance.

Below the Waterline. Except for stress relief and the maintenance prescribed for portions of the chafing chain below the waterline no other maintenance is applied to the legs. Design provides for a life cycle of 30 years for anchor chain and 10 years for the wire portion. Replacement of this latter element is discussed under the heading of Repair. Wear and abrasion observed on the chafing chain provides an indication of the condition of the anchor chain.

2.7.3 Repair

Above the Waterline. As in the case of maintenance requirements, machinery repair procedures are in accordance with the manufacturer's instructions. Minor repairs are effected by the platform crew with major repairs being accomplished by base support personnel. Repairs to the chafing chain may be required by virtue of its constant action on the fairleader and windlass. Worn sections can readily be replaced by the platform crew.

Below the Waterline. Because of the depths involved it is impractical to consider that any effective repairs can be made to an anchor leg other than replacement of the failed or degraded element. Because the wire portion of the anchor leg is the only element which does not meet the 30-year life cycle requirement, this element requires "repair by replacement" prior to the expiration of is designed 10-year life cycle. The procedure to accomplish this task follows.

Replacing the Wire Component of the Mooring Leg. When replacement of the wire component of the mooring leg becomes necessary, the work barge used for deployment of the legs is used in a modified reversal of the initial deployment procedure as follows:

When replacement of the wire component of the anchor leg becomes necessary, the workbarge used for deployment of the legs is used in a modified reversal of the initial deployment procedure. The workbarge modification includes an additional heavy duty cable grip at the after end and the relocation of the aft wire rope reel to the after end of the linear winch. This reel is for storage of the replacement wire rope. After this reel is payed out, it is returned to its original position to haul in the auxiliary rope. The other reel is used to store the auxiliary wire rope and to haul in the "old" wire rope after it is payed out. The modification is shown in Fig. 2-29. The procedure for wire rope change-out is as follows:

1. The workbarge is moored to the platform in the vicinity of the leg scheduled for replacement

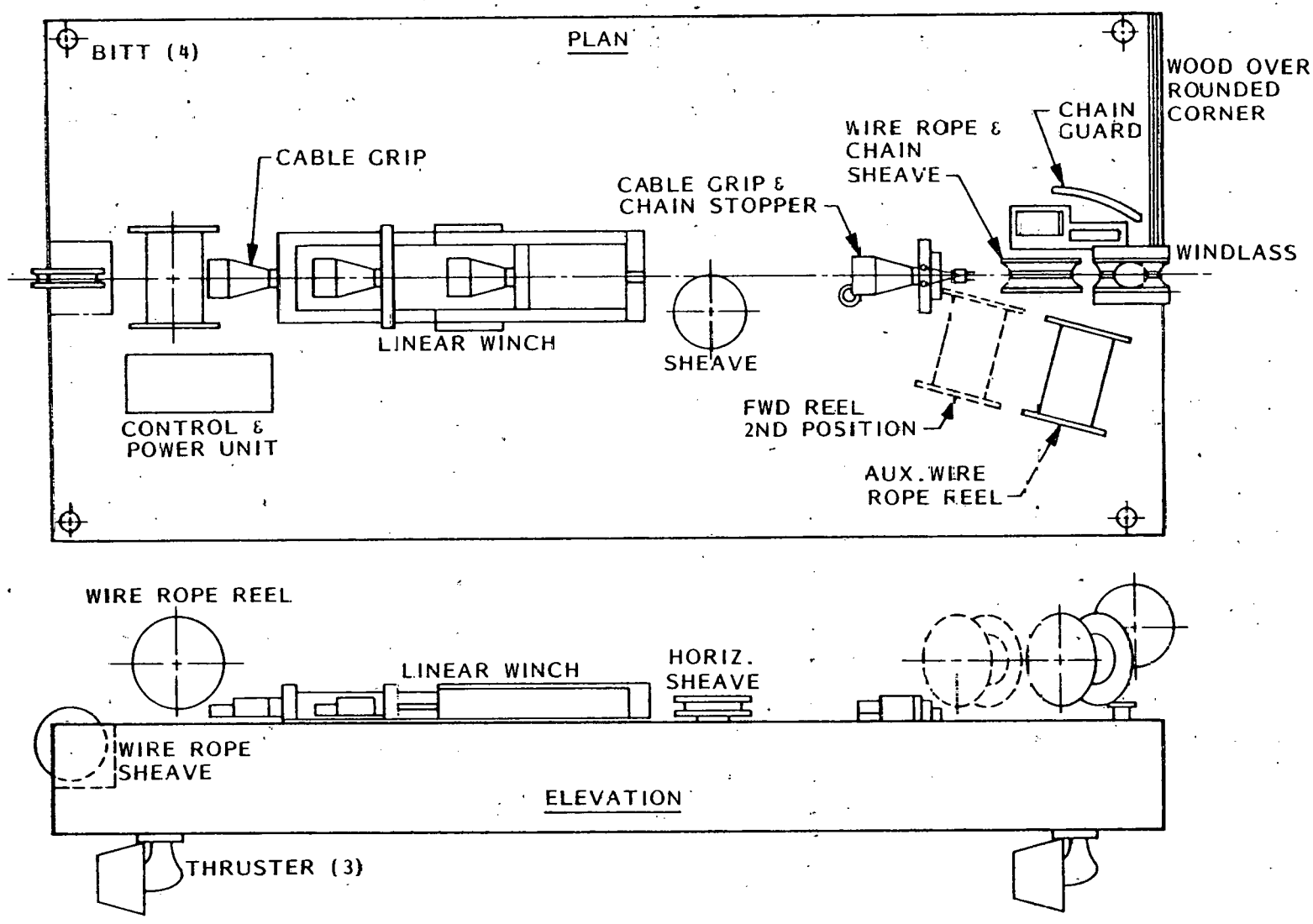

Fig. 2-29 Workbarge Arrangement for Wire Rope Changeout

2. The platform anchor windlass hauls in on the chafing chain of the leg until the connection between the chafing chain and the anchor wire is clear of the water and above deck height of the workbarge.
3. The workbarge is then maneuvered under the connection and the connection is lowered to the deck alongside the windlass.
4. While paying out 150 ft of chain, the barge is moved outboard in line with the anchor. The barge is securely moored to the platform in this orientation.
5. The 170 ft of load transfer wire rope (stored on the workbarge) is then layed in the grips of the linear winch, gripped, threaded under the sheave, hung over the wildcat, and connected to the end link of the wire rope and chain connection.
6. With the workbarge moored to the platform, the anchor leg chain is payed out to transfer the load to the linear winch. Using the linear winch, the wire rope is hauled in until the connection is outboard of the windlass. The chain is disconnected and hauled in to facilitate reconnection at the other end of the 170-ft wire rope. The chain is reconnected to the wire rope and the slack taken up. Mooring lines are gradually relieved.
7. The anchor leg is hauled in with the linear winch until the wire-rope-to-wire-rope connection is inboard of the forward heavy duty cable grip. both of the forward and aft heavy duty cable grips are engaged. The linear winch is then unloaded and the 170-ft wire disconnected at the forward cable grip.
8. The grips on the linear winch are reversed to pay out wire rope from the after end. The auxiliary wire rope from the storage reel is connected to the 170-ft wire. The load is then transferred from the aft cable grip to the linear winch.
9. The workbarge moves toward the anchor location while the auxiliary wire rope is payed out through the linear winch.
10. When the end of the auxiliary wire is reached, the wire is then connected to the "old" wire rope stoppered at the forward heavy duty cable grip slack is taken up.

11. The workbarge continues moving toward the anchor location as the "old" wire is pulled through the linear winch.
12. Thruster power is increased as required as the workbarge approaches the anchor location.
13. When the connection between the "old" cable and anchor chain is inboard of the chain stopper on deck, the load is transferred to the chain stopper and the windlass.
14. The aft heavy duty cable grip is engaged on the "old" wire rope and the linear winch is relieved.
15. After the grips are reversed on the winch, the replacement cable from the storage reel is placed in the grips and connected to the anchor chain. The anchor chain load is transferred from the windlass and chain stopper to the linear winch.
16. The replacement cable is then payed out. When the end of the wire rope is reached, the forward heavy duty cable grip is engaged, after which the winch is relieved and the cable set aside.
17. The grips of the linear winch are reversed and the "old" wire rope is layed in the grips.
18. The "old" wire is hauled in and wound on the auxiliary wire rope reel.
19. The empty storage reel is moved from its forward position to aft in front of the auxiliary wire rope reel.
20. When the end of the "old" wire rope is reached, the auxiliary wire rope is hauled in and wound on the storage reel in front of the auxiliary reel.
21. The procedure to complete the wire rope changeout is identical to the deployment procedural, Steps 14 through 18.

Changeout of the remaining legs is identical to the procedure described for leg No. 1. After each wire rope segment is replaced, the workbarge returns to port for unloading of "old" wire and loading of replacement wire rope. The auxiliary wire rope is reused. Setting of the anchors is established with the use of the windlasses and load cells.

2.8 INTERFACES

SKSS interfaces with other OTEC systems are presented in this section primarily to identify the potential interference between the SKSS and the platform, CWP, and riser cable.

2.8.1 Platform

The windlasses require platforms which extend the main deck 9 ft at each corner of the barge. These windlass platforms interfere with the deckhouse in the aft portion by as much as 9 ft. Platform structural scantlings below the platforms must be increased to support the weight and mooring loads. The large fairleaders on the barge sides require adequate foundation structure as well.

Below deck the chain lockers interfere with certain spaces between the main deck (El. 89) and the second deck (El. 65). Aft on both sides the chain lockers interfere with electrical and engineering workshops (El. 65) and future electrical spaces (El. 77). The chain lockers forward interfere with platform equipment and thruster access spaces port and starboard.

2.8.2 CWP

The anchor legs are generally well clear of the CWP in all but the Extreme Sea State. In this condition the active tensioning required to reduce leg tension causes leg No. 5 to be "slack" (see Fig. 2-1). This leg is "down current" and is 275 ft from the CWP inlet. The leg and CWP will touch if the CWP deflects in the current and or the dynamic oscillations of CWP and MAL are of sufficient magnitude and phasing to result in relative motion of 275 ft. This leg is essentially vertical at the platform so that the chafing chain is likely to contact the barge side plating.

2.8.3 Riser Cables

The watch circle of the barge is restricted by the allowable bend radius and tensions in the riser cable. Several riser cable concepts are presented in the Task II report which are compatible with the MAL. The direct descent catenary cables attached to the barge on the landward port side and descending to the seafloor between anchor legs 6 and 7 provide the least potential for interference between the MAL and ETS. The distance between the anchors on these legs is 2,800 ft, which would appear to be adequate to locate four riser cables connected to submarine cables on the seafloor, approximately 2 miles to shore. The touchdown point of the anchor legs is 1,700 ft to seaward of the riser cable touchdown point, minimizing cable-anchor leg interference.

2.9 SENSITIVITY TO REQUIREMENTS

The sensitivity of the MAL to design requirements is discussed, particularly in the area of environmental forces, depth and watch circle variation.

2.9.1 Forces

MAL sensitivity to errors in environmental load magnitude is examined by assuming that the wave drift force is exceeded by 25 percent of the design mean wave drift force in the Extreme Sea State. In this sea state the resultant force increase is 160,000 lb, which, added to the total force of 1.61×10^6 lb, causes an increase in leg tension of 160,000 lb. The resultant safety factor is 2 with active tensioning applied to increase anchor leg length, and 1.6 without active tensioning. This level of sensitivity highlights the importance of adequately predicting wave drift force. In addition, other loads of lesser magnitude such as vortex-induced loads on the anchor leg require further investigation in establishing anchor leg fatigue life. While the MAL has sufficient strength for loads higher than the design loads, the design safety factor is not realized for loads in error by more than 25 percent of wave drift force, or 10 percent of total sea state force.

2.9.2 Water Depth

The effect on the MAL of increasing water depth is to increase the required length of anchor leg. The longer the anchor leg, the greater the vertical component of tension at the barge. This penalizes the MAL since a greater fraction of the wire and chain breaking strength are required to support self weight. The limiting depth is the depth at which the chain can just support its weight. This depth is approximately 7,000 ft during wire rope replacement with an adequate safety factor.

In the case of a bottom slope of 15 deg, an increase in water depth from 5,140 to 6,140 ft results in a decrease in range to the anchor of 700 ft (5,600 to 4,300 ft) for constant horizontal restoring force (Section 2.2.2). Considering that the longest chain is 5,880 ft in this design with a mean water depth of 4,000, it is estimated that the limiting mean depth for the MAL is approximately 5,100 ft. This depth is greater if the sea floor is not sloped.

2.9.3 Watch Circle

The MAL is designed to constrain barge excursion to less than 400 ft in the Operational Sea State. Maximum excursion is 340 ft with a horizontal tension component of 300,000 lb. If the watch circle requirement is made less restrictive, this tension can be reduced with an equivalent reduction in anchor leg scantlings. For example, doubling the allowable excursion to 800 ft, or 20 percent of water depth, reduces the horizontal tension to 100,000 lb, or a 67-percent reduction of the design value. This leads to a 23-percent reduction in maximum tension if wire rope and chain size are unchanged. A reduction in the vertical tension component is achieved by reducing the cross-section of wire and chain. Although some reduction may be realized, the requirement to provide an adequate safety factor in the Extreme Sea State remains. Citing the example of the alternate MAL design (Section 2.4), there is relatively little sensitivity of MAL size and cost to allowing greater watch circle.

2.10 COMMERCIAL PLANT SKSS

The applicability of the MAL Active Tensioning SKSS to the 400-MW(e) Commercial Plant is addressed in this section. An estimate of environmental loads for the specified commercial ship concept is obtained and the required extrapolation of the MAL is indicated.

2.10.1 Environmental Loads

The principal characteristics of the Commercial ship concept specified for the study are given in Table 2-14 and a profile sketch is given in Appendix C, together with details of the loads analysis. The sea states and site are assumed to be identical to the specifications for the smaller OTEC barge. A summary of the environmental loads on the ship is presented in Table 2-15. The applied force is approximately three times that on the smaller barge.

Table 2-14 PRINCIPAL CHARACTERISTICS OF THE 400-MW (NET) SHIP OTEC PLATFORM

Length	620 ft (189m)
Beam	300 ft (91m)
Depth	85 ft (25.9m)
Draft	45 ft (13.7m)
Operating Displacement	310,000 L.T. (314,900 metric tons)
Principal Hull Material	Mild Steel
Cold Water Pipe System	
Inside Diameter	100 ft (30.5m)
Material	Mild Steel
Connection	Pinned (zero rotational stiffness)

Table 2-15 COMPARISON OF COMMERCIAL PLANT VS. PILOT PLANT LOADS

Heading	Sea State Return Period (years)	Force (10^6 lb)		Yaw Moment (10^6 ft-lb)	
		Pilot	Commercial	Pilot	Commercial
Head	3	0.38	1.22	-	1.1
Head	100	0.97	3.06	-	3.8
Beam	3	0.69	1.86	-1.0	-1.9
Beam	100	1.61	4.75	1.3	-2.7

2.10.2 Application of the MAL Active Tensioning SKSS

The MAL design has adequate strength and holding power to hold the Commercial Plant in sea states of return period of 3 years and less, with watch circle excursion of approximately 704 ft or 18 percent of depth. In higher sea states the greater loads on the Commercial Plant result in both overstressing the anchor legs and anchor slippage.

The MAL is capable of modification required for satisfactory performance as a Commercial Plant SKSS. One option is to increase the diameter of anchor leg components to provide the required breaking strength. The estimated anchor leg tension in the MAL under the Commercial Plant load in the Extreme Sea State is in excess of 3×10^6 lb (Fig. 2-30). The required anchor leg breaking strength is therefore in excess of 6×10^6 lb. Anchor chain is available in continuous length with a diameter up to and including 6-3/4 in., and strength of approximately 6×10^6 lb. Wire rope is available at least to 11 in. in diam with a strength of approximately 10×10^6 lb with a maximum continuous length of 1,100 ft.

Design and fabrication of a windlass which has a pulling capacity of 3×10^6 lb, twice the pull of one of the larger existing windlasses, would represent a significant step forward in the state of practice. Significant handling requirements are imposed on the deployment barge deck machinery. The

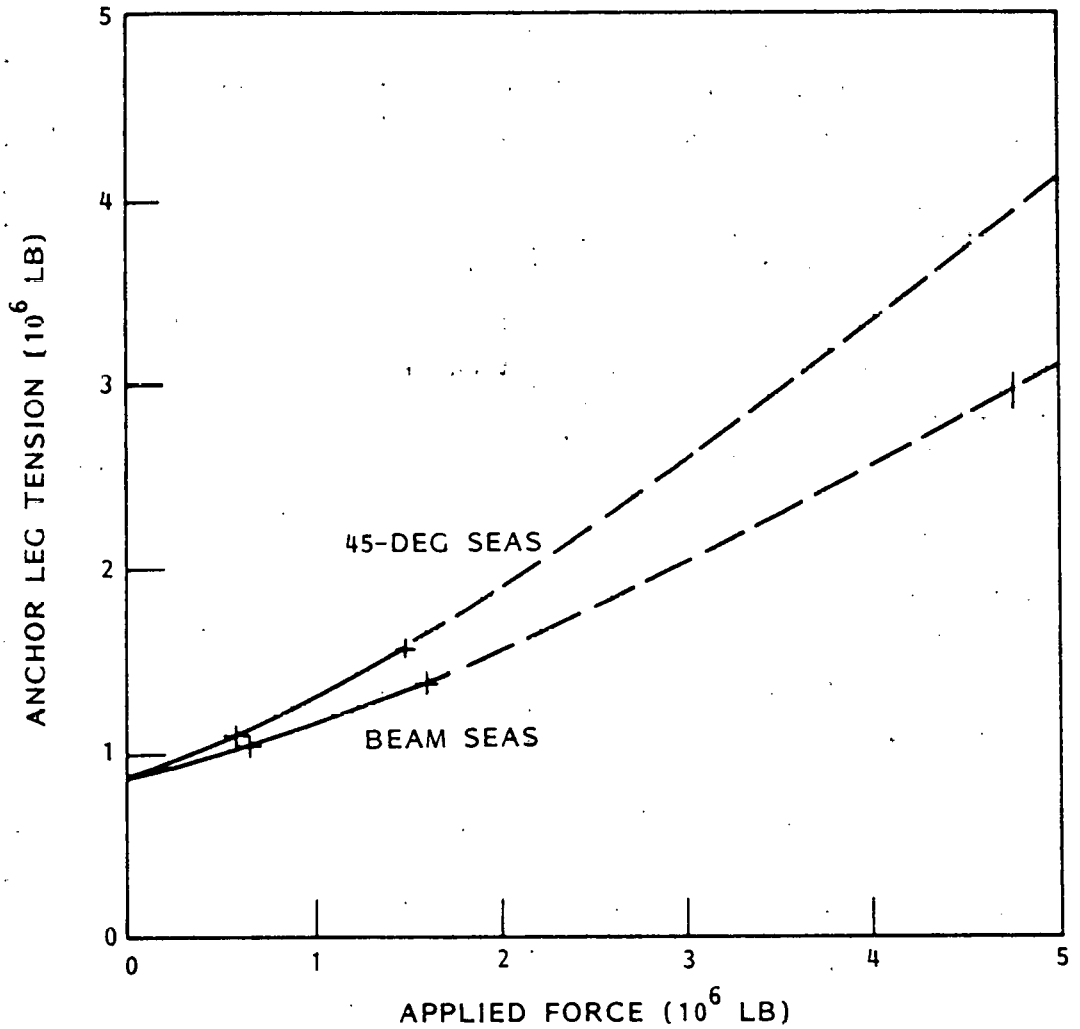

Fig. 2-30 Extrapolation of MAL SKSS to Higher Applied Force - Extreme Sea State

wire rope linear winch pull capacity of approximately 3×10^6 lb is a threefold increase in present capacity. This approach leads to anchor leg components that are at the limit of existing production capability, and to deck machinery pulling capacity which is significantly beyond existing capacity.

A second design approach to the Commercial Plant MAL is to increase the number of legs from eight to a number that is sufficient to carry the loads without increasing the breaking strength of each leg. A first estimate of the number of legs for the Commercial Plant MAL is 24, or an increase of 16 legs. Although this approach requires minimal extension of manufacturing capability, it does impose a requirement for operation and maintenance of 24 windlasses. This requirement is reduced to less than 24 windlasses if anchor leg strength is increased by selecting larger scantlings. The deck machinery is not required if the active tensioning feature of the MAL is not necessary for the Commercial Plant.

The MAL with active tensioning is applicable to the Commercial Plant SKSS by increasing the number of anchor legs. The resultant large quantity of windlasses on the Commercial Plant is excessive and an alternative aproach to active tensioning is needed. To effectively develop the SKSS, the requirements of the Commercial Plant SKSS, assumed here to be that of the smaller pilot plant SKSS, must be determined. In particular, the need for active tensioning requires consideration and comparison with potential benefits. The large beam of the Commercial Plant, significantly greater than that of existing platforms of comparable length, affects response in a seaway, so that motions in a beam sea, for example, must be compared to head sea response to assess the heading most favorable to motions and accelerations.

2.10.3 Development Program

A hardware development program for the Commercial Plant MAL is not recommended at this time. Definition of SKSS performance and operation requirements is

necessary before component sizing and development needs can be identified assist in assessing the requirement for active tensioning. A scale model test program is recommended. The objective of conducting these tests is to determine the importance of plant heading on seaway response. In the event that these tests indicate responses are relatively insensitive to heading, the requirement for heading control and for the extensive deck machinery is reduced or entirely removed.

2.11 REFERENCES

2.11.1 Cited References

2-1 Lockheed Missiles & Space Company, Inc., Preliminary Design for OTEC SKSS, Task II Final Report, LMSC-D676379, 27 Jul 1979

2-2 A. E. Loken and O. A. Olsen, "The Influence of Slowly Varying Wave Forces on Mooring Systems," Offshore Technology Conference Paper No. 3626, Houston, Texas, May 1979

2-3 D. E. Hairston, "Dynamics of Vessels Moored by Multiple Cables in Deep Waters," Marine Technology, Vol. 16, No. 2, Apr 1979

2-4 R. L. Webster and W. R. McCreight, "Analysis of Deep Sea Moor and Cable Structures," Offshore Technology Conference Paper No. 3623, Houston, Texas, May 1979

2-5 W. H. Michel, "Sea Spectra Simplified," Marine Technology, Jan 68

2-6 Civil Engineering Laboratory, Corrosion of Metals and Alloys in the Deep Ocean, by F. M. Reinhart, T. R. R834, Port Hueneme, California, Feb 1976

2-7 U.S. Naval Research Laboratory, Theoretical Considerations in the Cathodic Protection of Wire Rope, by M. H. Peterson, NRL Memo Rpt 1301, Wash., D. C., Apr 1962

2.11.2 Uncited References

- L. R. Glosten and Associates, Comprehensive Seakeeping Report for the OTEC Pilot Plant Ship Phase III, 811 First Ave., Seattle, Washington, Sep 78
- Lockheed Missiles & Space Co., Mathematical Modeling of Marine Riser Systems, by R. Cowan, Sunnyvale, Calif., Sep 78
- -----, Dynamics of Planar Cable-Body Systems, by J. V. Rattaya, Sunnyvale, Calif., Apr 73
- Lockheed Missiles & Space Company, Inc., OTEC SKSS Task I Design Requirements, Sunnyvale, Calif., Jun 79
- Department of Energy, OTEC Demonstration Plant Environmental Package, Washington, D.C., Dec 78
- A. Palmgren, "Die Lebensdauer von Kugellagern," Zeitschrift des Vereins Deutscher Ingenieure, Vol. 68, Nr. 14, Apr 1924
- M. A. Miner, "Cumulative Damage in Fatigue" J. Applied Mechanics, ASME Vol. 12, No. 3, Sep 45
- F. Matango, Jr., "Axial Fatigue Testing of Wire Rope," Marine Technology Society Journal, Vol. 6, No. 6, Nov-Dec 1972

Section 3
PRELIMINARY DESIGN OF TENSION ANCHOR LEG SKSS FOR OTEC SPAR

3.1 BACKGROUND

The mooring system design is based on a tension anchor leg (TAL) system composed of spar and cold water pipe (CWP) previously designed in other studies.

These are outlined as follows:

1. SPAR. A spar vessel designed by Gibbs & Cox was assumed in the design. A simplified geometrical model is shown in Fig. 3-1.
2. CWP. A Brown and Root CWP design was assumed for the mooring system design. There were originally five sections in the CWP and a tension leg between the inlet and the mooring base. Each section is made of a stiffened cylindrical shell. The sections are connected by universal joints of an unspecified design. The CWP sections are of varying length with the longest sections closer to the bottom.

The following information on the CWP was provided in the early stages of the preliminary design:

CWP structural weight	15,000 kips
CWP and CWP buoy net buoyancy	6,000 kips
CWP buoyancy tank weight	2,400 kips
CWP buoyancy tanks	8 x 15 ft diam x 200 ft long

Since the water depth for the preliminary design is reduced from 4,000 ft to 3,280 ft, the lengths of the CWP sections had to be reduced. The lengths of each section were proportioned using a procedure developed at LMSC. The assumed CWP geometry and characteristics are shown in Fig. 3-2.

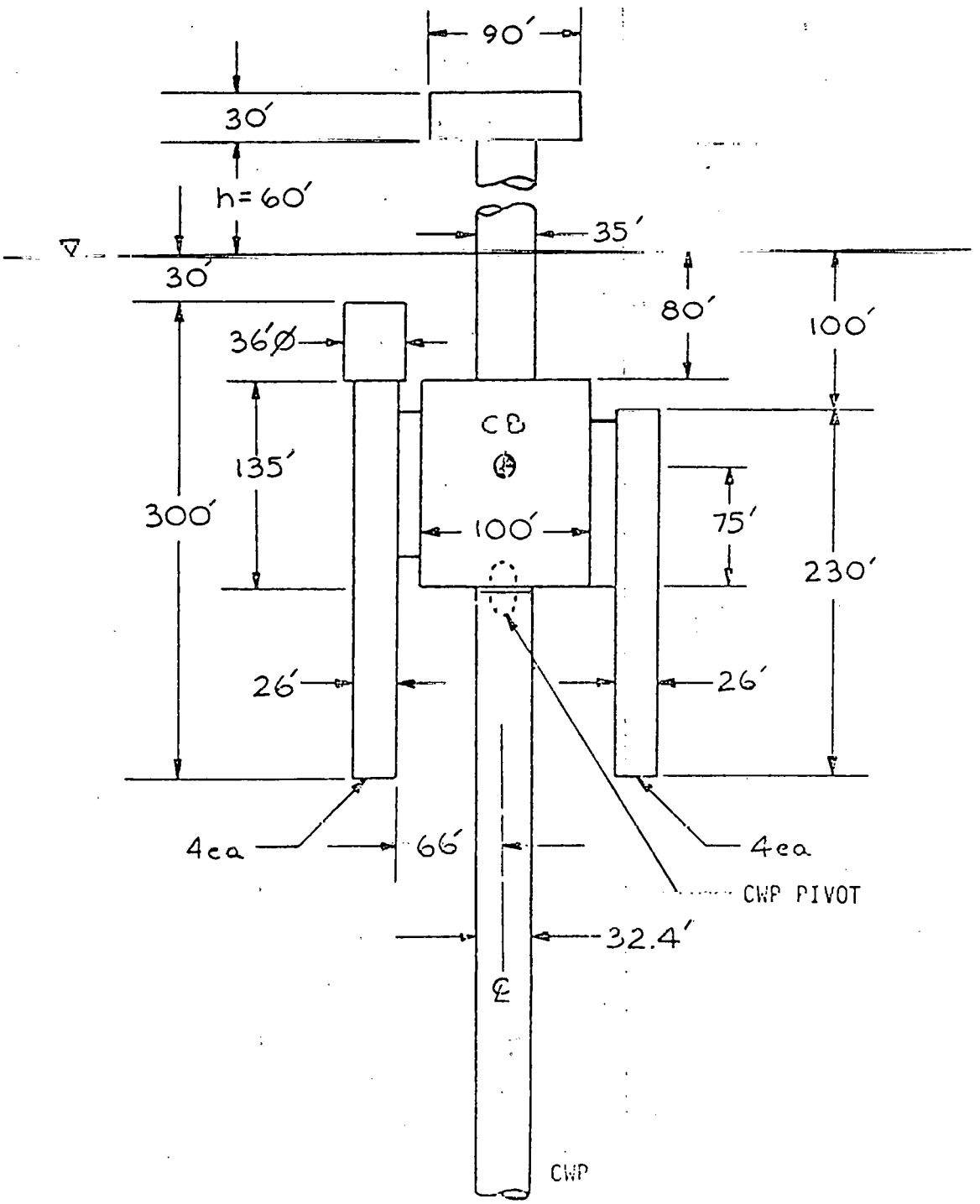

Fig. 3-1 OTEC Spar Dimensions

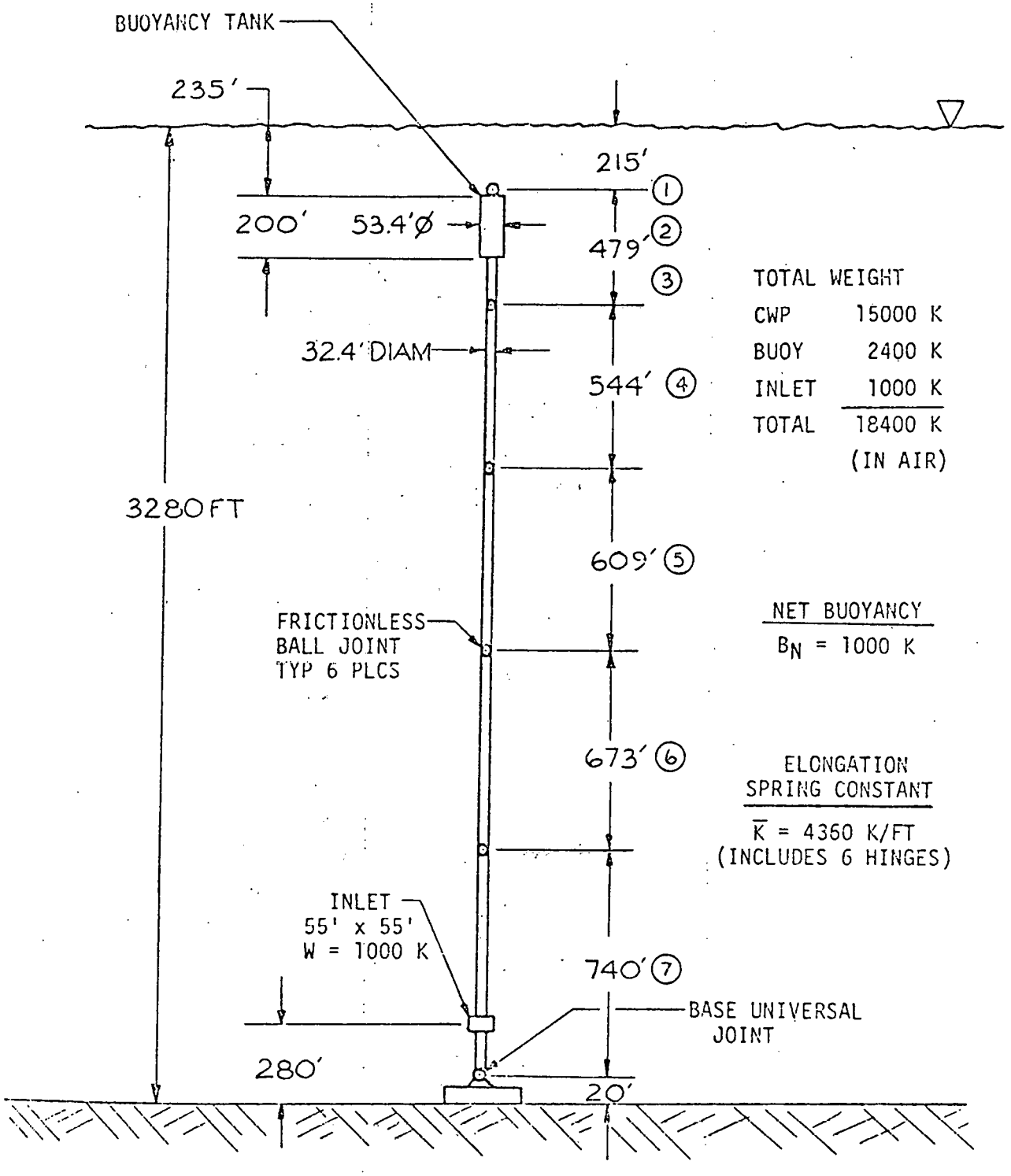

Fig. 3-2 OTEC CWP and Buoy

3.2 SPAR TAL GENERAL DESCRIPTION

The spar vessel, shown in Fig. 3-3, consists of a main body (containing the power plant) and eight vertical modules (containing the four evaporators and four condensers). The discharge pipes attached below the modules may be fabricated of flexible materials. An elevated platform structure is held above the water surface by a 35-ft-diameter cylinder projecting from the main body of the spar.

A hinge under the spar connects it to the top of the CWP. Net positive buoyancy in the spar maintains a constant tension in the hinge during still-water conditions.

The cold water pipe sections consist of a steel cylindrical shell with vertical and transverse stiffeners on the outside of the CWP shell. The stiffeners consist of bulb flat, angle, or wide flange sections. In the design it was considered that the shell would be 30 ft in diameter with external stiffeners that would increase the effective diameter to 32.4 ft.

The bottom section of the CWP extends down to the mooring base universal joint. The CWP inlet is located within this section of pipe. Due to the short distances between the inlet and the base (280 ft) it was not considered economical to place an extra universal joint under the inlet. The extra cost of such a universal joint would have had to have been offset by a reduced cost in the tension member of the lowest CWP section. Since bending moments are less critical near the bottom, little stress reduction in either member would have resulted from adding an extra universal joint.

The universal joint at the base allows angular motion between the CWP and the base, while transmitting the tension between the CWP and the base.

The mooring base consists of a steel shell and frame, filled with cement grout. Mooring loads are carried by the weight of the base and by friction between the base bottom and the soil. The TAL is shown in elevation in Fig. 3-4 and in isometric in Fig. 3-5.

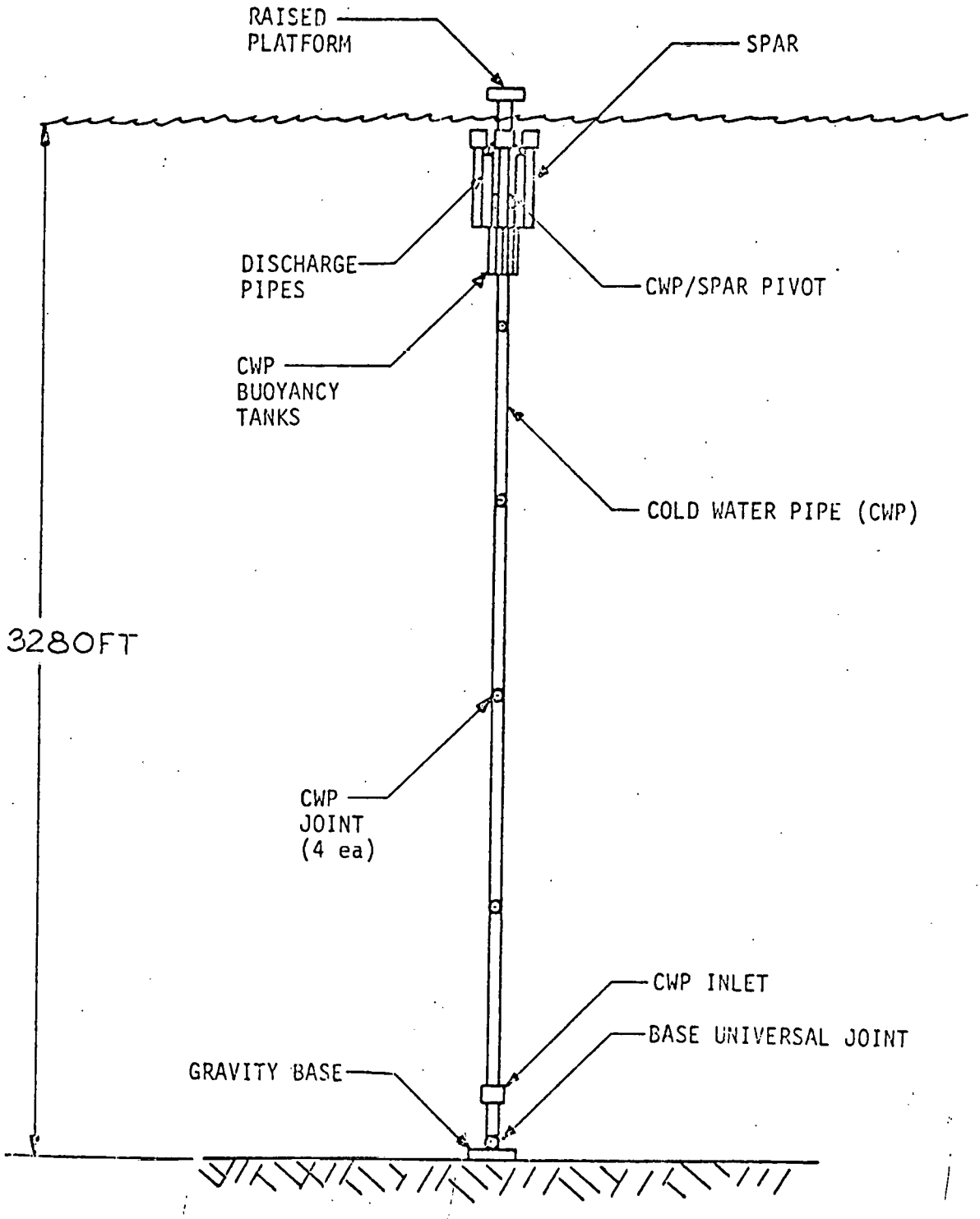

Fig. 3-3 OTEC Spar TAL

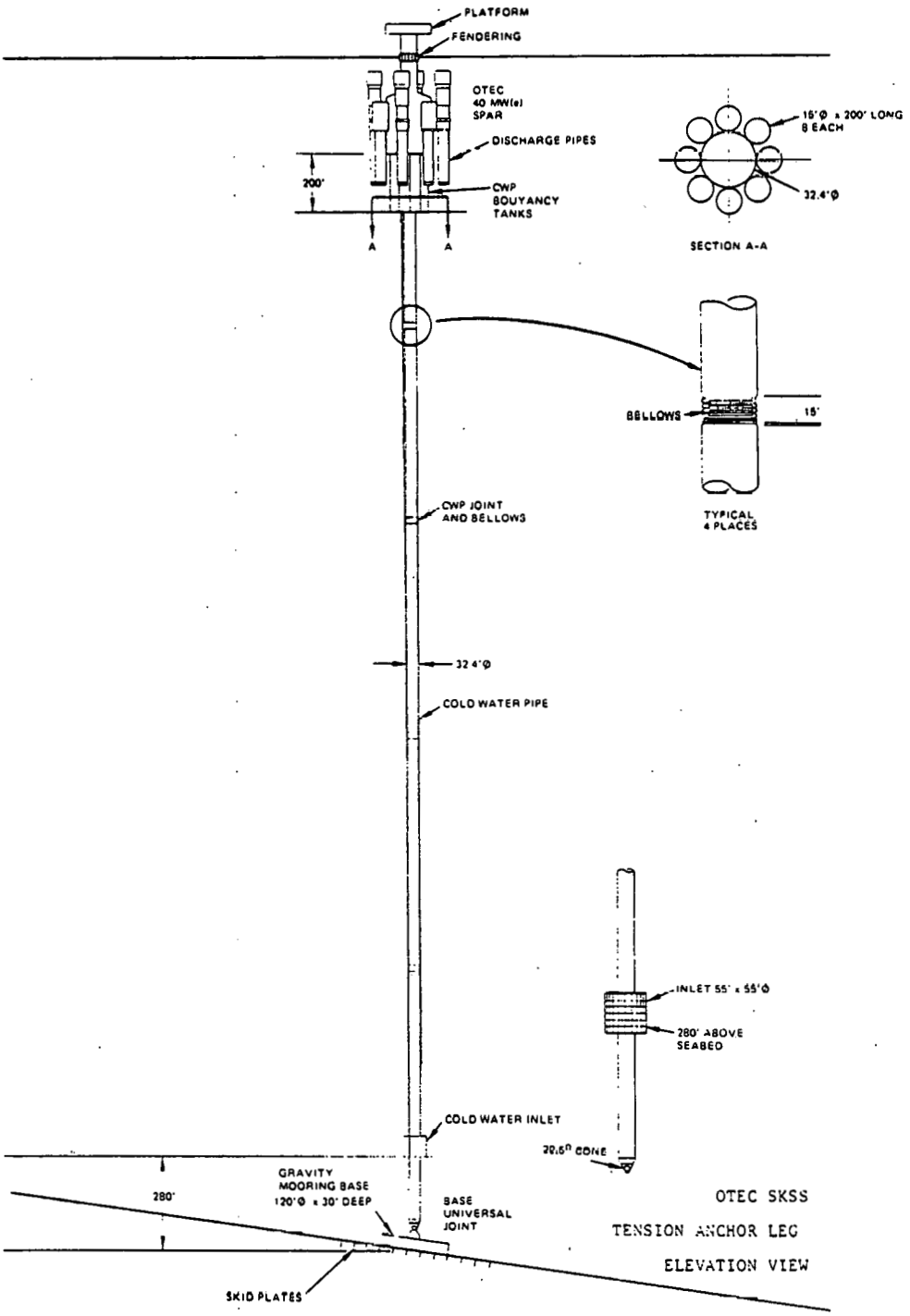

Fig. 3-4 OTEC SKSS Tension Anchor Leg Elevation View

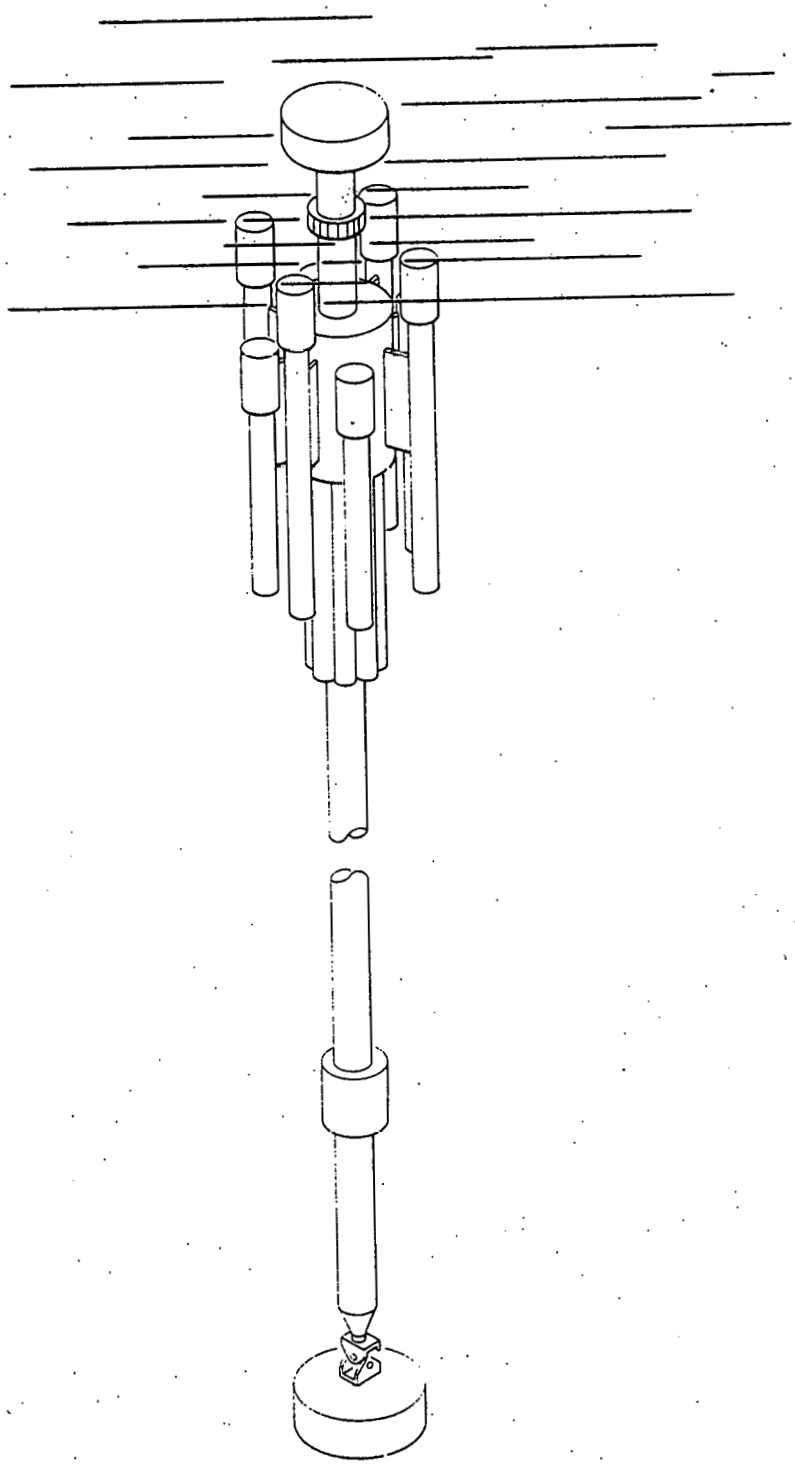

Fig. 3-5 OTEC Spar SKSS Tension Anchor Leg

3.3 SYSTEM LOAD ANALYSIS

3.3.1 General Description

External loads on the spar and CWP are caused primarily by wind, waves, and current.

3.3.2 Spar-CWP Models

The spar vessel, shown in Fig. 3-1, is simulated by a simplified model as shown in Fig. 3-6. In this model, the volumes and lengths are the same as for the actual spar. The vertically projected areas are also the same. Thus buoyancy and wave inertial forces will be similar.

It is assumed that the spar is a rigid body with no water flow across its boundaries. In reality, however, the discharge pipes may be flexible and "give" during wave action, which would reduce the loads. The flow in the discharge pipes could also affect the vertical wave forces. For example, if the discharge pipes were left open at the top and bottom, the wave forces on the projected areas at the top and bottom would act to accelerate the water in the discharge pipes rather than act upon the spar structure. Allowing the enclosed water to move in the storm wave would reduce the vertical loads in the spar. But since the pumps, condenser modules, and evaporator modules will restrict the vertical flow, the entrapped water is treated as being part of the spar. This water will add to both the buoyancy and the weight of the spar. The buoyancy will be proportional to the volume of the spar module, and the weight will be assumed to be whatever value is required to provide the net buoyancy of the spar.

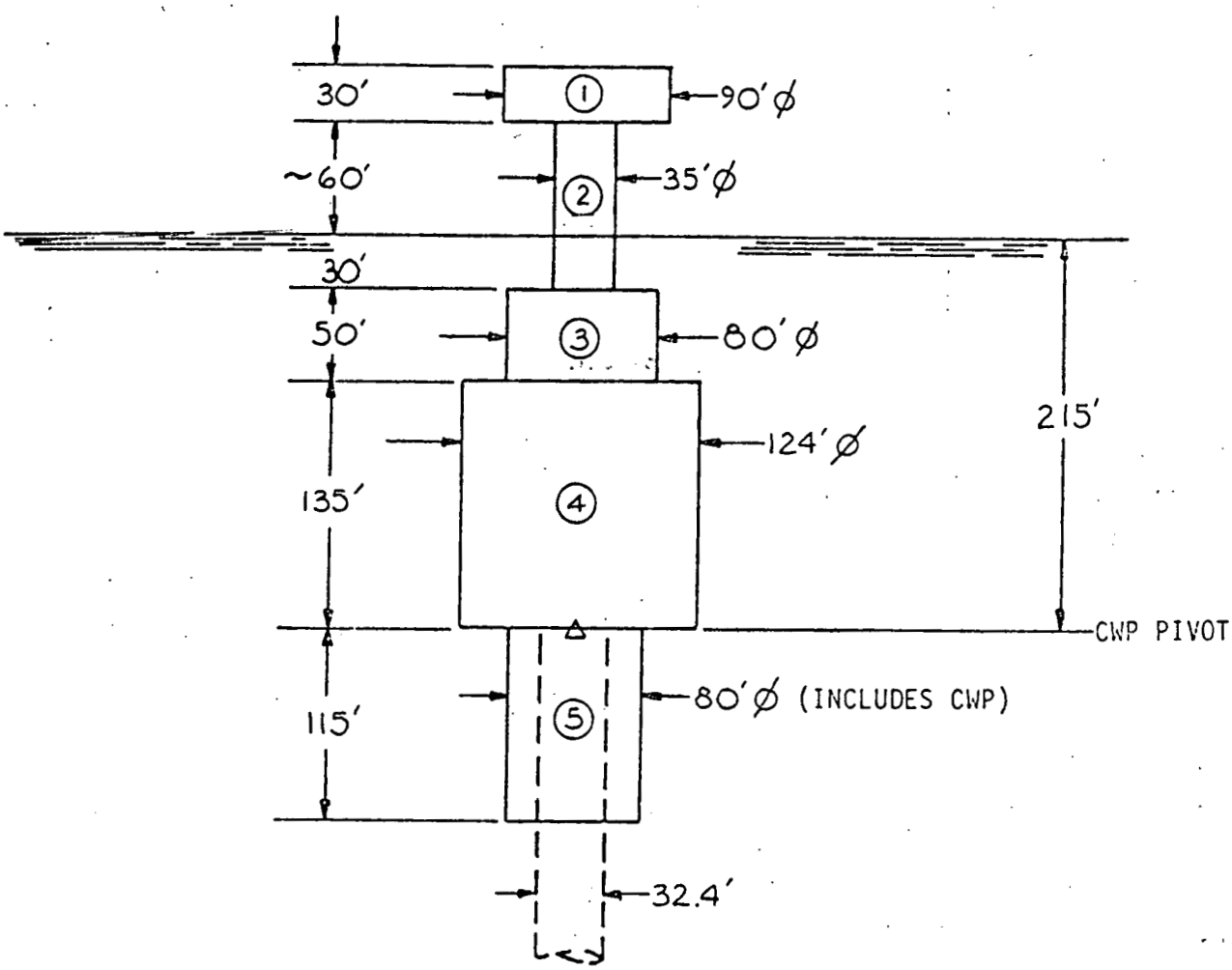

DIAMETERS PROVIDE SAME VOLUME AS REAL SPAR
(INCLUDING ENTRAPPED WATER)

Fig. 3-6 OTEC Spar Wave Load Model

The change in geometry affects the projected areas of the spar as seen from the front or side. This can be accounted for analytically by using a larger coefficient of drag, as seen in Table 3-1.

The CWP model, shown in Fig. 3-2, also models equivalent volumes. The diameter of the CWP is 32.4 ft, which includes 30 ft for the shell plus an additional diameter for the external stiffeners. These stiffeners will act to entrap the water and to increase the added mass value of the CWP and the projected areas for drag.

The mass of water in the CWP is assumed not to act with the CWP when calculating vertical motions. For horizontal motions it contributes to the mass, buoyancy, and weight of the CWP.

If the mass of the water in the CWP were to accelerate vertically with the spar, it would cause higher pipe stresses. If the spar moves sinusoidally with a 5-ft amplitude and an 8-sec period, for example, the maximum vertical acceleration would be 0.1 g.

To accelerate the 4,300 kslugs of water enclosed in the CWP to this value, assuming that water is an incompressible fluid, a force of 13,244 kips would be required, resulting in a water pressure change of 130 psi at the top of the CWP. Since the ambient water pressure at the upper pivot is 96 psi, an upward acceleration of the spar could cause vaporization of the water in the CWP. A downward acceleration will cause a hoop stress of approximately 30 ksi in the CWP shell. Therefore it could be an advantage to unseal the CWP at its upper end to decouple the water inside from the spar motions during the 100-year storm. This was assumed for the analysis herein.

This assumption could be self-fulfilling in that if the mass of the water were included, it would reduce the spar motions to a degree that these effects would not occur. A more detailed analysis would take this into account, treating the water as a compressible fluid.

Table 3-1 OTEC SPAR WAVE LOAD MODEL

CYL NO	DIAM FT	LENGTH	STILL WATER BUOY (KIPS)	HORIZONTAL		VERTICAL	
				C_m	C_D	C_M	C_D
1	90	30	0	—	.6	—	—
2	35	90	1847	2	.6	1.2	1.0
3	80	50	16085	2	1.5	1.2	1.0
4	124	135	104340	2	1.05	1.2	1.0
5	80	115	31654	2	.8	1.2	1.0

TOTAL DISPLACEMENT + 153900 KIPS AT DWL*

TOTAL WEIGHT = 152900 KIPS IN-AIR*

NET BUOYANCY = 1000 KIPS AT DWO

CG AT 20 FT ABOVE CWP PIVOT

* INCLUDES WATER IN DISCHARGE PIPES, AND IN THE TOP 115' OF THE CWP.

3.3.3 Wave Drift Forces

The wave drift forces on floating objects are the least known of the hydrodynamic forces. These forces are caused by the reflection and refraction of waves by the body, and by higher order wave motions such as the drift velocity. Much work has been done on predicting these forces, both theoretical and model testing. There is usually a great deal of discrepancy between the results of different methods. This scatter occurs even in model test based predictions because, although the wave surface effects are modeled correctly, the second order drift effects are usually left to chance. In other words, the water circulation patterns in different test basins can cause different wave drift forces.

In general most wave drift equations are for barge or ship shapes. Several of these equations were used to predict the drift forces on the spar. The results are shown in Table 3-2. Another method was used to predict the wave drift force on the spar, using a procedure described in Ref. 3-1, and described in Section 3.3.5 of this report. The spar has a displacement equivalent to that of a 55,000 DWT oil tanker when completely loaded. The spar and tanker were assumed to have equivalent wave drift forces. Although the spar has a greater projected area than an equivalent displacement tanker, this may be balanced by the fact that the majority of the spar displacement is located under the region of intense wave activity. A second prediction based on empirical formulae for circular cylinders yields a comparable force. Model tests are the most reliable method for deriving wave forces and are required to verify the given assumptions.

From model test graphs of significant wave energy versus tanker size and wave height, it was determined that a 35.1-ft significant wave will impart a significant wave energy of 10,100 kips-ft to the spar. A significant horizontal force must be found to absorb this energy with the spar buoyancy. Given a net buoyancy of 2,000 k, the horizontal stiffness of the spar CWP system is approximately 2.6 kips per foot of horizontal displacement. If

Table 3-2 WAVE DRIFT FORCES

Method Reference	Drift Force	Comments
Oceanographical Engineering Wiegel, p. 273	358 kips	Neglects Fluid Viscosity
OTC Report No. 1741	625 kips	For Ship Shapes
Task II Report LMSC-D676379 p. 2-4	648 kips	For Barge Shapes
Task III Report LMSC-D678771 p. A-6	430 kips	API Formulae for Cylinders

linearity is assumed for the horizontal force, the horizontal force required to absorb an energy of 10,110 kips-ft is F_H = 230 kips.

The wave drift force on the spar is assumed to be 250 kips during the 100-year storm. This is a significant value rather than an average value.

3.3.4 Wind and Current Forces

Wind forces are usually calculated using the 1 minute average of the maximum wind occurring during the 100-year storm. In this report, a sustained maximum value was used. The maximum current is based on the superimposed tidal, storm, and wind-driven currents occurring during the 100-year storm.

The drag term of the Morison equation is used to calculate both wind and current forces.

$$F = \frac{1}{2} \rho V^2 AC_d$$

The projected area of the portion of the spar which is above the water is 4,800 ft^3.

The maximum velocity is:

79.1 knots

79.1 knots x 1.689 ft/sec/knot = 133.6 ft/sec

The coefficient of drag was given in the Task 1 Report as 0.8. The maximum force on the spar due to the wind is 81,451.7 lb.

The force on the spar caused by the current is calculated using the procedure used for the wind force, with a C_D of 0.6. Total projected area is found for each different section.

Average Velocity (ft/sec)	Area (ft^2)	Force (lb)
4.0536	105	10,400
3.969	3,050	28,800
3.88	20,520	185,800
3.7156	12,121	100,400
3.5469	4,539	34,300
TOTAL		360,000

Current forces are calculated using the average current over each segment of the cold water pipe.

Length (ft)	Area (ft^2)	Average Velocity (ft/sec)	Force (lb)
279	9,765	2.36	54,387
544	19,040	1.52	43,990
609	21,315	1.01	21,743
673	23,555	0.69	11,214
740	25,900	0.17	748
TOTAL			132.1 kips

The sum of the wind and current forces over the entire structure is 573,000 lb.

3.3.5 Horizontal Load Analysis

Moment Balance - CWP as a Rigid Body. The watch circle can be calculated by balancing the moments around the bottom universal joint caused by the current, wind, wave drift, buoyancy, and weight. The angle at which the sum of the moments caused by these maximum forces equals zero is the maximum average angle the system will obtain. There will be some fluctuation about this position due to the waves passing by. The flexible cold water pipe and spar are modeled as a rigid body. It is assumed that this rigid model approximates

the deflected shape of the flexible pipe when exposed to storm conditions. The small variations encountered will not change significantly the magnitude of the forces. Because the buoyancy of the spar is not fixed at this stage of the design, it is best to draw a curve of the watch circle that will result for a range of buoyancies. The influence of the buoyancy on the watch circle can then be studied and an optimum buoyancy calculated. Summing the moments around the bottom universal joint gives the equation relating the buoyancy of the spar to the angle.

$$\text{Buoyancy} = 122{,}000/\tan\theta + 9{,}410{,}000$$

The total in-air weight of the cold water pipe is 18,400 kips. The weight in water is 15,989 kips. Therefore the net buoyancy of the spar and cold water pipe buoy must be at least 16,000 kips to keep the pipe in tension. As can be seen by the graph of net buoyancy vs. angle (Fig. 3-7), any increase in buoyancy above 23,000 kips does not add much stability. The increase in tension due to an increase of buoyancy over 23,000 kips is not justified by the small increase in stability. A satisfactory amount of net buoyancy is the minimum amount that will keep the cold water pipe in tension under all conditions. The maximum average angle the system will tilt at a buoyancy of 23,000 kips is 5 deg. This equals a horizontal displacement at the water surface of 287 ft, and a watch circle of 8.75 percent.

The preceding analysis is based on a net drift force. In reality a random oscillation will occur about the mean angle; this is calculated in the following sections.

Energy Procedure for the Determination of Horizontal Loads and Motions. To design the components of the Spar-TAL a reliable set of design loads must be calculated. Design loads for single point moorings are usually derived by a procedure that combines empirical and analytical methods. The mooring system of a specific project can be model tested prior to a final design.

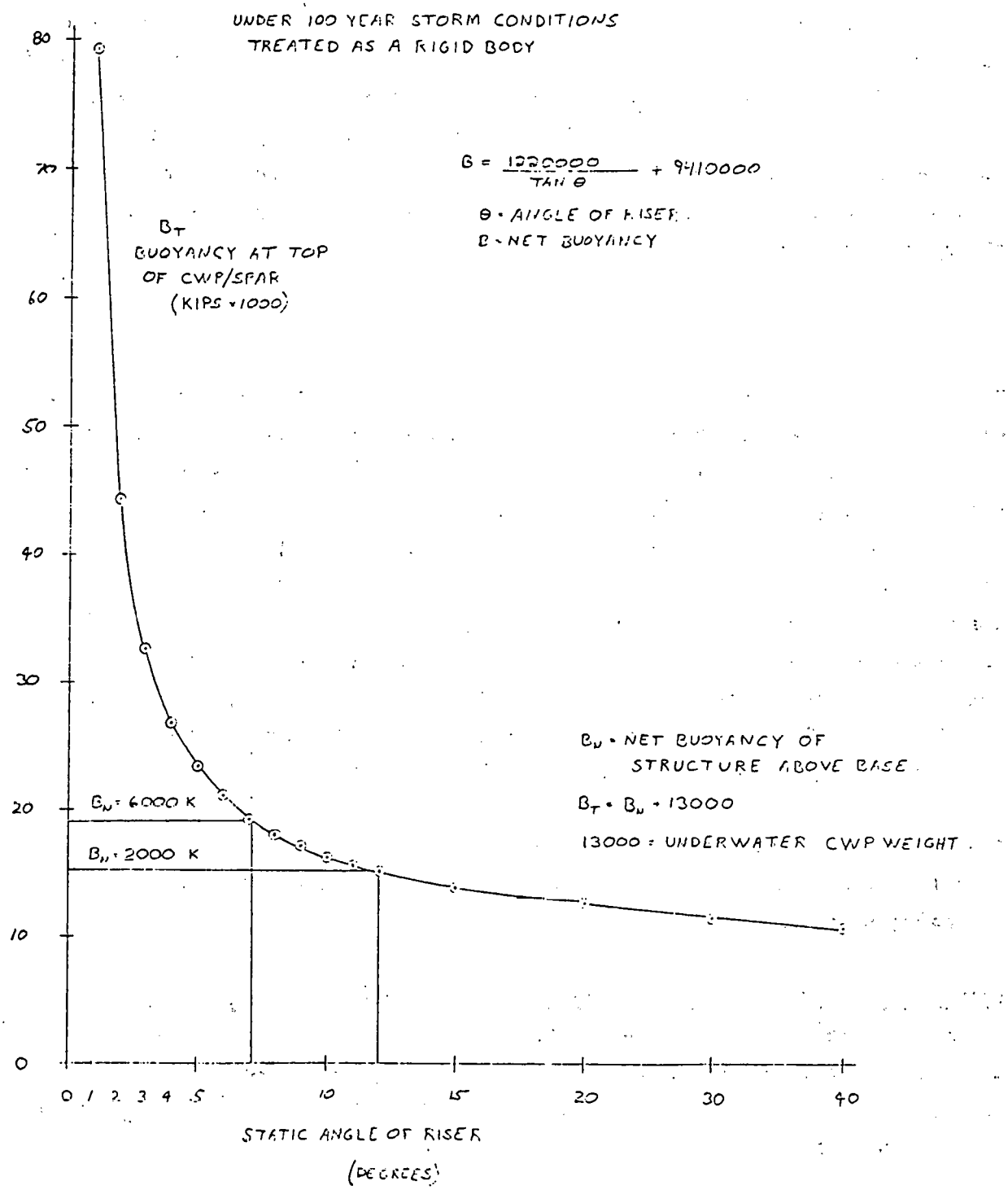

Fig. 3-7 Buoyancy of Spar vs. Static Analysis of CWP/Spar

The preliminary design loads for the SKSS were derived using a procedure similar to that described in Ref. 3-1. This procedure is outlined as follows:

1. A "significant" energy imparted to a tanker by the waves is found from model-test-generated curves. (The significant energy is related to significant wave height, which is defined as the average of the one-third highest waves in a spectrum.)
2. The wind and current static force on the tanker is calculated.
3. The static force-deflection curve of the mooring is found.
4. The horizontal force is found at which the significant energy is absorbed by the system (referred to as the significant horizontal force).
5. A ratio of maximum force to significant force is estimated. This is based on the expected duration of the storm and the desired probability of exceedence.
6. The significant horizontal force and the wind and current force are added, and the sum is multiplied by the above ratio.
7. Design loads and deflections are those occurring at the displacement position at which the horizontal force is equal to the force from Step 6. Maximum system excursions and maximum loads are all derived from this position. (Vertical loads are an exception for the Spar-TAL, and are derived in a later section.)

The above method is a static simulation of a dynamic system, and the results have been verified by model tests. The method is applicable to a wide range of mooring systems (Ref. 3-1).

The steps of the procedure are described in greater detail as follows:

1. Wave Significant Energy. This variable is found from graphs as a function of tanker size, significant wave height, and the tanker ballast condition (20 or 100 percent loaded). In general, the energy goes up with the square root of the tanker tonnage, and with the square of the wave height. These graphs have not been published extensively. As an approximation, a significant energy value can be derived from Fig. 9 of Ref. 3-1, using Froude scaling to correct for tanker size.

2. Maximum to Significant Force Ratio. The ratio of maximum to significant force is based on past model test experience for any mooring configuration being studied. Values usually range between 1.8 and 2.5, depending on the water depth and the degree of confidence desired. The ratios are higher in shallow water, where the motions of the vessel, such as pitch or roll, can have a greater affect on the loads. In deeper water, the mooring system is more flexible and motions do not cause significantly higher tensions. For the OTEC Spar-TAL, a ratio of 1.8 is considered to be a likely value.

Maximum Horizontal Force. The energy procedure is used in this section to determine the maximum horizontal force in the 100-year storm.

The following forces act on the spar during the 100-year storm:

Wave Drift	250 kips
Wind	81 kips
Current	360 kips
TOTAL	691 kips

A ratio of maximum force to significant force of 1.8 is assumed. Therefore, the spar maximum deflected position is that which occurs when a horizontal force of 1.8 (691) = 1,244 kips acts on the spar. This is in comparison to the value of 926 kips computed independently using other techniques (p. A-6); the higher value is used.

The horizontal base load is 1,244 kips plus the horizontal current forces on the CWP sections, 132 kips, for a total of 1,376 kips.

3.3.6 CWP Static Deflected Position

Methodology. Under pure tension, the CWP sections will be colinear, but with a side load on each CWP section the CWP will assume a curved or deflected shape. The distributed weight of the CWP sections also affects the deflected shape.

If the deflections are small, then the current forces on the pipe sections will remain constant and the deflected position is simple to calculate. The methodology used for this computation is demonstrated in Fig. 3-8. The angle of each CWP segment is determined so that the moment about the lower pivot is zero, determined in part by the sum of all the vertical and horizontal forces above the upper pivot.

Maximum Watch Circle Position. Given a horizontal spar force of 1,244 kips, and a distributed current loading, the spar CWP maximum deflected position is derived in Table 3-3.

For a net buoyancy of 2,000 kips in the spar and CWP, the watch circle is 18 percent, and for a net buoyancy of 6,000 kips the watch circle is 11 percent. The original requirement was that the watch circle be less than 10 percent in the operational conditions. The 6,000-kips net buoyancy nearly meets this requirement in the 100-year storm.

The static heave of the spar is also significant for either case. For the 2,000 k net buoyancy, the spar is pulled 67.4 ft under the water by the static loads. This would require an elevation of over 100 ft of the raised platform to prevent submergence. For the 6,000-kips net buoyancy, the submergence is 24.6 ft, requiring a platform height of approximately 70 ft to prevent submergence. For this reason a net buoyancy of 6,000 kips seems more appropriate, and is used except where otherwise noted as in Figs. 3-12 through 16.

These deflected positions are assumed as valid even though dynamic heave affects the CWP angles. This is approximately correct because the maximum heave is associated with the maximum wave, which does not occur at the same time as the maximum displacement. If it did, the energy imparted to the spar would force it over even more.

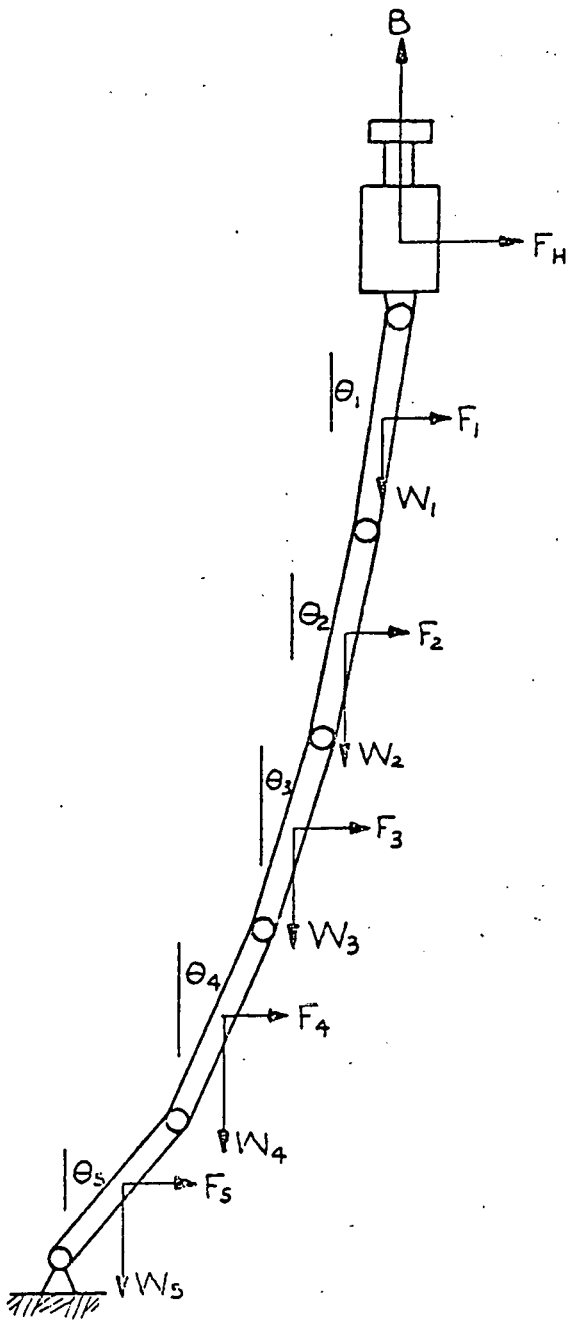

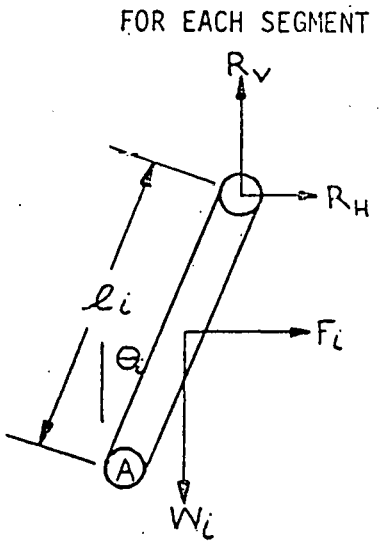

R_H = Σ HORIZONTAL FORCES ABOVE THE SEGMENT

R_V = Σ VERTICAL FORCES ABOVE THE SEGMENT

F_i & W_i ACT AT $\ell/2$

FOR $\Sigma M_A = 0$

$$\tan \theta_i = \frac{\frac{1}{2} F_i + R_H}{R_V - \frac{1}{2} W_i}$$

Fig. 3-8 CWP Static Deflection Methodology

Table 3-3 WATCH CIRCLE DEFLECTION - EXTREME SEA STATE

B_{NET} = 2000 KIPS

CWP SEG	W_i	DRAG F_i	LEN-GTH	R_V	R_H	Θ_i	Δx_i	Δy_i	
1	-12840	78.2	479	1000	1244	9.8°	81.5	6.99	
2	2329	35.7	544	13840	1322	6.03	57.15	3.0	
3	2607	16.4	609	11511	1358	7.6°	80.5	5.35	
4	2881	10	673	8904	1374	10.5	123	11.3	
5	4040	4	740	6023	1384	19.1	242	40.7	
	18%		WATCH CIRCLE				584'	67.4'	

B_{NET} = 6000 KIPS

1	-16840	78.2	479	1000	1244	7.76	64.7	4.4	
2	2329	35.7	544	17840	1322	4.6	43.6	1.8	
3	2607	16.4	609	15511	1358	5.5	58.4	2.8	
4	2881	10	673	12904	1374	6.86	80.4	4.8	
5	4040	4	740	10023	1384	9.8	126	10.8	
	11%		WATCH CIRCLE				373	24.6	

3.3.7 Vertical Load Analysis

The vertical loads in the CWP are of great importance because of their effect on the gravity base and universal joint designs. The basic idea behind the TAL is that the CWP can be used for mooring as well as transmitting cold water. It is hoped that the mooring system would not increase the CWP costs. The tension loads determine whether this will be the case. The tensions are also required for the base and universal joint stresses.

In the analysis of the vertical loads, determined largely by the heave of the spar, it is assumed that the heave motion and response are independent of the other directions.

The heave of the spar is determined mostly by the mass of the spar, the vertical loads on it, the spring stiffnesses of the CWP, and the damping present in the system.

The stiffness of the CWP is highly nonlinear. If the spar moves in the upward direction, it elongates the CWP shell and the universal joints. If the spar moves in the downward direction, the CWP segments will fold at the universal joints and move out of the way, due to the number of universal joints distributed along the CWP. The stiffness in the downward direction will be as great as that in the upward direction only if all of the joints are in a perfectly straight line and do not buckle under a load, which is a very unstable situation. This nonlinear CWP stiffness is demonstrated in Fig. 3-9 which models the CWP as a spring with two stiffnesses. This simplified model is used in the heave dynamic analysis.

The upward heave stiffness is determined by the cross-sectional area of the CWP shell and vertical stiffeners. In addition, the CWP joints also contribute to the CWP total axial stiffness. It is assumed that the stiffness of the joints is the same as the stiffness of the CWP shell and stiffeners. Thus the total stiffness is the CWP cross-sectional area stiffness divided by two.

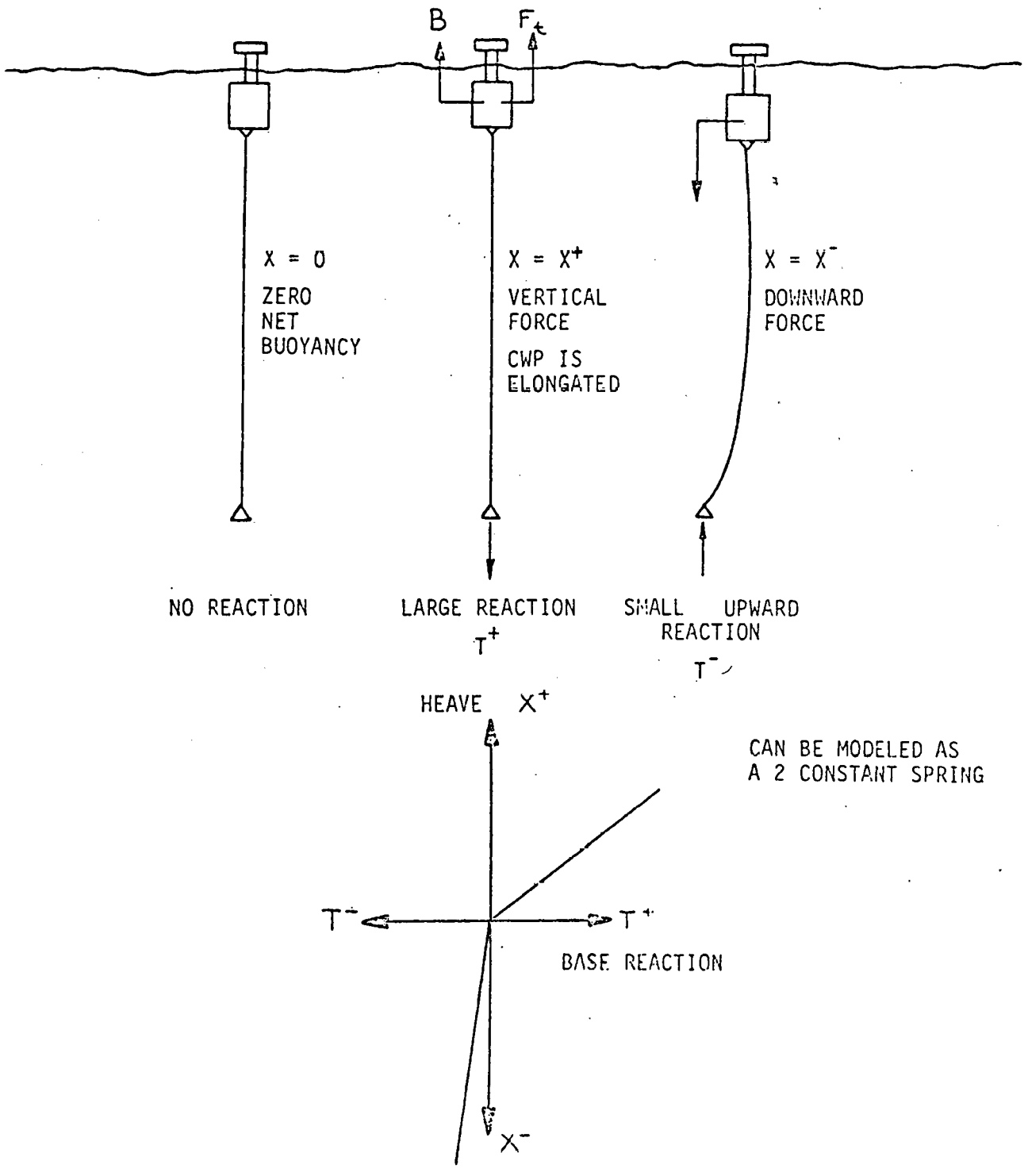

Fig. 3-9 Spar Heave Resistance

The downward heave stiffness could be approximated as zero without much affect on the heave dynamics. A small equivalent stiffness, however, is present which causes a variation of vertical base load with downward spar motion. This occurs because the CWP is lowered onto the seafloor, releasing its weight from the spar and adding it to the base. This is similar to an upward compressive force on the spar. This spring constant is approximated by dividing the underwater weight of the CWP by its length. The coupled pitch and sway response of each CWP section which is expected during spar motion in a seaway are considered in this simplified analysis through the damping force.

Simplified Model. The simplified dynamic model of the Spar-TAL, used to estimate heave motions, is shown in Fig. 3-10. This is a single mass, single degree of freedom system with two springs, each of which can only resist compressive forces. The two springs are the values discussed previously and provide the nonlinear force reactions.

The mass calculated in Fig. 3-10 consists of the spar mass, including the water contained in the discharge pipes; the CWP, not including the mass of the water in the CWP; the CWP inlet; the CWP buoyancy tanks; and added hydrodynamic mass corresponding to 20 percent of the spar mass. The greatest uncertainty in the total mass is the effect of the mass of the water inside the CWP and the added mass effects outside the CWP. The mass of the water inside the CWP is nearly as great as that of the spar itself. The fluid flow path of the power system may force the water to accelerate with the spar, which will increase its apparent mass and probably reduce the motions and the resulting loads. Thus the above mass is a low estimate and is probably conservative.

A damping force proportional to the square of velocity is incorporated into the simplified model. The damping constant has a great effect on the heave motions.

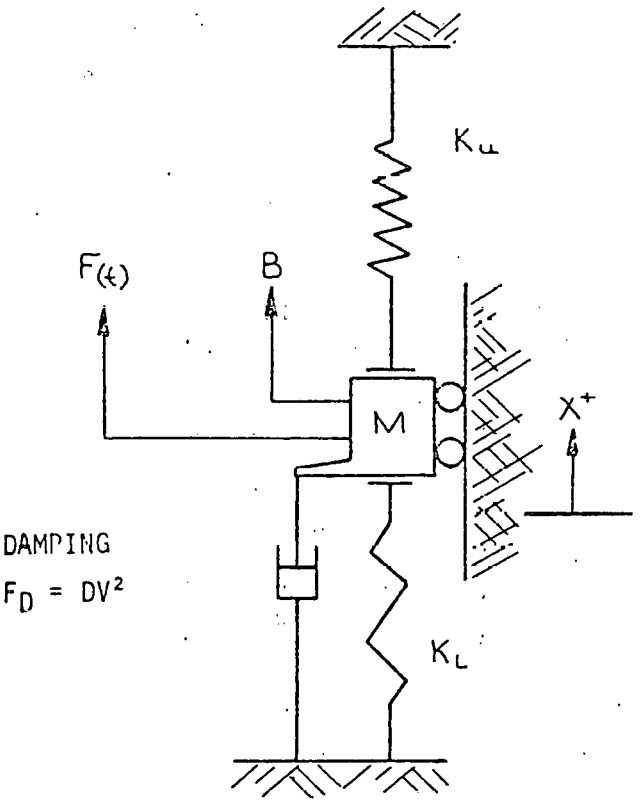

SPAR W	153900 K
	-1000 K
CWP	15000 K
INLET	1000 K
CWP BUOY	2400 K
WATER ADDED MASS	30780 K
TOTAL W	202080 KIPS

SPAR MASS = 6300 KSLUGS = M

K_u = 4360 K/FT

K_L = 4.5 K/FT

K_u = SPRING CONSTANT EQUAL TO AXIAL STIFFNESS OF CWP PLUS U.J.'S.COMPRESSION FORCE ONLY.

K_L = SPRING CONSTANT EQUAL TO WEIGHT OF CWP DIVIDED BY ITS LENGTH. COMPRESSION FORCE ONLY.

B = CONSTANT NET BUOYANT FORCE

$$F(t) = \Sigma F_i \cdot \cos\left(\frac{2\pi}{T_i} t + \phi_i\right)$$

D = DAMPING COEFFICIENT

Fig. 3-10 Spar-TAL Dynamic Model

Two forces are considered as acting on the spring-mass system. One is a constant vertical force corresponding to the net buoyancy of the Spar-CWP system above the base universal joint. The other is a time varying force consisting of a sum of a series of sine waves each with its own amplitude, period, and phase shift. Thus the forcing function provided by an irregular sea can be modeled.

Method of Solution - Program OTSPAR. The nonlinear damping term complicates the solution of the dynamic motions of the simplified model. A time domain solution, generated by a computer program, OTSPAR, was employed to find the motions. Although not an efficient method, the simplicity of the model resulted in minimizing the amount of computer time required.

A time domain solution is characterized by a transient phase in which transient motions generated by the assumed initial conditions are damped out, followed by a steady state phase in which the motions are repeatable. The decay of the transient motions depends on the damping constraint, so that for low values of damping the initial conditions can have some affect on the system response. In addition, the solutions diverge when a low net buoyancy is selected. This occurs because the mass spends most of its time in the region of low spring constant with an occasional impact on the stiffer spring required to balance the small vertical net load. This type of system requires a long time to reach equilibrium.

Vertical Loads. The vertical loads on the Spar-TAL are caused by the change in buoyancy of the column during the passage of waves, and by the wave loads on the spar.

The vertical wave forces are calculated by integrating the water pressure over the vertically projecting surfaces of the spar, as shown in Table 3-4 for the maximum wave treated as a regular wave. The net maximum vertical force, including a coefficient of mass of 1.2, is 13,500 kips, which alternately acts in the upward and downward directions as a sine wave. This value is much larger than the net buoyancy of the Spar-CWP.

Table 3-4 OTEC SPAR VERTICAL WAVE LOADS - METHOD 1

REGULAR WAVE : $H = 63.2$ FT
$T = 13$ SEC
$\lambda = 890$ FT

WAVE PRESSURE

$$P = \rho A g \frac{\cosh(kh + kz)}{\cosh(kh)} \cos(\omega t) - \rho g h$$

MAXIMUM IF $\cos(\omega t) = 1$

DEPTH	$\frac{\cosh()}{\cosh()}$	DYNAMIC PRESSURE K/FT^2	EFFECTED AREA (FT^2)	FORCE (KIPS)
30′	.81	1.65	4064	6706
80′	.569	1.16	7050	8178
215′	.22	.447	7050	-3151
330′	.097	.119	4202	-500
SEE FIG				

11233 = NET MAXIMUM VERTICAL FORCE

ASSUME $C_M = 1.2$

NET FORCE = $1.2(11233) = \pm 13500$ KIPS
(CAN ACT UP OR DOWN)

An irregular wave forcing function can be found in two ways. The first method, used in Table 3-5, distributes the forces at each frequency to the same proportion as the wave amplitude, in such a way that the sum of the individual components adds up to the same value as the maximum vertical force calculated previously for the 100-year storm wave when treated as a regular wave. This method is only approximate, since it ignores the effects of frequency on the decay of wave motion with depth. The values of wave spectral energy are obtained from the Task I Report. The phase angles for each frequency component are randomly selected.

The second method for creating a wave forcing function is more theoretically precise. The wave spectrum is first broken up into eight frequency components in Table 3-6. The pressure from each component is integrated over the four spar surfaces and provides a net force value at each frequency. Thus the RAO of force with frequency is taken into account. The maximum force predicted by this method is 17 percent lower than that predicted by the first method. A comparison of the two methods is shown in Fig. 3-11. The result is that an irregular sea state is modeled as the sum of eight superimposed sine waves.

The buoyancy change due to wave elevation at the spar is a maximum of about 2,000 kips, much less than the wave forces. The buoyancy force acts to reduce the wave force, as can be seen in the wave crest, where the extra buoyancy acts upward while the downward acceleration of the water particles causes a downward force.

The buoyancy forces were neglected for much of the analysis, which results in a 20-percent overestimation of the forces.

Damping. The damping coefficient has a great effect on the heave of the spar, and is the least determinant portion of the analysis.

The most important mode of damping is caused by horizontal translation of the CWP sections. This is calculated in Tables 3-7 and 3-8. In these tables the static deflection position of the CWP under a distributed horizontal load and

Table 3-5 WAVE FORCE MODEL - METHOD 1

N	Δf	$\bar{f}$	S_i * FT^2-SEC	$\sqrt{S_i}$	F_i	T_i	ϕ_i
1	.015	.055	226	15	1111	18.2	46
2	.015	.070	1298	36	2666	14.3	324
3	.015	.085	1313	36	2666	11.8	236
4	.015	.100	869	29.5	2185	10	200
5	.015	.115	521	22.8	1688	8.7	287
6	.015	.130	311	18.2	1348	7.7	114
7	.015	.145	190	13.8	1022	6.9	120
8	.015	.160	120	10.95	811	6.3	317
			TOTAL	182.3	13479		

ϕ_i ← RANDOM PHASE ANGLE

$$F(t) = \sum_{i=1}^{8} F_i \cos\left(\frac{2\pi}{T_i} t + \phi_i\right)$$

$$a = \frac{13500 \text{ KIPS}}{182.3} = 74.05 \qquad F_i = a\sqrt{S_i}$$

* FROM PUNTA TUNA PUERTO RICO OTEC 100-YEAR TWO PARAMETER WAVE SPECTRUM.

Table 3-6 STORM WAVE MODEL - METHOD 2

N	$\bar{f}$	S FT^2-SEC	ah	Hi	Ti	λ_i *	Ki
1	.055	226	15	5.4	18.2	1698	.0037
2	.070	1298	36	12.9	14.3	1048	.006
3	.085	1313	36	12.9	11.8	714	.0088
4	.100	869	29.5	10.5	10	512	.0123
5	.115	521	22.8	8.1	8.7	388	.0162
6	.130	311	18.2	6.5	7.7	304	.0207
7	.145	190	13.8	4.9	6.9	244	.0258
8	.160	120	10.95	3.9	6.3	203	.031
SUM		4848		65.1		UNITS: K, FT, SEC	

$H_{1/3} = 35.1$ FT

$\bar{H}^2 = \left(\frac{H_{1/3}}{1.41}\right)^2 = 620$

$\bar{H}^2 = \sum_1^8 (H_i)^2$

$ah = \sqrt{S_i}$

$\frac{\Sigma (ah)^2}{B^2} = \frac{4848}{B^2} = 620$

$B = 2.8$

$H_i = \frac{ah}{2.8}$

$\Sigma H_i^2 = 619.3$ ✓

* λ = WAVELENGTH $= \frac{gT^2}{2\pi}$

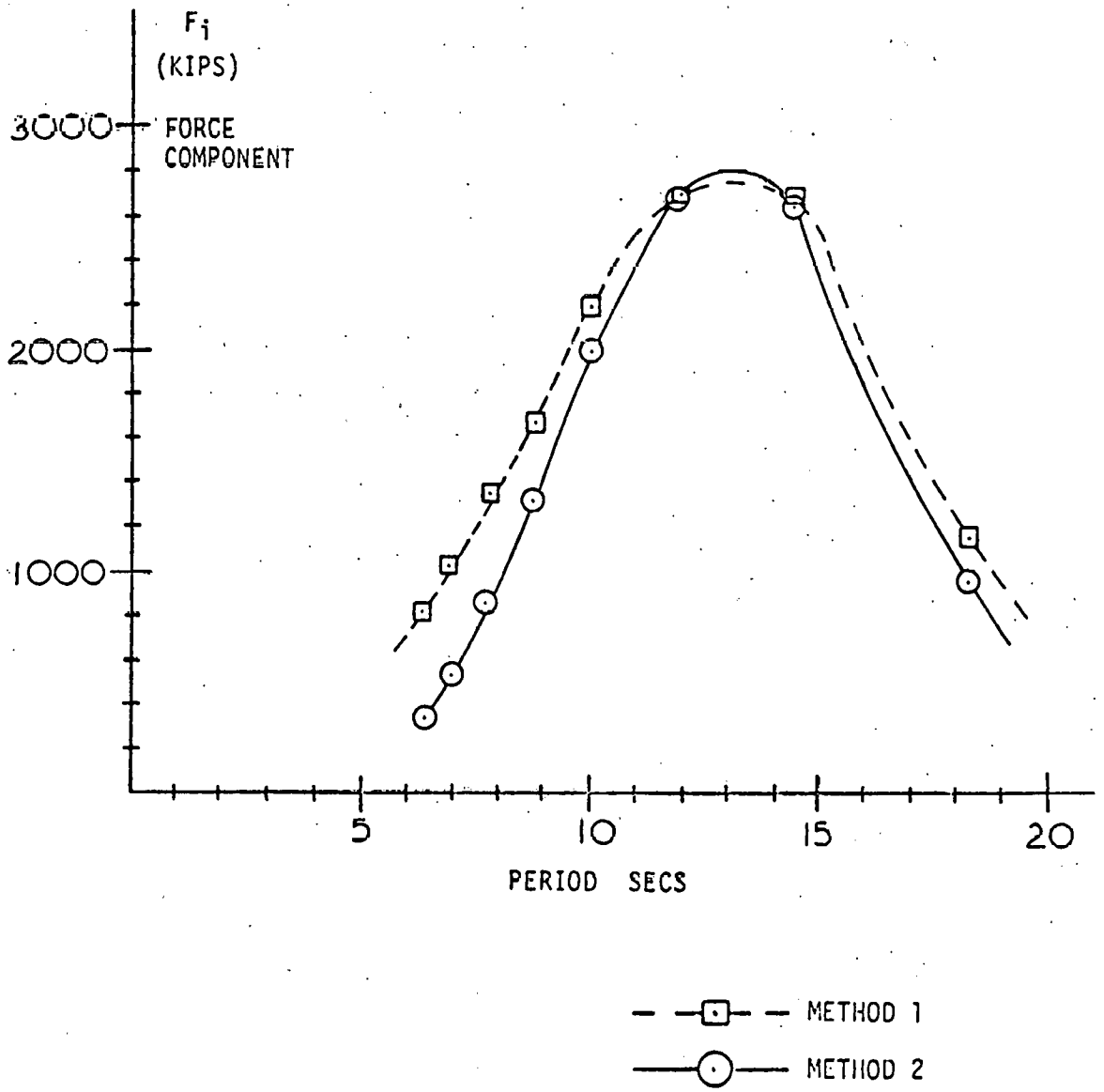

Fig. 3-11 Wave Force Comparison

Table 3-7 CWP DEFLECTIONS FOR DAMPING STUDY

CWP SECT	W_i NET WEIGHT	DRAG F_i	LENGTH	$F_H = 630$, $B_N = 6000$ R_V	R_H	θ	$F_H = 400$, $B_N = 2000$ R_V	R_H	θ	$F_H = 630$, $B_N = 2000$ R_V	R_H	θ
1	*	78.2	479	1000	485.7	3.2°	1000	256	2.28	1000	486	4.05
2	2329	35.7	544	17840	563.9	2°	13840	334	2.63	13840	564	2.63
3	2607	16.4	609	15511	599.6	2.45°	11511	369.6	2.1°	11511	600	3.4
4	2881	10	673	12904	616	3.1°	8904	386	3.0°	8904	616	4.8
5	4040	4	740	10023	626	4.5°	6023	396	5.68°	6023	626	8.9
		144										

$$\theta_i = \tan^{-1}\left(\frac{F_i + 2R_H}{2R_V - W_i}\right) \qquad X_T = 166 \qquad X = 174.8$$

* B_N	W_1
6000	-16840
2000	-12840

Table 3-8 CWP TRANSVERSE DAMPING

CWP SEG	LEN	① $F_H = 630$, $B = 2000$ θ	X_{TOP}	X_{MID}	② $F_H = 630$, $B = 6000$ θ	X_{TOP}	X_{MID}	③ $F_H = 400$, $B = 2000$ θ	X_{TOP}	X_{MID}
5	740	8.9	114.5	72′	4.5	58	29	5.68	73	37
4	673	4.8	170.8	143′	3.1	94.5	76	3.0	108.5	91
3	609	3.4	206.9	189	2.45	120.5	108	2.1	131	120
2	544	2.63	231.9	219	2.0	139.5	130	2.63	156	144
1	479	4.05	265.7	249	3.2	166	153	2.28	175	166
	3045									

$Y_T = 4.901$ $\quad Y_T = 5.92$

CWP SEG	②&③ ΔX_{MID}	F_D
5	21	6344
4	15	2944
3	12	1705
2	14	2073
1	13	1573
		14639

ASSUME CHANGE REQUIRES 1 SECOND.

$V_T = 5.92 - 4.901 = 1.02$ FPS

$V_i = \Delta X_{MID}$ FT/SEC

$\sum F_D \cdot V_i = 247320$ K-FT/SEC

POWER DISSAPATED = POWER INPUT

$247320 = F_T \cdot V_T = F_T \cdot 1.02$ FPS

$F_T = 242470$ K $\quad = BV_T^2$

$B = 233055$ K/(FPS)^2

$F_D = C_D \frac{1}{2} \rho V^2 A$

$F_D = (.6)\left(\frac{1}{2}\right)(2)\left(\frac{\Delta X_{MID}}{1}\right)^2 \frac{LEN \cdot 32.4}{1000}$

net buoyancy is calculated for several combinations. What is desired is to know how much the CWP sections move horizontally for a given vertical displacement in the spar. The vertical and horizontal velocities can then be related. A vertical damping constant is found that provides the same energy dissipation by the spar as if it acted alone, as is dissipated by the CWP sections translating through the water.

F_H is the horizontal force on the spar and B_N is the net buoyancy of the Spar-CWP. The reference point occurs at B_N = 6,000 kips and F_H = 630 kips, two values considered likely to occur. Another combination, F_H = 400 kips and B_N = 2,000 kips, is found so that the horizontal position of the spar is the same as for the first combination. The positions of the CWP section midpoints can be compared for the two cases.

It is readily apparent from Table 3-8 that a small change in spar elevation causes a large horizontal motion of the CWP sections. For the example given, a 1-ft change in spar elevation causes a 21-ft horizontal displacement of the lowest CWP section, and a 13-ft displacement of the upper CWP segment.

When these displacement changes are converted to drag forces with C_D = 0.6, based on the projected area of the CWP sections, a heave damping constant of 233,000 k/(fps)^2 is calculated for the case presented.

This value provides only the relative importance of this mode of damping. It is obvious from the preceding calculations that transverse CWP induced damping is geometry dependent, varying with the horizontal and vertical displacements of the spar, and with the buoyancy and current forces on the spar and CWP. In addition, each CWP section has its own mass, and accelerations which will cause it to move and dissipate energy in a different way than the simple static method described. But it is shown that a great deal of damping is possible from CWP oscillations.

A second form of damping is vertical drag resistance of the spar vessel. The V^2 damping constant for this mode is approximately 15 k/(fps)^2, very much less than for CWP damping.

A third form of damping is provided by friction in the CWP universal joints. If the universal joints are made of self-lubricated aluminum bronze, with a coefficient of friction of 0.1, the large tensions in the CWP will result in energy dissipation when the joint is deflected through any angle. The magnitude of this effect is calculated in Table 3-9, in which the changes in angles from Table 3-8 are used to calculate the energy dissipation.

It is important to note that this type of friction is Coulombian friction, and is independent of the velocity. It is also geometry dependent and therefore cannot be solved exactly. If this mode of friction is converted to an approximate V^2 damping term, the drag constant is 87 k/(fps)^2 which is still much smaller than the CWP transverse damping (Table 3-9).

Another type of damping is wave making caused by heave of the spar. Due to the small projected area of the spar column, and its constant cross section, this affect is ignored. The longitudinal drag on the CWP is also relatively unimportant.

In conclusion, the damping of the Spar-TAL cannot be determined accurately for the simplified model used herein. Instead, the affects of a range ot damping values are studied.

One method of estimating a damping value is to compute a value of damping that will provide a desired spar orbit diameter. This concept is used in the graph in Fig. 3-12. Spar heave of 5 ft in amplitude in the maximum storm wave is assumed. Program OTSPAR was run with zero values of spring stiffness and with a sinusoidal force corresponding to the maximum storm wave force, and the values of damping constant were varied. The net buoyancy is treated as zero so that the spar would not drift. The orbit diameter as a function of damping constant is shown in Fig. 3-12 for two values of spar mass. The lighter spar mass does not include the water mass inside the discharge pipes.

Table 3-9 CWP BUSHING DAMPING

UNIVERSAL JOINT BUSHING RADIUS = 3 FT
COEFF OF FRICTION = .1

ENERGY DISSIPATED PER JOINT

$E_i = R_v \; .1 \; \Delta x$ $\qquad$ R_v = TENSION ACROSS U.J.

$= R_v \; (.0052) \; \Delta\theta$

CWP SEC	R_v	③ ② $\Delta\theta$	E_i K-FT
1	1000	1.2	6.1
2	13840	.1	7.2
3	11511	.35	21.0
4	8904	.63	29.2
5	6023	.92	28.8
			92.3 K-FT

POWER CONSERVED

B = VERTICAL DAMPING COEFF

$P = BV^2 \cdot V = 92.3$ K-FT/SEC

$P = B(1.02)^3 = 92.3$

$B = 87$ K/(FPS)^2

SMALL COMPARED TO CWP TRANSVERSE DAMPING

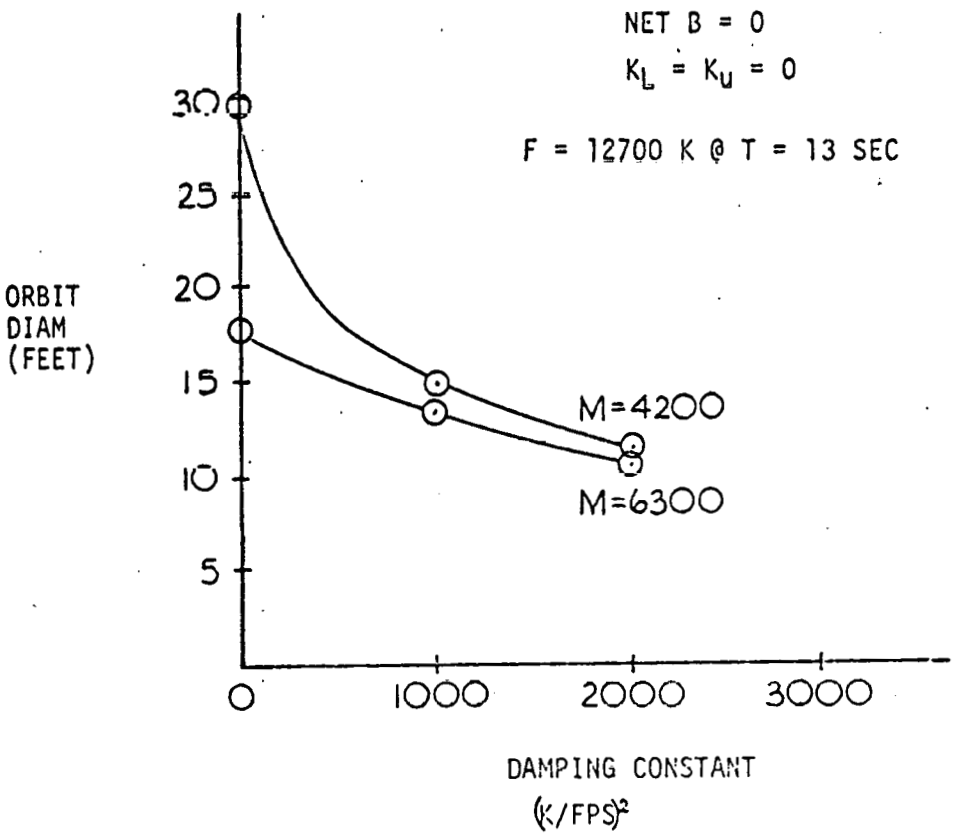

Fig. 3-12 Damping Effects

The damping constant corresponding to an orbit diameter of 10 ft is 2,000 k/(fps)^2. This value, smaller than the value previously calculated, is used throughout the load analysis.

Strictly speaking, the sinusoidal force used in Fig. 3-12 should be different for the two masses. The orbit diameter at zero damping should be more equal for each mass. The curve for M = 6,300 is probably the more accurate representation. A damping value of over 10,000 k/(fps)^2 is selected for design load analysis.

Snapping Loads. The spar can respond in heave in two ways. If the net buoyancy is much greater than the wave load amplitude, the CWP will never go into compression and the spar acts like a simple spring mass system. If the wave load amplitude is greater than the net buoyancy, then the downward wave load can cause the CWP to become slack. The spar is then allowed to build up kinetic energy in the longitudinal direction of the CWP. When the spar moves back in the upward direction, it pulls on the CWP, and the kinetic energy of the spar is absorbed by elongation in the CWP. This snap load is therefore studied.

In model testing of single anchor leg moorings, for example, if sufficient buoyancy is lost in the waves to cause the chain to become slack, the subsequent retightening of the chain usually causes a load beyond the breaking strength of the chain. The low energy absorbtion of steel results in rather high stresses.

In plotting wave-induced tension versus net buoyancy, one would expect to see a peak in the lower buoyancies caused by snap loads. To study this phenomenon, several OTSPAR runs were made using a sinusoidal force equal to the significant value in the maximum storm wave. The maximum CWP tension (at the base) versus net buoyancy is shown in Fig. 3-13. As can be seen there is a peak in the lower buoyancies for D = 2,000 but it is not as pronounced as expected. For the highest value of damping no peak at all is observed. For a

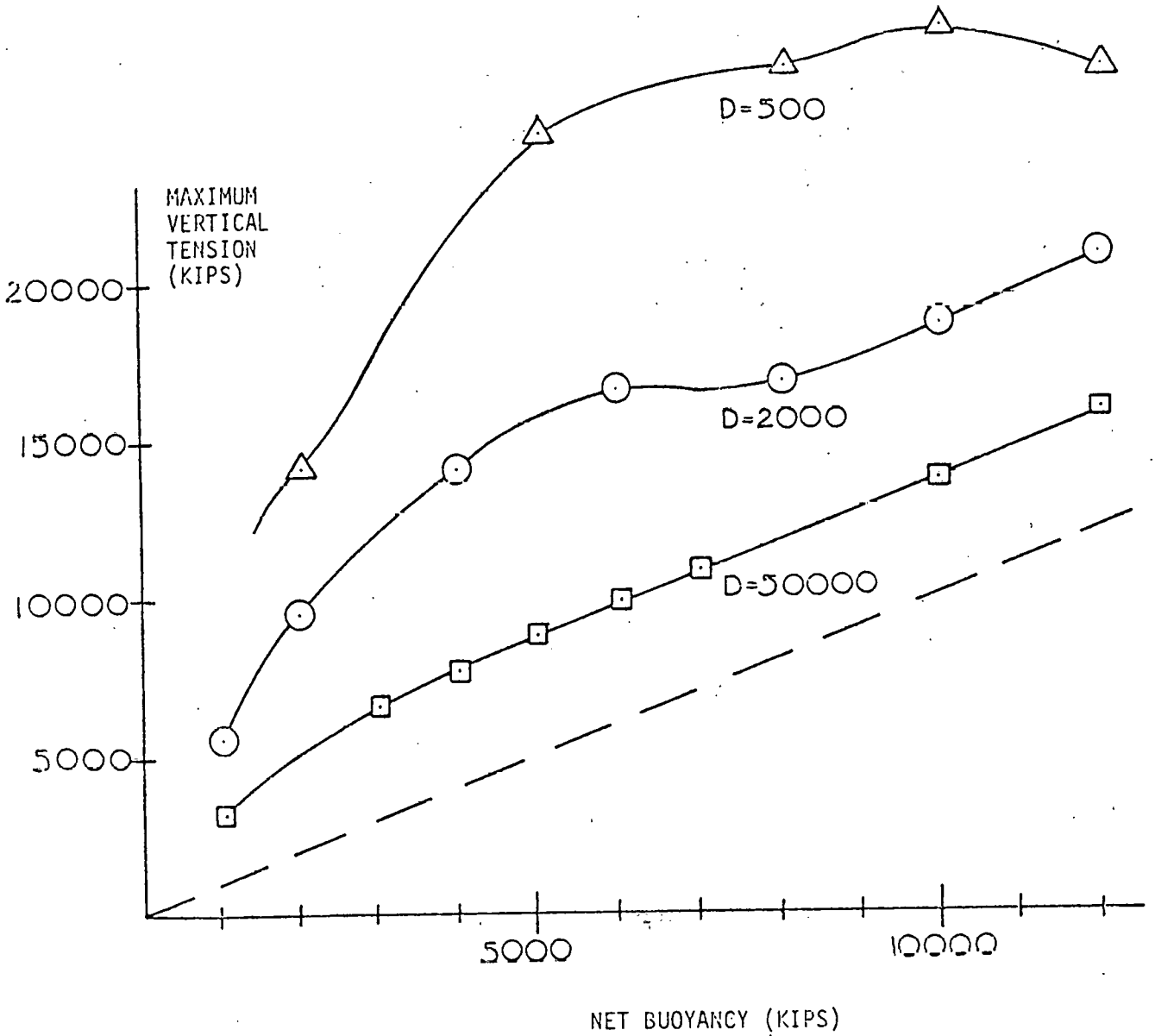

H1/3 = 32 FT

T = 13 SEC

F = 6800 @ T = 13 SEC

M = 4020 KSLUGS

K_u = 4362 K/FT

K_L = 4.3 K/FT

Fig. 3-13 Regular Wave Tensions

lower value of damping, the peak shifts toward higher net buoyancies, since the CWP goes slack at these higher buoyancies with low damping.

Two conclusions are reached from Fig. 3-13. The first is that the CWP is sufficiently long and flexible that significant snap loads do not occur. The second is that the values of damping present in the system can greatly reduce any snapping that would occur. Snap loads do not seem to be a problem for the Spar-TAL based on the damping values examined. The validity of this conclusion needs to be verified in model tests.

The minimum negative spar displacement versus net buoyancy is plotted in Fig. 3-14 for D = 2,000. This shows that the net buoyancy at which the CWP no longer goes slack (B_N = 8,000) corresponds to the net buoyancy to the right of the peak in Fig. 3-13.

Resonance. A spring mass system has a natural period of

$$T = 2\pi\sqrt{\frac{M}{K}}$$

For the Spar-CWP system in heave, the natural period is

$$T = 2\pi \sqrt{\frac{6,300}{4,360}} = 7.6 \text{ sec}$$

This period is effective if the CWP does not become slack, or if the CWP can go into compression.

If the CWP becomes slack this period is greatly changed. The situation is analogous to a rubber ball bouncing on a flat surface. If the ball is glued to the surface, it will have a small natural period. If the ball is allowed to bounce, its period not only greatly increases but is also dependent upon the height of the bounce.

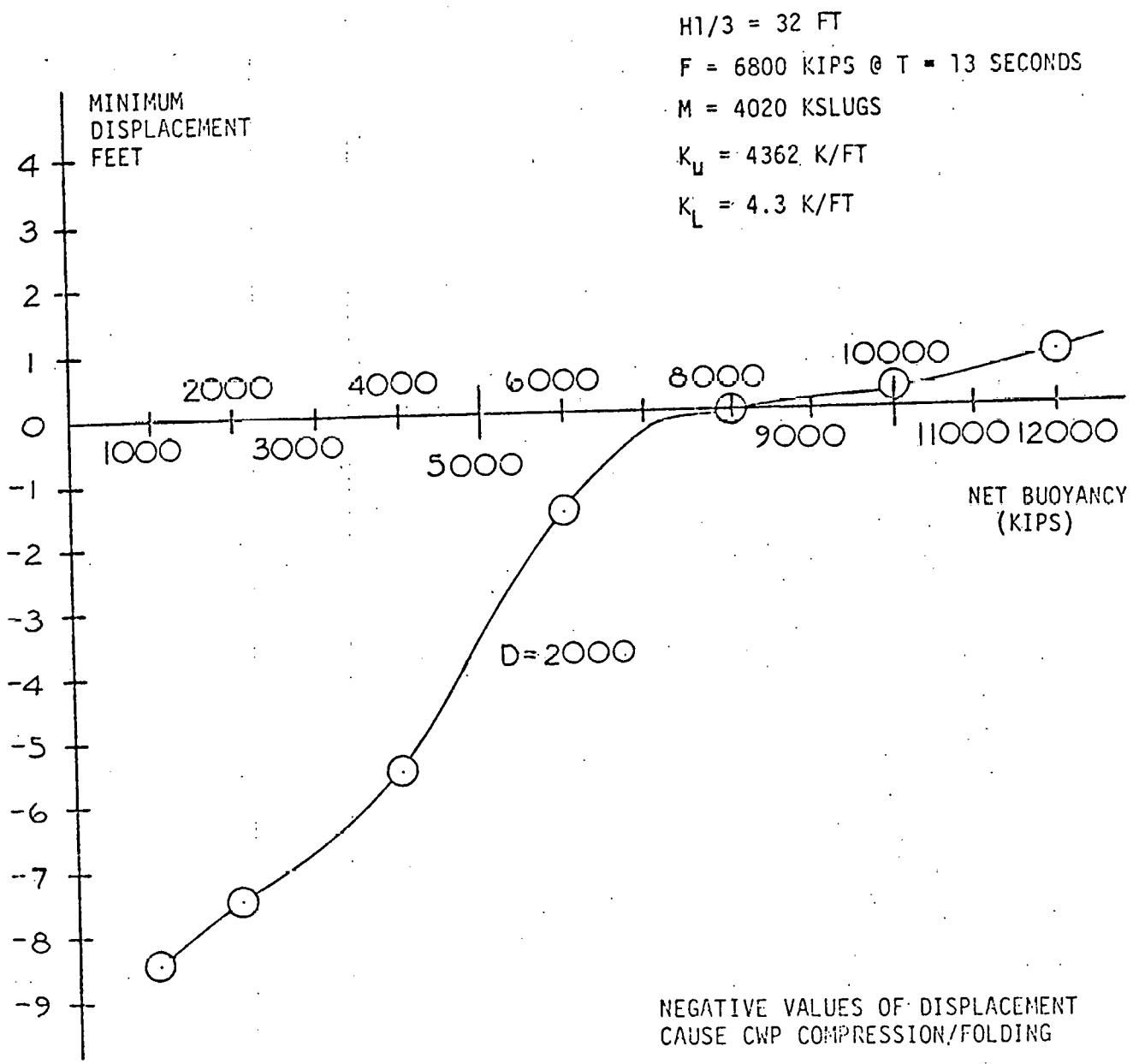

Fig. 3-14 Regular Wave Motions

The same will be true of the Spar-CWP spring mass system. Several OTSPAR runs were made to study this phenomenon. The following were held constant:

- Net buoyancy = 2,000 k
- Damping constant = 2,000 k/(fps)^2
- Upper spring constant = 4,360 kips/ft
- Forcing function F = 6,800 sin (2w t/T)

The maximum CWP tension is found as a function of exciting period, T, for two values of the lower spring constant. In the first case, the lower spring constant is set equal to the upper spring constant, KL = 4,360 kips/ft. This models the Spar-CWP as a simple spring-mass system with a linear spring, so that the CWP can carry compression. The tension response for this case peaked at around 8 sec, and behaves like a typical harmonic oscillator with damping, as shown in Fig. 3-15.

In the second case, the lower spring was given a constant of 4.3 k/ft, similar to the real CWP response. The tension versus wave period, shown in Fig. 3-15, demonstrates a behavior very different from the first case. The peak at 8 sec has disappeared and the true peak appears to be greater than 30 sec. This compares well with the bouncing ball analogy. This peak is outside the frequency range of the 100-year storm spectrum. It can be concluded that folding of the CWP sections may reduce the problem of heave resonance.

Irregular Wave Cases. Finally, several OTSPAR runs were made using the irregular force spectrum of the 100-year storm wave. The maximum tension is plotted as a function of net buoyancy in Fig. 3-16, for several values of damping. The minimum downward displacement versus net buoyancy is plotted for D = 2,000.

The maximum value for each case is the maximum that occurs in a 20-minute run, with the same forcing function for each case.

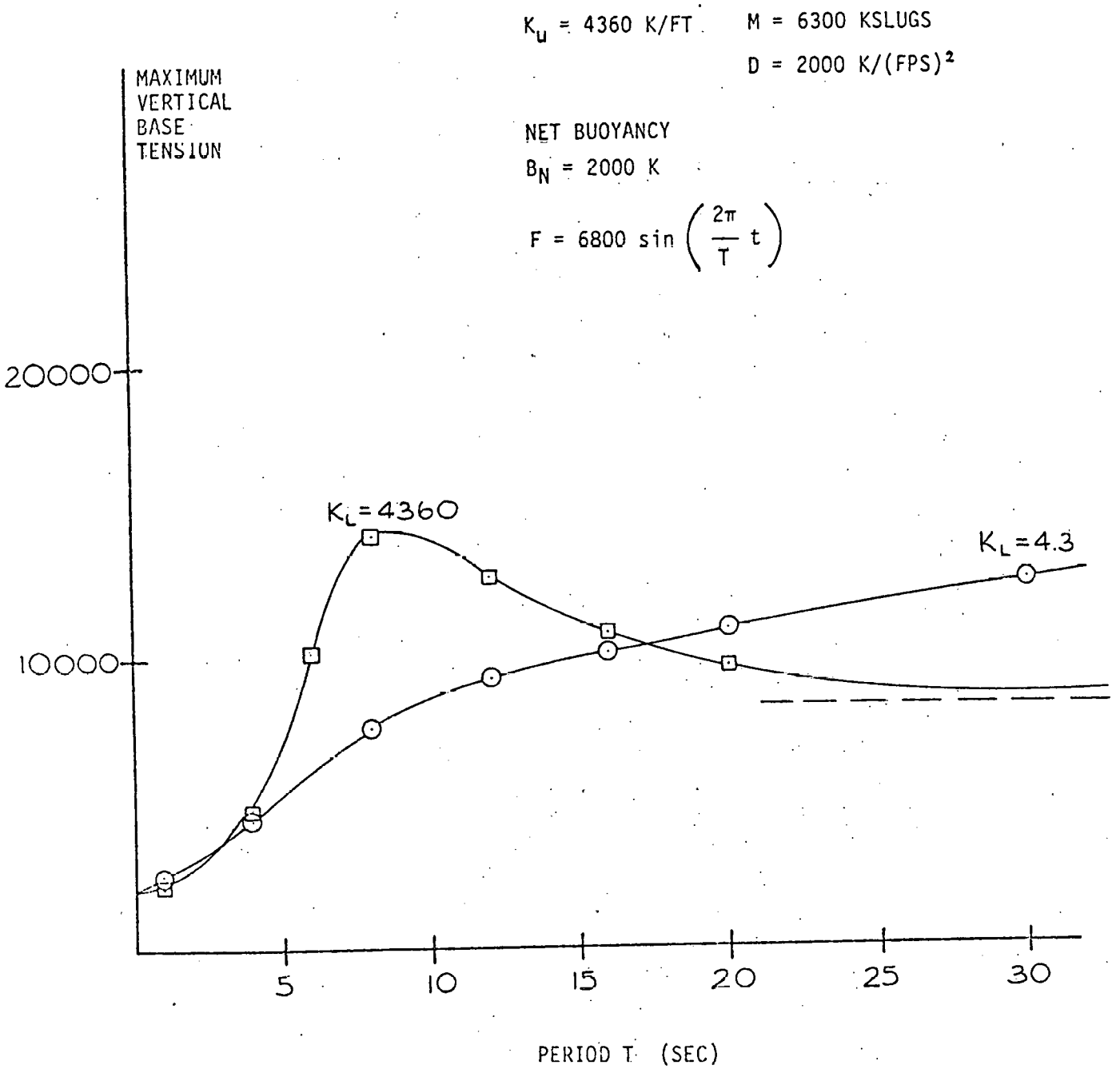

Fig. 3-15 Tension vs. Period

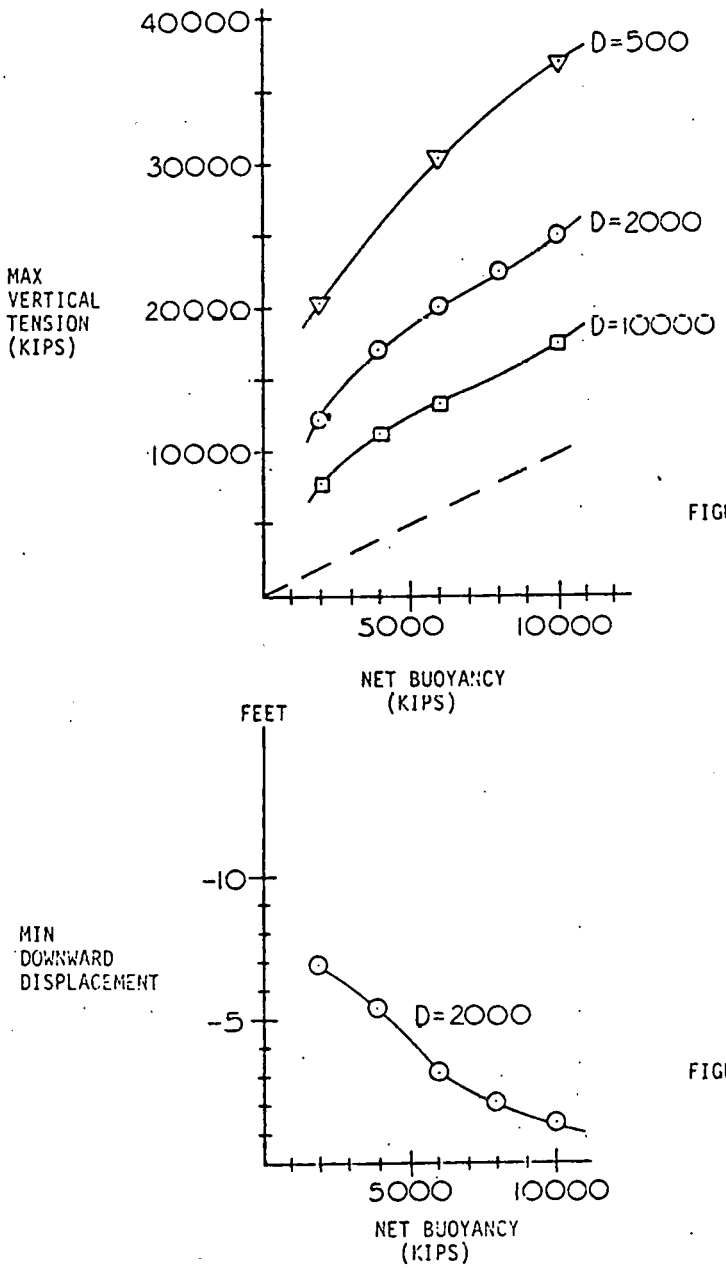

Fig. 3-16 Irregular Wave Results

3.3.8 OTEC Simulation Computer Programs

Program Description. Two frequency domain computer programs have been written to determine the coupled CWP-Spar/barge response and stresses:

1. The Paulling Program, written by J. Randolph Paulling of University of California, Berkeley
2. The NOAA/DOE program

These programs were originally written to analyze CWP systems suspended from free-floating OTEC plants. They were later modified to handle tension leg systems. It is beyond the scope of this report to describe the theory and methodology of the programs. The NOAA/DOE program was not ready in time to provide results for this design effort.

Program Applicability. For the following reasons the applicability of the frequency domain computer programs may be limited when applied to the Spar-TAL.

1. Frequency domain analysis is based on linear superposition of response. This assumes linearity of response to wave height at each frequency. Due to the nonlinear stiffness in heave, shown in Fig. 3-9, the heave is not a linear function of wave height. The response in heave for small waves is linear until the wave height is sufficient to cause the CWP to become slack. Not only will the larger waves have a different response, but the frequency response characteristics will shift with heave amplitude as demonstrated in Fig. 3-15. Thus the theoretical basis of the programs is open to question with regard to the heave of the spar, the most important mode of response for the Spar-TAL.
2. The CWP motions are based on small amplitudes of deflections in the CWP. Thus the transverse CWP damping is unlikely to be transferred into heave damping of the spar. Therefore the potentially most important mode of damping will not occur in the frequency domain analysis, and the heave motions will be overestimated.

Program Results. A Paulling Program run was performed for IMODCO by Giannotti and Associates through Gibbs and Cox. The existing Gibbs and Cox spar model was used, with a total system net buoyancy of 2,000 kips. The CWP properties were the same as from Fig. 3-3. The 100-year storm conditions were run. No damping was added at the universal joints.

The program predicts a peak heave response at around 7 sec, which indicates that it treated the spar response as a simple harmonic oscillator. The rms value of CWP tension is 32,400 k, which results in an approximate maximum CWP tension of

$$T = 2{,}000 + (2)(32{,}400)(1.86)$$

$$T = 122{,}500 \text{ kips}$$

which is considerably more than the design values chosen.

It is anticipated that the reason for these high loads is the unrealistic heave resonance at 7 sec combined with an underestimation of the true heave damping.

OTSPAR/Paulling Program Comparison. An OTSPAR run was conducted in an attempt to match the assumptions and results of the Paulling program. The following was modeled to simulate the characteristics of the Paulling program:

- Spar mass - 6,300 kslugs
- Damping constant - includes spar drag effects only - 25 k/(fps)^2
- Irregular wave forcing function from Method 2
- Lower spring constant of 4,360 k/ft, equal to the upper spring constant

In this run a marked heave resonance occurred with a period of approximately 8 sec. The maximum vertical tension was 240,000 kips, about double that predicted by the Paulling program.

This result demonstrates two concepts. The first is that if the CWP stretch nonlinearity and the CWP transverse damping are not taken into account,

exceedingly high loads can be predicted. The second is that the wave-making damping, computed by the Paulling program but not by OTSPAR, is as significant as the spar drag, since OTSPAR overpredicted the Paulling program results by a factor of two. If wave-making drag were included in OTSPAR, the results could match more closely.

3.3.9 Design Loads

Selecting the design loads requires some engineering judgment and selection of a value for net buoyancy. The results of Fig. 3-16 show that a high value of net buoyancy is not required to reduce the loads. The watch circle places a limitation on buoyancy. Any net buoyancy greater than 1,900 kips will prevent a negative buoyancy in the storm wave trough.

If a net buoyancy of 6,000 k and a damping coefficient of slightly more than 10,000 are selected, the maximum load should be less than 12,000 kips. The following mooring base loads were selected for further component design:

Vertical Base Load	12,000 kips
Horizontal Base Load	1,500 kips

It could be argued that a lower value of vertical load could be selected because the heave damping will be greater than 10,000 $k/(fps)^2$. If the surge motion of the spar were included in the analysis, however, it might be found that the surge energy would also cause tightening of the CWP, which in conjunction with the storm wave could then allow the vertical wave load to be transmitted directly to the base. The vertical tension would then be

$$T = 6,000 + 11,197 = 17,200 \text{ kips}$$

Any design tension significantly below this value could be contradicted by model tests.

The maximum tension in the CWP will be 13,000 kips higher than the vertical base load, since the pivot below the buoyancy section must carry the suspended

weight of the CWP. This tension will be approximately 25,000 kips, a value that may be too high for the assumed CWP design.

The load analysis included herein is not intended as a final set of results. The purpose is to study the concepts involved and to derive a preliminary design to determine the relative feasibility of the Spar-TAL. If the concept proves to be viable, model tests will be required in order to determine an exact set of design loads.

3.4 MOORING BASE

3.4.1 Description

The mooring base for the tension anchor leg OTEC spar is the gravity type. The weight of the base is designed to counteract the greatest expected vertical force with a specified safety factor. The soil conditions and materials are considered in the calculations of the required minimum dimensions of the base and the required anti-skid foundation of the base (see Fig. 3-17).

Vertical forces are transmitted through eight bulkheads to the base structure. These bulkheads divide the circular base structure into eight separate compartments into which the grouting material is poured.

3.4.2 Design Criteria

The loads used for the design of the base are the maximum expected loads. On a gravity base, the safety factors are 1.5 and 2.0 for the vertical and horizontal loads, respectively.

The controlling factor in the diameter of the base is the bearing stress the soil can withstand without failure. Since this stress is undetermined at the

time of this writing, an expected value is assumed. The factor of safety used for the failure of foundation is 3.

The structure of the base is designed using the ABS rules for allowable stress levels. These are:

- o 60 percent of yield strength for tensile stresses
- o 60 percent of either the local buckling or yield strength, whichever is less, for compression stresses
- o 57 percent of either the buckling or yield strength, whichever is less, for compression stresses
- o 40 percent of tensile yield strength for shear

The base is to be fabricated of ASTM-A36 steel. The ABS rules for the selection of plate thickness and section modulus of stiffeners are:

$$t = \sqrt{\frac{sh}{460}} + 0.1$$

where

- t = plate thickness in inches
- s = stiffener spacing in inches
- h = maximum design water head above plate in feet

Section modulus = $0.0041 \cdot h \cdot s \cdot l^2$ in.^{3}

where

- l = unsupported length of stiffener in feet
- s = stiffener spacing in feet
- h = water head to center of l in feet

The base is designed to meet the ABS grades for the different thicknesses.

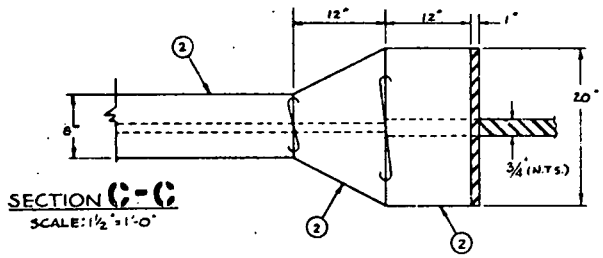

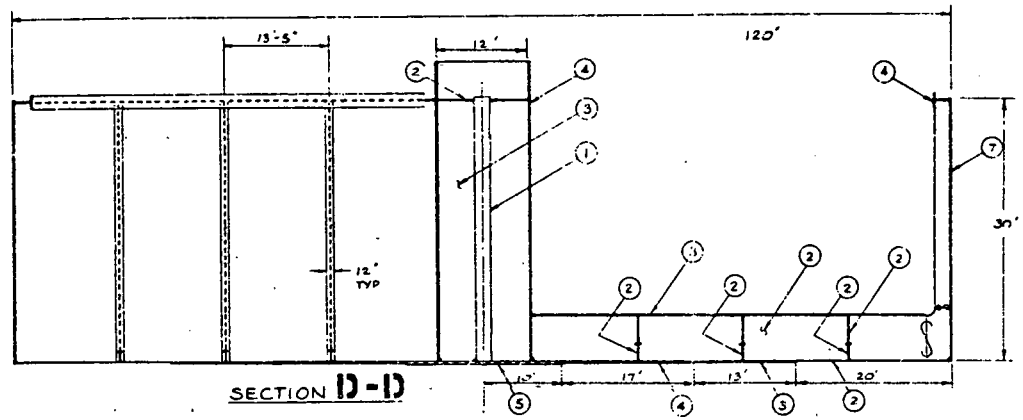

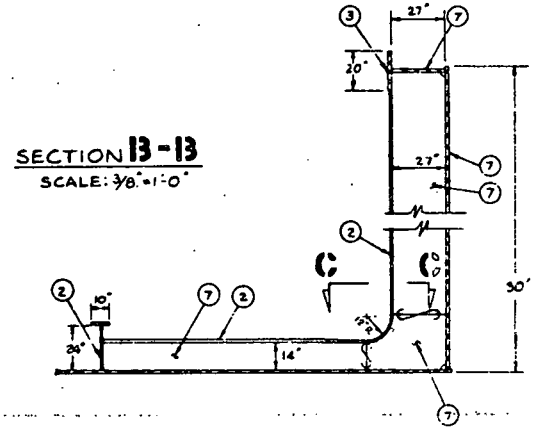

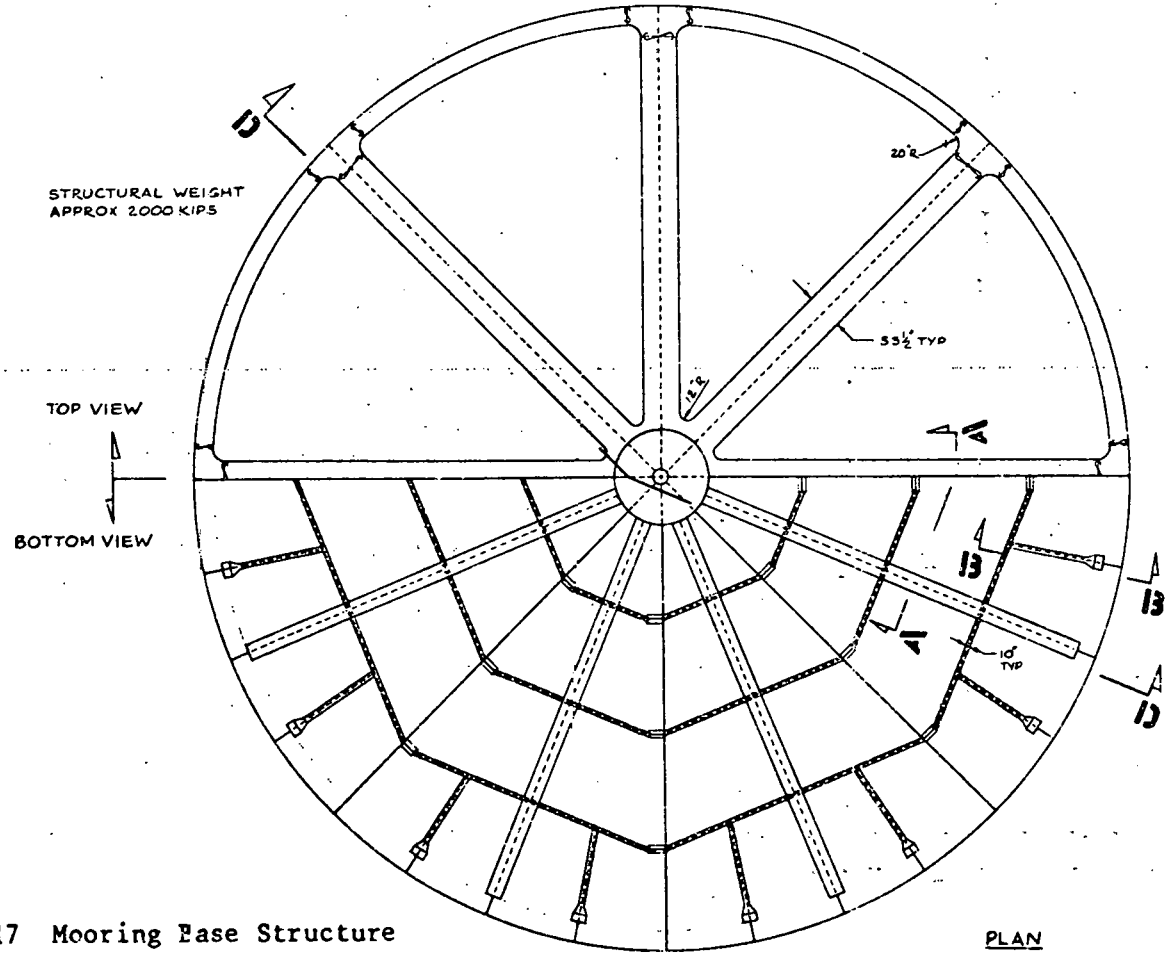

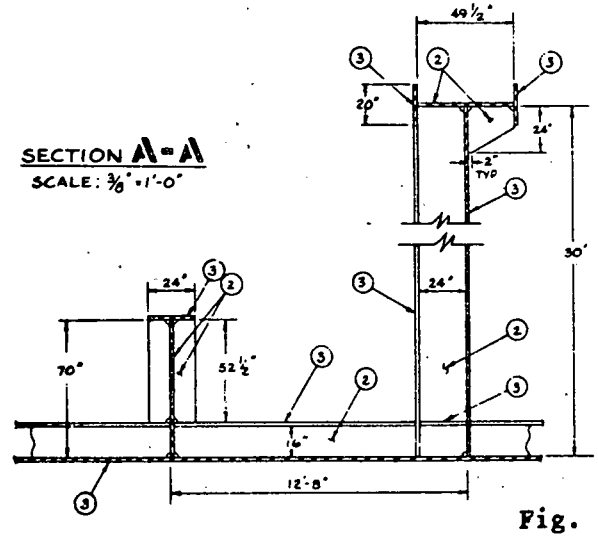

Fig. 3-17 Mooring Base Structure

Complete soil analyses are needed in order to calculate the bearing stress and angle of internal friction of the soil. These values in turn are needed to calculate the shear skirts on the bottom on the base and the soil stability when the base is set down on the soil. These values were estimated in the design of the base for this report. It is recommended that soil samples be taken and analyzed before a base design is finalized.

3.4.3 Design Method

Base Size. The base must be capable of holding the spar and cold water pipe at the position it was installed under the largest predicted loads the system will carry. Because of the uncertainty of the ocean environment and the statistical nature of the forces that can be predicted, factors of safety must also be used in the development of a design.

The forces acting on the base are reaction forces which are created by the environmental forces acting on the spar and cold water pipe, and the total net buoyancy of the system, as calculated previously. The design loads are a horizontal load of 1,500 kips and a vertical load of 12,000 kips acting on the base.

Based on the static balance formula,

$$W = 1.5\, F_v + \frac{2\, F_h}{\mu}$$

where

F_H = horizontal load

F_V = vertical load

W = weight of base

μ = coefficient of friction of soil

the weight needed depends on the coefficient of friction between the base and the soil. The bottom quality is given in the Task I Report, but the depths of the soil layers and their angle of internal frictions are not given. It is assumed that the base can be designed to make the best use of the soil given any type of stratification. Angle of internal friction is calculated from the table (Ref. 3-2 page 107) which lists values for some types of soils. The assumed angle of internal friction provides a base/soil coefficient of friction of 0.3. Substituting these values into the above equation, a base weight required is 30,000 kips underwater weight.

There are any number of different diameters and heights that can provide this weight. The general equation would be:

$$W = \frac{\pi D^2}{4} \cdot H \cdot w$$

where

D = diameter of base (ft)

H = height of base (ft)

W = weight of grout (lb/ft^3)

The grout is assumed to weigh the maximum that can be supplied, 150 lb/ft^3 (underwater weight 86 lb/ft^3).

The minimum dimensions to prevent overturning are

$$0 \geq 3{,}000\ H - (30{,}000\ k - 18{,}000)\ D/2$$

$$2D \geq H$$

The bearing stress on the soil caused by the base alone is checked first. A sand layer is used for the calculations. The general formula for the bearing capacity from Ref. 3-3 is

$$qdr = 1.2c\,N_c + \gamma D_f\,N_q + 0.6\gamma_r\,N_g$$

where

N_c = bearing capacity factor for cohesion

N_q = bearing capacity for factor for surcharge

N = bearing capacity for factor for soil weight

c = cohesion

γ = weight of soil

D_f = depth of foundation in soil

r = radius of foundation

Sand can be assumed to be cohesionless, the first term will equal zero. The foundation rests on top of the soil, so D_f equals zero and the second term equals zero. The bearing capacity factor for soil weight is estimated from a graph of the bearing capacity factors vs. angle of internal friction. This factor is estimated to be 4.2. The weight for sand is 120 lb/ft^3.

The weight per unit area of the base is calculated

$$W = \frac{30,000,000\ (4)}{\pi D^2} = \frac{38,197,186}{D^2}$$

The weight per foot is increased by the safety factor to:

$$W = \frac{114,600,000}{D^2}$$

This is the maximum bearing capacity the soil must support.

Equating expressions yields

$$\frac{114,600,000}{4r^2} = 0.6\gamma_r\,N_\gamma$$

$$r = 60\ ft$$

In the above equation, the slope of the bottom (12 deg) is taken into account by multiplying the bearing factor N by a correction factor 0.44 (Ref. 3-3).

For the base with the above radius and the soil conditions assumed, there will be a safety factor of 3 against soil failure for the static case.

The bearing pressure when the base is under the maximum loads must also be checked. The net vertical bearing stress on the soil due to the weight of the base is superimposed on the stress caused by the moment resulting from the horizontal load.

$$\sigma = \frac{P}{A} \pm \frac{MC}{I}$$

where

P = net vertical load

A = area of base

M = moment

I = moment of inertia of the base area

C = base radius

The loads are added to find the maximum stress and subtracted to find the minimum.

At the minimum side, the stress should not be less than zero to avoid uplift leading to soil in stability. Using the 60-ft radius calculated above, the height of the base to meet the weight requirement is found to be 30.8 ft. Assuming the horizontal force is applied 40 ft above the bottom, the minimum stress will be 1.24 kips/ft^2.

At the maximum stress side, the stress should not be greater than the bearing capacity divided by the safety factor.

The maximum stress is calculated to be 1.95 kips/ft^2. The maximum allowable is

$$q = 0.6\gamma_r N_\gamma \frac{1}{3}$$

$$q = 2.67 \text{ kips/ft}^2$$

Therefore, the diameter of the base of 120 ft and a height of the base of 30 ft will meet all of the requirements and is acceptable.

In the early stages of the design, a universal joint elevation of 20 ft was assumed. This has been shown to be too low a value.

Base Structure. The base has eight bulkheads which distribute the loads throughout the structure. The loads are transmitted to the bulkheads from a large circular tube. The vertical force causes the center of the base to be pulled up while the weight of the base holds it down. This combination of forces creates a bending moment in the bulkhead with maximum compression and tension at the center of the base. The 12 ft cylinder requires internal stiffeners to withstand these high compressive and tension forces so the bulkheads meet at a pipe in the center. The pipe facilitates welding the bulkheads into a common center. The weight of base structure is 2,000 k.

The bottom plating thickness is varied to save weight and cost. The bending stresses decrease away from the center so less steel is needed at the outer sections of the base.

The bulkheads have vertical stiffeners to decrease the length of the unsupported plate and therefore eliminate the chance of plate buckling. These stiffeners also give the plate added stiffness in the event that the compartments fill unevenly. A beam stiffener along the top of the bulkheads support against buckling in the two conditions mentioned above.

The bottom plating between the bulkheads must be able to support the weight of the grout on an uneven seafloor. One large stiffener is used in each compartment. This stiffener is designed to carry the total load in the compartment. Smaller stiffeners are used to give the rest of the plate support. The walls of the base are stiffened using the same criteria. The stiffeners are continuous through the bottom radial stiffeners to provide moment continuity. All connections between stiffeners are continuous to allow stresses to flow evenly from one area to another with a minimum of concentrations. This results in a stiff, stable structure.

Shear skirts project from the bottom of the base into the sand layer. The sand layer is assumed to have the highest internal angle of friction of those soils listed in the Task I Report (Table 2-1). The shear skirts are arranged in a matrix pattern.

Not shown in the base drawing is the guide tube for the installation of the CWP and universal joint. This is an arched square cylinder with large radii for direct contact with the cable. No pulleys are used.

3.4.4 Fabrication Procedure

The fabrication of the TAL-SPAR mooring base is carried out in the conventional method for offshore structures. All welds are full penetration welds and ultrasonically tested. All steel is ABS grade mild steel; grade B for thickness from 3/4 up to 1 in., grade D for thickness from 1 to 2 in., grade E for thicknesses over 2 in. All steel plate 2-1/4 in. thick and over is tested and accepted according to ASTM A 435 prior to welding. Any access holes needed in the fabrication are cut, then welded closed when no longer needed.

Fabrication site is selected with the installation method in mind. Passage of the base through any waterways and past obstructions and bridges must be considered. Since the base is floated out to the installation site, the base must be either lifted from the yard and put into the water, lowered down ways into the water, or built in a drydock and floated out after completion.

3.5 BASE UNIVERSAL JOINT

3.5.1 General Description

The base universal joint connects the lower end of the CWP tube to the center of the gravity base. It allows two angular degrees of freedom between the CWP and the base. It is designed to pitch at least 30 deg in any direction, 10 deg of which is required for the sloping seabed. If the seabed slopes more than 10 deg at the site, the universal joint design will be unaffected, providing the central tube in the mooring base is tilted into the vertical direction. The structure is designed to carry the design load in any azimuthal direction (see Fig. 3-18).

The pedestals of the universal joints are fabricated from steel plate, and are provided with press-fitted, self-lubricated bushings to transfer radial and thrust loads. These bushings are equivalent to those manufactured by Merriman. Journal surfaces in contact with the bushings are protected against corrosion by a weld deposited overlay of Monel, and are finished to a maximum surface roughness of 1.6 microns. The pivot pins are of forged steel. All pedestal/bushing and bushing/pivot-pin contact surfaces are parallel to assure maximum load-carrying contact.

Suitable inspection and testing procedures are maintained to ensure that all forgings, bearings, bushings, castings, and other items used in the fabrication of the universal joints are free of defects. Prior to delivery, the completed universal joint is tested to assure free rotation within the desired envelope.

The material of the universal joint components is mild steel, such as ABS Grade E with a yield strength of 34 ksi. This will ease the welding of the large plate thicknesses of up to 8 in. The location of the universal joint at the bottom of the CWP eliminates the need for weight reduction in the universal joint, since this weight actually reduces the vertical load on the base. Standard industry practice for the fabrication of large universal joints for tension anchor leg mooring systems is to use mild steel, even if the weight of the universal joint is supported by a buoyancy tank. An example of this is the Hondo field SALM, where the universal joints are made of mild steel equivalent to A36, and weigh 60 tons each, for a vertical load of approximately 1,000 kips. The weight of the OTEC base universal joint is approximately 300 tons, for a vertical load of 12,000 kips.

A mechanical connection is provided for securing the bottom of the universal joint to the mooring base. This connector is similar to those manufactured by FMC or Vetco for offshore use as pile connectors. A specially designed unit is required for OTEC due to the large dimensions and loads.

The connector operates by means of a segmented sawtooth ring, which is wedged into matching sawtooth grooves on the inside cylinder. These rings are forced into place by actuator screws accessible from the outside. The actuator screws can act to either install or remove the lockring, so that the unit can be easily disconnected after use. A setscrew is used to lock the actuator screw into position. High-strength materials are used for the connector unit. The connector unit is welded at either end to the universal joint tube and to the base center tube. Design of a connector to ensure disconnection after 30 years is feasible. Since the connector will not be re-used, damage may be allowed during the disconnection operation.

The lower portion of the universal joint has a stab-in tapered guide which, when coupled with guidewire equipment, allows for more positive positioning and securing into the mooring base during the installation sequence. This design also allows the universal joint to be detached from the base and reinstalled to permit the removal of the CWP if necessary, for overhaul and

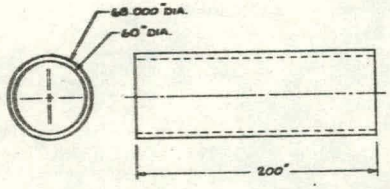

BASE UNIVERSAL JOINT PIN

SCALE: 1/4"=1'-0"

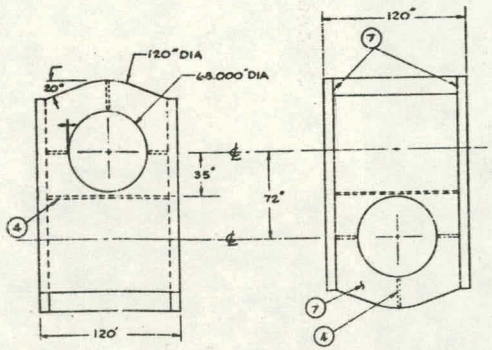

BASE UNIVERSAL JOINT COUPLER

SCALE: 1/4"=1'-0"

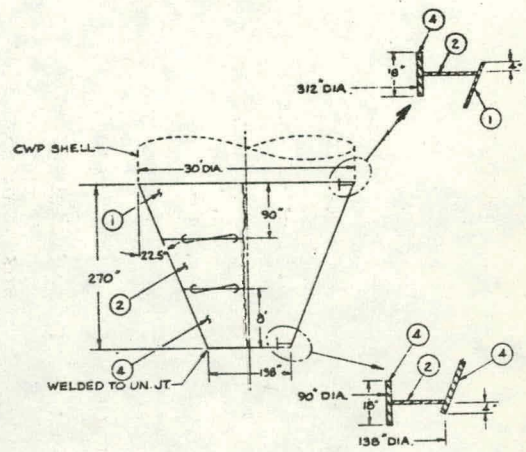

BASE UNIVERSAL JOINT TO CWP STRUCTURE

SCALE: 1/8"=1'-0"

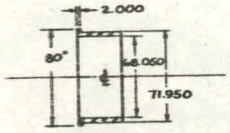

UNIVERSAL JOINT LUBRITE BUSHING

SCALE: 1/4"=1'-0"

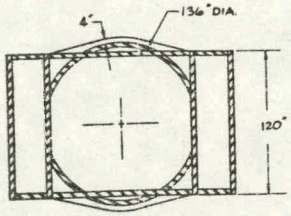

SECTION A-A

PARTS LIST

Item 1	3/4-in. Plate
Item 2	1-in. Plate
Item 3	1-1/2-in. Plate
Item 4	2-in. Plate
Item 5	3-in. Plate
Item 6	4-in. Plate
Item 7	8-in. Plate

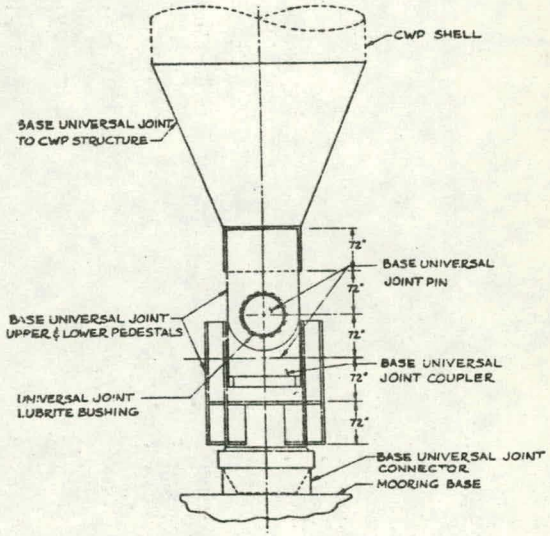

BASE UNIVERSAL JOINT

SCALE: 1/8"=1'-0"

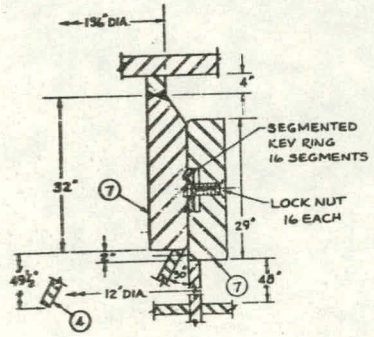

SECTION

BASE - UNIVERSAL JOINT CONNECTOR

SCALE: 1"=1'-0"

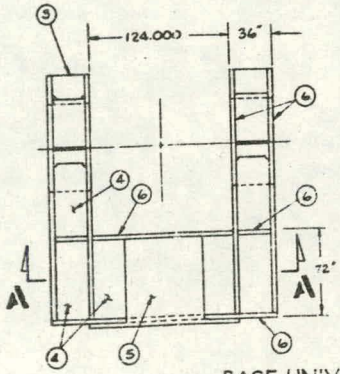

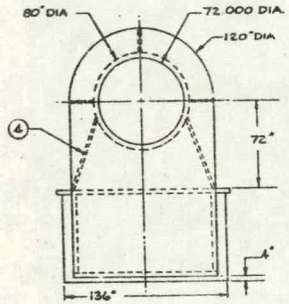

BASE UNIVERSAL JOINT

UPPER AND LOWER PEDESTALS

SCALE: 1/4"=1'-0"

Fig. 3-18 Base Universal Joint

THIS PAGE

WAS INTENTIONALLY

LEFT BLANK

repairs, even after prolonged submergence. The universal joint is designed to operate in seawater with minimum maintenance requirements. Based on SALM experience, expected bearing life is 20 years.

The bearing pedestals are continuous with a horizontal beam welded through to a cylindrical shell. Two of these pedestal structures are required, one for attachment of the CWP and the other for attachment to the base mechanical connector. The four bushings are press fit into the four bearing pedestals.

A coupler structure connects the two bearing pedestal structures. The pin centerlines of the coupler are vertically offset by 6 ft. The pins fit through the central coupler with metal-to-metal bearing contact rather than through Lubrite bushings. The pins are keyed to the coupler to prevent relative rotation and to ensure that sliding occurs on the bushing surfaces in the bearing pedestals. The coupler plates have a maximum thickness of 8 in.

The pins are of forged material, of a thickness to resist the shear and bending loads in the pins. They are keyed to the coupler.

The top pedestal structure is connected to the CWP extension by a conical shell, of a wall thickness varying from 2 to 3/4 in. Lateral stiffeners are required at the ends of the cone to carry hoop stresses. Additional stiffeners may be required. The conical structure weighs approximately 90 kips. Conical transition zones are commonly used in offshore tension anchor leg moorings, such as the Hondo field SALM.

The stab cone underneath the inner ring of the mechanical connection is used to guide the universal joint into the base. A padeye inside the cone, welded to the baseplate of the universal joint, provides an attachment for the installation guidewire. This guidewire cannot be detached from the universal joint after it is installed, but instead is left in place as a short leader section. The guide cone makes positive contact with the baseplate prior to installation of the actuator screws.

3.5.2 Universal Joint Design Criteria

The universal joint is designed in accordance to ABS rules for the design of single point moorings. The major deviation is that Section 5.5.1 was used for storm loads instead of Section 5.5.2, which means that the one-third allowable stress increase for the maximum storm was not used. Thus the universal joint design is considered conservative with respect to ABS rules. With the possibility of resonance and fatigue in the structure, however, it is felt that a lower design stress is the more applicable value.

A detailed fatigue analysis of the stress concentration would probably verify this reduction.

The following are allowable design stresses:

Tension	0.6 Fy
Bending	0.6 Fy
Shear	0.4 Fy

The design loads are as follows:

Tension	12,000 kips
Side Load	1,500 kips (any direction)

3.5.3 Design Methods

The universal joint is designed using standard industry practice. Simplified cuts are taken through various sections of the structure and the stresses are calculated using beam theory, assuming that plane sections remain planar after bending. The important sections are listed below:

1. Tearout shear on the circular padeyes
2. Bending in the pedestals
3. Shear in the pedestal webs
4. Bending in the pedestal cross beam
5. Bending in the central tube

6. Tearout shear in the coupler pin holes
7. Tension in the conical CWP transition

This method of design has been previously verified for universal joints of tension anchor leg moorings by comparison with the results of finite element computer analyses.

It is possible that the universal joint cost could be reduced by using higher strength steel, which would reduce the weld volume required.

3.5.4 Fabrication Procedure

The welding procedures for the 8-in. and 4-in. plates must be carefully defined. Extensive preheating of the structure is required. In addition, stress relieving in an oven may be required.

Access holes are provided into the structure so that the majority of the welds can be two-sided full-penetration welds. Welds accessible from only one side have backup bars to contain the weld. Access holes are welded closed after inspection. The machining is performed only after the welding, stress relieving, and monel overlaying are complete.

3.6 INSTALLATION

3.6.1 Installation Procedure

For the mooring system installation it is assumed that the Spar-CWP system is previously placed in a vertical orientation with the CWP hanging from the spar. The basic procedure, outlined as follows, is illustrated in Fig. 3-19.

1. The gravity base is floated under its own buoyancy and towed to the site by a tug.
2. The gravity base is lowered to the seafloor by a crane. A series of slings are required, with each sling of a length equal to the vertical elevation lifting capacity of the crane barge. The base is lowered in a series of steps, with each step equal to the length of a

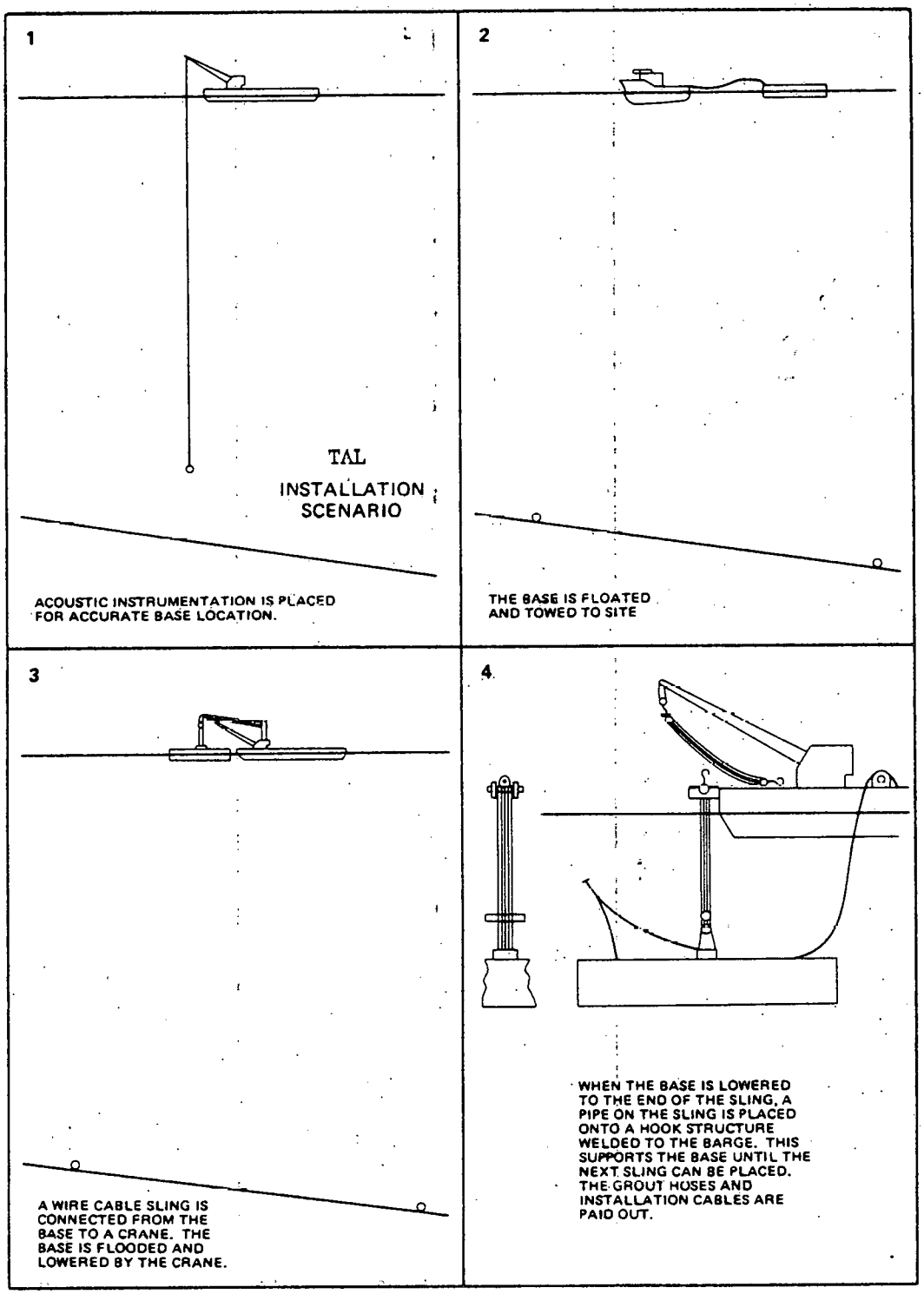

Fig. 3-19 Installation Procedure

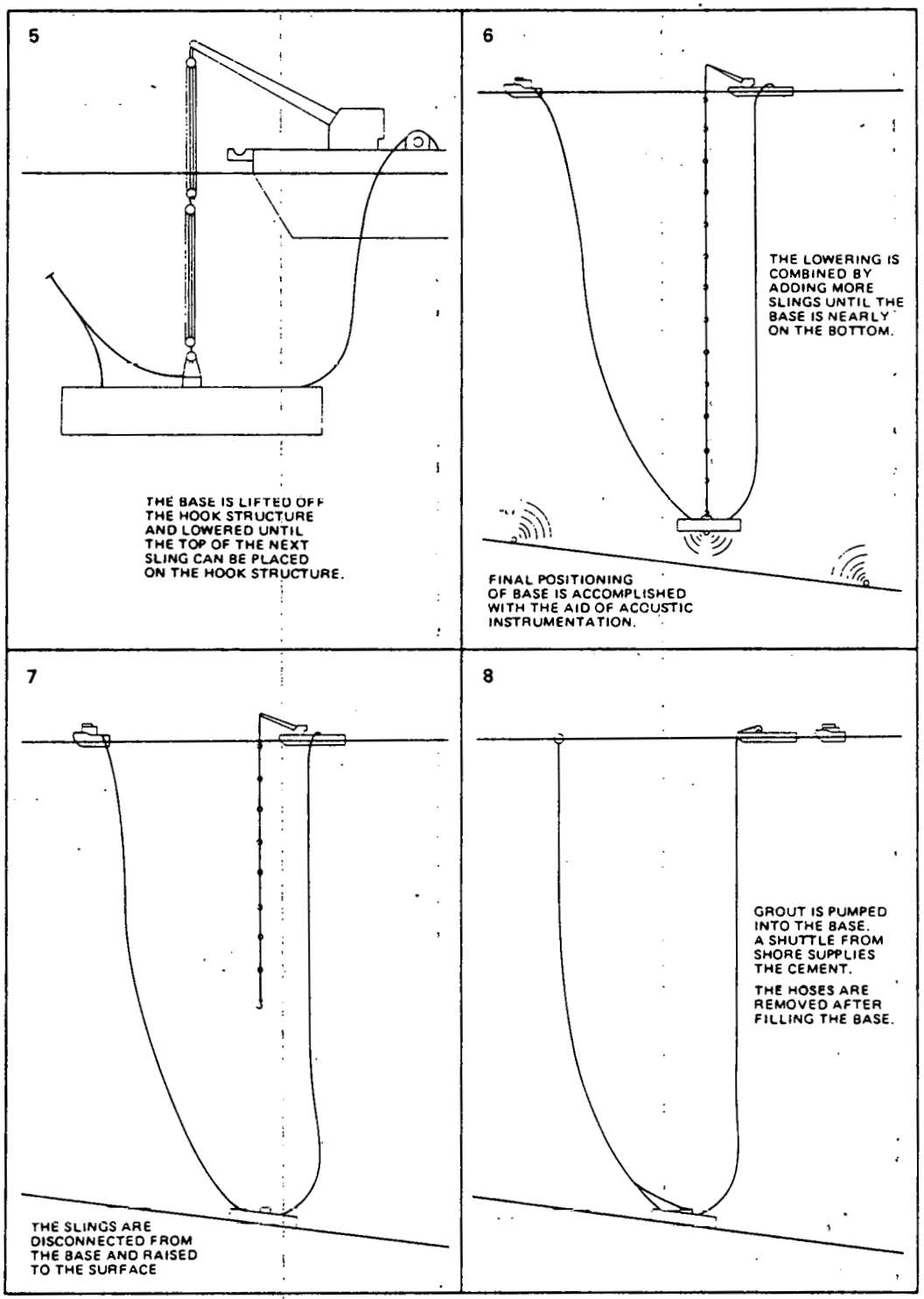
5
THE BASE IS LIFTED OFF THE HOOK STRUCTURE AND LOWERED UNTIL THE TOP OF THE NEXT SLING CAN BE PLACED ON THE HOOK STRUCTURE.
6
THE LOWERING IS COMBINED BY ADDING MORE SLINGS UNTIL THE BASE IS NEARLY ON THE BOTTOM.
FINAL POSITIONING OF BASE IS ACCOMPLISHED WITH THE AID OF ACOUSTIC INSTRUMENTATION.
7
THE SLINGS ARE DISCONNECTED FROM THE BASE AND RAISED TO THE SURFACE
8
GROUT IS PUMPED INTO THE BASE. A SHUTTLE FROM SHORE SUPPLIES THE CEMENT.
THE HOSES ARE REMOVED AFTER FILLING THE BASE.

Fig. 3-19 (Cont.)

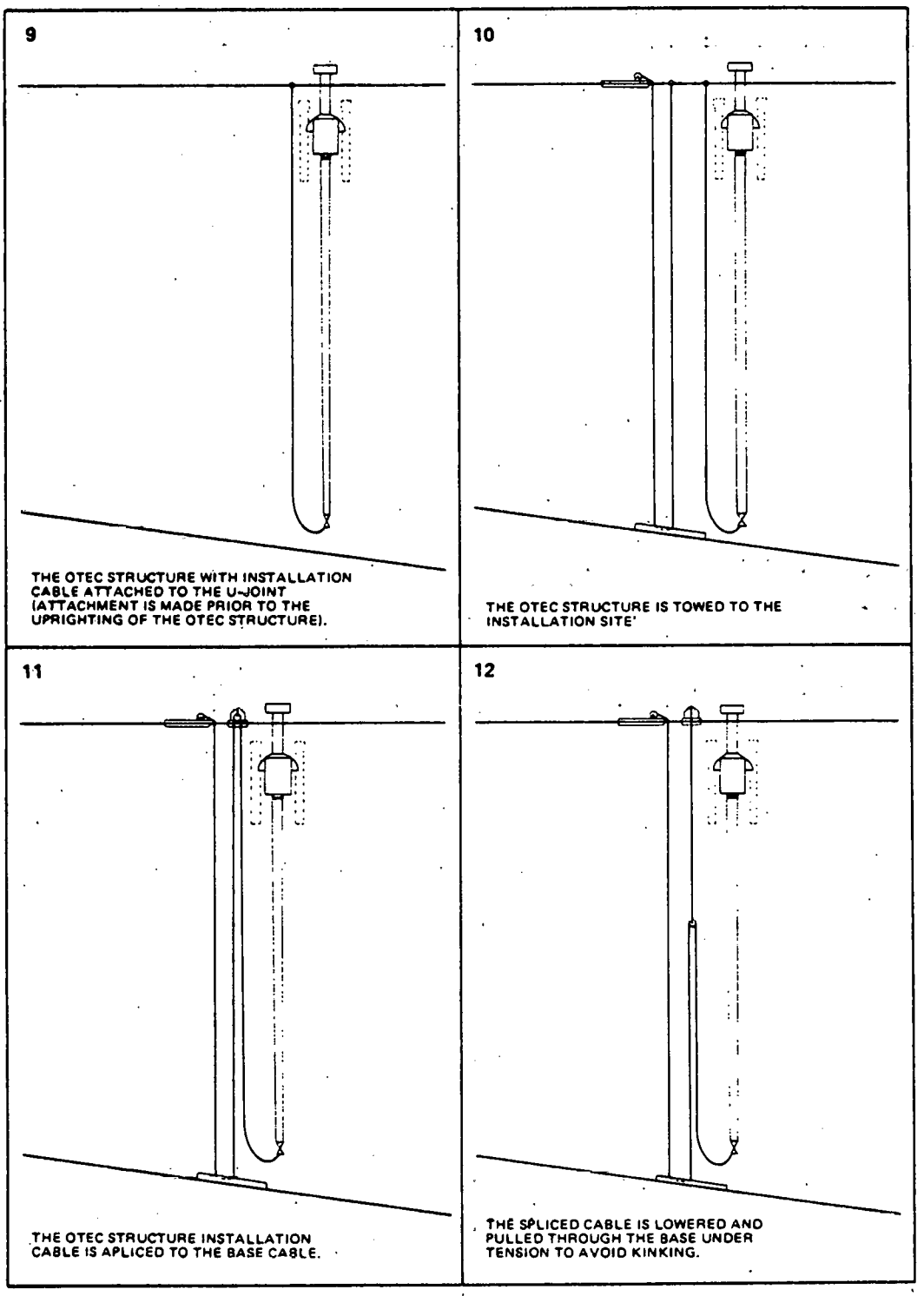
9
THE OTEC STRUCTURE WITH INSTALLATION CABLE ATTACHED TO THE U-JOINT (ATTACHMENT IS MADE PRIOR TO THE UPRIGHTING OF THE OTEC STRUCTURE).
10
THE OTEC STRUCTURE IS TOWED TO THE INSTALLATION SITE'
11
THE OTEC STRUCTURE INSTALLATION CABLE IS APLICED TO THE BASE CABLE.
12
THE SPLICED CABLE IS LOWERED AND PULLED THROUGH THE BASE UNDER TENSION TO AVOID KINKING.

Fig. 3-19 (Cont.)

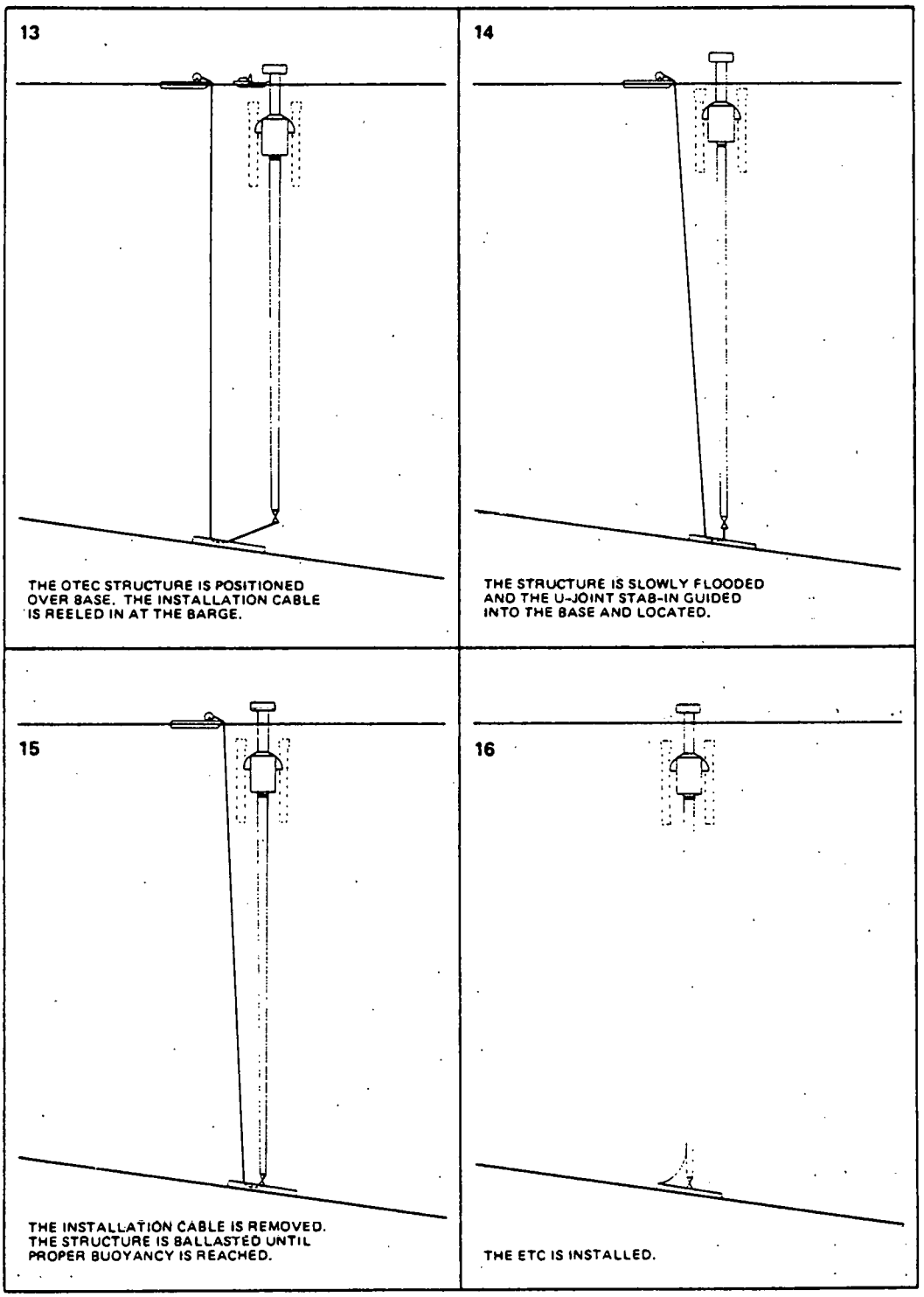
13
THE OTEC STRUCTURE IS POSITIONED OVER BASE. THE INSTALLATION CABLE IS REELED IN AT THE BARGE.
14
THE STRUCTURE IS SLOWLY FLOODED AND THE U-JOINT STAB-IN GUIDED INTO THE BASE AND LOCATED.
15
THE INSTALLATION CABLE IS REMOVED. THE STRUCTURE IS BALLASTED UNTIL PROPER BUOYANCY IS REACHED.
16
THE ETC IS INSTALLED.

Fig. 3-19 (Cont.)

sling. The top beam of each sling is supported on a structure projecting from the side of the barge, while carrying the base weight, in order that the next sling can be positioned.

3. When the base is nearly lowered to the seafloor, transponders on the base are used to position the barge until the base is over the desired location. The base is lowered the remaining distance until it rests on the seabed.
4. The slings and cables are raised onto the crane barge. The sling is hooked to the base in such a way that when tension in the sling is removed the sling slides off the base lifting pads. Thus divers or machines are not required to remove the base sling.
5. The gravity base is filled with cement grout. Eight 3-in. ID grout hoses are lowered with the gravity base. These hoses are connected to a piping system in the base that distributes the grout evenly within the base. Grout is pumped from a grout mixer on board an installation barge. Since a large volume of grout is required, a workboat shuttle from a nearby land-based cement plant or a storage facility is required. These workboats carry grout sacks which are to be continuously offloaded onto the installation barge. The grout mixture is formulated so that it can be mixed with seawater.

   The grout is pumped into each of the eight base compartments one at a time. The setting time is regulated so that the compartment can be filled before the grout begins to harden. Television cameras lowered from the surface are used to monitor the grout installation, and to determine when the compartments are filled. This procedure is similar to that used in large concrete structures in the North Sea.

   The grout hoses are disconnected from the base by either breaking a weak link in the hoses, or by removal by either a mechanical manipulator or a diver in a pressurized diving suit.
6. The CWP and spar are maneuvered over the base and connected to a guidewire passing through the base socket. The spar is ballasted with water until the universal joint mechanical connector is pulled into place in the base. A mechanical manipulator or a diver in a

pressure suit is then used to secure the mechanical connector by wedging the rams of the connector with actuator screws used for that purpose.

7. The guidewire is then removed from the base, with a leader left in the guide tube for future CWP removal.

3.6.2 Equipment Availability

The crane that lowers the base must have a lift capacity of 2,000 kips at the horizontal reach required to lift directly over the center of the base, or approximately 60 ft plus the width of the barge overhang. If a crane of this capacity is not available during the installation, buoyancy tanks can be placed in the base structure. The largest crane barge presently in use has a maximum lift capacity of 3,000 tons. After the base is lowered below the barge keel and suspended from the barge rail, these tanks are flooded. The crane capacity is greater at this shorter reach and the base can be lowered to the seafloor as previously described.

It is unlikely that sufficient grout hose will be readily available for this installation. Thus the grout hose must be purchased specially for this project, increasing the installation costs.

Standard depth measurement techniques generally provide accuracy of 1 percent; or 33 ft at this site. To obtain the accuracy required for TAL installation, 0.3 percent, salinity and temperature measurements are required.

3.6.3 Installation Aids

Pressurized Diving Suits. Pressurized diving suits, such as the JIM suit, are rated to 3,000 ft of water depth. This system offers the advantage of direct eye contact with the underwater work, increasing the reliability of the installation. Although presently rated to a depth of 3,000 ft, it is possible that this depth could be extended by the time of installation of the OTEC/SKSS.

Underwater Manipulation RCV. Manned and unmanned underwater manipulators are available which can perform a variety of underwater tasks, such as tightening bolts with impact wrenches, lifting objects, and making connections and disconnections.

Manned underwater submersibles such as the General Electric Diver Equivalent Manipulator System (DEMS) are depth limited to approximately 3,000 ft, requiring little additional depth for the OTEC base installation. The major limitation will be the 65-lb lifting capacity of the manipulator arm.

The depth limitation of the unmanned manipulator submersible is less stringent than for the manned submersible. These units are operated from the surface by television cameras.

3.6.4 Universal Joint to Base Connector

This connector is similar to units used as structural pipe connectors in the offshore industry. Steel rams are forced into place by threaded actuator screws with setscrews. These threaded parts are turned by an impact wrench during installation, operated from an RCV or a pressurized diving suit.

3.6.5 Retrieval Procedure

Retrieval of the Spar/CWP requires no guidewires. The spar is ballasted until it submerges sufficiently to indicate that the uplift on the base is removed. The mechanical connector is unfastened by an RCV, and the spar is floated free with the universal joint attached. Complete retrieval of the TAL is not satisfied as removal of the base plate from the seafloor is not feasible (see Fig. 3-20).

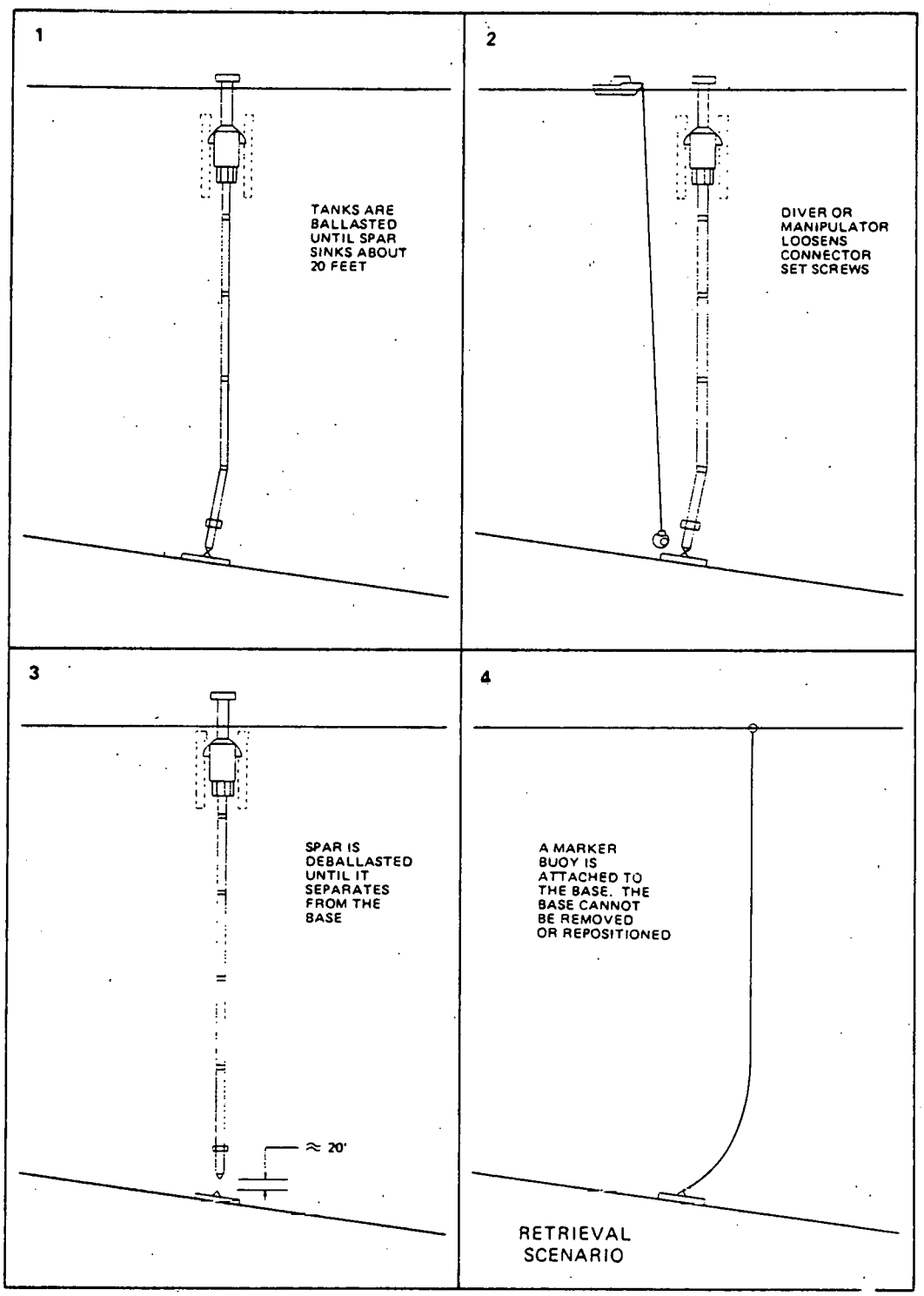

Fig. 3-20 Retrieval Procedure

3.7 SPAR-TAL PHYSICAL LIMITATIONS

3.7.1 Watch Circle Limitations

As previously described, placing the buoyancy required to support the CWP at the top of the CWP results in a large uprighting moment that helps keep the spar within a 20-percent watch circle during the 100-year storm.

If the CWP weight is increased to handle higher tensions, this uprighting moment will also increase. Watch circle radius is not a severe problem for the TAL system. The CWP also has no tendency to make contact with the bottom.

3.7.2 Depth and Position Errors

The spar vertical elevation should be fixed within 10 ft (plus or minus) to prevent submergence of the elevated platform in the wave crests, and to prevent the power modules from being exposed in the storm wave troughs. Ten feet represents an error of 0.3 percent (plus or minus) which is an extremely accurate value in these water depths.

Depths are difficult to establish accurately in deep water because the water temperature gradient must be known in order to compensate the hydroacoustic devices. In short, great care must be exercised in locating the gravity base, because once it is in place it cannot be removed. It is not certain whether this accuracy has been attained. The elongation in the CWP must also be considered when placing the base.

At a slope of 10 deg, the base must be placed within plus or minus 57 ft along the direction of slope of the seabed to maintain plus or minus 10 ft of vertical accuracy. Along the bottom contour lines, the allowable error can be much greater.

3.7.3 Water Depth

Increase to 5,000 Ft. If the water depth is increased, the longer CWP will be more flexible. The natural period of the spring-mass system for low oscillations will increase into the range of periods of the waves. It seems unlikely, however, that this will greatly increase the vertical or horizontal loads, since the CWP nonlinearity shifts the natural periods above the wave periods. The major requirement is that the spar buoyancy must be greater to support the heavier CWP.

The greatest problem at a 5,000-ft depth is the installation procedure. Five thousand feet exceeds the depth limit of pressurized diving suits and of most underwater RCVs.

Limiting Depth. Depth limitations are imposed by installation difficulties and costs. Present state of the art for installation of this type of structure probably is limited to 3,000 ft. With no great effort this could be increased to 3,280 ft by the time of installation of the 40-MW(e) OTEC plant. It is not certain whether 5,000 ft could be attained by that time. Any further depth will require an increase in the capabilities of the private offshore industry. In short, any depth could be attained with the expenditure of sufficient resources over a period of time.

Another effect caused by a deeper system is that the CWP deflections are greater, causing the spar to be more deeply submerged in the offset position. This requires a longer column to elevate the raised platform above the wave crests.

3.7.4 Effects on Platform Design

Ballast must be added to the spar so that the net buoyancy (of the spar alone) is the desired value, which is 1,000 kips for the preliminary design. If the buoyancy is insufficient, the spar volume must be increased. The spar structure near the CWP pivot must be strengthened to carry the large tension

loads. The spar raised platform must be at least 70 ft above the still waterline to prevent wave crest impact, with a total net buoyancy of 6,000 kips (spar and CWP tanks).

3.7.5 Limiting Environmental Conditions

The Spar-TAL could be designed for more severe wind, wave, and current criteria if necessary. The following components would require modification:

- Spar platform would be raised
- Power modules would require lowering to prevent their being exposed during wave troughs
- CWP tension capacity would need to be increased
- Gravity base size would become larger
- Universal joints would carry higher tensions and would increase in size

3.8 ELECTRICAL POWER CABLE

3.8.1 Design Concept

The Spar-TAL offers versatility in the ETC design in that either the vertical descent, catenaried direct descent, or the standoff buoy arrangements can be used. The recommended arrangement for the Spar-TAL is the vertical descent method, in which the electrical cable is attached directly to the CWP, with flexible loops around the CWP joints. At the base universal joint, a catenary loop of cable can extend from the CWP to the edge of the base. Bending restrictors at each end of the suspended loop can reduce bending in the cable at the rigid attachment.

The minimum bend radius of the cable is 15 ft, according to Simplex. An arrangement to scale is shown in Fig. 3-21 that meets this requirement.

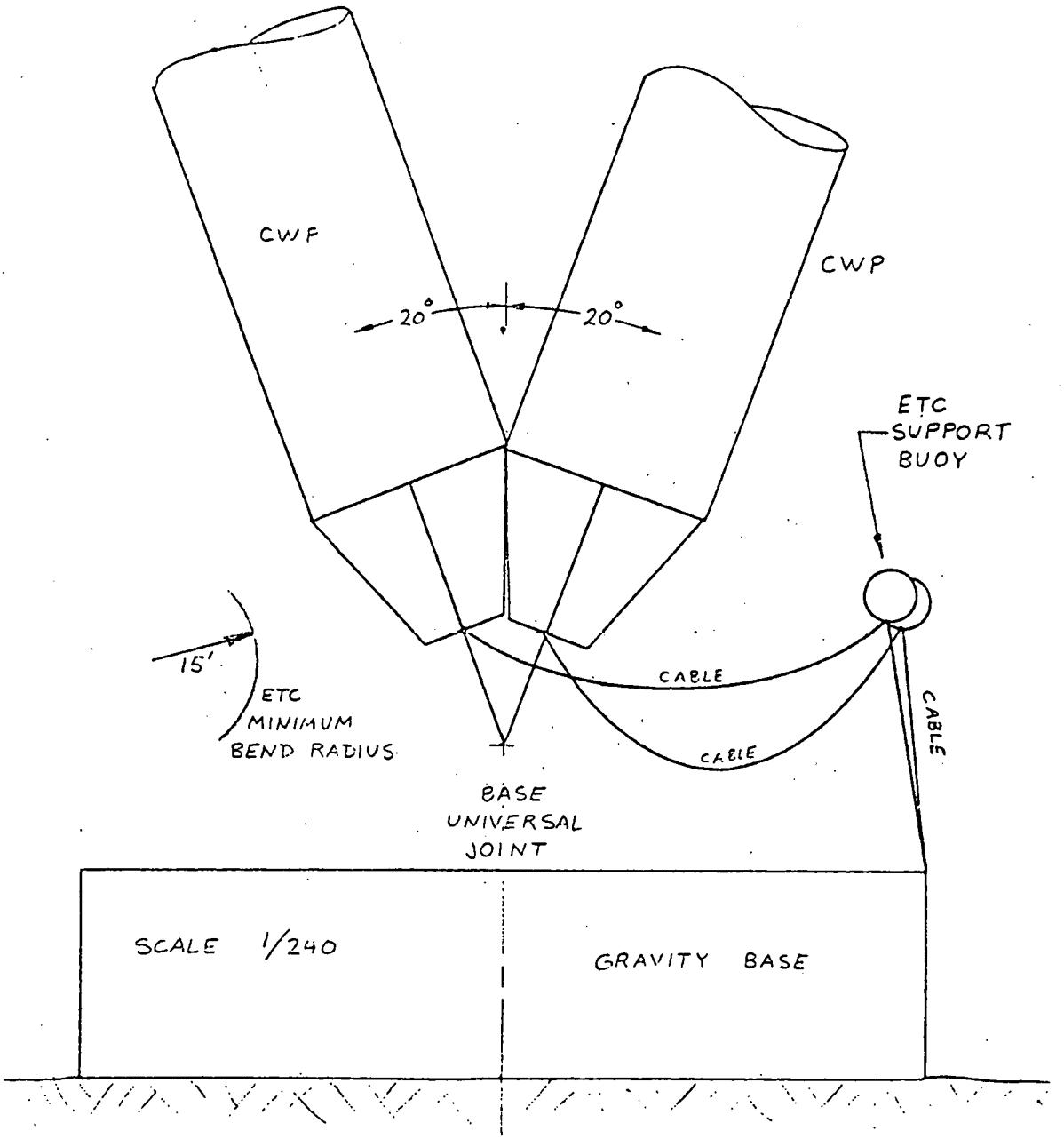

Fig. 3-21 Electrical Cable Base Layout

3.8.2 ETC Installation

The ETC can be installed on the CWP and base in two ways. The first is to pull it through a series of guides from the seabed to the surface. The second method is to clamp it to the CWP and base by using an RCV or diver.

3.9 OTEC COMMERCIAL PLANT APPLICABILITY

The commercial spar has an approximate displacement of 250,000 tons and a CWP diameter of 100 ft. This displacement is more than three times that of the 40-MW(e) plant. The wave forces are approximately three times higher and the gravity base is therefore three times as large, neglecting resonance in the CWP. But since the CWP has three times the diameter and somewhat more than three times the axial stiffness, while the spar mass also increases by a factor of 3, the frequency response in heave (proportional to $\sqrt{K/M}$) is not drastically altered. Thus, the size of the gravity base and universal joint can be linearly proportioned to the displacement of the spar.

If the gravity base steel weight were tripled to 6,000 kips, it would exceed the lifting capacity of large offshore cranes, which presently can lift 3,000 tons. Steps could be taken to allow lowering of a 6,000-ton base, such as the placement of buoyancy tanks in the structure, or the use of high-strength steels. The commercial OTEC plant presents technological difficulties for the TAL design concept.

3.10 MAINTENANCE

3.10.1 Required Maintenance

The steel in the base and universal joint should not corrode excessively in the oxygen-poor waters present at a depth of 3,280 ft. The corrosion allowance is sufficient to maintain design strength over the life of the OTEC/SKSS. In addition, the base design is largely determined by installation

loads, which are nonrelevant after the grout is cured. In short, no painting of the base or universal joint is required after installation.

The Lubrite bushings are designed for long life. There is a remote possibility they could wear more quickly than expected and require replacement during the life of the SKSS. This would necessitate removal of the spar and CWP with the universal joint attached. The pivots in the CWP could also be maintained at this time.

3.10.2 Inspection

Inspection by RCVs and television cameras is recommended at periodic intervals with the following items carefully observed:

- Search for cracks on all exposed steel surfaces, especially near welds and joints
- Inspect the Lubrite bushings for wear; a feeler gauge can be inserted between the pin and the bushing to measure the wear
- Inspect the ETC elements, and the CWP flexible bellows
- Inspect the soil around the base for evidence of scour - rather unlikely at these depths
- Inspect the setscrews of the mechanical connector to check for loosening

3.10.3 Replacement

Scheduled replacement of parts is not required for the Spar-TAL mooring system. Repair will be required only as dictated by the regular inspections.

3.11 RELIABILITY AND PERFORMANCE

The precise reliability of the Spar-TAL is difficult to determine statistically, since none has ever been built. Some general statements can be made about the system:

- The constant tension in the tension member will amplify the significance of any structural defects in the tension system.
- Fatigue and corrosion fatigue require attention.
- The mode of failure of the mooring system could be dangerous. If a 2,000-kips net buoyancy is present and the mooring system fails, the spar will suddenly rise over 310 ft, exposing the evaporator modules. This occurs because static equilibrium requires the Spar/CWP to float higher in the water if not held down by a universal joint. Once the system fails, there is no backup to prevent the Spar-TAL from drifting ashore and thereby suffering great damage.

3.12 CONCLUSIONS AND SUMMARY

The Spar-TAL system loads have proven to be higher than previously expected. An exact load analysis is rather complex, and simplifying assumptions are made to derive a set of design loads. The uncertainty of the effects of damping requires model tests for verification of the final design loads.

The mooring base and universal joint are shown to be feasible structures, utilizing state of the art technology.

The installation of the base and Spar-TAL is possible within present state of the art techniques.

The Spar-TAL concept is shown to be a feasible configuration for mooring an OTEC power plant and warrants continued design development.

3.13 REFERENCES

3.13.1 Cited References

3-1 N. Maddox, "An Energy Basis for the Design of Open-Ocean Single-Point Moorings," OTC paper 1536, 1972, Vol. 1

3-2 K. Terzaghi and R. Peck, Soil Mechanics in Engineering Practice, John Wiley and Sons, 2nd edition, 1967

3-3 H. Winterkorn, and H. Fang, editors, Foundation Engineering Handbook, Van Nostrand Reinhold Company, 1975

3.13.2 Uncited References

- M. McCormick, Ocean Engineering Wave Mechanics, John Wiley and Sons, 1973
- R. Wiegel, Oceanographical Engineering, Prentice-Hall, Inc., 1964
- Lockheed Missiles & Space Company, Inc. Preliminary Designs for Ocean Thermal Energy Conversion (OTEC) Stationkeeping Subsystems (SKSS), Task I: Design Requirements, LMSC-D673832, Sunnyvale, Calif., Jun 1979
- -----, Preliminary Designs for Ocean Thermal Energy Conversion (OTEC) Stationkeeping Subsystems (SKSS), LMSC-D676379, Sunnyvale, Calif., 27 Jul 1979
- J. R. Paulling, "Analysis and Design of the Cold Water Pipe (CWP) for the OTEC System with Application to OTEC-1," Presented to Northern California Section of SNAME, 11 Jan 1979
- Science Applications, Inc., Hydrodynamic Design Loads for the OTEC Cold Water Pipe, by D. Hove, W. Shih, and E. Albano, Report SAI-79-559-LA, prepared for NOAA, Sep 1978
- J. Paulling, "A Linearized Dynamic Analysis of the Coupled OTEC Cold Water Pipe and HMB-I Barge System," prepared for Morris Guralnick Associates, Inc., Aug 1977
- Giannotti & Buck Associates, Inc., Simulation of Platform Wave Induced Motions and Loads for the OTEC 10-MW(e) Modular Applications Spar Platform, Report No. 78-020-009, prepared for Gibbs & Cox, Inc., Dec 1978

- General Electric Brochure, Diver Equivalent Manipulator System (DEMS).
- G. Remery and G. Van Oortmerssen, "The Mean Wave, Wind and Current Forces on Offshore Structures and Their Role in the Design of Mooring Systems," OTC paper 1741, 1973, Vol. 1

Section 4
COSTS AND SCHEDULES

This section considers, in separate subsections, the capital costs associated with the two SKSS designs presented in Sections 2 and 3; the overall life cycle costs implied by these capital costs; and the scheduling of activities required for construction, deployment, and operation of the SKSSs.

4.1 CAPITAL COSTS

Tables 4-1 and 4-2 present capital cost estimates for the ship-MAL and the Spar-TAL SKSS design concepts, respectively; late 1979 dollars are used throughout. It is noted that the two cost estimates are not comparable on a line by line basis, as the design concepts they are respectively associated with are radically different from one another, as are the cost estimating and cost allocation philosphies behind the two estimates. The total capital costs indicated, however, can be compared to each other with a reasonable degree of confidence. In particular, allowances for contingency, home office, engineering and fees are included within the amounts given for each component of the TAL system, while they are calculated separately, as a global figure, for the MAL design. The overall capital cost of the ship-MAL system is roughly 30 percent higher than that of the Spar-TAL. The two summary cost tables are discussed separately in some detail.

All individual component estimates shown for the MAL SKSS are direct from the actual or potential manufacturers; for those components not currently available, such as the windlasses, the costs shown represent the manufacturer's best ROM estimate on the basis of past experience. These manufacturers include: for windlasses, Western Gear Corporation, Lucker Manufacturing Company, Houston Systems Manufacturing Company, and Mitsubishi; for wire rope, British Ropes Limited, Fatzer AG, U.S. Steel Corporation,

Table 4-1 MAL BARGE ACTIVE TENSIONING SKSS CAPITAL COSTS

	1979 ($K)
MOORING SYSTEM COMPONENTS	
Swivel	150
Chain	5,885
Chain Stoppers	180
Fairleaders	1,520
Wire Rope	2,085
Anchors	470
Windlasses	6,720
Miscellaneous	170
Total Component Cost	17,180
Contingency, Home Office, Engineering, and Fees	7,730
Subtotal	24,910
MOORING SYSTEM DEPLOYMENT	
Installation Labor and Support Equipment	310
Deployment Barge Lease	875
Mobilization/Demobilization	375
Total Deployment Cost	1,560
Contingency, Home Office, Engineering and fees	700
Subtotal	2,260
OVERALL MOORING SYSTEM TOTAL	27,170

Elken Spigerverket, and Thyssen; and for chain, Hamanaka International, Inc., and Ramnas. Windlass and chain costs each account for over one-third of total component costs, while fairleaders and wire rope are also important cost components, each account for roughly 10 percent of component costs. As is seen later, wire rope costs are of greater importance to life cycle costs because wire rope is assumed to require replacement at least twice over the life of the OTEC plant.

Table 4-2 SPAR TAL SKSS CAPITAL COSTS

	1979 ($K)
MOORING SYSTEM COMPONENTS	
Universal Joint	8,315
Pile Connector	1,700
Gravity Base	6,950
Total Component Cost	-
Contingency, Home Office, Engineering, and Fees	(Included Above)
Subtotal	16,965
MOORING SYSTEM DEPLOYMENT	
Installation Labor, Support Equipment, and Mobilization/Demobilization	4,165
Total Deployment Cost	-
Contingency, Home Office, Engineering, and Fees	(Included Above)
Subtotal	4,265
OVERALL MOORING SYSTEM TOTAL	21,230

The last entry in the component cost sector of the table covers a miscellany of special purpose links, shackles, and sockets. Mooring system deployment is costed on the basis of the deployment procedure discussed in Section 2.6; this procedure requires a specially equipped barge which is assumed to be available for lease at a rate of $73,000/day. Should this barge have to be built to order for the specific purpose of OTEC SKSS deployments, its cost is estimated at approximately $15,000,000. Labor costs are included in the deployment cost estimate at a rate of $50/hr, and support craft (other than the deployment barge) are expected to cost roughly $8,000/day.

To arrive at an overall estimate of SKSS capital costs, allowances are added to basic component and labor cost to cover costs associated with administrative and engineering activities, estimated at roughly 10 percent of basic costs, to provide for fees of approximately 10 percent, and to include a contingency buffer of some 20 percent of basic costs; it might be noted that transportation from the Gulf Coast to the operating site is included within

this contingency, as component costs are given FOB Gulf Coast. Combining these three allowances multiplicatively, an overall combined allowance of some 45 percent is arrived at, and this is reflected in the allowances shown for these items in Table 4-1. Ideally, different allowances should be applied to each cost component for each of the factors mentioned above, in particular, contingency allowances should perhaps be higher for deployment costs than for component costs, given their respective degree of definition. However, the additional estimating effort required is not justified by the somewhat spurious improvement in accuracy that would result, and consequently this approach is not followed. The overall cost estimate arrived at by applying a uniform allowance across the board to all cost components is as accurate an estimate of SKSS costs as can be formulated at this stage of the design process.

The TAL capital cost estimates include the following items:

Item 1. Universal Joint

- o Universal Joint Fabrication
- o Bushings
- o Miscellaneous IMODCO Supply
- o Freight (West Coast to East Coast, Maryland)

Item 2. Pile Connector

- o Pile Connector Fabrication
- o Pile Connector Half Weld to Item 1
- o Freight (West Coast to East Coast, Maryland)

Item 3. Gravity Base

- o Gravity Base Fabrication
- o Pile Connector Half Weld to Item 3
- o Miscellaneous IMODCO Supply
- o Installation Rigging Equipment

Item 4. Installation - Gravity Base

- o Equipment Mobilization/Demobilization
- o Gravity Base Tow to Site
- o Installation Prerigging
- o Gravity Base Installation
- o Ballast of Base by Concrete (50×10^6 lb)

The following items are excluded from the cost estimates:

Item 1. Universal Joint

- o Installation to OTEC Machine

Item 2. Gravity Base

- o Floating BAL/DEBAL Installation Tanks
- o Location Positioning Equipment
- o Location Positioning Marker Floats
- o Location Position Triggering Transponders
- o Seabed Leveling Grout
- o Sub-Base Location Template
- o Towing from East Coast to Pt. Tuna

Item 3. Installation - Gravity Base

- o Weather Downtime
- o Fuel Cost
- o OTEC Machine Stab-In into Gravity Base
- o Seabed Preparation
- o RCV Underwater Vehicles and Support Equipment
- o Seabed Cleanup

The dominant cost elements in the costs estimated for the TAL SKSS (Table 4-2) are the universal joint and the gravity base, which together account for some 90 percent of total component costs and 70 percent of total installed system costs. The high cost of these items is due largely to their very large size and plate thickness and, in the case of the universal joint, to the extensive use of monel and lubrite. Deployment costs for the TAL system, wherein the

cold water pipe and spar are assumed to be on site, are estimated to be roughly twice as high as those for the MAL SKSS design; however, as already noted, the overall installed cost of the Spar-TAL is some 30 percent lower than that of the ship-MAL. The costs associated with modification of the cold water pipe required to accommodate the mooring loads are not include.

4.2 LIFE CYCLE COSTS

The life cycle costs (LCCs) associated with both SKSS designs are estimated using the LCC model described in the Task II Conceptual Design Final Report (LMSC-D676379), with some minor modifications. For the sake of completeness, a brief description of the model is included below, incorporating the modifications mentioned above.

The first step in calculation of LCCs is to generate a cash disbursement schedule spanning the entire life of the SKSS. The program operates on the capital cost data in Tables 4-1 and 4-2, according to the following rules:

- The OTEC platform and SKSS are to start operation at the beginning of 1985 and have a 30-year operational life, thus ending operation at the end of 2014.
- Capital cost expenditures take place at an even rate over the period from order placement to equipment delivery; thus, they are time-phased following the schedules presented in the next subsection.
- Scrapping or disposal costs are assumed to be one-half of deployment costs, and to occur in 2015, the year following the end of operations.
- Yearly local tax and marine insurance charges are expected to be roughly 3.5 percent of initial capital cost.
- The yearly cost of inspection and routine maintenance of the platform is estimated at approximately 1 percent of initial capital cost.
- All costs escalate at a yearly rate of 7 percent except for tax and insurance charges which remain fixed as a proportion of original (accounting) cost.

Once the disbursement schedule has been generated, each year's cash flows are totaled and their present value in 1979 is then obtained following the end-of-year financial analysis convention and a 10-percent discount rate; the result of this operation is the overall LCC of each system for a given cost scenario. It might be noted that the values as given above for escalation and discount rates are those suggested for use in the recently completed Power System Development-II Study.

Table 4-3 shows the disbursement schedule and life cycle cost for the ship-MAL SKSS concept. The overall LCC is approximately $45,000,000, some two-thirds higher than capital costs. This reflects the inclusion in LCCs of the costs of maintenance and eventual scrapping of the SKSS, taxes and insurance charges on it, and the cost of two replacements of the wire ropes, which are assumed to have a 10-year service life. The present cost of these two replacements is slightly over 10 percent of the total LCC. This high proportion of wire rope replacement costs in LCC is due partly to assuming that the cost of the operations involved in retrieving and disposing of old wire ropes, and replacing them with new ones, is approximately the same as the cost of the new ropes themselves. This assumed operational cost is almost certainly too high, as it is roughly equal to the cost of the original deployment operation; this high estimate was retained to introduce some conservativeness into the LCC estimate, thus compensating for the perhaps optimistically long assumed wire rope service life. To test the sensitivity of LCC to this parameter, a separate calculation is carried out for a 5-year wire rope life, resulting in a LCC increase of roughly one-quarter, to approximately $57,000,000. By contrast, assumption of a 10-day delay in deployment and scrapping operations, at a weather downtime rate of $100,000/day (in 1979 dollars), only increases the total LCC by about 5 percent.

Table 4-4 shows the disbursement schedule and total life cycle cost for the Spar-TAL SKSS. The overall LCC is approximately $31,000,000, roughly one-half higher than the capital cost estimate. It might be noted that no actual maintenance is planned for this system. The amounts shown under this heading

Table 4-3 SHIP-MAL LIFE CYCLE COSTS

	1983	1984	1985	1986	1987	1988	1989	1990
SWIVEL	0.	210.	0.	0.	0.	0.	0.	0.
CHAIN	0.	8254.	0.	0.	0.	0.	0.	0.
STOPPER	0.	252.	0.	0.	0.	0.	0.	0.
FAIRLEAD	0.	2132.	0.	0.	0.	0.	0.	0.
WIREROPE	0.	2924.	0.	0.	0.	0.	0.	0.
ANCHORS	0.	659.	0.	0.	0.	0.	0.	0.
WINDLASS	0.	9425.	0.	0.	0.	0.	0.	0.
MISC	0.	238.	0.	0.	0.	0.	0.	0.
CHOEF	0.	10842.	0.	0.	0.	0.	0.	0.
DEPLOYMENT	0.	3170.	0.	0.	0.	0.	0.	0.
SCRAP	0.	0.	0.	0.	0.	0.	0.	0.
SUBTOTAL	0.	38107.	0.	0.	0.	0.	0.	0.
TAX & INS	0.	0.	1334.	1334.	1334.	1334.	1334.	1334.
MAINT	0.	381.	408.	436.	467.	500.	534.	572.
TOTAL	0.	38488.	1742.	1770.	1801.	1833.	1868.	1906.

	1991	1992	1993	1994	1995	1996	1997	1998
SWIVEL	0.	0.	0.	0.	0.	0.	0.	0.
CHAIN	0.	0.	0.	0.	0.	0.	0.	0.
STOPPER	0.	0.	0.	0.	0.	0.	0.	0.
FAIRLEAD	0.	0.	0.	0.	0.	0.	0.	0.
WIREROPE	0.	0.	0.	11505.	0.	0.	0.	0.
ANCHORS	0.	0.	0.	0.	0.	0.	0.	0.
WINDLASS	0.	0.	0.	0.	0.	0.	0.	0.
MISC	0.	0.	0.	0.	0.	0.	0.	0.
CHOEF	0.	0.	0.	0.	0.	0.	0.	0.
DEPLOYMENT	0.	0.	0.	0.	0.	0.	0.	0.
SCRAP	0.	0.	0.	0.	0.	0.	0.	0.
SUBTOTAL	0.	0.	0.	11505.	0.	0.	0.	0.
TAX & INS	1334.	1334.	1334.	1334.	1634.	1634.	1634.	1634.
MAINT	612.	655.	701.	750.	802.	858.	918.	983.
TOTAL	1946.	1989.	2034.	13589.	2436.	2492.	2552.	2617.

Table 4-3 (Cont.)

	1999	2000	2001	2002	2003	2004	2005	2006
SWIVEL	0.	0.	0.	0.	0.	0.	0.	0.
CHAIN	0.	0.	0.	0.	0.	0.	0.	0.
STOPPER	0.	0.	0.	0.	0.	0.	0.	0.
FAIRLEAD	0.	0.	0.	0.	0.	0.	0.	0.
WIREROPE	0.	0.	0.	0.	0.	22632.	0.	0.
ANCHORS	0.	0.	0.	0.	0.	0.	0.	0.
WINDLASS	0.	0.	0.	0.	0.	0.	0.	0.
MISC	0.	0.	0.	0.	0.	0.	0.	0.
CHOEF	0.	0.	0.	0.	0.	0.	0.	0.
DEPLOYMENT	0.	0.	0.	0.	0.	0.	0.	0.
SCRAP	0.	0.	0.	0.	0.	0.	0.	0.
SUBTOTAL	0.	0.	0.	0.	0.	22632.	0.	0.
TAX & INS	1634.	1634.	1634.	1634.	1634.	1634.	2024.	2024.
MAINT	1051.	1125.	1204.	1288.	1378.	1475.	1578.	1688.
TOTAL	2685.	2759.	2838.	2922.	3012.	25741.	3601.	3712.

	2007	2008	2009	2010	2011	2012	2013	2014
SWIVEL	0.	0.	0.	0.	0.	0.	0.	0.
CHAIN	0.	0.	0.	0.	0.	0.	0.	0.
STOPPER	0.	0.	0.	0.	0.	0.	0.	0.
FAIRLEAD	0.	0.	0.	0.	0.	0.	0.	0.
WIREROPE	0.	0.	0.	0.	0.	0.	0.	0.
ANCHORS	0.	0.	0.	0.	0.	0.	0.	0.
WINDLASS	0.	0.	0.	0.	0.	0.	0.	0.
MISC	0.	0.	0.	0.	0.	0.	0.	0.
CHOEF	0.	0.	0.	0.	0.	0.	0.	0.
DEPLOYMENT	0.	0.	0.	0.	0.	0.	0.	0.
SCRAP	0.	0.	0.	0.	0.	0.	0.	82530.
SUBTOTAL	0.	0.	0.	0.	0.	0.	0.	82530.
TAX & INS	2024.	2024.	2024.	2024.	2024.	2024.	2024.	0.
MAINT	1806.	1933.	2068.	2213.	2368.	2534.	2711.	0.
TOTAL	3830.	3956.	4092.	4237.	4391.	4557.	4735.	82530.

LCC IN 1979 IN $K: 44885.0

ASSUMPTIONS : .07 ESCALATION; .10 DISCOUNT RATE; .035 TAX AND INS

Table 4-4 SPAR-TAL LIFE CYCLE COSTS

	1983	1984	1985	1986	1987	1988	1989	1990
U-JOINT	0.	11662.	0.	0.	0.	0.	0.	0.
PILE CON	0.	2384.	0.	0.	0.	0.	0.	0.
GRAV BASE	0.	9748.	0.	0.	0.	0.	0.	0.
DEPLOYMENT	0.	5982.	0.	0.	0.	0.	0.	0.
SCRAP	0.	0.	0.	0.	0.	0.	0.	0.
SUBTOTAL	0.	29776.	0.	0.	0.	0.	0.	0.
TAX & INS	0.	0.	1042.	1042.	1042.	1042.	1042.	1042.
MAINT	0.	298.	319.	341.	365.	390.	418.	447.
TOTAL	0.	30074.	1061.	1383.	1407.	1432.	1460.	1489.

	1991	1992	1993	1994	1995	1996	1997	1998
U-JOINT	0.	0.	0.	0.	0.	0.	0.	0.
PILE CON	0.	0.	0.	0.	0.	0.	0.	0.
GRAV BASE	0.	0.	0.	0.	0.	0.	0.	0.
DEPLOYMENT	0.	0.	0.	0.	0.	0.	0.	0.
SCRAP	0.	0.	0.	0.	0.	0.	0.	0.
SUBTOTAL	0.	0.	0.	0.	0.	0.	0.	0.
TAX & INS	1042.	1042.	1042.	1042.	1042.	1042.	1042.	1042.
MAINT	478.	512.	547.	586.	627.	671.	718.	768.
TOTAL	1520.	1554.	1590.	1628.	1669.	1713.	1760.	1810.

	1999	2000	2001	2002	2003	2004	2005	2006
U-JOINT	0.	0.	0.	0.	0.	0.	0.	0.
PILE CON	0.	0.	0.	0.	0.	0.	0.	0.
GRAV BASE	0.	0.	0.	0.	0.	0.	0.	0.
DEPLOYMENT	0.	0.	0.	0.	0.	0.	0.	0.
SCRAP	0.	0.	0.	0.	0.	0.	0.	0.
SUBTOTAL	0.	0.	0.	0.	0.	0.	0.	0.
TAX & INS	1042.	1042.	1042.	1042.	1042.	1042.	1042.	1042.
MAINT	822.	879.	941.	1006.	1077.	1152.	1233.	1319.
TOTAL	1864.	1921.	1983.	2049.	2119.	2194.	2275.	2361.

	2007	2008	2009	2010	2011	2012	2013	2014
U-JOINT	0.	0.	0.	0.	0.	0.	0.	0.
PILE CON	0.	0.	0.	0.	0.	0.	0.	0.
GRAV BASE	0.	0.	0.	0.	0.	0.	0.	0.
DEPLOYMENT	0.	0.	0.	0.	0.	0.	0.	0.
SCRAP	0.	0.	0.	0.	0.	0.	0.	74202.
SUBTOTAL	0.	0.	0.	0.	0.	0.	0.	74202.
TAX & INS	1042.	1042.	1042.	1042.	1042.	1042.	1042.	0.
MAINT	1412.	1510.	1616.	1729.	1850.	1980.	2118.	0.
TOTAL	2454.	2553.	2658.	2771.	2892.	3022.	3161.	74202.

LCC IN 1979 IN $K: 30938.0

ASSUMPTIONS : .07 ESCALATION; .10 DISCOUNT RATE; .035 TAX AND INS.

in the computer printout are intended to cover the cost of periodic submarine inspection. It is noticed that consideration of overall LCCs increases the apparent relative cost advantage of this concept over the ship-MAL SKSS as the latter's LCC (Table 4-3) exceeds that for the Spar-TAL SKSS by some 50 percent. This increased advantage is primarily due to the lack of components requiring periodic replacement in the Spar-TAL concept; all items in this design are expected to last out the 30-year operational life of the OTEC plant. In closing, it might be noted that TAL LCC costs are somewhat more sensitive to weather downtime than those of the previous system. A 10-day weather delay, costed now at the (appropriate) higher rate of $250,000/day, results in an increase of over 20 percent on overall LCC.

4.3 SCHEDULES

Figures 4-1 and 4-2 depict, for the MAL and TAL SKSS designs, respectively, schedules for component order placement, SKSS integration and deployment, operations and recurring replacements, and eventual scrapping of the SKSS at the end of its useful life.

It is assumed in both cases that deployment is planned to take place in the last quarter of 1984, followed by operations beginning in early 1985. It is emphasized that this schedule is primarily for the purpose of LCC analysis and consequently does not take into account weather window considerations. Should such considerations dictate a preference for a different seasonal period for deployment operations, the entire schedule can be shifted in either direction by the appropriate number of months. The impact on LCCs of such shifting is relatively small, on the order of one or two percentage points.

The longest lead items in the MAL SKSS concept are the chain, with a 24-month order lead time, followed by windlasses, which should be ordered some 18 months prior to need. The balance of components for this SKSS design can be ordered 3 to 6 months prior to need. Mobilization, system integration and installation, and demobilization, lasting somewhere between 1 and 2 months, are assumed to take place within the last quarter of 1984, as discussed

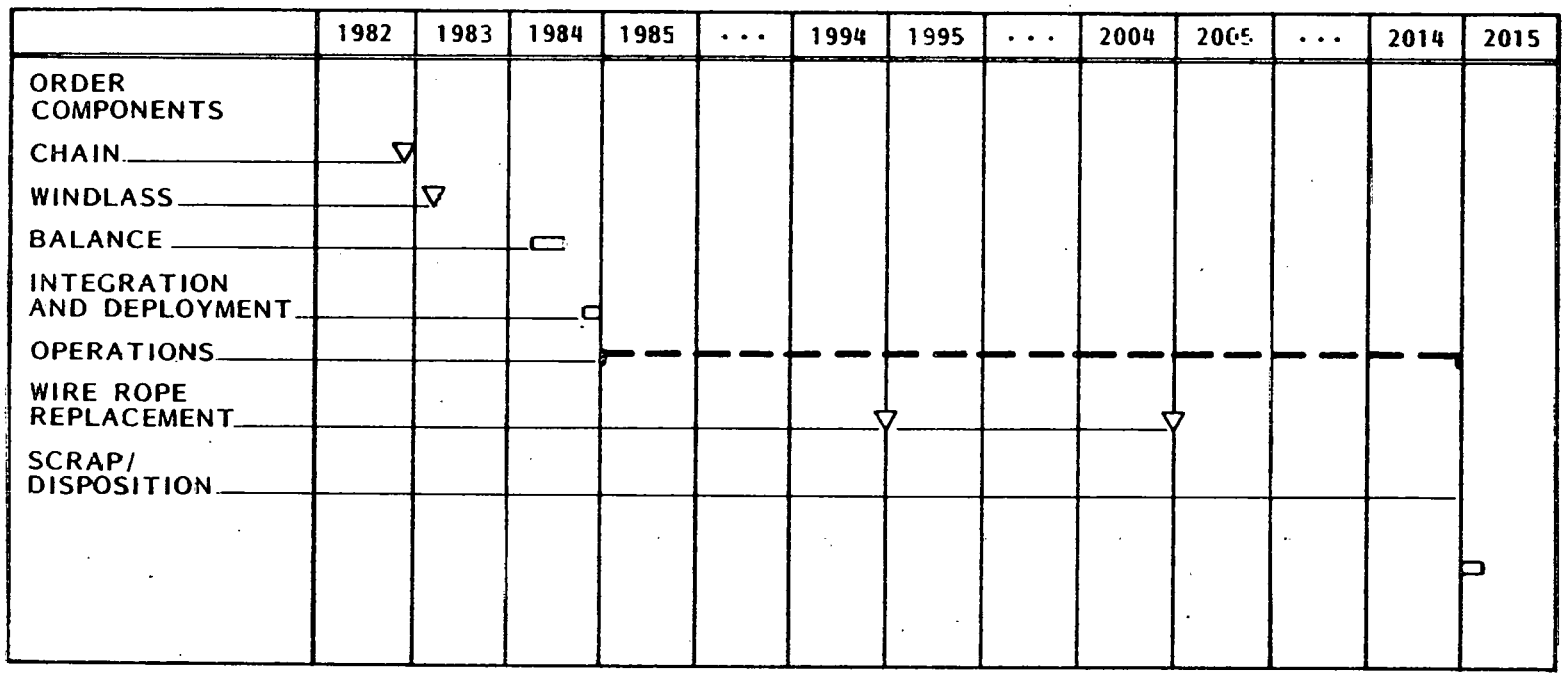

Fig. 4-1 Ship-MAL Schedule

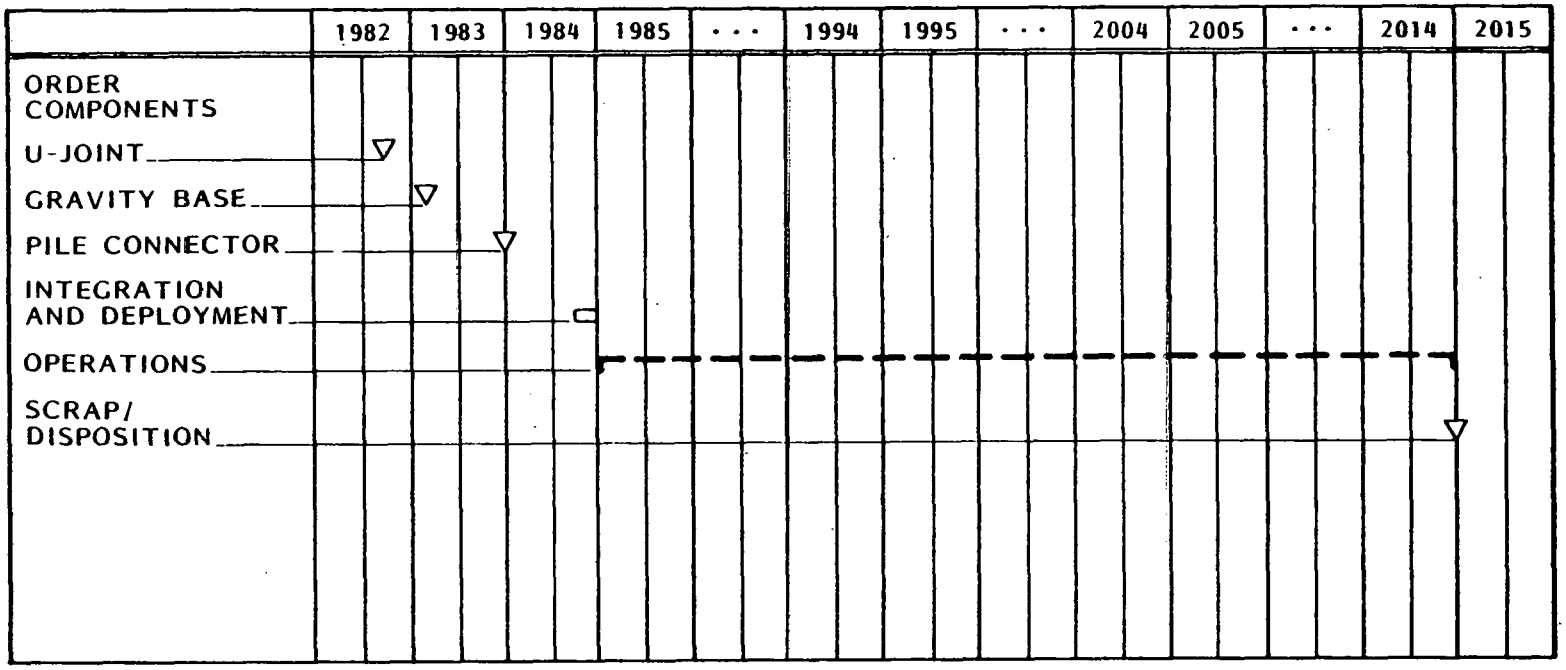

Fig. 4-2 Spar-TAL Schedule

earlier. Routine maintenance in the course of operations takes place on a continuous basis over the 30-year life of the SKSS. In addition, major maintenance operations occur at 10-year intervals to replace worn wire ropes. Finally, removal and scrapping of the SKSS are planned to occur in the first quarter of 2015, the year following termination of operations.

In the case of the TAL SKSS, orders for the universal joint and the gravity base must be placed 24 and 18 months, respectively, in advance of need, and the pile connector must be ordered 9 months in advance. Again, deployment is assumed to take place in the last quarter of 1984, and the system is assumed to be scrapped in the first quarter of 2015.

The installation of the lower universal joint into the gravity base should form part of the total installation sequence in which the OTEC spar is connected to the CWP sections in a vertical orientation.

If connecting the base universal joint to the mooring base is priced out separately, the costs excluding divers and remote control vehicles, are as follows:

Mobilization/Demobilization	$ 50,000
1 Tug, 5 days	40,000 plus fuel
1 Materials Barge, 5 days	25,000
Miscellaneous Equipment	5,000
TOTAL	$120,000

Section 5
CONCLUSIONS AND RECOMMENDATIONS

Preliminary designs are completed for two OTEC Stationkeeping Subsystems; the MAL with active tensioning for the barge and the spar TAL. Engineering description at the level of detail required for preliminary design are provided and supported by extensive discussions of design development and methodology.

The stationkeeping performance requirements for the barge are satisfied by the MAL active tensioning SKSS. The MAL maintains station in the Extreme Sea State under conservative design loads and with loss of the windward leg. The system provides sufficient holding power to maintain station with the required excursion, is capable of altering leg lengths to effectively distribute loads, provides heading control of up to 90 deg, and is suitable for extrapolation to the commercial plant SKSS. MAL SKSS capital cost estimate is $27.2 M, and life cycle cost is $45 M. The MAL requires approximately two years from order of hardware to installation.

A development and testing program presented in the separate Task IV report, is recommended to provide confirmation of design assumptions and hardware development necessary for successful installation of the MAL in 1985. The MAL design is based on existing or minor extensions of manufactured components.

Active tensioning is shown to be an effective technique for reducing leg tension. The barge heading is controllable by lengthening all legs, thereby transferring tension to pendant lines. The extent of heading change, proportional to the extent of load sharing between pendant and chafing chains, is limited to 90 deg clockwise rotation. MAL cost sensitivity to watch circle is small as the Extreme Sea State requirement limits reduction in anchor leg scantlings.

A detailed deployment plan defines the steps and equipment required to install the MAL in the great depths at the Puerto Rico site. Procedures for inspection, maintenance and repair indicate the extensive operation required for wire rope replacement. Interfacing the MAL with the barge is shown to be noncritical, although large bending and heel moments are induced in the barge by the SKSS. The potential interference between the CWP and a slack anchor leg in the Extreme Sea State, and between anchor legs and riser cables, requires further investigation to assess criticality.

The TAL is shown to potentially satisfy the SKSS design requirements for the spar platform. The design, based on extrapolation of existing SALMs, is sized to react loads which are significantly larger than the loads determined in conceptual design. Hence, the universal joint and gravity base structure are heavier and more costly than both the earlier concept and existing SALMs. The required service life is 10 years longer than present design requirements. The loads on the CWP, acting as an integral component of the SKSS, are determined. A CWP design iteration is required to assess the impact on the CWP, particularly in the area of tension carrying capacity of the pipe joints. Extension of analytical models is required to adequately predict TAL performance in a seaway. The capital cost is $21.2 M and life cycle cost is $31 M.

TAL installation involves lowering the gravity base and grouting in place, followed by stab-in of the U-joint attached to the bottom of the CWP. This procedure, critically dependent on accurate measurement of water depth, is considered to be within the state-of-the-art in offshore engineering.

In comparing the MAL with the TAL, consider that the TAL is not appropriate to the ship while the MAL with modification is appropriate to the spar. A relative comparison is made in consideration of the choice of a SKSS for the spar.

Factor	SKSS
Installation	MAL is closer to SOA than TAL, considering depth and service life.
Electrical Riser	TAL provides more direct interface; less interference than MAL.
Failure	MAL has graceful mode of failure; TAL does not.
CWP Interface	MAL requires minimal interface with CWP; TAL major interface with CWP.
Platform Interface	TAL has minimal interface with platform; MAL has significant interface.
Life Cycle Cost	TAL has potential for lower life cycle cost.
Water Depth	TAL allows shallower site, thereby potentially lower costs.
Risk-Criticality	MAL is found to have less risk than the TAL.
Schedule Risk	MAL has lower delivery risk because of fewer special fabrication items.
Deployment	TAL has lower economic risk as the high cost work barge needed for MAL deployment is not required for the TAL.

Design and analysis effort is recommended to further develop the two SKSS designs. Areas which may lead to cost reductions and which require development include:

- For the MAL: wire rope sheathing and other corrosion inhibiting techniques, continuous pulling machines for chain, high efficiency drag embedment anchors for tandem configuration, fore and aft asymmetry of anchor legs, shorter chain segment, verification of fatigue loading predictions and development of empirical S-N curves for wire rope.
- For the TAL, lower cost alternatives to the U-joint, analytical model for prediction of spar-TAL response in a seaway, and CWP design iteration for TAL application.

MAL and TAL design refinement is recommended to reduce design costs and to conduct trades of SKSS requirements with other OTEC subsystems to assess the cost effectiveness of the prescribed performance requirements. Potential cost reductions may be found in reducing water depth, increasing watch circle, and in development of environmental criteria supported by analysis of the sea state induced by Hurricane Frederick which recently passed nearby the Puerto Rico site.

Appendix A
ENVIRONMENTAL LOADS COMPUTER LISTINGS

THIS PAGE

WAS INTENTIONALLY

LEFT BLANK

```
 1            C:     "SKSSLOAD".............
 2            C:      WRITTEN BY : R.L.POTASH   14 JUNE,1979.
 3            PI = 3.141592
 4       10   CONTINUE
 5            WRITE(1,100)
 6            ACCEPT"RETURN PERIOD OF STORM(YRS)= ",RT
 7            ACCEPT "PLATFORM HEADING=",BETA1,"DEG.(0 IS EAST)"
 8            ACCEPT "WIND FROM          ",BETA2,"DEG."
 9            ACCEPT "CURRENT FROM       ",BETA3,"DEG."
10            ACCEPT "WAVE FROM         ",BETA4,"DEG."
11            CALL SITE(RT,HS,TO,BETA2,BETA3,BETA4,VW,VC)
12            C:DISPLAY RT,HS,TO,VW,VC
13            WRITE(1,101)HS
13.1          WRITE(1,111) TO
14            WRITE(1,102)VW
15            WRITE(1,103)VC
16            WRITE(1,104)
17            WRITE(1,105)
 3            CALL WIND(BETA1,BETA2,VW,FX,FY,FXI,FYI,RNW,FXS,FYS)
19            WRITE(1,106) FX,FY,FXI,FYI,RNW,FXS,FYS
20            C:DISPLAY BETA1,BETA2,VW,FX,FY,FXI,FYI,RNW
21            C:DISPLAY FXS,FYS
22            CALL CURRENT(BETA1,BETA3,VC,FXC,FYC,FXCI,FYCI,RNC,FXCIS,FYCIS)
23            C:DISPLAY BETA1,BETA3,VC,FXC,FYC,FXCI,FYCI,RNC
24            WRITE(1,107)FXC,FYC,FXCI,FYCI,RNC,FXCIS,FYCIS
25            CALL WAVE(BETA1, BETA4,HS,TO,FXW,FYW,FXWI,FYWI,
                        RNWA,FXWS,FYWS,FXWIS,FYWIS)
26            C:DISPLAY BETA1,BETA4,HS,TO,FXW,FYW,FXWI,FYWI,RNWA,FXWS,
                       FYWS,FXWIS,FYWIS
27            WRITE(1,108) FXW,FYW,FXWI,FYWI,RNWA,FXWIS,FYWIS
28            C:SUM OF FORCES AND MOMENTS.
29            FXT = FX + FXC + FXW
30            FYT = FY + FYC + FYW
31            RNT = RNW + RNC + RNWA
32            FXIT = FXI + FXCI + FXWI
33            FYIT = FYI + FYCI + FYWI
34            FXITS = FXS + FXCIS + FXWIS
35            FYITS = FYS + FYCIS + FYWIS
36            WRITE (1,109) FXT,FYT,FXIT,FYIT,RNT,FXITS,FYITS
37            C: VECTOR SUM.
38            FBT = SQRT(FXIT**2 + FYIT**2)
39            FST = SQRT(FXITS**2 + FYITS**2)
40            WRITE(1,110)FBT,FST
 \      100   FORMAT(//,13X,"PLATFORM ENVIRONMENTAL STATIC LOADS")
-2      101   FORMAT(/,"SIGNIFICANT WAVE HEIGHT(FT)= ",F4.1)
43      102   FORMAT("WIND SPEED(KT)= ",F5.1)
44      103   FORMAT("SURFACE CURRENT(KT)= ",F5.1)
45      104   FORMAT(/,"PLATFORM    ......BARGE.....................
           ", 5X,"....SPAR...")
46      105   FORMAT(11X,"FX(LB)   FY(LB)   FXI      FYI    M(FT-LB)
             FXI      FYI",/)
```

```
      106   FORMAT("WIND",3X,4(1X,F8.0),F10.0,2(1X,F8.0))
      107   FORMAT("CURRENT",4(1X,F8.0),F10.0,2(1X,F8.0))
      108   FORMAT("WAVE",3X,4(1X,F8.0),F10.0,2(1X,F8.0))
      109   FORMAT("TOTAL",2X,4(1X,F9.0),F10.0,2(1X,F9.0),//)
      110   FORMAT("VECTOR SUM",7X,F9.0,36X,F9.0)
      111   FORMAT("MODAL WAVE PERIOD(SEC.)=",F5.1)
            GO TO 10
            END
            SUBROUTINE WIND(BETA1,BETA2,VW,FX,FY,FXI,FYI,RNW,FXS,FYS)
            C:WIND SURGE AND SWAY FORCE AND YAW MOMENT ON BARGE,SPAR.
            DATA A/13434./,BS/7460/,BH/3816/,BP/8605./
            DATA ASS/2750./,SAC/1675./
            PI = 3.141592
            VW = VW * 1.689
            C = PI/ 180.
            DATA RL/371./,RHO/0.002378/,CDW/0.8/
            DATA C1/2.7840921/,C2/6.2597722/,C3/-.21383899/,
              C4/3.614305E-03/,C5/-3.05913E-05/,C6/1.2404335E-07/,
              C7/-1.8893059E-10/
            DATA D1/4.1436649E-02/,D2/1.2217967E-02/,D3/-1.0305026E-04/,
             D4/1.8651768E-07/,D5/9.1391493E-10/
            B12 = BETA2 - BETA1
            CC = SIGNUM(B12)
            IF(B12.EQ.0)CC=1
            TW =ABS(B12)
            TW2 = TW* TW
            TW3 = TW2 * TW
            TW4 = TW3 * TW
            TW5 = TW4 * TW
            TW6 = TW5 * TW
            RLOL = D1 + D2*TW + D3*TW2 + D4*TW3 + D5*TW4
            ALPHA = C1 + C2*TW + C3*TW2 + C4*TW3 + C5*TW4
                      + C6*TW5 + C7*TW6
            ALPHA = CC * ALPHA
            TW = TW *CC
            C:DISPLAY ALPHA,RLOL
            VW2 = VW * VW
            TWC = TW * C
            ALPHAC = ALPHA * C
            STW = SIN(TWC)
            STW2 = STW * STW
            CTW = COS(TWC)
            CTW2 = CTW * CTW
            CATW = COS(ALPHAC - TWC)
            FW = CDW *0.5 *RHO * VW2*( A*STW2 + BP*CTW2) / CATW
            C:DISPLAY FW
            C:BARGE FRAME COMPONENTS.
            FX = -FW*COS(ALPHAC)
            FY = - FW*SIN(ALPHAC)
            C: INERTIAL FRAME COMPONENTS.
            BETA1C = BETA1 * C
            BMA = ALPHAC + BETA1C
            FXI = -FW * COS(BMA)
            FYI = -FW * SIN(BMA)
            C: YAW MOMENT.
            RNW = - FY*COS(ALPHAC)*RL  * (0.5 - RLOL)
            C: SPAR WIND DRAG(SIDE FORCE AND MOMENT ARE ZERO).
            FSW = 0.5 * RHO* VW2 *(ASS*1. + SAC*0.55)
            BETA2C = BETA2 * C
            FXS = - FSW *COS(BETA2C)
            FYS = - FSW * SIN(BETA2C)
            RETURN
            END
```

```
101           SUBROUTINE CURRENT(BETA1,BETA3,VC,FX,FY,FXI,FYI,RNC,FXIS,FYIS)
102           C:CURRENT SURGE,SWAY AND YAW MOMENT ON BARGE AND SPAR.
103           DATA CD/0.6/,AC/24770/,BC/7865/,RHO/1.98/,PI/3.14159/
104           DATA RL/371./,AP/22040/,ACWP/88050./
105           DATA D1/4.1436649E-02/,D2/1.2217967E-02/,D3/-1.0305026E-04/,
               D4/1.8651768E-07/,D5/9.1391493E-10/
106           DATA ASCD/40480/,ACWPS/83550/
107           C = PI/180.
108           VCF = VC * 1.689
109           VC2 = VCF * VCF
110           TC = ABS(BETA3 - BETA1)
111           TC2 = TC * TC
112           TC3 = TC2* TC
113           TC4 = TC3 * TC
114           RLOL = D1 + D2*TC + D3*TC2 + D4*TC3 + D5*TC4
115           TCC = TC * C
116           F = - CD * 0.5 * RHO * VC2
117           C2 = (COS(TCC))
118           S2 = (SIN(TCC))
119           C: BARGE FRAME COMPONENTS-HULL.
120           FXH = F * BC * C2
121           C:DISPLAY "FXH= ",FXH
122           FYH =- F * AC * S2
123           C:DISPLAY "FYH= ",FYH
124           FC = SQRT(FXH**2 + FYH**2)
125           C:DISPLAY "FC = ",FC
126           RLAMB = ATAN2(-FYH,-FXH)
127           C:DISPLAY "RLAMB=",RLAMB
128           BML = BETA1 * C + RLAMB
129           C:YAW MOMENT
130           RNC = -FYH*RL *(0.5 - RLOL)*COS(RLAMB)
131           C: DISPLAY "FC,RL,RLOL,RLAMB=",FC,RL,RLOL,RLAMB
132           C:DISCHARGE PIPES.
133           FCP = - F * AP * 0.9**2
134           C:DISPLAY "FCP=",FCP
135           BETA3C = BETA3*C
136           BETA1C = BETA1 * C
137           B3M1 = BETA3C - BETA1C
138           C: COLD WATER PIPE DRAG.
139           CDCWP = 0.066 * VC ** 0.196
140           FCWP = 0.5 *RHO * ACWP * VC2 * CDCWP
141           C:DISPLAY"FCWP=",FCWP
142           FXP = - ( FCP + FCWP ) * COS( B3M1)
143           FYP = - ( FCP + FCWP ) * SIN(B3M1)
144           FX = FXH + FXP
145           FY = FYH + FYP
146           C: INERTIAL FRAME COMPONENTS.
147           FXI = - ( FC + FCP + FCWP ) * COS( BML )
148           FYI = - ( FC + FCP + FCWP) * SIN ( BML)
149           C:SPAR CURRENT DRAG.
150           FSC = 0.5*RHO*CD*ASCD*0.81*VC2
151           CDCWPS = 0.051*VC**0.183
152           FCWPC = 0.5*RHO*CDCWPS*ACWPS*VC2
153           FS = FSC + FCWPC
154           FXIS = -FS*COS(BETA3C)
155           FYIS = -FS * SIN(BETA3C)
156           RETURN
157           END
```

```
158           SUBROUTINE WAVE(BETA1,BETA4,HS,TO,FX,FY,FXI,FYI,RNW,
                              FXS,FYS,FXIS,FYIS)
159           C:SURGE,SWAY AND YAW MOMENT ON BARGE DUE TO WAVE DRIFT.
160           DATA PI/3.141593/,DS/200./
161           TS = TO/1.06
162           R = HS / 35.
163           FHEAD = 419563. *R**2.17
              FBEAM = 777761.* R**1.64
  5           C:DISPLAY"FHEAD=",FHEAD
166           C:DISPLAY "FBEAM=",FBEAM
167           C = PI / 180.
168           BETA1C = BETA1 * C
169           BETA4C = BETA4 * C
170           AC = BETA4C - BETA1C
171           CAC = COS (AC )
172           SAC = SIN(AC)
173           CAC2 = CAC * CAC
174           SAC2 = SAC * SAC
175           F1 = 2. * CAC2/(1.+CAC2)
176           F2 = 2. * SAC2/(1.+SAC2)
177           FW = F1 * FHEAD + F2*FBEAM
178           C:DISPLAY"FWAVE(SHIP)=",FW
179           FX = - FW * CAC
180           FY = - FW * SAC
181           CB = COS( BETA4C )
182           SB = SIN ( BETA4C )
183           FXI = - FW * CB
184           FYI = - FW * SB
185           C: YAW MOMENT.
186           RNW = - 1.35E+06* (R**0.57)* SIN (3*AC)
187           C: WAVE DRIFT FORCE ON SPAR.
188           FDS = 2.28*(HS/TS)**2 * DS**2
189           FDS = FDS * EXP(-((2*PI/TO)**2)*80./32.17)
  0           FXS = - FDS* CB
191           FYS = - FDS * SB
192           FXIS = FXS
193           FYIS = FYS
194           RETURN
195           END
196           SUBROUTINE SITE(RT,HS,TO,BETA2,BETA3,BETA4,VW,VC)
197           C: PT. TUNA, PUERTO RICO ENVIRONMENTAL CONDITIONS
198           C:   REFERENCE: LMSC-D673832. REV. 11 JULY.
199           DATA VNS/1.2/,PI/3.14159/
200           PI2 = PI/2.
201           HS = 4.51 *LOG(27.83*RT)
202           IF(HS.GT.21)GO TO 10
203           VW = 10.96 * LOG(23.27*RT)
204           TO = EXP(0.507*LOG(5.*HS))
205           VC = 1.8
206           VO = 0.0166 * VW
207           GO TO 20
208       10  CONTINUE
209           C: HURRICANE.
210           TO = EXP( 0.412*LOG(14.51*HS))
211           VW = 10.96 * LOG(23.27*RT)
212           VO = 0.0166 * VW
213       20  CONTINUE
214           VC = SQRT(VO**2 + 1.414*VO*VNS + VNS**2)
  7           C: COMPASS DIRECTIONS FROM WHICH WIND(2),CURRENT(3),
                   AND WAVE(4) ARE TRAVELING.
216           B2 = 90 - BETA2
217           B3 = 90 - BETA3
218           B4 = 90 - BETA4
219           C:DISPLAY"PROB(100<B3<30) = 0.5   B3= ", B3
220           RETURN
221           END
```

PLATFORM ENVIRONMENTAL STATIC LOADS

RETURN PERIOD OF STORM(YRS)= 100
PLATFORM HEADING=0
DEG.(0 IS EAST)WIND FROM 0
DEG.CURRENT FROM 0
DEG.WAVE FROM 0
DEG.
SIGNIFICANT WAVE HEIGHT(FT)= 35.8
MODAL WAVE PERIOD(SEC.)= 13.1
WIND SPEED(KT)= 85.0
SURFACE CURRENT(KT)= 2.4

PLATFORM	.....BARGE.....					....SPAR...		
	FX(LB)	FY(LB)	FXI	FYI	M(FT-LB)	FXI	FYI	
WIND	-168565.	-8197.	-168565.	-8197.	1392937.	-89896.		0.
CURRENT	-367306.	0.	-367306.	0.	0.	-405831.		0.
WAVE	-439854.	0.	-439854.	0.	0.	-429994.		0.
TOTAL	-975725.	-8197.	-975725.	-8197.	1392937.	-925721.		0.

VECTOR SUM 975760. 925721.

PLATFORM ENVIRONMENTAL STATIC LOADS

RETURN PERIOD OF STORM(YRS)= 100
PLATFORM HEADING=30
DEG.(0 IS EAST)WIND FROM 0
DEG.CURRENT FROM 0
DEG.WAVE FROM 0
DEG.
SIGNIFICANT WAVE HEIGHT(FT)= 35.8
MODAL WAVE PERIOD(SEC.)= 13.1
WIND SPEED(KT)= 85.0
SURFACE CURRENT(KT)= 2.4

PLATFORM	.....BARGE.....					....SPAR...		
	FX(LB)	FY(LB)	FXI	FYI	M(FT-LB)	FXI	FYI	
WIND	-74280.	255772.	-192214.	184365.	-4736954.	-89896.		0.
CURRENT	-318097.	267048.	-367126.	222259.	-3910346.	-405831.		0.
WAVE	-605721.	349713.	-699427.	0.	1366852.	-429994.		0.
TOTAL	-998098.	872534.	-1258767.	406625.	-7280448.	-925721.		0.

VECTOR SUM 1322814. 925721.

PLATFORM ENVIRONMENTAL STATIC LOADS

RETURN PERIOD OF STORM(YRS)= 100
PLATFORM HEADING=45
DEG.(0 IS EAST)WIND FROM 0
DEG.CURRENT FROM 0
DEG.WAVE FROM 0
DEG.
SIGNIFICANT WAVE HEIGHT(FT)= 35.8
MODAL WAVE PERIOD(SEC.)= 13.1
WIND SPEED(KT)= 85.0
SURFACE CURRENT(KT)= 2.4

PLATFORM	.....BARGE.....					....SPAR...	
	FX(LB)	FY(LB)	FXI	FYI	N(FT-LB)	FXI	FYI
WIND	-58438.	246839.	-215863.	133219.	-2000861.	-89896.	0.
CURRENT	-259725.	377663.	-418238.	216648.	-1875977.	-405831.	0.
WAVE	-587312.	587312.	-830584.	0.	966510.	-429994.	0.
TOTAL	-905475.	1211814.	-1464685.	349867.	-2949329.	-925721.	0.

VECTOR SUM 1505892. 925721.

PLATFORM ENVIRONMENTAL STATIC LOADS

RETURN PERIOD OF STORM(YRS)= 100
PLATFORM HEADING=60
DEG.(0 IS EAST)WIND FROM 0
DEG.CURRENT FROM 0
DEG.WAVE FROM 0
DEG.
SIGNIFICANT WAVE HEIGHT(FT)= 35.8
MODAL WAVE PERIOD(SEC.)= 13.1
WIND SPEED(KT)= 85.0
SURFACE CURRENT(KT)= 2.4

PLATFORM	.....BARGE.....					....SPAR...	
	FX(LB)	FY(LB)	FXI	FYI	N(FT-LB)	FXI	FYI
WIND	-42542.	252004.	-239513.	89160.	-689961.	-89096.	0.
CURRENT	-183653.	462541.	-475593.	169462.	-627712.	-405831.	0.
WAVE	-433409.	750687.	-866818.	0.	-.	-429994.	0.
TOTAL	-659604.	1465232.	-1581924.	258622.	-1317674.	-925721.	0.

VECTOR SUM 1602925. 925721.

PLATFORM ENVIRONMENTAL STATIC LOADS

RETURN PERIOD OF STORM(YRS)= 100
PLATFORM HEADING=90
DEG.(0 IS EAST)WIND FROM 0
DEG.CURRENT FROM 0
DEG.WAVE FROM 0
DEG.
SIGNIFICANT WAVE HEIGHT(FT)= 35.8
MODAL WAVE PERIOD(SEC.)= 13.1
WIND SPEED(KT)= 85.0
SURFACE CURRENT(KT)= 2.4

PLATFORM	.....BARGE.....					....SPAR...	
	FX(LB)	FY(LB)	FXI	FYI	N(FT-LB)	FXI	FYI
WIND	17751.	263162.	-263162.	17752.	-14981.	-89896.	0.
CURRENT	-.	534097.	-534097.	.	.	-405831.	0.
WAVE	.	806023.	-806023.	0.	-1366852.	-429994.	0.
TOTAL	17751.	1603282.	-1603282.	17752.	-1381833.	-925721.	0.
VECTOR SUM		1603380.				925721.	

PLATFORM ENVIRONMENTAL STATIC LOADS

RETURN PERIOD OF STORM(YRS)= 100
PLATFORM HEADING=0
DEG.(0 IS EAST)WIND FROM 30
DEG.CURRENT FROM 0
DEG.WAVE FROM 30
DEG.
SIGNIFICANT WAVE HEIGHT(FT)= 35.8
MODAL WAVE PERIOD(SEC.)= 13.1
WIND SPEED(KT)= 85.0
SURFACE CURRENT(KT)= 2.4

PLATFORM	.....BARGE.....					....SPAR...	
	FX(LB)	FY(LB)	FXI	FYI	N(FT-LB)	FXI	FYI
WIND	-74280.	-255772.	-74280.	-255772.	4736954.	-77852.	-44948.
CURRENT	-367306.	0.	-367306.	0.	0.	-405831.	0.
WAVE	-605721.	-349713.	-605721.	-349713.	-1366852.	-372385.	-214997.
TOTAL	-1047307.	-605486.	-1047307.	-605486.	3370102.	-856069.	-259945.
VECTOR SUM		1209738.				894665.	

PLATFORM ENVIRONMENTAL STATIC LOADS

RETURN PERIOD OF STORM(YRS)= 100
PLATFORM HEADING=0
DEG.(0 IS EAST)WIND FROM 0
DEG.CURRENT FROM 0
DEG.WAVE FROM 90
DEG.
SIGNIFICANT WAVE HEIGHT(FT)= 35.8
MODAL WAVE PERIOD(SEC.)= 13.1
WIND SPEED(KT)= 85.0
SURFACE CURRENT(KT)= 2.4

PLATFORM	.....BARGE.....					....SPAR...	
	FX(LB)	FY(LB)	FXI	FYI	N(FT-LB)	FXI	FYI
WIND	-168565.	-8197.	-168565.	-8197.	1392937.	-89896.	0.
CURRENT	-367306.	0.	-367306.	0.	0.	-405831.	0.
WAVE	.	-806023.	.	-806023.	1366852.	.	-429994.
TOTAL	-535871.	-814220.	-535871.	-814220.	2759789.	-495727.	-429994.
VECTOR SUM		974737.					656232.

PLATFORM ENVIRONMENTAL STATIC LOADS

RETURN PERIOD OF STORM(YRS)= 100
PLATFORM HEADING=75
DEG.(0 IS EAST)WIND FROM 0
DEG.CURRENT FROM 0
DEG.WAVE FROM 0
DEG.
SIGNIFICANT WAVE HEIGHT(FT)= 35.8
MODAL WAVE PERIOD(SEC.)= 13.1
WIND SPEED(KT)= 85.0
SURFACE CURRENT(KT)= 2.4

PLATFORM	.....BARGE.....					....SPAR...	
	FX(LB)	FY(LB)	FXI	FYI	M(FT-LB)	FXI	FYI
WIND	-13674.	262221.	-256825.	54659.	-72294.	-89896.	0.
CURRENT	-95066.	515898.	-518402.	92687.	-105943.	-405831.	0.
WAVE	-215679.	804926.	-833320.	0.	-966511.	-429994.	0.
TOTAL	-324420.	1583045.	-1608547.	147347.	-1144747.	-925721.	

VECTOR SUM 1615282. 925721.

PLATFORM ENVIRONMENTAL STATIC LOADS

RETURN PERIOD OF STORM(YRS)= 3
PLATFORM HEADING=0
DEG.(0 IS EAST)WIND FROM 0
DEG.CURRENT FROM 0
DEG.WAVE FROM 0
DEG.
SIGNIFICANT WAVE HEIGHT(FT)= 20.0
MODAL WAVE PERIOD(SEC.)= 10.3
WIND SPEED(KT)= 46.5
SURFACE CURRENT(KT)= 1.8

PLATFORM	.....BARGE.....					....SPAR...	
	FX(LB)	FY(LB)	FXI	FYI	M(FT-LB)	FXI	FYI
WIND	-50561.	-2459.	-50561.	-2459.	417812.	-26964.	0.
CURRENT	-207719.	0.	-207719.	0.	0.	-230977.	0.
WAVE	-123967.	0.	-123967.	0.	0.	-152428.	0.
TOTAL	-382247.	-2459.	-382247.	-2459.	417812.	-410369.	

VECTOR SUM 382255. 410369.

PLATFORM ENVIRONMENTAL STATIC LOADS

RETURN PERIOD OF STORM(YRS)= 3
PLATFORM HEADING=30
DEG.(0 IS EAST)WIND FROM 0
DEG.CURRENT FROM 0
DEG.WAVE FROM 0
DEG.
SIGNIFICANT WAVE HEIGHT(FT)= 20.0
MODAL WAVE PERIOD(SEC.)= 10.3
WIND SPEED(KT)= 46.5
SURFACE CURRENT(KT)= 1.8

PLATFORM	.....BARGE.....					....SPAR...	
	FX(LB)	FY(LB)	FXI	FYI	N(FT-LB)	FXI	FYI
WIND	-22280.	76719.	-57655.	55300.	-1420851.	-26964.	0.
CURRENT	-179890.	151804.	-208114.	125993.	-2248081.	-230977.	0.
WAVE	-199240.	115031.	-230062.	0.	980056.	-152428.	0.
TOTAL	-401410.	343554.	-495831.	181293.	-2688876.	-410369.	

VECTOR SUM 527935. 410369.

PLATFORM ENVIRONMENTAL STATIC LOADS

RETURN PERIOD OF STORM(YRS)= 3
PLATFORM HEADING=60
DEG.(0 IS EAST)WIND FROM 0
0DEG.CURRENT FROM
DEG.WAVE FROM 0
DEG.
SIGNIFICANT WAVE HEIGHT(FT)= 20.0
MODAL WAVE PERIOD(SEC.)= 10.3
WIND SPEED(KT)= 46.5
SURFACE CURRENT(KT)= 1.8

PLATFORM	.....BARGE.....					....SPAR...	
	FX(LB)	FY(LB)	FXI	FYI	N(FT-LB)	FXI	FYI
WIND	-12760.	75589.	-71842.	26744.	-206954.	-26964.	0.
CURRENT	-103860.	262932.	-270174.	96267.	-360876.	-230977.	0.
WAVE	-157442.	272697.	-314883.	0.	-.	-152428.	0.
TOTAL	-274062.	611218.	-656898.	123011.	-567830.	-410369.	

VECTOR SUM 668317. 410369.

PLATFORM ENVIRONMENTAL STATIC LOADS

RETURN PERIOD OF STORM(YRS)= 3
PLATFORM HEADING=75
DEG.(0 IS EAST)WIND FROM 0
DEG.CURRENT FROM 0
DEG.WAVE FROM 0
DEG.
SIGNIFICANT WAVE HEIGHT(FT)= 20.0
MODAL WAVE PERIOD(SEC.)= 10.3
WIND SPEED(KT)= 46.5
SURFACE CURRENT(KT)= 1.8

PLATFORM	.....BARGE.....					....SPAR...	
	FX(LB)	FY(LB)	FXI	FYI	N(FT-LB)	FXI	FYI
WIND	-4102.	78653.	-77035.	16395.	-21684.	-26964.	0.
CURRENT	-53762.	293263.	-294638.	52680.	-60907.	-230977.	0.
WAVE	-81360.	303641.	-314352.	0.	-693005.	-152428.	0.
TOTAL	-139224.	675557.	-686025.	69075.	-775596.	-410369.	
VECTOR SUM		689494.					410369.

PLATFORM ENVIRONMENTAL STATIC LOADS

RETURN PERIOD OF STORM(YRS)= 3
PLATFORM HEADING=90
DEG.(0 IS EAST)WIND FROM 0
DEG.CURRENT FROM 0
DEG.WAVE FROM 0
DEG.
SIGNIFICANT WAVE HEIGHT(FT)= 20.0
MODAL WAVE PERIOD(SEC.)= 10.3
WIND SPEED(KT)= 46.5
SURFACE CURRENT(KT)= 1.8

PLATFORM	.....BARGE.....					....SPAR...	
	FX(LB)	FY(LB)	FXI	FYI	N(FT-LB)	FXI	FYI
WIND	5325.	78935.	-78935.	5325.	-4494.	-26964.	0.
CURRENT	-.	303608.	-303608.	.	.	-230977.	0.
WAVE	.	309512.	-309512.	0.	-980056.	-152428.	0.
TOTAL	5324.	692056.	-692056.	5325.	-984550.	-410369.	
VECTOR SUM		692076.					410369.

PLATFORM ENVIRONMENTAL STATIC LOADS
RETURN PERIOD OF STORM(YRS)= 100
PLATFORM HEADING=10
DEG.(0 IS EAST)WIND FROM 0
DEG.CURRENT FROM 0
DEG.WAVE FROM 0
DEG.
SIGNIFICANT WAVE HEIGHT(FT)= 35.8
MODAL WAVE PERIOD(SEC.)= 13.1
WIND SPEED(KT)= 85.0
SURFACE CURRENT(KT)= 2.4

PLATFORM	.....BARGE.....					....SPAR...	
	FX(LB)	FY(LB)	FXI	FYI	M(FT-LB)	FXI	FYI
WIND	-146122.	158454.	-171418.	130673.	-13808662.	-89896.	0.
CURRENT	-361726.	92745.	-356479.	123055.	-4769292.	-405831.	0.
WAVE	-473010.	83404.	-480307.	0.	683426.	-429994.	0.
TOTAL	-980858.	334603.	-1008203.	253728.	-17894528.	-925721.	0.
VECTOR SUM		1039640.				925721.	

PLATFORM ENVIRONMENTAL STATIC LOADS
RETURN PERIOD OF STORM(YRS)= 100
PLATFORM HEADING=20
DEG.(0 IS EAST)WIND FROM 0
DEG.CURRENT FROM 0
DEG.WAVE FROM 0
DEG.
SIGNIFICANT WAVE HEIGHT(FT)= 35.8
MODAL WAVE PERIOD(SEC.)= 13.1
WIND SPEED(KT)= 85.0
SURFACE CURRENT(KT)= 2.4

PLATFORM	.....BARGE.....					....SPAR...	
	FX(LB)	FY(LB)	FXI	FYI	M(FT-LB)	FXI	FYI
WIND	-103262.	241495.	-179631.	191613.	-8939650.	-89896.	0.
CURRENT	-345155.	182672.	-350740.	193612.	-5173646.	-405831.	0.
WAVE	-546294.	198835.	-581354.	0.	1183728.	-429994.	0.
TOTAL	-994711.	623001.	-1111725.	385225.	-12929568.	-925721.	0.
VECTOR SUM		1176576.				935721.	

PLATFORM ENVIRONMENTAL STATIC LOADS

RETURN PERIOD OF STORM(YRS)= 3
PLATFORM HEADING=10
DEG.(0 IS EAST)WIND FROM 0.DEG.CURRENT FROM 0.DEG.WAVE FROM
SIGNIFICANT WAVE HEIGHT(FT)= 20.0
MODAL WAVE PERIOD(SEC.)= 10.3
WIND SPEED(KT)= 46.5
SURFACE CURRENT(KT)= 1.8

PLATFORM	.....BARGE.....					....SPAR...	
	FX(LB)	FY(LB)	FXI	FYI	M(FT-LB)	FXI	FYI
WIND	-43829.	47528.	-51417.	39195.	-4141913.	-26964.	0.
CURRENT	-204563.	52721.	-201683.	69620.	-2741894.	-230977.	0.
WAVE	-138059.	24344.	-140189.	0.	490028.	-152428.	0.
TOTAL	-386452.	124593.	-393289.	108815.	-6393778.	-410369.	

VECTOR SUM 408065. 410369.

PLATFORM ENVIRONMENTAL STATIC LOADS

RETURN PERIOD OF STORM(YRS)= 3
PLATFORM HEADING=20
DEG.(0 IS EAST)WIND FROM 0.DEG.CURRENT FROM 0.DEG.WAVE FROM
SIGNIFICANT WAVE HEIGHT(FT)= 20.0
MODAL WAVE PERIOD(SEC.)= 10.3
WIND SPEED(KT)= 46.5
SURFACE CURRENT(KT)= 1.8

PLATFORM	.....BARGE.....					....SPAR...	
	FX(LB)	FY(LB)	FXI	FYI	M(FT-LB)	FXI	FYI
WIND	-30974.	72436.	-53880.	57474.	-2681451.	-26964.	0.
CURRENT	-195192.	103840.	-198624.	109643.	-2974359.	-230977.	0.
WAVE	-170173.	61938.	-181095.	0.	648753.	-152428.	0.
TOTAL	-396339.	238214.	-433599.	167117.	-4907057.	-410369.	

VECTOR SUM 464690. 410369.

PLATFORM ENVIRONMENTAL STATIC LOADS

RETURN PERIOD OF STORM(YRS)= 3
PLATFORM HEADING=5,DEG.(0 IS EAST)WIND FROM 0.DEG.CURRENT FROM 0

SIGNIFICANT WAVE HEIGHT(FT)= 20.0
MODAL WAVE PERIOD(SEC.)= 10.3
WIND SPEED(KT)= 46.5
SURFACE CURRENT(KT)= 1.8

PLATFORM	.....BARGE.....					....SPAR...	
	FX(LB)	FY(LB)	FXI	FYI	M(FT-LB)	FXI	FYI
WIND	-48597.	27127.	-50777.	22788.	-3515308.	-26964.	0.
CURRENT	-206929.	26461.	-205765.	37783.	-1752054.	-230977.	0.
WAVE	-187673.	11170.	-128161.	0.	253657.	-152428.	0.
TOTAL	-383199.	64758.	-384703.	60571.	-5013705.	-410369.	

VECTOR SUM 389442. 410369.

Appendix B

COST TRADE STUDY DATA

THIS PAGE

WAS INTENTIONALLY

LEFT BLANK

UPDATE OF COST TRADE STUDY

Latest Cost Estimates

Wire (in.)	3.5	4.5	6	7
Cost ($/ft)	30	45	107	160
Chain (in.)	2.8	3.6	5.1	6.0
Cost ($/ft)	53	84	160	220
Anchor	$0.60/lb			
Windlass	$800,000/unit			

Case	1	2	3	4
Number Legs	17	11	8	6
Wire Diam. (in.)	3.5	4.5	6	7
Total Wire Length (ft)	61,200	39,600	28,800	21,600
Total Wire Cost ($M)	1.83	1.78	3.08	3.46
Chain Diam. (in.)	2.8	3.6	5.1	6.0
Total Chain Length (ft)	76,500	49,500	36,000	27,000
Total Chain Cost ($M)	4.06	4.16	5.76	5.94
Total Anchor Weight (10^6 lb)	0.62	0.48	0.42	0.58
Total Anchor Cost ($M)	0.38	0.29	0.25	0.35
Total Number of Windlass	17	11	8	6
Unit Cost ($M)	0.53	0.93	0.80	0.93
Total Windlass Cost ($M)	9.01	10.23	6.4	5.6
1. Sum of Major Component Costs ($M)	15.28	16.46	15.49	15.35
2. Chain Locker Cost ($M)	0.16	0.17	0.21	0.20
3. Deployment Cost$_{(3)}$ ($M)	7.8	5.0	5.1	4.1
Subtotal ($M) (1+2+3)	23.2	21.6	20.8	19.65

Windlass

Pull	1×10^6 lb	1.5
Cost	$680,000	$800,000
Assume Pull = 1/2 B.S. of Wire		
	$0.68/lb	$0.53/lb

Anchor

$$\text{Anchor weight} \geq \text{holding power}/30 = \frac{2 \times \text{chain tension @ anchor}}{30}$$

Tension (10^6 lb)	0.59	0.66	0.79	1.45
Holding Power (10^6 lb)	1.3	1.45	1.58	2.9
Anchor Weight (lb)	44,928	48,400	53,000	97,000

Chain Locker

Assume storage for 700 ft of chain on barge (per leg).

Case	1	2	3	4
Volume Required/100 Fathoms				
(ft^3)	400	650	1,150	1,430
ft^3/ft	0.667	1.080	1.917	2.383
Total Length of Chain (ft)	11,900	7,700	5,600	4,200
Volume Required (ft^3)	7,937	8,316	10,735	10,009

Estimate of cost of 1 ft^3 of APL barge volume.

40-MW(e) Spar (G & C) platform $71 M constr. + deployment

weight = 22,691 LT (= 0.79×10^6 ft^3 sw)

Fully submerged $\therefore$ cost ($/$ft^3$) = 89.4

APL barge platform system $33 M (1978).

$\forall$ = $378 \times 121 \times 89 = 4.07 \times 10^6$ ft^3

Assume half is flooded; cost ($/$ft^3$) = 16.2 assume 20

Δ = 67,000 LT (= 2.35×10^6 ft^3)

Cost of Volume ($M)	0.16	0.17	0.21	0.20

Deployment

Assume $5 M for 10-leg MAL (contractor ROM not available)

1. Cost proportional to total weight deployed.

Case	1	2	3	4
Wire (lb/ft)	22	36	65	90
Total Wire wt (10^6 lb)	1.35	1.43	1.86	1.94
Chain (lb/ft)	80	123	247.6	343
Total Chain wt (10^6 lb)	6.79	6.09	8.91	9.26
Total Anchor wt (10^6 lb)	0.62	0.48	0.42	0.58
Total Leg wt (10^6 lb)	8.09	8.00	11.19	11.78
Total wt/Total wt_2	1.01	1.0	1.4	1.5
Cost ($M)	5.1	5.0	7.0	7.5

2. Cost proportional to total leg length deployed.

Total Leg Length (10^6 ft)	0.137	0.089	0.065	0.049
Length/$Length_2$	1.54	1.0	0.73	0.55
Cost	7.7	5.0	3.7	2.8

3. Cost proportional to weight and length deployed.

Cost ($M)	7.8	5.0	5.1	4.1

Inspection, Maintenance, Repair

ROM not available.

Assume fixed cost/leg.

COST COMPARISON OF MAL WITH AND WITHOUT ACTIVE TENSIONING

	Active Tens.			No Active Tens.		
Component	Size	Unit Cost	Total Cost ($M)	Size	Unit Cost	Total Cost ($M)
Wire Rope	5-3/4 in.	$88/ft	2.29	6-1/4 in.	$115/ft	3.16
Chain	4-7/8 in.	$135/ft	4.96	5-3/8 in.	$160/ft	5.88
Windlass	1.5×10^6 lb	$800,000	6.4	-	-	0
Anchor	60,000 lb	$ 36,000	0.58	68,000 lb	40,800	0.66
Chain Locker			0.21			0.22
Deployment			5.1			6.3
Kenter Shackle			0.8			1.0
Sum (partial)			20.34			17.22

$$\Delta = \frac{20.34 - 17.22}{20.34} \times 100 = 15\%$$

If only change is windlass,

$$\Delta = \frac{6.4}{20.34} \times 100 = 31.5\%$$

WIRE-ROPE/CHAIN COSTS VS DIAMETER

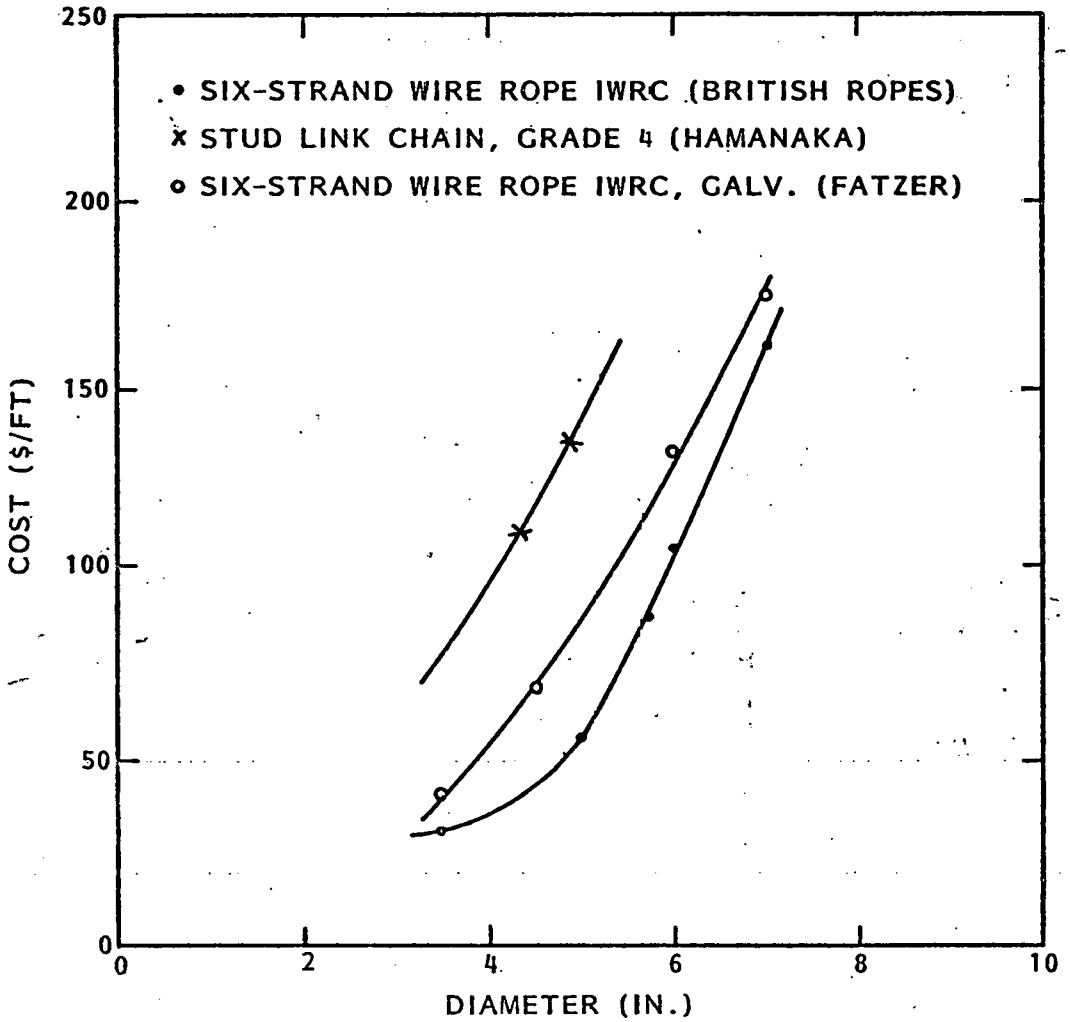

VOLUME REQUIRED FOR STORING CHAIN

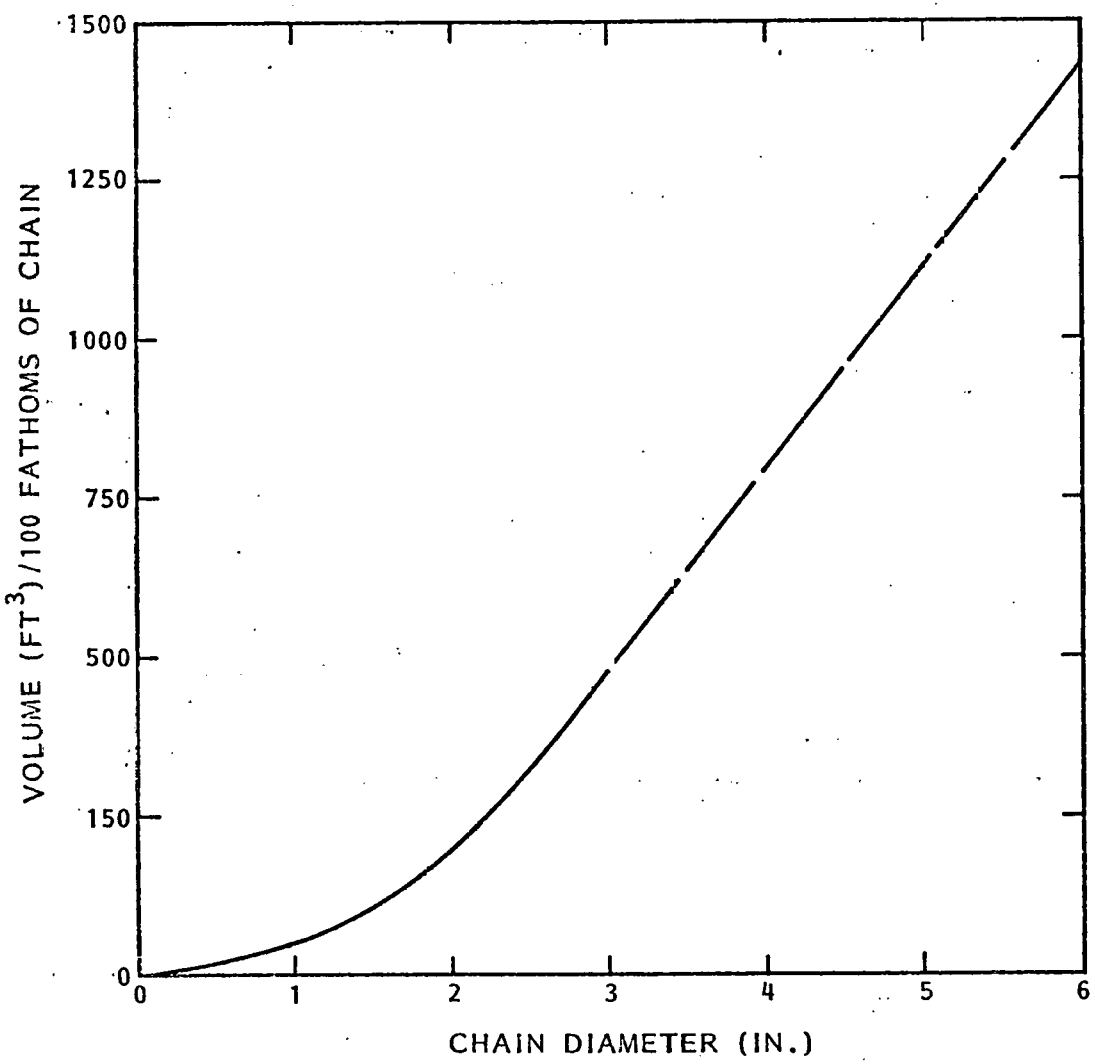

WINDLASS COST

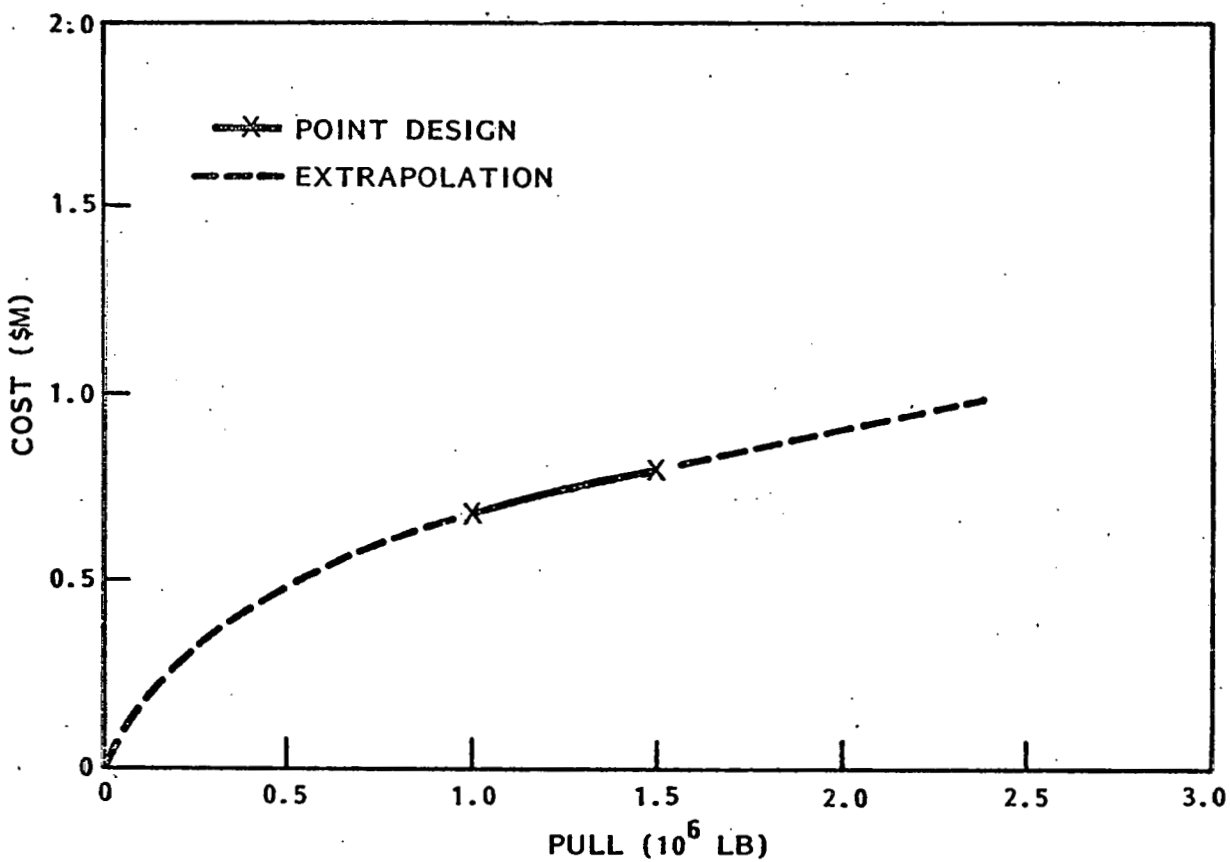

Appendix C

COMMERCIAL PLANT LOADS

THIS PAGE

WAS INTENTIONALLY

LEFT BLANK

COMMERCIAL PLANT LOADS

C.1 AREAS

C.1.1 Wind

FREEBOARD = 85 - 45 = 40

LOA = 620

BEAM = 300

FRONTAL $A_F \cong$ 40 × 300 + 35 × 300 = 22,500 ft²
(HULL) + (SUPERSTRUCTURE)

ABEAM $A_B \cong$ 40 × 620 + 35 × 180 = 31,100 ft²

C.1.2 Current

1. CWP

ID 100 ft ; ASSUME OD = 105 ft

OUTLET DEPTH = 45 FT

INLET DEPTH ASSUME 3,000 ft

AREA = (3000 - 45) × 105 = 310,275 ft²

2. Discharge Pipes

LENGTH = 200 FT

INLET DEPTH = 245 FT

OUTLET DEPTH = 45 FT

AVERAGE DIAMETER = 45 FT

QUANTITY = 4

ASSUME BLOCKAGE, CURRENT ABEAM

CURRENT ABEAM A = 4 × 45' × 200' = 36,000 ft²

CURRENT AHEAD A = 45 × 200 = 9,000 ft²

3. Hull

CURRENT ABEAM A_B = 620 × 45 + 245 × 50 = 33,400 ft²
HULL + PUMPS

CURRENT AHEAD A_F = 45 × 300 + 55 × 50 = 16,250 ft²

C.2 CWP CURRENT DRAG

V_c (KT)	F (LB)	C_D
1	0.8279×10^5	0.0945
2	0.3566×10^6	0.102
3	0.8185×10^6	0.104

$$F = \tfrac{1}{2} \rho A V_c^2 \bar{C}_D$$

$$= 0.5 \times 1.98 \times 310,275 \times V_c^2 \bar{C}_D \times 1.689^2$$

$$F = 8.763 \times 10^5 V_c^2 \bar{C}_D$$

$$C_D = a V_c^b$$

$$\ln C_D = \ln a + b \ln V_c$$

$$-2.359 = \ln a, \quad a = 0.095$$

$$-2.263 = -2.359 + b(0.693)$$

$$b = 0.139$$

$$\therefore C_D = 0.095 V_c^{0.139}$$

C.3 WAVE DRIFT FORCE

Faltinsen & Michelsen Theory, Fig. 28

C.3.1 Beam Seas

$\lambda/B = 5.017\,T^2$

$\omega = \frac{1}{\sqrt{B}}\sqrt{\frac{2\pi g}{\lambda/B}} = \frac{1}{\sqrt{300}}\sqrt{\frac{2\pi \cdot 32.2}{\lambda/B}} = 0.821/\sqrt{\lambda/B}$

T (sec)	λ/B	ω (r/s)	f (Hz)	F	$\sum_3$ (FT³/sec)	$\sum_{100}$ (FT³/sec)	Δω	$\sum_3 \Delta\omega F$	$\sum_{100} \Delta\omega F$
10	1.74	0.62	0.099	0.5	366	947	0.08	14.6	37.9
11	2.10	0.57	0.090	0.4	346	1234	0.05	6.9	24.7
12	2.5	0.52	0.083	0.34	273	1426	0.05	4.6	24.2
13	2.93	0.48	0.076	0.28	157	1500	0.04	1.8	16.8
14	3.4	0.45	0.071	0.26	80	1395	0.03	0.6	10.9
15	3.91	0.42	0.066	0.36	28	1120	0.03	0.3	12.1
16	4.44	0.39	0.062	0.30	8	799	0.03	0.2	14.8
17	5.02	0.37	0.058	0.30	1	471	0.02	0	7.8
5	0.425	1.26	0.20	0.5	32	43	0.20	3.2	4.3
6	0.612	1.05	0.167	0.5	73	105	0.21	7.7	11.0
7	0.833	0.90	0.143	0.5	144	210	0.15	10.8	15.8
8	1.088	0.79	0.125	0.5	231	369	0.11	12.7	21.2
9	1.38	0.70	0.111	0.5	317	630	0.09	14.3	28.4
								77.7	227.0

BEAM WAVE DRIFT FORCE

$F = \rho g L \int S F \, d\omega \times \frac{1}{2\pi} \times 2$

$= 1.98 \times 32.2 \times 620 \times 77.7 \times \frac{1}{2\pi} \times 2 = 977{,}851$ LB Beam, 31 KTS

" $\times 227$ " $= 2.86 \times 10^6$ LB Beam, 100 KTS

HEAD SEAS

$F = 2.86 \times 10^6 \left(\frac{H_{1/3}}{35.9}\right)^a$

$\therefore a = 1.83$

C.3.2 Head Seas

$$\omega = \frac{1}{\sqrt{32.2}} \frac{\sqrt{2\pi g}}{\sqrt{\lambda/L}} = 0.591/\sqrt{\lambda/L}$$

T (sec)	λ/L	ω (r/s)	f (Hz)	F	$\sqrt{S_3}$ (FT²/sec)	$\sqrt{S_{100}}$ (FT²/sec)	$\Delta\omega$ (r/s)	$\sqrt{S_3}\,\Delta\omega F$	$\sqrt{S_{100}}\,\Delta\omega F$
5	0.425	0.876	0.139	0.5	150	243	0.20	18.0	24.3
6	0.612	0.730	0.116	0.5	286	527	0.15	21.5	39.5
7	0.833	0.626	0.10	0.5	366	916	0.10	18.3	45.8
8	1.088	0.547	0.087	0.5	318	1324	0.08	12.7	53.0
9	1.380	0.486	0.077	0.5	172	1495	0.06	5.2	44.9
10	1.74	0.433	0.069	0.5	53	1302	0.05	1.3	32.6
11	2.10	0.394	0.063	0.4	12	866	0.04	0.2	13.9
12	2.5	0.361	0.057	0.34	1	394	0.03	0	4.0
13	2.93	0.334	0.053	0.28	0	160	0.03	0	1.3
14	3.4	0.310	0.049	0.26	0	34	0.03	0	0.3
15	3.91	0.289	0.046	0.36	0	9	0.02	0	0
16	4.44	0.271	0.043	0.70	0	1	0.02	0	0
17	5.02	0.255	0.041	0.30	0	0	0.02	0	0
3	0.153	1.46	0.23	0.5	17	22	0.36	3.1	4
4	0.272	1.1	0.17	0.5	69	95	0.36	12.4	17.1
								89.6	280.6

$$F = 1.984 \times 32.2 \times 300 \times 89.6 \times \frac{1}{2\pi} \times 2 = 545,500 \text{ LB} \quad H_{1/3}, 300$$

$$= \text{"} \times 280.6 \text{ "} = 1.71 \times 10^6 \text{ LB} \quad H_{1/3}, 100$$

$$F = 1.71 \times 10^6 \left(\frac{H_{1/3}}{35.9}\right)^q$$

$$\frac{0.55 \times 10^6}{1.71 \times 10^6} = \left(\frac{120}{35.9}\right)^q$$

$$\ln(0.32) = q \ln 3.34$$

$$q = 1.94$$

C.4 WAVE DRIFT MOMENT

BEAM SEAS, KIM & CHOU

λ/L	$\bar{M}$	ω	f	S_3	S_{100}	$\Delta\omega$	$\int_3 \Delta\omega \bar{M}$	$\int_{100} \Delta\omega \bar{M}$
—	—	(r/s)	(H_z)	(FT^2-SEC)	(FT^2-SEC)	—		
0.2	0.01	1.84	0.29	5.3	6.9	0.54	0.03	0.04
0.4	0.01	1.3	0.21	25.6	33.9	0.54	0.14	0.18
0.6	0.01	1.06	0.17	68.5	94.8	0.34	0.23	0.32
0.8	0.005	0.92	0.15	117.5	171.4	0.19	0.08	0.12
1.6	0.	0.82	0.13	202.8	327.9	0.10	—	0
							0.48	0.66

$$M = 0.5 \times 1.98 \times 32.2 \times 620^2 \times 0.48 \times 2 \times \frac{1}{2\pi} = 1.87 \times 10^6 \text{ FT-LBS (3 years)}$$

$$.66 \qquad = 2.57 \times 10^6 \text{ FT-LBS (100 years)}$$

ASSUME SAME FUNCTION OF $H_{1/3}$ AS FOR BARGE (1/40).

ASSUME

$$M = 2.57 \times 10^6 \left(\frac{H_{1/3}}{35.9}\right)^a \text{ FT-LBS}$$

$$a = 0.54$$

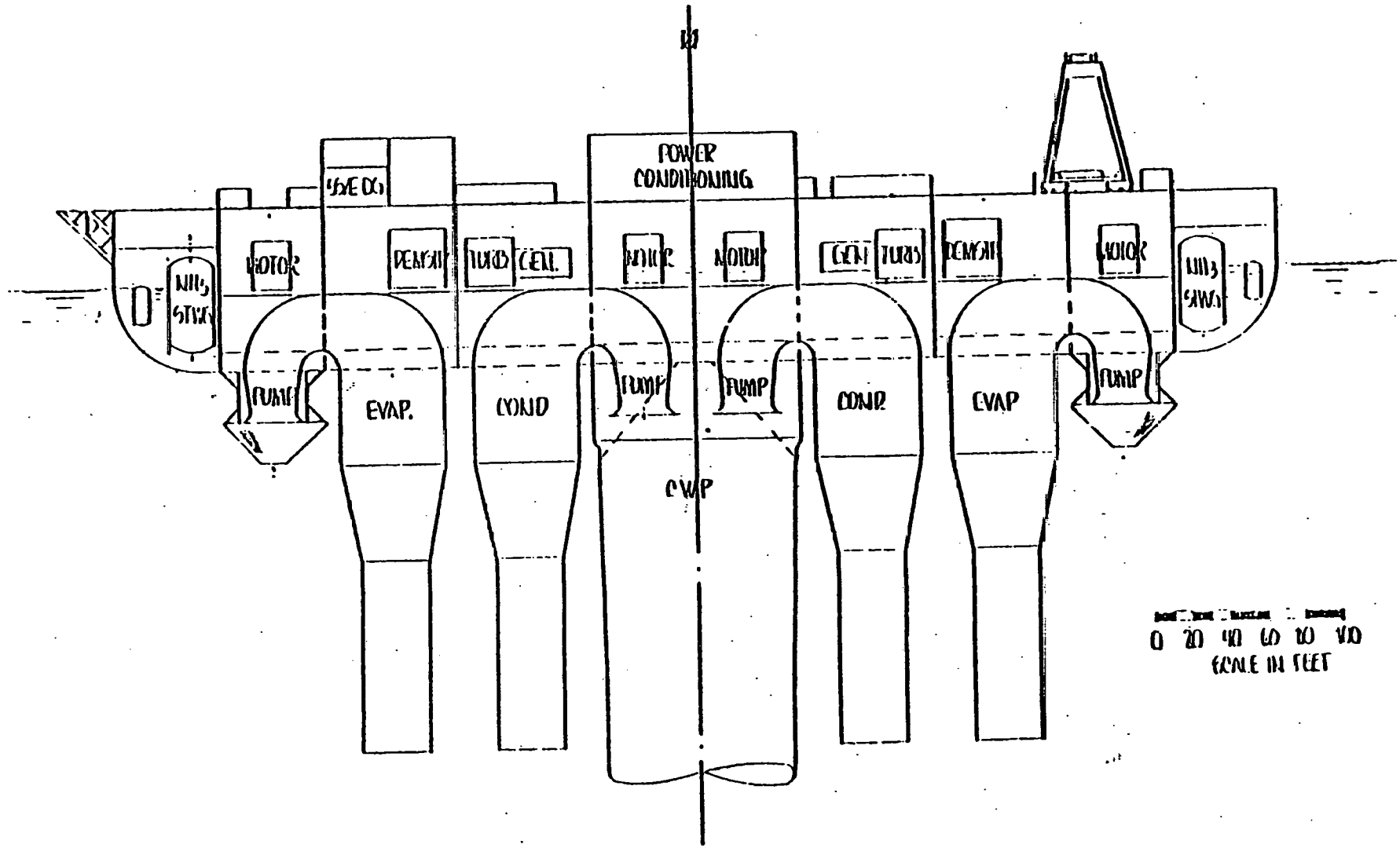

Fig. C-1 400-MW(e) Ship Profile

Appendix D
STATIC LOADS ANALYSIS METHODOLOGY

THIS PAGE

WAS INTENTIONALLY

LEFT BLANK

D.1 CHARACTERISTICS OF SLACK MOORING LEGS

A typical configuration of a slack mooring leg consists of an anchor at rest on the sea bottom, with a length of chain attached, followed by a mooring line secured to a moored platform. That portion of the anchor chain adjacent to the anchor, is resting on the sea bottom in the slack mooring condition. This configuration is illustrated in Fig. D-1.

Forces due to wind and wave action tend to move the moored platform away from the mooring line anchor resulting in a countering horizontal force in the mooring system. This horizontal restoring force is partially generated by the change in angle of the mooring line toward the horizontal. Additional restoring force is due to an increase in tension when a greater length of chain is lifted from the ocean floor, as is depicted in Fig. D-1.

Slack Mooring Legs on Sloping Bottoms

Discussion of the sloping bottom will be simplified to some extent by defining the slope as positive when the depth decreases traveling away from the platform toward the anchor, as in Fig. D-2. This illustration also shows a particular effect of various sloping bottoms on both the length of line required, and the range to the anchor, when generating a constant amount of restoring force at the upper end. A positive slope causes the chain to hang in a catenary with its lowest point below both the anchor location and the point of first contact with the bottom.

The mooring leg configurations in Fig. D-2 are developed by application of catenary equations. This analysis is presented in the following section of this report.

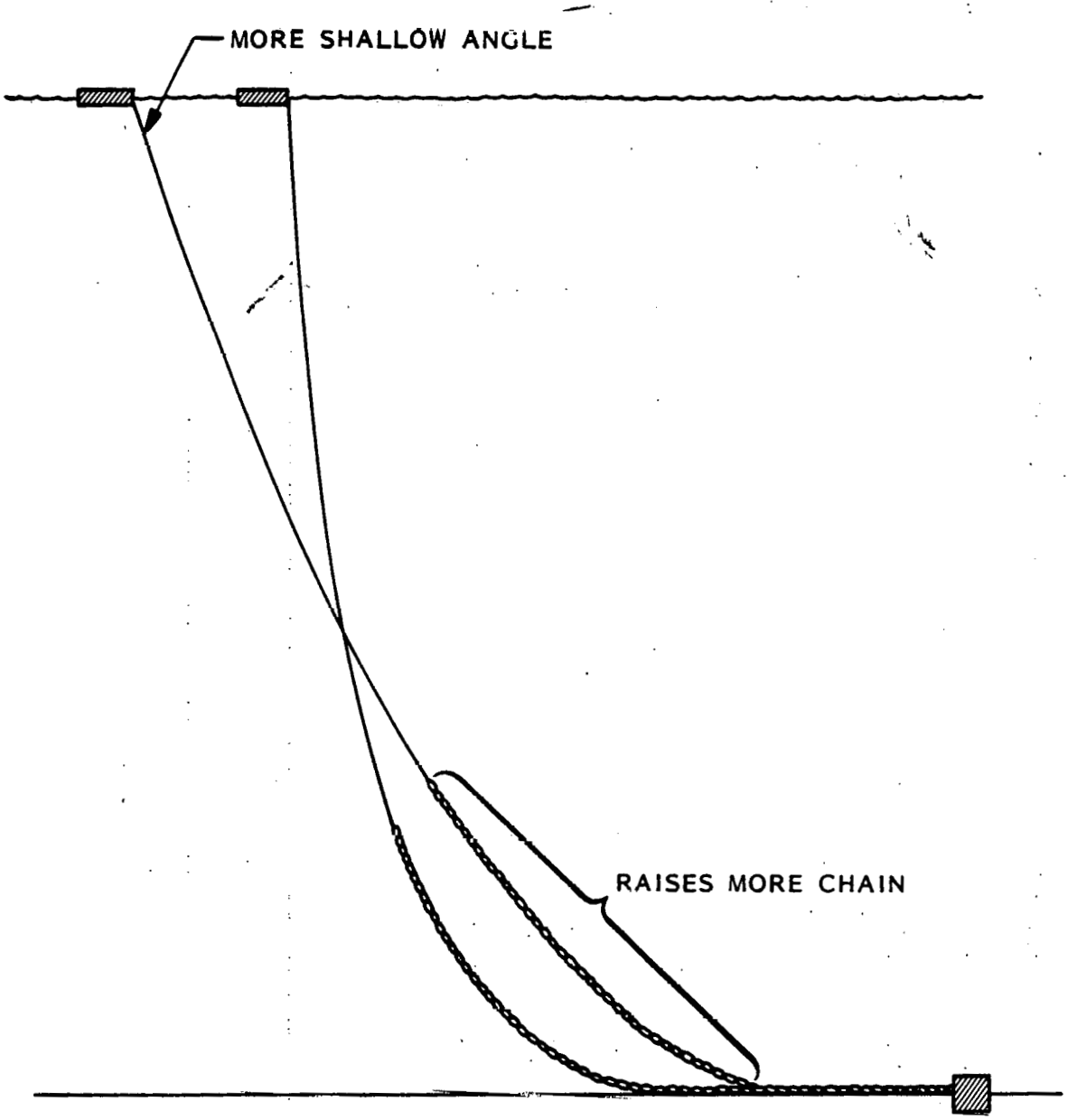

Fig. D-1 Slack Moor Configuration

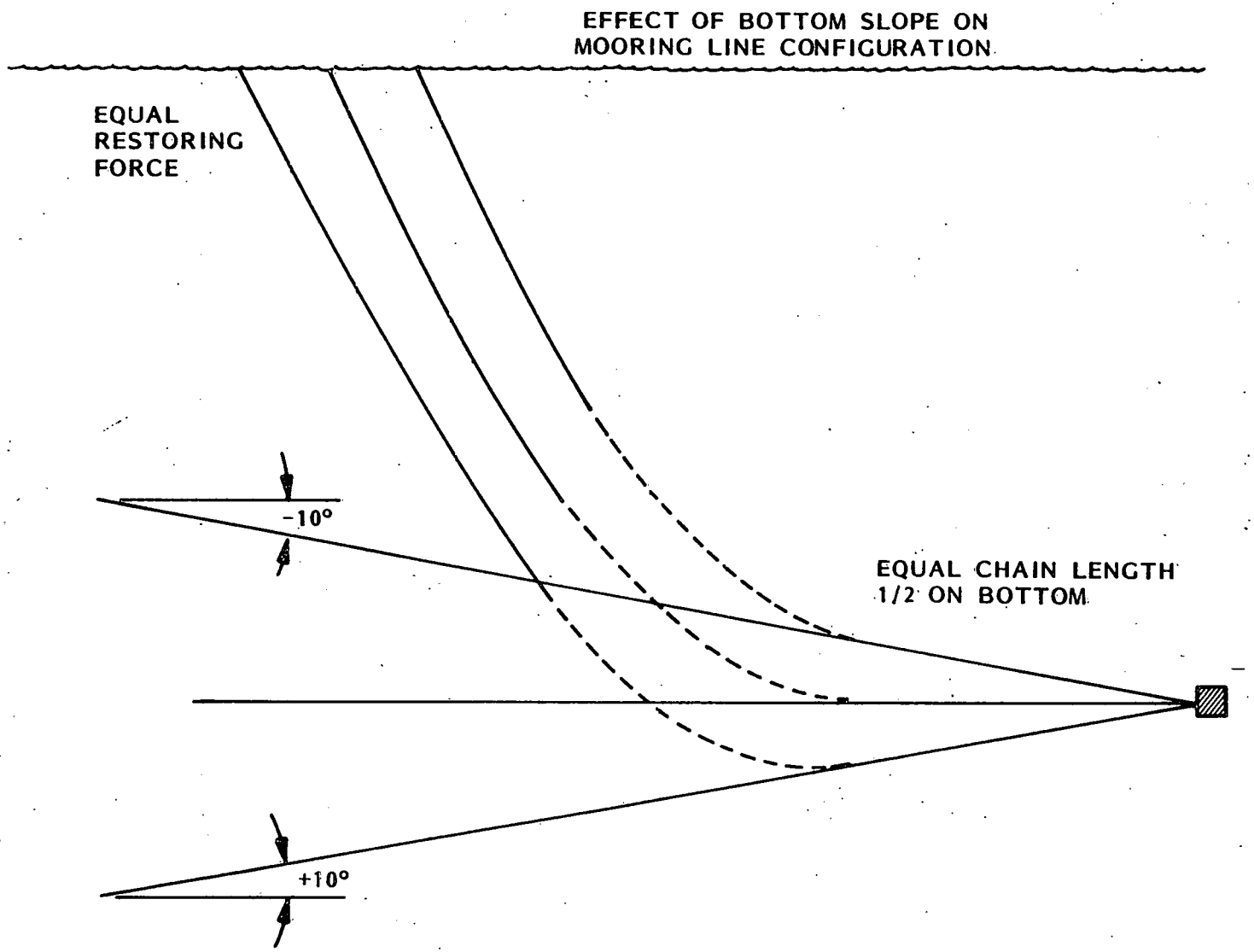

Fig. D-2 Effect of Bottom Slope on Mooring Line Configuration

D.2 METHOD OF SOLUTION

The characteristics of composite mooring lines on a sloping bottom and without an imposed current are considered in the remaining sections. A catenary analysis was necessary for general knowledge of the problem. These catenary generated configurations are used also as a starting point for subsequent numerical integration.

Two simplifications are made in the following analysis:

- o The platform orientation to the storm load is held fixed during each calculation. Platform rotation to relieve the mooring-system-induced moments is not considered.
- o Bottom slope for each anchor is constant in the plane of the mooring line.

D.2.1 Calculation of an Unloaded Single Mooring-Leg Configuration using Catenary Equations

The approximate configuration of an unloaded, two-component, single mooring leg is determined by applying a set of catenary equations to the known boundary conditions.

Values for several environmental variables must be available before this solution can proceed. The necessary parameters are depth of the anchor, bottom slope of the region adjacent to the anchor, and horizontal range from the platform mooring line attachment point to the anchor. Necessary mooring-leg characteristics are the length, and wet weight per foot of the chain attached to the anchor plus the wire rope length, and weight in water.

Two distinct categories based on the sign of the bottom slope contain all practical solutions: negative zero slope, and positive slope.

D.2.1.1 Negative or Zero Slopes. Solution of the configuration illustrated in Fig. D-3 is reached by applying an appropriate set of equations over restricted regions of consistent characteristics.

- Region I comprises the section of chain lying on the bottom slope adjacent to the anchor.
- Region II is the next section of chain suspended off the bottom slope and attached at the upper end to the wire rope mooring line.
- Region III is the wire rope mooring line attached to the chain at one end and to the surface platform at the other end.

Several characteristics of this mooring leg must be known to provide results at the end of the calculation procedure:

- Weight of chain per foot in water W_c lb/ft
- Weight of wire per foot in water W_w lb/ft
- Length of chain S_c ft
- Angle of bottom slope Θ deg
- Fraction of chain on bottom $K_c \leq 0$ ratio ≤ 1
- Horizontal tension at anchor H lb

Subscripts refer to regions for lengths or point number for tensions.

The horizontal tension is constant in a catenary and can be regarded in this instance as platform restoring force. This restoring force acts to pull the platform toward the anchor, and is used as a variable in the calculation to provide a particular anchor range or wire rope length. Fraction of chain on the bottom is also used as a calculation variable but has a nominal value of 0.5.

Region I Equations. (Chain lying on the bottom)

- Horizontal and vertical distances

$$x_1 = K_c S_c \cos\Theta$$

$$d_1 = K_c S_c \sin\Theta$$

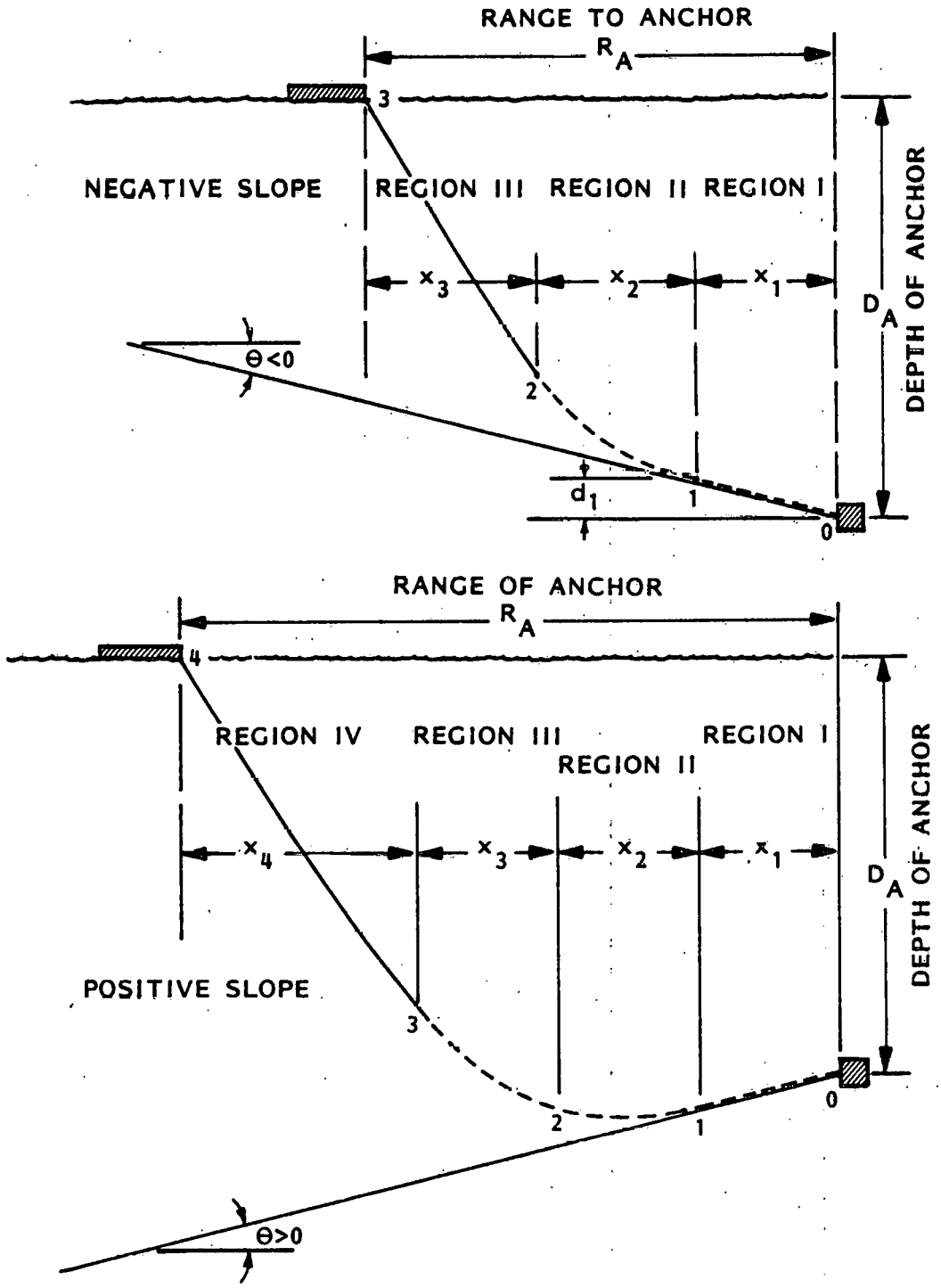

Fig. D-3 Solution Regions for Negative and Positive Seafloor Slopes

- Length of chain on bottom

$$S_{c_1} = K_c S_c$$

- Tension components at point 1

$$V_1 = -H \tan \Theta \text{ vertical tension}$$

$$T_1 = H/\cos \Theta \text{ total tension}$$

Region II Equations. (Chain suspended in catenary curve)

- Length of chain suspended

$$S_{c_2} = (1 - K_c) S_c$$

- Tensions at point 2

$$V_2 = S_{c_2} W_c + V_1$$

$$T_2 = \sqrt{H^2 + V_2^2}$$

- Horizontal and vertical distances

$$x_2 = H/W_c \left[\ln (T_2 + V_2) - \ln (T_1 + V_1)\right]$$

$$d_2 = (T_2 - T_1)/W_c$$

Region III Equations. (Wire rope to the surface)

- Distance to surface

$$d_3 = d_A + d_1 - d_2$$

- Tension components at point 3, surface attachment point

$$T_3 = d_3 W_w + T_2$$

$$V_3 = \sqrt{T_3^2 - H^2}$$

- Length of wire to reach the surface

$$S_3 = (V_3 - V_2)/W_w$$

- Horizontal distance

$$x_3 = \frac{H}{W_w} \left[\ln (T_3 + V_3) - \ln (T_2 + V_2)\right]$$

- Total range to the anchor

$$R_A = X_1 + X_2 + X_3$$

- Total length of mooring leg

$$S_T = S_c + S_3$$

D.2.1.2 Positive Slope. The positive slope configuration shown in Fig. D-3 is similar in many respects to that configuration resulting from a negative slope. Differences from the preceding development exist only in the first two regions.

- Region I. Includes, as before, the section of chain lying on the bottom slope adjacent to the anchor. Depth in this region increases in contrast to the previous Region I.
- Region II. This section of chain reverses the bottom slope, and is calculated as a full symmetric catenary.
- Region III. Same as the previous Region II. This last chain section starts at the antisymmetric slope angle.
- Region IV. The wire rope section that reaches the surface, and is the same as the previous Region III.

Nomenclature used here is similar to that in the previous section, with the addition of a subscript 4.

Region I Equations. (Chain lying on bottom)

- Length of chain on bottom

$$S_{c_1} = K_c S_c$$

- Horizontal and vertical distance

$$X_1 = K_c S_c \cos \Theta$$

$$d_1 = K_c S_c \sin \Theta$$

- Tension components at point 1

$$V_1 = H \tan \Theta \text{ (vertical tension}$$

$$T_1 = H/\cos \Theta \text{ (total tension)}$$

Region II Equations. (Chain suspended in symmetric catenary)

- Tension components by symmetry at point 2

$$V_2 = V_1 = H \tan \Theta$$

$$T_2 = T_1 = H/\cos \Theta$$

- Horizontal Distance

$$X_2 = \frac{2H}{W_c} \left[\ln (V_3 + T_3) - \ln (H) \right]$$

- Length of chain section

$$S_{c_2} = \frac{2V_3}{W_c}$$

Region III Equations. (Final chain section)

- Length of chain section

$$S_{c_3} = S_c - S_{c_1} - S_{c_2}$$

- Tension components at point 3 upper end of chain

$$V_3 = V_2 + S_{c_3} W_c$$

$$T_3 = \sqrt{V_3^2 + H^2}$$

- Horizontal and vertical distances

$$X_3 = H/W_c \left[\ln (T_3 + V_3) - \ln (T_2 + V_2)\right]$$

$$d_3 = (T_3 - T_2)/W_c$$

Region IV Equations. (Wire rope to the surface)

- Distance to the surface

$$d_4 = d_A + d_1 - d_2 - d_3$$

- Tension components at point 4, surface attachment point

$$T_4 = T_3 + d_4 W_w$$

$$V_4 = \sqrt{T_4^2 - H^2}$$

- Length of wire to reach the surface

$$S_4 = (V_4 - V_3)/W_w$$

- Horizontal distance

$$x_4 = H/W_w \left[\ln (T_4 + V_4) - \ln (T_3 + V_3)\right]$$

- Total range to the anchor

$$R_A = X_1 + X_2 + X_3 + X_4$$

- Total length of the mooring leg

$$S_T = S_c + S_4$$

D.2.2 Applications of Equations

These two sets of equations are solved iteratively for different combinations of anchor range and wire rope mooring line length by varying the horizontal tension H and the fraction K_c of chain resting on the bottom.

The configuration differences resulting from slope variations (±10 deg and zero) with constant anchor depth, horizontal tension and chain fraction is shown in Fig. D-2.

This catenary solution technique is used to provide unloaded equilibrium mooring leg configurations as an initial starting point for the full mooring array solution.

D.3 SOLVING CABLE VECTOR EQUATIONS BY NUMERICAL INTEGRATION

A simple static cable configuration can be solved by integrating the governing differential equations along the length of the cable when the tension vector at the starting point is known. These differential equations represent the cable, at rest, and in equilibrium with the forces acting on it.

Figure D-4 shows (1) the forces acting on a small section of cable, and (2) the associated nomenclature used in the vector differential equations.

The differential equations for a flexible inextensible cable are:

$$\frac{d}{ds}(\vec{T}) + \vec{F}_t + \vec{F}_N + \vec{W} = 0 \qquad (1)$$

$$\frac{d}{ds}(\vec{R}) \times \vec{T} = 0 \qquad (2)$$

The hydrodynamic normal and tangential forces appearing in Eq. (1) are expressed as:

$$F_N = 1/2 \quad C_D \, D \, C_N^2 \, \hat{C}_N \qquad (3)$$

$$F_t = 1/2 \quad C_D \, D \left[-0.035|C_t| + 0.083 \, (C \cdot C)^{1/2}\right] C_t \, \hat{t} \qquad (4)$$

These loading functions representing the normal and tangential components of hydrodynamic force are due to Whicker (1957).

The Axis System

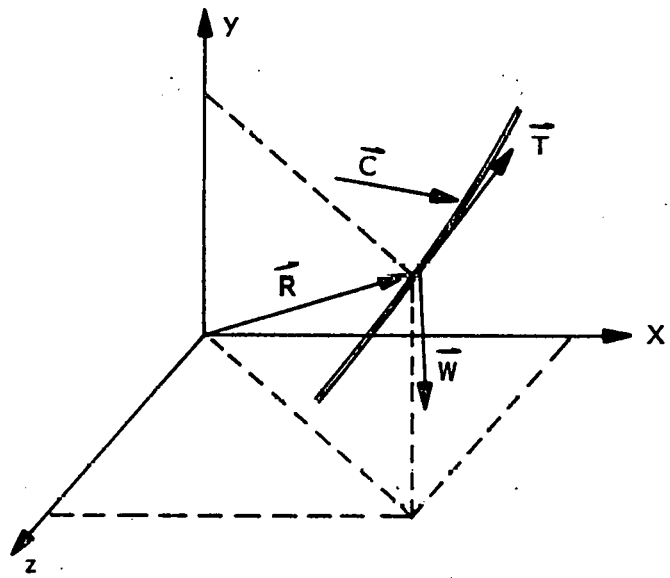

NOMENCLATURE

$\vec{R}$	three-component position vector
$\vec{T}$	three-component tension vector
$\vec{C}$	three-component current vector
$\vec{W}$	weight vector acting in the -Y direction
$\hat{t}$	unit vector in the direction of tension $\vec{T}$
$\hat{C}_N$	unit vector in the direct of the normal current component
C_t, C_n	tangential and normal components of current with respect to cable direction
C_D	cable normal drag coefficient
$\vec{F}_t$	hydrodynamic tangetial force vector acting on a cable element
$\vec{F}_n$	hydrodynamic normal force vector acting on a cable element
S	distance measured along cable in feet
D	cable diameter in feet

Fig. D-4 Vector Equations and Nomenclature for the Cable

The normal coefficient of current C_N is:

$$C_N^2 = (t \times C) \cdot (t \times C)$$

and its direction $\hat{C}_N$ is

$$C_N = \frac{(\hat{t} \times \vec{C}) \times \hat{t}}{\left\{\left[(\hat{t} \times \vec{C}) \times \hat{t}\right] \cdot \left[(\hat{t} \times \vec{C}) \times \hat{t}\right]\right\}^{1/2}}$$

The tangential component of current C_t is found by taking the projection of the current on the cable direction t.

$$C_t = \hat{t} \cdot \vec{c}$$

and the direction is $\hat{t}$.

The weight vector has just a y component.

$$W = \begin{pmatrix} 0 \\ W \\ 0 \end{pmatrix}$$

Equation (1) yields expressions for the x, y, z components of dT/ds.

Equation (2) asserts that the cable direction is always the same as the local tension vector, such that $\vec{dR}/ds = t$ current is described as a vector quantity $\vec{C}$ which can have any prescribed spatial variation.

The above equations are then integrated by the Runge-Kutta technique, providing a three-component tension vector and a three-component position vector for each integration step along the length of the cable.

Stretch has been incorporated in the calculation procedure by allowing the integration step size Δs, diameter, and weight to vary as a function of the total tension along a particular cable element.

The digital computer subroutine, coded to perform the preceding calculations, uses as input the following information:

- o Coordinates of the starting point
- o Initial tension vector
- o Cable characteristics
  - Diameter
  - Weight/ft
  - Drag coefficient
  - Length of section
  - Stretch characteristics
- o Current vector

Variables R and T are integrated as functions of unstretched distance along the cable. The subroutine terminates when the total length of that particular cable section is reached. At this point the cable characteristics can be changed and another section calculated starting at the end point of the last section. Composite mooring lines consisting of alternating sections of chain and wire rope are handled in this fashion.

D.3.1 Calculation of a Single Mooring Line Configuration from the Anchor to the Surface

The mooring line under consideration is a composite with a length of chain adjacent to the anchor followed by a wire rope from the chain to the surface. This slack mooring line condition will allow at least some length of the chain section to rest on the ocean floor.

The geometry of the chain section in contact with the bottom is a matter of some speculation. This analysis assumes that the chain follows a straight line defined by the bottom slope and the horizontal tension components.

Coordinates of the point of chain lift off are calculated as

$$\vec{x}_o = \vec{x}_A - \hat{t} \cdot K_c \cdot S_c \qquad (5)$$

where

x_A represents the x, y, z coordinates of the anchor location,

t the unit vector in direction of tension at anchor,

K_c the fraction of chain on the bottom, and

S_c the total length of chain

The vertical tension component at the chain lift-off point is always adjusted to a value which ensures the tangency condition with the bottom slope.

Equations (1) and (2) are integrated numerically from the chain lift-off point described by Eq. (5) to the end of the chain section, a distance of $(1 - K_c)$ S_c ft. At this point, the cable properties are changed to reflect the wire rope and the integration continues to the end. The end of the wire rope, however, may not be sufficiently close to the depth of the attachment point at this stage of the circulation. Variations in the value of the constant K_c, which represents the fraction of chain resting on the sloping bottom, will

bring the platform end of the mooring line to the correct depth. Control of this procedure rests in a first guess of $K_c = 0.5$ followed by a series of perturbations determined by linear extrapolation. This process is illustrated in Fig. D-5 and

$$K_{c_{i+1}} = K_{c_i} + \Delta K_{c_i}$$

and the sequence of terms $\Delta K_c \rightarrow 0$.

D.3.2 Calculation of a Single Mooring Line Configuration to a Specified Point on the Surface

The preceding section discussed a technique used to solve for a configuration with the upper end at some attachment point depth without regard for the horizontal coordinates of that end point. Changing the horizontal tension components at the starting or anchor end will move the upper end of the cable to a new position in the horizontal plane. Systematic choice of horizontal tension increments will achieve any specific point in the range of that mooring line. This effective position adjustment is illustrated in Fig. D-6.

Choice of tension increments at the anchor depends upon idealizing the mooring line response to these increments as a linear process, in the following manner:

$$\begin{aligned} C_{11}\ \Delta T_X + C_{12}\ \ T_z &= \Delta_X \\ C_{21}\ \Delta T_X + C_{22}\ \ T_z &= \Delta_z \end{aligned} \qquad (6)$$

The linear influence coefficients C_{ij} can be evaluated by applying the differential operators $\partial / \partial T_x$ and $\partial / \partial T_z$ to both equations.

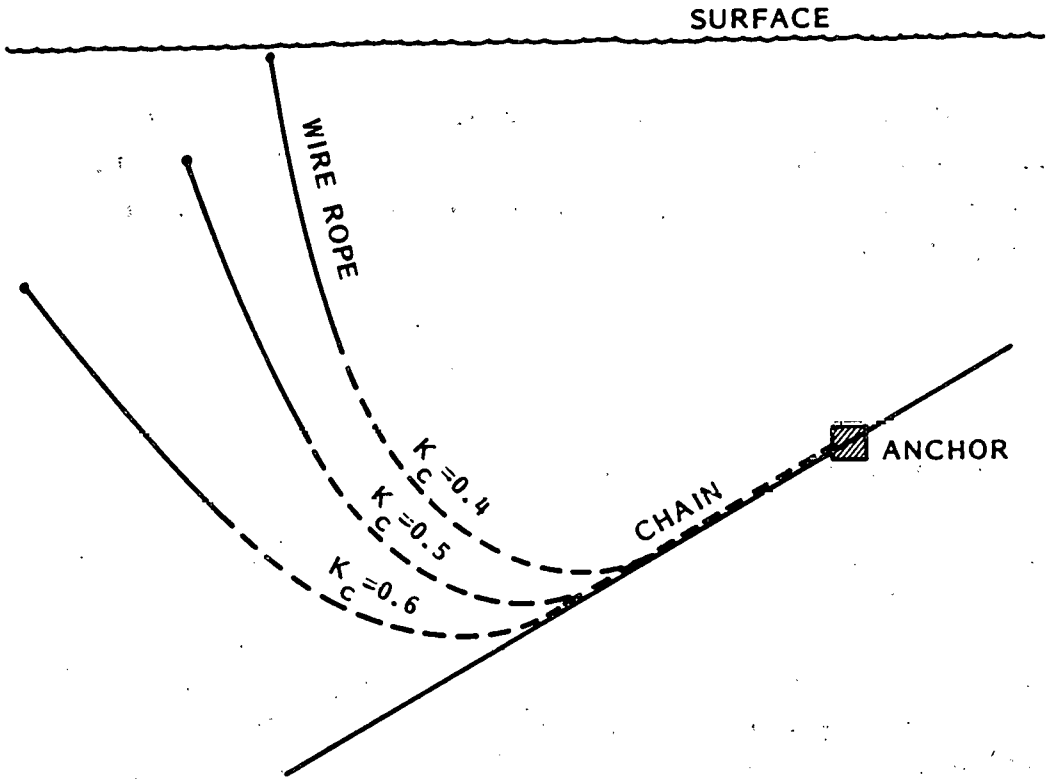

Fig. D-5 Influence of Bottom Chain Length on Anchor Leg Catenary Configuration

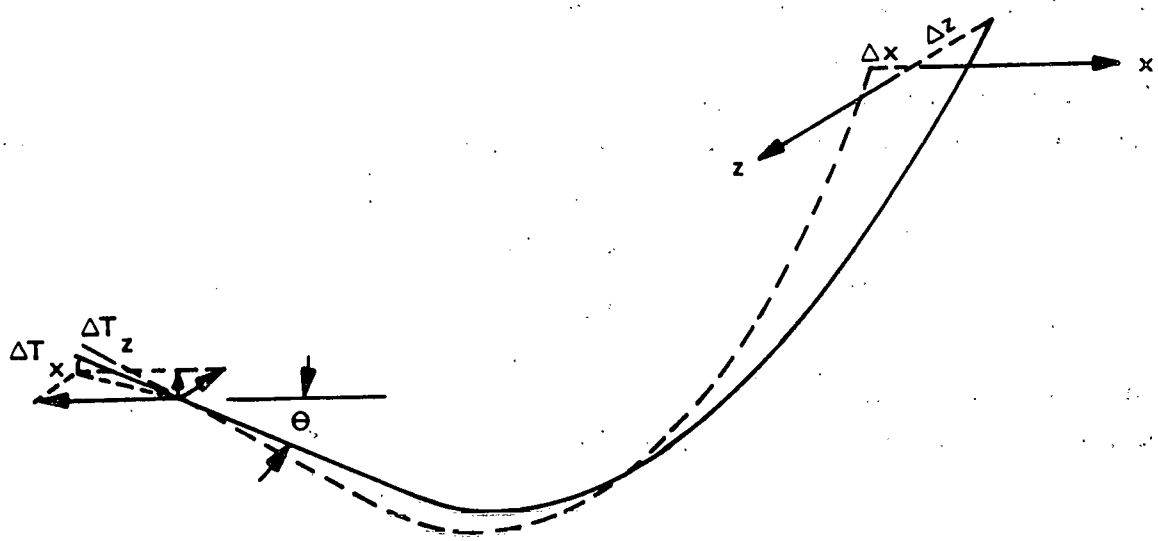

Fig. D-6 Influence of Horizontal Tension Component on Anchor Leg Catenary Configuration

Then

$$C_{11} = \frac{\partial \Delta x}{\partial \Delta T_x} \quad ; \quad C_{12} = \frac{\partial \Delta x}{\partial \Delta T_z}$$

$$C_{21} = \frac{\partial \Delta z}{\partial \Delta T} \quad ; \quad C_{22} = \frac{\partial \Delta z}{\partial \Delta T_z} \tag{7}$$

Evaluating these constants involves solving for a cable configuration with several different starting tension vectors:

- The basic case yields a set of differences from the desired final location of the platform end of the mooring line in this fashion

$$T_{x_0}, T_{z_0} \xrightarrow[\text{subroutine}]{\text{cable}} x_0, \Delta z_0$$

- Next the x component of starting tension is perturbed and

$$\left\{T_{x_0} + \Delta T_x, T_{z_0}\right\} \xrightarrow[\text{subroutine}]{\text{cable}} \left\{\Delta x_1, \Delta z_1\right\}$$

- The z component then receives similar treatment:

$$\left\{T_{x_0}, T_{z_0} + \Delta T_z\right\} \xrightarrow[\text{subroutine}]{\text{cable}} \left\{\Delta x_2, \Delta z_2\right\}$$

So

$$C_{11} = \frac{\partial \Delta x}{\partial \Delta T_x} \approx \frac{\Delta x_0 - \Delta x_1}{\Delta T_x}$$

$$C_{12} = \frac{\partial \Delta x}{\partial \Delta T_z} \approx \frac{\Delta x_0 - \Delta x_2}{\Delta T_z}$$

$$C_{21} = \frac{\partial \Delta z}{\partial \Delta T_x} \approx \frac{\Delta z_0 - \Delta z_1}{\Delta T_x}$$

$$C_{22} = \frac{\partial \Delta z}{\partial \Delta T_z} \approx \frac{\Delta z_0 - \Delta z_2}{\Delta T_z}$$

Each of these evaluations assumes that the vertical attachment depth criterion has been met. Now the set of Eq. (6) can be solved for the set of T_k values necessary to move the cable to the required position. This solution is:

$$C_{ij}^{-1} \begin{bmatrix} x_0 \\ z_0 \end{bmatrix} = \begin{bmatrix} \Delta T_{x_1} \\ \Delta T_{z_1} \end{bmatrix}$$

Apply these to the original set of tensions:

$$T_{x_1} = T_{x_0} + \Delta T_{x_1}$$

$$T_{z_1} = T_{z_0} + \Delta T_{z_1}$$

The new solution should yield errors smaller than the original basic case errors. Repeated application of the influence coefficient inverse matrix $[C_{ij}]^{-1}$ to the error vector

$$\begin{bmatrix} \Delta x \\ \Delta z \end{bmatrix}$$

should bring the mooring line to the required point within a very few cycles.

This solution process is not guaranteed to converge because of the system nonlinearities. When the sequence of additive ΔT_i act to greatly

decrease the total line tension, each succeeding iteration might be farther from the required solution, since the line motion becomes more sensitive to lateral force increments. Increasing total line tension slows down convergence somewhat, but will not introduce divergent behavior.

Control of the divergent behavior is exercised by rejecting Δx_i, Δz_i which are too nonlinear, and then reducing the ΔT_x, ΔT_z values to achieve desired results.

D.3.3 Multiple Anchor Leg Configurations

The previous section details an iterative solution to the problem of calculating the configuration of a composite mooring line from an anchor, embedded on a sloping bottom, to a specified surface attachment point. Additional difficulties are introduced when the surface attachment point is a floating platform tethered by a number of such mooring lines, as illustrated in Fig. D-7.

Deflection of mooring lines under the platform load is an unknown quantity and a satisfactory solution requires matching horizontal-force components as well as the position coordinates.

Generalizing the set of linear Eq. (6) which appear in the preceding section offers a method of solving these relationships if a set of similar force balance equations is added.

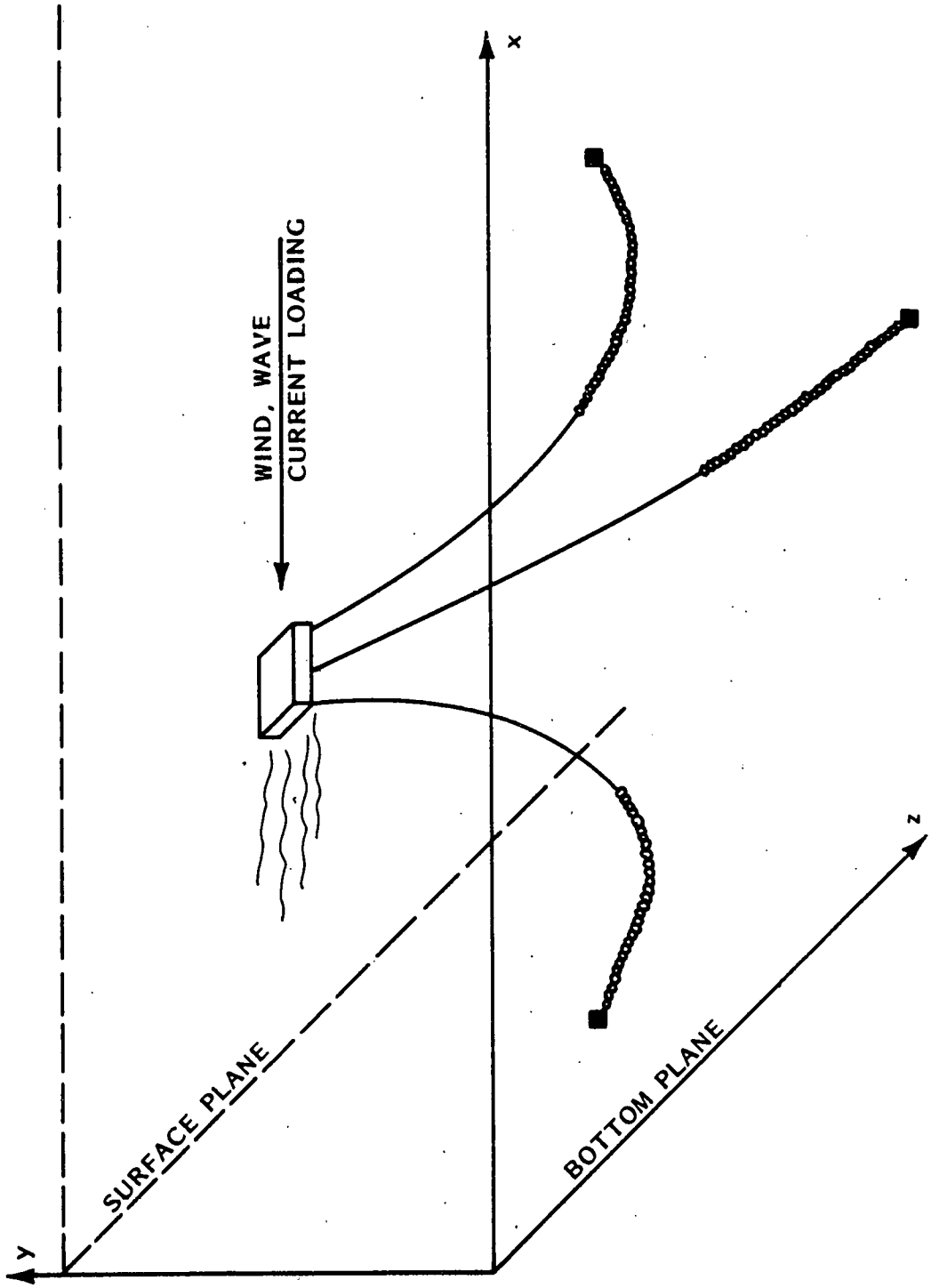

Fig. D-7 Typical MAL Configuration

D.3.4 Linear Influence Coefficients

The equations take the following form:

$$\sum_{j=1}^{2n} C_{ij} \Delta T_j = \Delta x_i \quad \text{where} \quad i = 1, 2 \ldots 2n-2 \tag{8}$$

plus the force balance equations

$$\sum_{j=1}^{2n} C_{ij} \Delta T_j = \Delta F_k \tag{9}$$

where

$i = 2n-2 + k$

$k = 1$

$n =$ the number of mooring legs

The quantities x_i are differences between the horizontal coordinates of the upper ends of all mooring legs referenced to leg number 1.

$$\Delta x_{2i-1} = X_1 - X_{i+1} \qquad i = 1, \ldots, n-1$$

$$\Delta x_{2i} = z_1 - z_{i+1}$$

Force balance between mooring system and platform is provided by the F_k in Eq. (9) above:

$$\Delta F_1 = \sum_{i=1}^{n} T_{x_1} + F_{x\ \text{PLATFORM}}$$

$$\Delta F_2 = \sum_{i=1}^{n} T_{z_i} + F_{z\ \text{PLATFORM}} \tag{10}$$

where the $F_{PLATFORM}$ are forces external to the mooring system.

The linear influence coefficient matrix $[C_{ij}]$ consists of terms like those explained in the preceding section.

$$C_{ij} = \frac{\partial \Delta x_i}{\partial \Delta T_{x_j}} \qquad \begin{matrix} i = 1, 2, \ldots 2n - 2 \\ j - 1, 2, \ldots 2n \end{matrix}$$

with the force balance coefficient

$$C_{ij} = \frac{\partial \Delta F_k}{\partial \Delta T_{x_j}} \qquad \begin{matrix} i = 2n - 1, 2n \\ j = 1, 2, \ldots, 2n \end{matrix}$$

Actual values for the coefficients given are calculated by finite difference methods. Perturbing the tensions by ΔT_{x_j} to obtain coordinate changes Δx_i and force changes ΔF_k

D.3.5 Formation of the Influence Coefficient Matrix

The cable integration subroutine is given a starting tension vector $\vec{T}_{o_i}$ for each mooring leg i.

The coordinates and tensions $\left\{ \vec{X}_{o_i} \right\}$, $\left\{ \vec{T}_{o_i} \right\}$ at the upper end of each cable are stored after the integration is completed.

This process is repeated after the tensions are perturbed in the X coordinate as $\left\{ \vec{T}_{0_i} + \vec{T}_{1_i} \right\}$ resulting in $\left\{ \vec{X}_{1_i} \right\}$ and $\left\{ \vec{T}_{1_i} \right\}$. The same for the z coordinate direction: $\left\{ \vec{T}_{0_i} + \vec{T}_{2_i} \right\}$ produces $\left\{ \vec{X}_{2_i} \right\}$, $\left\{ \vec{T}_{2_i} \right\}$

The effects of these perturbations are then evaluated by calculating and storing two sets of numerical partial derivatives for each of the mooring legs.

$$Q_{ijk} = \frac{\vec{X}_{ok} - \vec{X}_{jk}}{\Delta\vec{T}_{jk}}$$

$i = 1, 2, x, z$ vector components
$j = 1, 2, x, z$, perturbations
$k = 1, 2, \ldots n$ mooring leg number

Calculating force balance coefficients in the same fashion:

$$P_{ijk} = \frac{\vec{T}_{ok} - \vec{T}_{jk}}{\Delta\vec{T}_{jk}}$$

with the same index range as Q_{ijk}

These indexed collections of quantities are 2n, 2 x 2, matrices containing all of the necessary information required to form the influence coefficient matrix. The final task remaining is to place the coefficients in the proper order to satisfy the relations expressed in Eqs. (8) and (9).

Definitions of the Δx_i show that each double row of the matrix (i.e., 1, 2, or 3, 4, etc.) involves just two mooring legs, and only four of the perturbing tension increments. Each set of two rows involve mooring leg 1 plus the leg number entering the coordinate difference calculation on the other side of the equation.

The first two rows concern only legs 1 and 2. Essentially the Q_{ijk} matrices are all formulated in the same fashion. Therefore, forcing the ends of the cables together requires that the matrices be of opposite sign, generating motion in opposite directions.

Now the Q_{ijk} and P_{ijk} can be used to load the influence coefficient matrix C_{lm}. This can be represented pictorially in the following fashion:

$$[C_{lm}] = \begin{bmatrix} Q_{ij1} & -Q_{ij2} & 0 & 0 & 0 \\ Q_{ij1} & 0 & -Q_{ij3} & 0 & 0 \\ Q_{ij1} & 0 & 0 & -Q_{ij4} & 0 \\ & & & & \\ Q_{ij1} & 0 & 0 & 0 & -Q_{ijn} \\ P_{ij1} & P_{ij2} & P_{ij3} & P_{ij4} & P_{ijn} \end{bmatrix} \tag{11}$$

where 0, P_k and Q_k are all 2 x 2 matrices.

The influence coefficient matrix is complete and the first of several iterative cycles will be illustrated.

This linear system will be written in matrix form as:

$$[C_{ij}]\,\Delta T = \begin{pmatrix} \Delta \vec{X} \\ \Delta F \end{pmatrix} \tag{12}$$

The Δx has been defined previously as:

$$\Delta x_{2i-1} = X_1 = X_{i+1} \qquad i = 1, 2 \ldots n-1$$
$$\Delta x_{2i} = z_1 - z_{i+1}$$

and the $\Delta \vec{F}$ is again

$$F_1 = \sum_{i=1}^{n} T_{xi} + F_{x\ \text{PLATFORM}}$$

$$F_2 = \sum_{i=1}^{n} T_{zi} + F_{z\ \text{PLATFORM}}$$

Solving the Eq. (12)

$$\Delta\vec{T} = \left[C_{ij}\right]^{-1} \begin{pmatrix} \Delta\vec{X} \\ \Delta\vec{F} \end{pmatrix} \qquad (13)$$

The next set of coordinate distance errors $\Delta\vec{x}$ and force errors $\Delta\vec{F}$ are generated by repeating the cable computations with a new set of tensions, $\vec{T}_{k+1}$

$$\vec{T}_{k+1} = \vec{T}_k + \Delta\vec{T}$$

k is just the iteration index in this equation.

Equation (13) is utilized after every complete integration cycle of the n mooring legs. The iterative procedure continues until all of the horizontal coordinate errors are within some preset tolerance.

Vertical coordinate errors are minimized before each mooring leg integration is accepted.

The influence coefficient matrix need not be recalculated for most configurations, although nonlinear mooring leg response will invalidate some of the C_{ij} coefficient values frequently. Other methods of maintaining a linear response will be discussed subsequently.

The preceding technique would result in all the cables converging at a single point when the errors were reduced. This is not a necessary consequence, however, since coordinates of attachment points can be subtracted from the end coordinates of the mooring legs. Introducing the coordinates of the attachment points causes convergence at the origin of the platform coordinate system, usually the center.

D.3.6 Nonlinear Mooring Leg Response

Local cable angular orientations are the same as the local tension vector directions. This method utilizes incremental changes in the tension vector at the anchor end of the mooring leg to achieve convergence at the platform end. When these incremental tension values act to decrease the total tension vector greatly, then much larger direction changes occur.

Normally this type of line behavior is evident on the downstream side of the platform where the mooring legs have a tendency to go slack.

The opposing condition of increased total line tension also leads to nonlinear behavior because here the directional changes or increments are much less than expected.

These two examples pose a different problem to the iterative solution, however. Decreased tension leads to overcorrection and at the extreme divergent behavior, which renders this solution impossible. Increased tension will provide an undercorrection and slow convergence but not prevent it.

Several methods are examined to correct the above defects in this procedure. All attempts were based on the goal of decreasing the linear tension increments to the more sensitive lines on the slack side of the mooring system.

The method selected has two advantages over those previously tried:

- o The method is automatically applied and altered when necessary.
- o Increased tension in the lines is treated by increasing the tension increments.

D.3.7 Iteration Control Technique

The matrix Q_{ijk} contains the necessary elements to predict the linear line response Δx_p, Δz_p to a particular set of tension increments, ΔT_{x_k}, ΔT_{z_k}, for a typical mooring leg k.

That is,

$$\Delta x_{pk} = Q_{11k}\ \Delta T_{xk} + Q_{12k}\ \Delta T_{zk}$$
$$\Delta z_{pk} = Q_{21k}\ \Delta T_{xb} + Q_{22k}\ \Delta T_{zk}$$

The mooring leg end point coordinates are calculated in the normal fashion by integrating the cable equations after the tension increments ΔT_{xk}, ΔT_{zk} are added to the starting tensions.

A change in end point coordinates Δx_k, Δz_k are then compared with the linear predictions.

If the result is in the range

$$0.5 \left(\Delta x_{pk}^2 + \Delta z_{pk}^2\right)^{1/2} < \left(\Delta x_k^2 + \Delta z_k^2\right)^{1/2} < 1.5 \left(\Delta x_{pk}^2 + \Delta z_{pk}^2\right)^{1/2} \qquad (14)$$

then the integration is accepted. If the result is such that

$$\left(\Delta x_k^2 + \Delta z_k^2\right)^{1/2} > 1.5 \left(\Delta x_{pk}^2 + \Delta z_{pk}^2\right)$$

then the tension increments are halved: ΔT_{xk} is replaced by 1/2 ΔT_{xk}, ΔT_{zk} is replaced by 1/2 ΔT_{zk}, and the calculations are repeated until inequality, Eq. (14), is satisfied.

If the result is such that

$$\left(\Delta x_k^2 + \Delta z_k^2\right)^{1/2} < 0.5 \left(\Delta x_{pk}^2 + \Delta z_{pk}^2\right)^{1/2}$$

Then the tension increments are increased by a factor of 1.75

$$\Delta T_{xk} \text{ is replaced by } 1.75\ \Delta T_{xk}$$

and

$$\Delta T_{zk} \text{ is replaced by } 1.75\ \Delta T_{zk}$$

This system has the capability of brining some very slack lines into convergence within a reasonable number of iterations.

D.3.8 Mooring Leg Induced Moments Acting on the Surface Platform

Storm loads on the surface platform are selected on the basis of severity and angular orientation of wind and wave. Computations are then performed with platform orientation held constant. Rotational moments, exerted on the platform by the directional tensions in the mooring lines, are not compensated by a corresponding platform rotation.

These platform rotational moments are calculated about all three axes, to aid in estimating the actual impact on platform heading.

Mooring line attachment points are specified in the surface platform coordinate system, $\vec{R}_i$ for the ith attachment point.

Line tension is calculated in the platform coordinate system as $\vec{T}_i$ for the ith mooring line. The total torque on the platform is:

$$\vec{M} = \sum_{i=1}^{n} \vec{R}_i \times \vec{T}_i$$

Specifically for the rotational moment about the vertical axis, this becomes:

$$M_y = \sum_{i=1}^{n} \left(R_{z_i} T_{x_i} - R_{x_i} T_{z_i} \right)$$

Appendix E
MAL CALCULATIONS

THIS PAGE

WAS INTENTIONALLY

LEFT BLANK

Prepared	NAME IWASHITA	DATE 10/10/79	LOCKHEED CORPORATION Stress Sheet	Page	TEMP.	PERM
Checked			TITLE ANCHOR	Model		
Approved				Report No.		

MAXIMUM ANCHOR PULL - SEE 100YR STORM
ANCHOR LEG #3

T_x = 50572 #
T_z = 662,228 #
$T_{RESULTANT} = \sqrt{T_x^2 + T_z^2}$ = 664 KIPS
ADD 10% DYNAMIC = 66.4
TOTAL 730
FACTOR OF SAFETY OF 2 730
ANCHOR HOLDING POWER = 1460 KIPS
4 7/8" DIA CHAIN BREAKING STRENGTH = 2932 KIPS
1/2 OF BREAKING STRENGTH = 1466 KIPS
∴ ANCHOR HOLDING POWER ≤ 1/2 B.S.

HOLDING POWER IN SAND ≈ 20 TIMES ANCHOR WT
HOLDING POWER IN MUD ≈ 9 TIMES ANCHOR WT
ASSUMING AN AVERAGE OF 15
ANCHOR WEIGHT x 15 = 1460 KIPS
A.W. = 97.3 KIPS
FOR REDUNDANCY AND RELIABILITY, TWO ANCHORS ARE ARRANGED IN TANDEM. IN THIS ARRANGEMENT, THE EFFECTIVE HOLDING POWER IS 170% (VICE 200%)
∴ INDIVIDUAL ANCHOR WT = 97.3/1.7
= 57.2 KIPS
USE 60,000# ANCHORS THEN:
HOLDING POWER IN SAND = 60 x 1.7 x 20 = 2040 KIPS
HOLDING POWER IN MUD = 60 x 1.7 x 9 = 918 KIPS

HOLDING POWER OF ONE ANCHOR
IN SAND = 60 x 20 = 1200 KIPS > $T_{RESULTANT}$
IN MUD = 60 x 9 = 540 KIPS < $T_{RESULTANT}$

HOLDING POWER IS DEPENDENT ON SEAFLOOR. SHANK ANGLE IS ALTERED FOR A COMBINATION OF SAND AND MUD BOTTOM.

Prepared	NAME IWASHITA	DATE 10/12/79	LOCKHEED CORPORATION Stress Sheet	Page	TEMP.	PERM
Checked			TITLE CHAIN	Model		
Approved				Report No.		

MAXIMUM STATIC CHAIN TENSION - SEE 100 YEAR STORM ANCHOR LEG #3

T_{TOTAL} STATIC.	= 1119 KIPS
12% DYNAMIC	= 134 KIPS
TOTAL	1253 KIPS
F.S. OF 2.0	1253 KIPS
MIN BR. STR.	2506 KIPS

USE 4 7/8" DIA, GRADE 4 ALLOY CHAIN, BR. STR. OF 2,932 KIPS (HAMANAKA CHAIN MFG. CO., LTD. HIMEJI, JAPAN HAS CAPABILITY), 229 #/FT

FACTOR OF SAFETY = 2932/1253 = 2.3

MAX. LENGTH OF CHAIN REQUIRED FOR WIRE ROPE CHANGE OUT IS MAX. ANCHOR DEPTH PLUS 20% FEET FOR CONTINGENCY.

MAX. ANCHOR DEPTH FOR ANCHOR LEG #2 = 5680'

WEIGHT OF CHAIN HANGING VERTICAL

$$229\left(1-\frac{64}{490}\right)\times 5680 = 199\times 5680 = 1130 \text{ KIPS}$$

WEIGHT OF CHAIN WITH ANCHORS

$$1130 + 60\left(1-\frac{64}{490}\right)\times 2 \cong 1234 \text{ KIPS}$$

FACTOR OF SAFETY = 2932/1234 = 2.4 (STATIC.)

NOTE: ANCHOR LOWERING OPERATION IS ASSUMED DURING A QUIET SEA STATE

ALLOWABLE DYNAMIC LOADING FOR A F.S. OF 2.

$$\left(\frac{2932}{2} - 1234\right)\frac{100}{1234} = 18\ \%$$

Prepared	NAME IWASHITA	DATE 10/12/79	LOCKHEED CORPORATION Stress Sheet	Page	TEMP.	PERM
Checked			TITLE WIRE ROPE	Model		
Approved				Report No.		

MAXIMUM STATIC WIRE ROPE TENSION - SEE 100 YEAR STORM ANCHOR LEG # 3

T TOTAL STATIC	=	1335 KIPS
12% DYNAMIC	=	160 KIPS
TOTAL	=	1495 KIPS
F.S. OF 2	=	1495 KIPS
MIN. BR. STR.	=	2990 KIPS

USE 5 3/4" DIA, 6x97 IWRC, GALV., BR. STR. OF 3000 KIPS, 65 #/FT (BRITISH ROPES HAS CAPABILITY).

CORROSION:

REF. JOURNAL OF OCEAN TECH, VOL 2, NO. 1, 1967 GUIDELINES FOR SELECTION OF MARINE MATERIALS

EXPECTED CORROSION - 3 TO 6 MILS PER YEAR. 10 YEAR CORROSION OF 1/16" AT DEPTH OF MORE THAN 200 FEET DOES NOT APPEAR TO BE SIGNIFICANT WITH RESPECT TO MATERIAL LOSS.

FATIGUE

THE CABLE IS NOT EXPOSED TO THE NORMAL BENDING FATIGUE AROUND SHEAVES. FOR THE MOST PART THE CABLE FLEXES AT A CATENARY RADIUS AT LOADS GENERALLY BELOW 33% OF ITS BREAKING STRENGTH. MOST EXPERIMENTAL DATA ON TENSION FATIGUE IS RELATED TO HIGH AMPLITUDE CONDITIONS HOWEVER IT IS POSSIBLE TO EXTRAPOLATE THE RESULTS TO PREDICT PERFORMANCE LEVELS FOR A RANGE OF MEAN LOADS BUT WITH LOW AMPLITUDE VARIATION.

EXAMPLE: FOR A MEAN LOAD OF 33% WITH A FATIGUE LIFE OF 1×10^7 THE AMPLITUDE IS

Prepared	NAME	DATE	LOCKHEED CORPORATION Stress Sheet	Page	TEMP.	PERM
Checked			TITLE	Model		
Approved				Report No.		

± 6% OF MINIMUM BREAKING LOAD. THE AMPLITUDE SHOULD BE RESTRICTED TO 1,000 KIPS ± 180 KIPS$_{ea}$ FOR 6×10^7 CYCLES - AND 33% OF MEAN LOAD, THE AMPLITUDE SHOULD BE RESTRICTED TO 1,000 KIPS ± 150 KIPS.

FURTHER IN DEPTH ANALYSIS IS RECOMMENDED FOR FINAL DESIGN

Prepared	NAME IWASHITA	DATE 10/11/79	LOCKHEED CORPORATION Stress Sheet	Page	TEMP.	PERM
Checked			TITLE FAIRLEAD	Model		
Approved				Report No.		

DESIGN CHAFING CHAIN LOAD = 1,500. KIPS
MATERIAL - A36 STEEL
YIELD STRENGTH = 36,000 PSI
ALLOWABLE TENSILE = 60% OF YIELD
ALLOWABLE COMPRESSIVE = 75% OF YIELD
ALLOWABLE SHEAR = 40% OF YIELD
LOAD DIAGRAM:

$R = \sqrt{1500^2 + 1500^2 - 2(1500^2)\cos 45^\circ}$

$R = 1148$ KIPS

$\therefore A_{TENSILE} = \frac{148 \times 2}{.6 \times 36} = 106\ IN^2$

$A_{COMP} = \frac{1148 \times 2}{.75 \times 36} = 85\ IN^2$

$A_{SHEAR} = \frac{1148 \times 2}{.4 \times 36} = 159\ IN^2$

FOR WILDCAT PIN, RECOMMEND OIL QUENCHED HIGH STRENGTH STEEL WITH A YIELD OF 75 KIPS.

PIN DIAMETER = $\sqrt{\frac{4}{\pi}\left(\frac{1148 \times 2}{.4 \times 75}\right)} = 9.87$ INCHES; USE 10"

YOKE PLATE: COMP AREA = 6"x10"x2 = 120 IN^2 > 85 IN^2
TENSION AREA = 6"x6.5"x4 = 156 IN^2 > 106 IN^2
SHEAR AREA = 6"x10"x4 = 240 IN^2 > 159 IN^2

BEARING BLOCKS: COMP AREA = 10"x10"x2 = 200 IN^2
TENSION AREA = 10"x10"x4 = 400 IN^2
SHEAR AREA = 10"x8.5"x4 = 340 IN^2

SUPPORT PLATE MINIMUM WELD CROSS SECTION:
TOTAL LENGTH OF WELD = 37"x8 = 296"
$\therefore$ MINIMUM WIDTH OF WELD = $\frac{159}{296} = .54$"

PIVOT ASSEMBLY BOLT SIMILAR TO WILDCAT PIN.

Prepared	NAME IWASHITA	DATE 10/12/79	LOCKHEED CORPORATION Stress Sheet	Page	TEMP.	PERM
Checked			TITLE CHAFING & PENDANT CHAIN	Model		
Approved				Report No.		

MAXIMUM STATIC CHAFING CHAIN TENSION IS THE SAME AS WIRE ROPE

BREAKING STRENGTH - 3×10^6 POUNDS

THE PHYSICAL DIMENSIONS OF THE CHAFING AND PENDANT CHAINS ARE IDENTICAL TO THE ANCHOR CHAIN. THIS FACILITATES ECONOMICAL AND MECHANICAL CONVENIENCES. SINCE THE ANCHOR CHAIN OF GRADE 4 (HAMANAKA CHAIN CO.) QUALITY WITH A BREAKING STRENGTH OF 2932 KIPS, THE CHAFING AND PENDANT CHAINS WILL REQUIRE ALLOY MODIFICATION TO MEET THE REQUIRED BREAKING STRENGTH OF 3000 KIPS.

CHAIN SIZE - 4 7/8"
BREAKING STRENGTH - 3000 KIPS
WEIGHT PER FOOT - 229 #
MATERIAL - MODIFIED GR 4 (HAMANAKA)

LENGTHS:

CHAFING CHAIN - 700' PROVIDES OPTIMUM PAYING OUT AND HAULING IN OF CHAIN FOR ACTIVE TENSIONING CONTROL BETWEEN ON STATION EQUILIBRIUM AND 100 YEAR STORM CONDITIONS.

PENDANT CHAIN - LENGTHS ARE VARIABLE TO INCLUDE ACTIVE TENSIONING REQUIREMENTS AND STILL EFFECT A CHANGE OF HEADING AS MUCH AS 90 DEGREES.

Prepared	NAME IWASHITA	DATE 10/12/79	LOCKHEED CORPORATION Stress Sheet	Page	TEMP.	PERM
Checked			TITLE ANCHOR RETRIEVAL	Model		
Approved				Report No.		

CHAIN 4 7/8" DIA

WEIGHT 220/FT (DRY)
199/FT (WET)

BREAKING STRENGTH 2,932,000#

MAXIMUM DEPTH = 5680 FEET

MAXIMUM CHAIN LOAD:
199 x 5680 = 1,130,320#

MAXIMUM WINDLASS PULL:
500 HP x 63000 x π x 12 / 72" x 0 FPM = 1,649,336#

MAXIMUM AVAILABLE FORCE DIFF (1ST ANCHOR).
1649336 - 1130320 = 519,016

MAXIMUM ANCHOR HOLDING POWER
600,000 x 20 = 1,200,000#

AVAILABLE BREAK FORCE:
519,016/1,200,000 = 43% OF HOLDING POWER
519,016/60 KIPS x 15 = 58% " " "

MAXIMUM AVAILABLE FORCE DIFF (2ND ANCHOR)
(519,016 - 52163)/1,200,000 = 39% OF HOLDING POWER
(519,016 - 52163)/60 KIPS x 15 = 52% " " "

∴ WITH MINIMUM BREAKOUT FORCE AS LOW AS 20% AND THE MAXIMUM AROUND 50%, ANCHOR BREAKOUT IS FEASIBLE.

Form LAC 362-1

Prepared	NAME	DATE	LOCKHEED CORPORATION Stress Sheet	Page	TEMP.	PERM
	WASHITA	9/20/79				1
Checked			TITLE DEPLOYMENT	Model		
Approved			CATENARY LOADS	Report No.		

X	S	C	V	H	Y	T	YC	2S	θ
3044	4524	1400	255600	107350	4906	27734	3006	9048	67.7
"	3680	1800	207923	158200	4624	26256	1824	7360	52.7
"	3467	2400	195900	192100	4856	27364	1456	6934	45.6
"	3346	4000	189073	226000	5214	29459	1214	6692	39.9
"	3271	4600	184815	259900	5644	31886	1044	6542	35.4
"	3201	5500	180,901	310750	6264	35548	864	6402	30.2

DEPLOYMENT CONFIGURATION

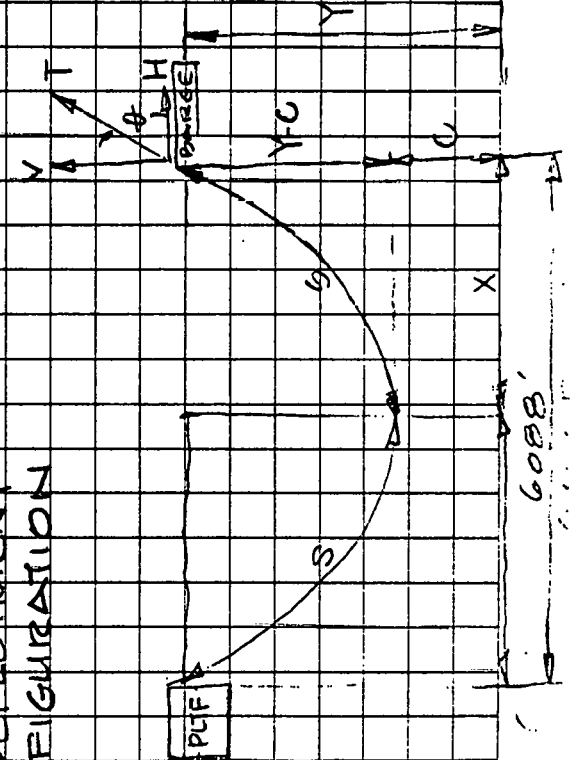

WIRE ROPE = 5 3/4"
WEIGHT = 65 #/FT (DRY)
50.5 #/FT (WET)

$Y^2 = S^2 + C^2$

$Y = C \cosh \frac{X}{C}$

$S = C \sinh \frac{X}{C}$

V = WS
H = WC
T = WY

Form LAC 362-1

Prepared	NAME IWASHITA	DATE 9/20/79	LOCKHEED CORPORATION Stress Sheet	Page	TEMP.	PERM 2
Checked			TITLE DEPLOYMENT	Model		
Approved			BARGE THRUSTERS	Report No.		

EXPECTED BOLLARD PULL = 226,000#

NOTES: 1. THREE THRUSTERS RECOMMENDED
2. TWO AFT MAY BE FIXED.
3. FWD THRUSTER SHOULD BE ROTATABLE FOR HEADING CONTROL.

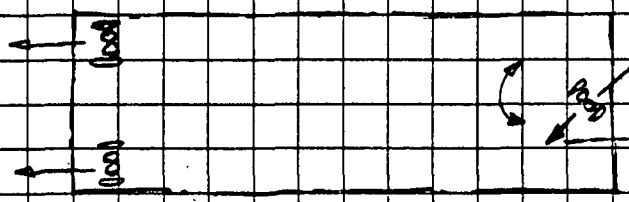

45° ASSUMED FOR HEADING CONTROL DURING DEPLOYMENT

NET THRUST $\times (2 + .707) = 226{,}000$

1. THRUST = 83.5 KIPS EACH
2. HORSEPOWER AT 25#/HP = 3340
3. VARIABLE SPEED - 0/180
4. 440 VOLT, 3 ϕ

Form LAC 362-1

Prepared	NAME IWASHITA	DATE 9/21/79	LOCKHEED CORPORATION Stress Sheet	Page	TEMP.	PERM 3
Checked			TITLE DEPLOYMENT BARGE DRAFT	Model		
Approved				Report No.		

BARGE WEIGHTS:

BARGE STEEL - 525 SHORT TONS	1,050,000
CHAIN - 5980' x 299#/FT	1,788,000
WIRE ROPE - 6,600 x 65#/FT	429,000
170' WIRE ROPE	11,100
WINDLASS	150,000
FAIRLEAD/SHEAVES/SNATCH BLOCK	242,500
WIRE ROPE REELS	15,000
LINEAR WINCH	3,000
WIRE ROPE/CHAIN STOPPERS	1700
MISC - THRUSTERS, EQUIP., CRANE, ETC.	431,300
TOTAL	4,121,600
CUBIC FEET	64,400
TONS	840

DRAFT - 64400/150'x70' ≈ 6 FEET

Prepared	NAME IWASHITA	DATE 9/21/70	LOCKHEED CORPORATION Stress Sheet	Page	TEMP.	PERM 4
Checked			TITLE DEPLOYMENT	Model		
Approved			ANCHOR LOWERING	Report No.		

CHAIN:

4 7/8" DIAM

229 #/FT (DRY)

199 #/FT (WET)

LENGTH = DEPTH PLUS 200 (FOR SERVICING)

BREAKING STRENGTH = 2,932,000#

DEPTH AT 6,000' ANCHOR RANGE

MAXIMUM AT 5680'

STATIC LOAD:

1. CHAIN = 5680' x 199 #/FT = 1130320
2. 2 ANCHORS AT 60 KIPS = 104326

SUB-TOTAL = 1234646

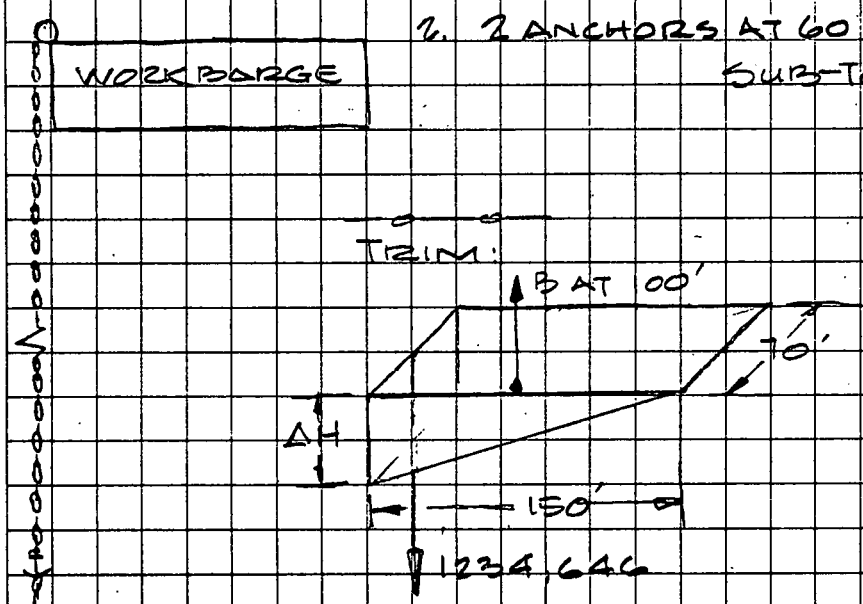

$\Sigma MOM = 0 = \frac{\Delta H}{2} \times 70 \times 150 \times 64 \times 100 = 1.234 \times 150 \times 10^6$

$\Delta H = 5.51$ FEET

.15 CONTINGENCY

$\Delta H = 6.26$

Form LAC 362-1

Prepared	NAME IWASHITA	DATE 9/21/79	LOCKHEED CORPORATION Stress Sheet	Page	TEMP.	PERM
Checked			TITLE WINDLASS	Model		
Approved				Report No.		

DEPLOYMENT WINDLASS

MAX LOAD - ANCHORS & CHAIN = 1,358,111 #

SPEED 10 FPM

WILDCAT DIAM:

1) WIRE ROPE - 9'-7"

2) CHAIN - 12'-0"

CHAIN BREAKING STRENGTH - 2,932 KIPS

LINE TENSION - 1358111 AT 10 FPM

BRAKE CAPACITY - 150% OF 1358111 #

HORSEPOWER:

$$\frac{1358111 \times 72'' \times 10}{63{,}000 \times \pi \times 12} = 412$$

PLATFORM DECK WINDLASS

MAX LOAD (1/2 BR. STR) = 1500,000 #

SPEED - 10 FPM

LINE TENSION - 1,500,000 AT 10 FPM

BRAKE CAPACITY 150% OF 1,500,000

WILDCAT

1) CHAIN DIA 4 7/8

2) LINK LENGTH 29.25"

3) LINK WIDTH 17.55"

4) LENGTH OF FIVE LINKS 8'-11 1/4"

5) FIVE WHELPS

6) CRITICAL PITCH DIA. ≈ 67.68"

HORSEPOWER:

$$\frac{1500000 \times 33.84'' \times 10}{63000 \times \pi \times 5.64} = 455$$

Prepared	NAME IWASHITA	DATE 9/26/79	LOCKHEED CORPORATION Stress Sheet	Page	TEMP.	PERM 1
Checked			TITLE DEPLOYMENT	Model		
Approved			DECK EQUIPT LOADS	Report No.		

MAX LOAD ON WINDLASS:

DEPTH MAX = 5680
WEIGHT/FT OF CHAIN = 199 #/FT (WET)
WEIGHT OF ANCHORS = 104,326 (WET)

MAX LOAD = 5680 × 199 + 104,326 = 1,234,646 #
× 1.1
INCL DYNAMIC = 1,358,111 #

WIRE ROPE REELS + ROPE DIA = 5 3/4"

SUPPLY REEL

DRUM. DIA = 5 3/4" × 15 = 86 1/4" ≈ 7'-4" (88")
DRUM. LENGTH = 23 × 1.15 × 5.75 = 12'-8" (152")
FIRST WRAP DIAM = 88 + 5.75" = 93.75'
CIRC. = 294.52" = 24.54'
LENGTH OF FIRST LAYER = 24.54' × 23 = 564.5'
TOTAL LENGTH = 3465'
LENGTH OF SECOND = π × 102.87 × 21/12 = 566.6'
" " 3RD = π × 111.99 × 23/12 = 674.3'
" " 4TH = π × 121.11 × 21/12 = 665.8'
" " 5TH = π × 130.23 × 23/12 = 784.2'
" " 6TH = π × 139.35 × 21/12 = 766.1'
TOTAL = 4021.5'

FLANGE DIAM. = 139.35 + 5.75 = 145" ≈ 12'-3"
CABLE CAPACITY = 4021 FEET
NO. OF LAYERS = 6
NO. OF TURNS = 132 (FULL)
LINE SPEED = 10 FPM & 20 FPM
LINE TENSION = 33,000 (INCL. BEND TENSION)
TORQUE = 33,000 # × 139.35/2 = 2,299,275 # IN
DELIVERED HP = $\frac{\text{TORQUE} \times \text{RPM}}{63000}$

$= \frac{2,299,275 \times 10 \text{ FPM}}{63,000' \times \pi \times 11.61} = 10$ HP

Prepared	NAME	DATE	LOCKHEED CORPORATION Stress Sheet	Page	TEMP.	PERM
	WASHITA	10/16/79				1
Checked			TITLE DEPLOYMENT COST	Model		
Approved			TIME STUDY	Report No.		

	M-HRS	TIME
LOADING WORKBARGE		
1. CHAIN (1ST LEG - 5840' #1)		
1) DOCKSIDE CRANE (RENTAL)	-	6.0
2) CRANE OPERATOR (1)	6.0	6.0
3) LINE HANDLING (5)	30.0	6.0
2. ANCHOR PREP & HOOKUP		
1) MOBILE CRANE (RENTAL)	-	8.0
2) MOBILE CRANE OPER. (1)	8.0	8.0
3) LINE HANDLING (2)	16.0	8.0
3. WIRE ROPE (1ST LEG - 3170' #1)		
1) SUPPLY REEL OPER (1)	3.0	3.0
2) LINE HANDLING (2)	6.0	3.0
4. AUXILIARY WIRE ROPE (170')		
1) AUX REEL OPER (1)	0.2	0.2
2) LINE HANDLING (2)	0.4	0.4
5. MISCELLANEOUS		
1) FUELING - D.G. .45 #/SHP/HR - 5100 GAL		
2) PREPARE FOR SEAWAY (2)	2.0	1.0
6. TOTAL - LOADING	71.6	8
ENROUTE TO AND FROM SITE INCL MOORING TO D.T.F		
1) CREW (9)	18.0	2.0
DEPLOYMENT		
1ST ANCHOR LEG (3340 WR, 5840 CHAIN)		
1) HANG ANCHORS, CONN. 170' AUX W.R., ENGAGE LIN WINCH, MOVE OUT 800'		1.0
2) PAY OUT REMAINING W.R.		2.0
3) ANCHOR LOWERING (3 FPM-AVE)		7.0
4) ENGAGE LIN. WINCH, PAY OUT 150' CH + 400' W.R.		1.0
5) PAY OUT REMAINING W.R.		3.5
6) ENGAGE STOPPERS, MOOR WORK-BARGE, SLACK CHAIN, DISCONN & RECONNECT CHAIN		1.0
7) TRANSFER LOAD FROM LINEAR WINCH TO CHAIN, WORK WORK-BARGE FROM UNDER ANCHOR LEG, DISCONNECT AUX 170' WR.		1.0

Prepared	NAME	DATE	LOCKHEED CORPORATION Stress Sheet	Page	TEMP.	PERM 2
Checked			TITLE	Model		
Approved				Report No.		

DEPLOYMENT SUPPORT

	MHRS	TIME
1) CREW (9)	148.5	16.5
2) MOBILE CRANE RENTAL	—	16.5

NOTE: 17 HOURS OF TUG(S) SUPPORT IS REQUIRED IF PLATFORM AND/OR WORK BARGE DO NOT HAVE THRUSTERS

SUMMARY

	MHRS	COST
BARGE CREW - 1ST LEG	148.5	
DOCKSIDE CRANE - 6 HOURS	—	
MOBILE CRANE - 17 HOURS	—	
FUEL - D.G. 5100 GALS	—	
DOCKSIDE CREW	71.6	
TOTAL	220.1	

Prepared	NAME	DATE	LOCKHEED CORPORATION Stress Sheet	Page	TEMP.	PERM 3
Checked			TITLE	Model		
Approved				Report No.		

	MHRS	TIME
LOADING WORKBARGE		
1. CHAIN (2ND LEG - 3910' #8)		
1) CRANE RENTAL	-	4.0
2) CRANE OPER (1)	4.0	4.0
3) LINE HANDLING (5)	20.0	4.0
2 ANCHOR PREP & HOOKUP		
1) MOBILE CRANE RENTAL	-	8.0
2) CRANE OPER (1)	8.0	8.0
3) LINE HANDLING (2)	16.0	8.0
3 WIRE ROPE (2ND LEG - 3110' #8)		
1) SUPPLY REEL OPER (1)	2.5	2.5
2) LINE HANDLING (2)	5.0	2.5
4 AUXILIARY WIRE ROPE (3400' + 170')		
1) AUX REEL OPER (1)	3.0	3.0
2) LINE HANDLING (2)	6.0	3.0
5 MISCELLANEOUS		
1) FUELING - D.G .45#/SHP/HR - 5100 GALS		
2) PREPARE FOR SEAWAY (2)	2.0	1.0
6 TOTAL - LOADING	66.5	8
ENROUTE TO AND FROM SITE & MOORING TO PLATE		
1) CREW (9)	18.0	2.0
DEPLOYMENT		
2ND ANCHOR LEG (3910' CHAIN, 6680' WR)		
1) HANG ANCHORS, CONN 170' AUX WR, AUX WR, ENGAGE LIN. WINCH, MOVE 800'		1.0
2) PAY OUT REMAINING W.R.		5.0
3) ANCHOR LOWERING (13 FPM)		5.0
4) ENGAGE LIN. WINCH, PAY OUT 150' CHAIN + 400' W.R.		1.0
5) PAY OUT & HAUL-IN REMAINING WR		5.7
6) ENGAGE STOPPERS, MOOR WORKBARGE, SLACK CHAIN, DISCONN. & RECONN CH.		1.0
7) TRANSFER LOAD FROM LINEAR WINCH TO CHAIN, WORK WORKBARGE FROM UNDER ANCHOR LEG, DISCONN. AUX 170' WR.		1.0

Prepared	NAME	DATE	LOCKHEED CORPORATION Stress Sheet	Page	TEMP.	PERM 4
Checked			TITLE	Model		
Approved				Report No.		

DEPLOYMENT SUPPORT

	MHRS	TIME
1) CREW (9)	145.8	16.2
2) MOBILE CRANE RENTAL	—	16.2

NOTE: 6 HOURS OF TUG(S) SUPPORT IS REQUIRED IF PLATFORM AND/OR WORKBARGE DO NOT HAVE THRUSTERS

SUMMARY	MHRS	COST
BARGE CREW - 2ND LEG	145.8	
DOCKSIDE CRANE - 4 HOURS	—	
MOBILE CRANE - 16.2 HOURS	—	
FUEL - D.G. 5100 GALS	—	
DOCKSIDE CREW	66.5	
TOTAL - 2ND LEG	212.3	

GENERAL NOTE:

1. ABOVE SUMMARY IS SIMILAR TO EACH OF THE THREE REMAINING LANDWARD ANCHOR LEGS

Prepared	NAME	DATE	LOCKHEED CORPORATION Stress Sheet	Page	TEMP.	PERM 5
Checked			TITLE	Model		
Approved				Report No.		

LOADING WORKBARGE

		MHRS	TIME
1.	CHAIN (3RD LEG - 5640' #3)		
	1) DOCKSIDE CRANE	-	6.0
	2) CRANE OPERATOR (1)	6.0	6.0
	3) LINE HANDLING (5)	30.0	6.0
2	ANCHOR PREP & HOOKUP		
	1) MOBILE CRANE (RENTAL)	-	8.0
	2) MOBILE CRANE OPER (1)	8.0	8.0
	3) LINE HANDLING (2)	16.0	8.0
3	WIRE ROPE (3RD LEG - 3255' #3)		
	1) SUPPLY REEL OPER (1)	3.0	3.0
	2) LINE HANDLING (2)	6.0	3.0
4	AUXILIARY WIRE ROPE (3400 + 170')		
	1) AUX REEL OPER (1)	3.0	3.0
	2) LINE HANDLING	6.0	3.0
5	MISCELLANEOUS		
	1) FUELING - D.G. 45#/SHP/HR - 5100 GALS		
	2) PREPARE FOR SEAWAY (2)	2.0	1.0
6.	TOTAL - LOADING	80.0	8
ENROUTE TO AND FROM SITE INCL MOORING TO PLTF			
	1) CREW (9)	18.0	2.0

DEPLOYMENT

3RD ANCHOR LEG (5640' CHAIN, 6825' WIR)		1.0
1) HANG ANCHORS, CONN. 170' AUX WIR. ENGAGE LIN WINCH, MOVE OUT 800'		
2) PAY OUT REMAINING W.R.		5.0
3) ANCHOR LOWERING (13 FPM)		7.0
4) ENGAGE LIN WINCH, PAY OUT 150' CHAIN, + 400' WR		1.0
5) PAY OUT AND HAUL-IN REMAINING WR		5.5
6) ENGAGE STOPPERS, MOOR WORKBARGE, SLACK CHAIN, DISCONN. & RECONN. CH.		1.0
7) TRANSFER LOAD FROM LINEAR WINCH TO CHAIN, WORK WORKBARGE FROM UNDER ANCHOR LEG, DISCONN. AUX 170' WR.		1.0

Prepared	NAME	DATE	LOCKHEED CORPORATION Stress Sheet	Page	TEMP.	PERM 6
Checked			TITLE	Model		
Approved				Report No.		

DEPLOYMENT SUPPORT

	MHRS	TIME
1) CREW (9)	162.0	18.0
2) MOBILE CRANE RENTAL	—	18.0

NOTE: 18 HOURS OF TUG(S) SUPPORT IS REQUIRED IF PLATFORM AND/OR WORKBARGE DO NOT HAVE THRUSTERS

SUMMARY

	MHRS	COST
BARGE CREW - 3RD LEG	162.0	
DOCKSIDE CRANE - 6 HOURS	—	
MOBILE CRANE - 18 HOURS	—	
ELEC - D.G. 5100 GALS	—	
DOCKSIDE CREW	80.0	
TOTAL 3RD LEG	242.0	

GENERAL NOTE:

ABOVE SUMMARY IS SIMILAR TO EACH OF THE TWO REMAINING SEAWARD ANCHOR LEGS.

IWASHITA 11/5/79

ANCHOR SETTING CALCULATION

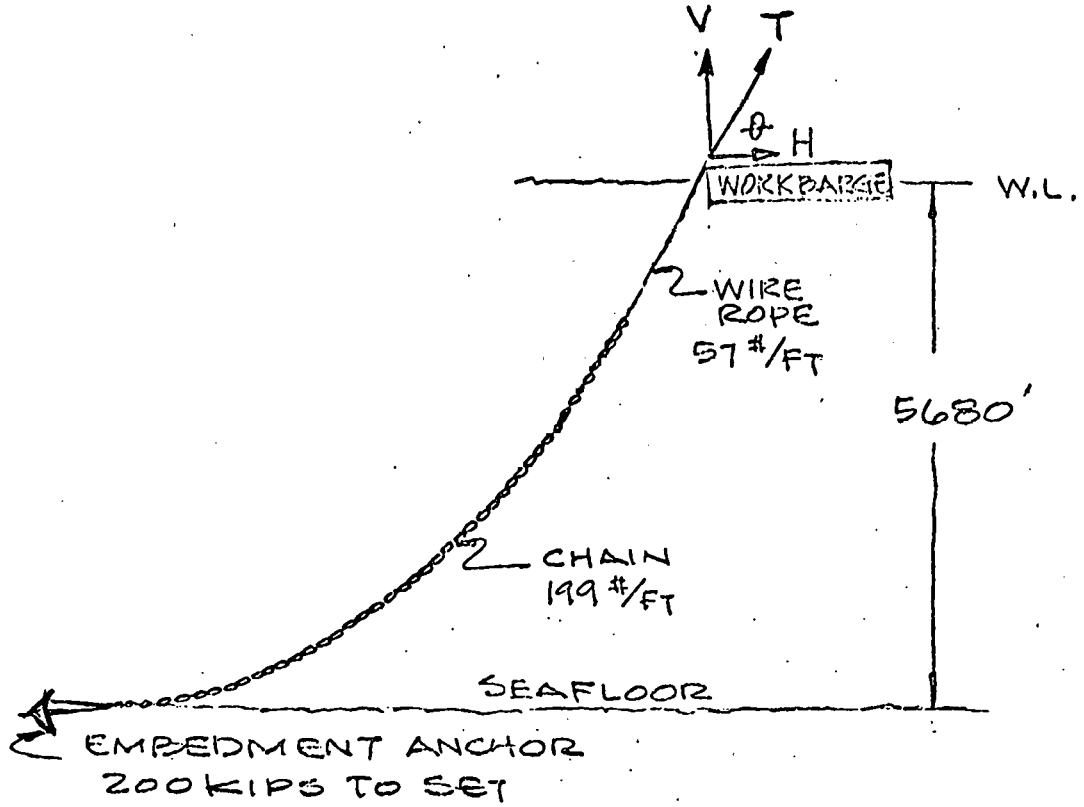

PROBLEM:

1. DEFINE CATENARY CHARACTERISTICS TO SET ANCHOR.
2. WHAT ARE VALUES OF T, V & θ

GIVEN

1 ANCHOR LEG #2 (LONGEST LEG & DEPTH)
2 ANCHOR PULL ANGLE IS 0°.

CATENARY NOMENCLATURE

1. $W_{(n+1)}$ = WIRE ROPE WEIGHT PER FOOT
2. W_n = CHAIN WEIGHT PER FOOT
3. $S_{(n+1)}$ = WIRE ROPE LENGTH
4. S_n = CHAIN LENGTH
5. $T_{(n+2)}$ = MOORING LINE TENSION AT TOP
6. $P_{(n+2)}$ = SLOPE OF MOORING LINE AT TOP
7. $V_{(n+1)}$ = MOORING LINE VERTICAL LOAD AT TOP
8. $H_{(n+1)}$ = MOORINGLINE HORIZONTAL LOAD AT TOP
9. D = DEPTH OF MOOR
10. X_T = HORIZONTAL PROJECTION OF MOORING LINE

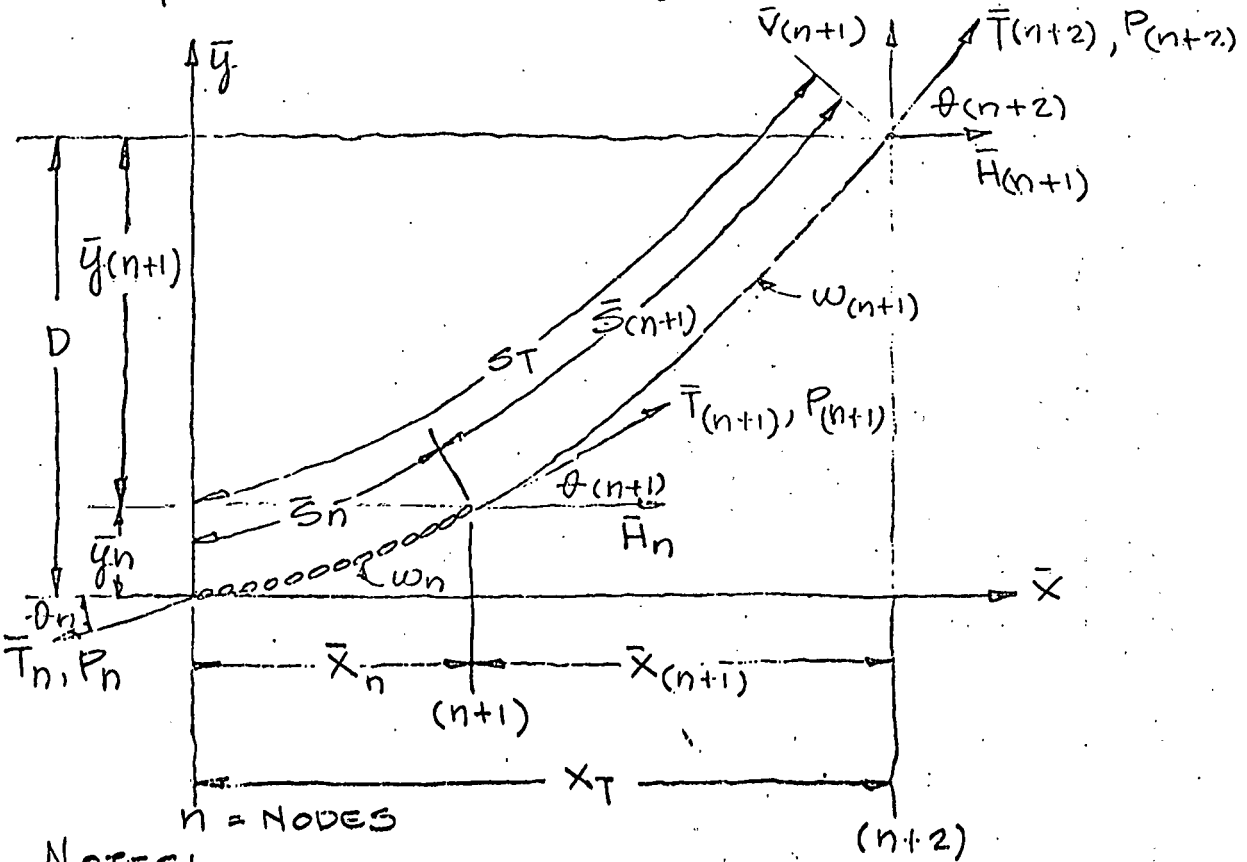

NOTES:

1. SYMBOLS WITH BARS (-) DENOTES DIMENSIONLESS ENTITIES WITH RESPECT TO D, DEPTH OF MOOR.
2. EQUATIONS ARE PUT IN DIMENSIONLESS FORM BY SCALING ALL LENGTHS WITH RESPECT TO D.

ANCHOR SETTING CATENARY CHARACTERISTICS

WIRE ROPE
- 5 3/4" DIAMETER
- 3000 KIPS BREAK STRENGTH
- 65 #/FT (DRY) 57 #/FT (WET)

CHAIN
- 4 7/8" DIAMETER
- 3000 KIPS BREAK STRENGTH
- 199 #/FT (WET)

DEPTH :- 5680'

$\theta_{(n+2)} = 80.5°$

$P_{(n+2)} = 5.976$

$\bar{T}_{(n+2)} = T_{n+2}/D \times W_{n+1} = \frac{200 KIPS}{\cos 80.5 \times 5680 \times 57} = 3.743$

$\bar{H}_{(n+1)} = \bar{T}_{(n+2)} \cos(\tan^{-1} P_{(n+2)}) = 4.179 \cos(\tan^{-1} 6.691) = .618$

$\bar{w}_n = w_{n+1}/w_n = 57/199 = .286$

$\bar{H}_n = \bar{H}_{(n+1)} \times \bar{w}_n = .618 \times .286 = .177$

$\bar{S}_{(n+1)} \cong S_{n+1}/S_n = 700/5880 = .119$

$\bar{P}_{(n+1)} = P_{(n+2)} - \bar{S}_{(n+1)}/\bar{H}_{(n+1)} = 5.976 - .119/.618 = 5.783$

$\bar{y}_n = \bar{H}_n\left[\sqrt{1+P^2_{(n+1)}} - \cosh(\sinh^{-1} P_n)\right] = .177\left[\sqrt{1+5.783^2} - 1\right] = .862$

$\bar{y}_{(n+1)} = \bar{H}_{(n+1)}\left[\sqrt{1+P^2_{(n+2)}} - \cosh(\sinh^{-1} P_{(n+1)})\right]$

$= .618\left[\sqrt{1+5.976^2} - \cosh(\sinh^{-1} 5.783)\right] = .118$

$F = 1 - (\bar{y}_n + \bar{y}_{(n+1)}) = 1 - .862 - .118 \cong .02$

$\bar{S}_n = \bar{H}_n(P_{(n+1)} - P_n) = .177(5.783) = 1.024$

$\bar{T}_n = \bar{H}_n(P_{(n+1)} - P_n) = .177(5.783) = 1.024$

$\bar{T}_{(n+1)} = \bar{y}_n + \bar{H}_n \cosh(\sinh^{-1} P_n) = .862 + .177(1) = 1.039$

$\bar{X}_n = \bar{H}_n(\sinh^{-1} P_{(n+1)} - \sinh^{-1} P_n) = .177(\sinh^{-1} 5.783) = .435$

$\bar{X}_{(n+1)} = \bar{H}_{(n+1)}(\sinh^{-1} P_{(n+2)} - \sinh^{-1} P_{n+1})$

$= .618(\sinh^{-1} 5.976 - \sinh^{-1} 5.783) = .02$

DIMENSIONAL DATA SUMMARY

$H = \bar{H}_n \times D \times W_n = .177 \times 5680 \times 199 = 200,067$ POUNDS

$H = \bar{H}_{(n+1)} \times D \times W_{(n+1)} = .618 \times 5680 \times 57 = 200,084$ POUNDS

$y_n = \bar{y}_n \times D = .862 \times 5680 = 4896$ FEET

$y_{(n+1)} = \bar{y}_{(n+1)} \times D = .118 \times 5680 = 670$ FEET

$S_n = \bar{S}_n \times D = 1.024 \times 5680 = 5816$ FEET ⇒ 5880 − 5816 = 64 ft of chain in aquifer

$64 \times 199 \times .7 = 9000.16$

$S_{(n+1)} = \bar{S}_{(n+1)} \times D = .119 \times 5680 = 676$ FEET

$S_T = S_n + S_{(n+1)} = 6492$ FEET

$X_n = \bar{X}_n \times D = .435 \times 5680 = 2470$ FEET

$X_{(n+1)} = \bar{X}_{(n+1)} \times D = .02 \times 5680 = 114$ FEET

$X_T = X_n + X_{(n+1)} = 2584$ FEET

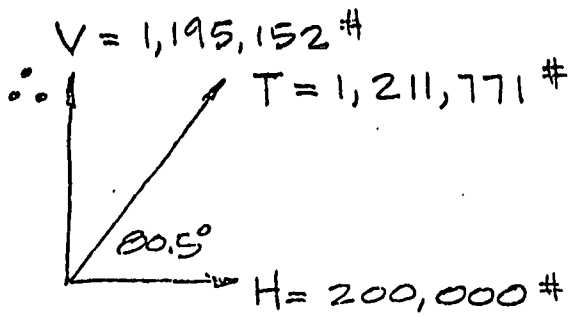

Appendix F
DYNAMIC LOADS ANALYSIS METHODOLOGY

F.1 METHOD OF ANALYSIS

The methods for determining mooring line dynamic tension extremes and fatigue life use a linearized frequency-domain approach. The computer programs utilized are "STORM" for analyzing the extreme dynamic tension conditions and "FATIGUE" for performing the fatigue life study. Figure F-1 shows the total dynamic study block diagram and illustrates the common areas used in both "STORM" and "FATIGUE."

F.2 COMMON AREAS

The barge transfer functions or unit response amplitude operators and their corresponding phase angles are from Glosten's report (Ref. F-1) for the OTEC pilot plant ships. The sheaves or fairleads are located on the corner of the barge. Unit RAOs for the three orthogonal translational motions of the corna point are computed by combining the translational and rotational RAOs of the barge center with the position vector to the barge corner point. This method is described in Ref. F-2.

Results from the static analysis (Section 2.2.2) are used as input to the dynamic programs for computing the line tension RAOs due to unit excitations at the top in two separate directions (horizontal and vertical). A two-dimensional cable dynamic frequency domain program, "FREQCABLE," is used as a subroutine in this process (Ref. F-3). Small perturbations about the static equilibrium position are assumed. The cable is divided into 20 segments, boundary conditions of unit harmonic translation at the top and pinned at the bottom, are applied. Transfer matrices are generated progressively along the cable, and solution of the cable tension amplitudes and phase angles are

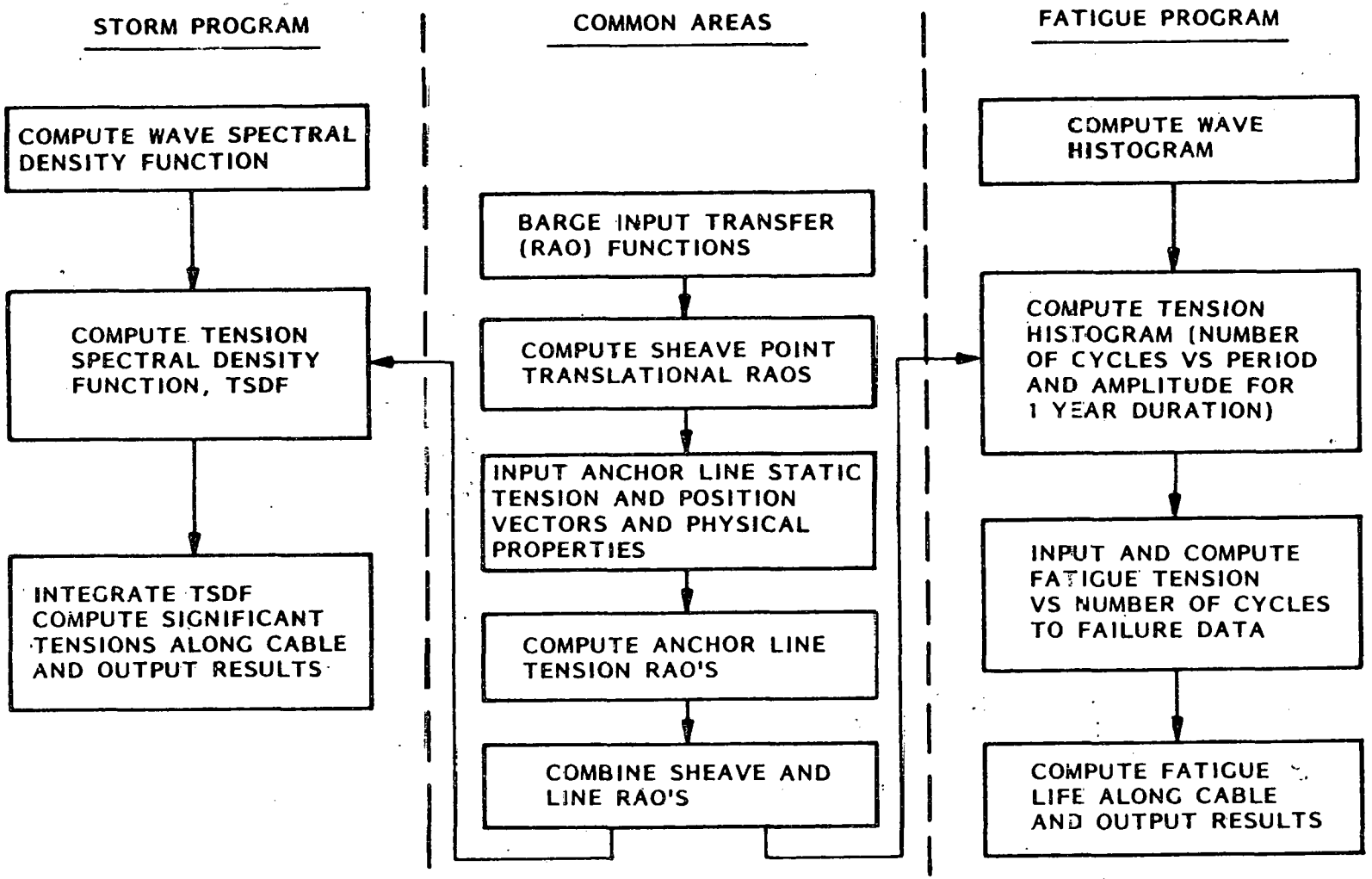

Fig. F-1 Dynamic Analysis Block Diagram

obtained. This technique has limitations because the two dimensional cable solution only considers motion in the vertical plane of the cable and the hydrodynamic damping is dependent only on current, and is independent of motion amplitude. Concerning the vertical plane limitation, some motion does occur normal to the vertical plane of the cable. This analysis conservatively assumes that the horizontal resultant motion of the sheave point is applied in the cable plane. There is no problem with the corner heave motion.

The tension RAOs and sheave translational RAO for two orthogonal motions, are converted to complex numbers and the products obtained to establish line tension amplitude RAO for all 20 points along the cable. The two sets of line tension RAO top vertical and horizontal motion are added together in complex form to obtain the total tension amplitude RAO, lb of tension/ft of wave height versus frequency or period.

F.3 STORM COMPUTATIONS

The storm conditions for evaluating the cable tensions during the 3-year and 100-year storms are represented by a wave spectrum of significant wave heights and period (see Section 1.4). The tension amplitude RAO distributions are squared and multiplied by the Bretschneider wave amplitude squared function to obtain tension amplitude squared spectral density distributions (lb^2/RAD) versus frequency. The areas under these distributions for all 20 points along the cable are computed and the significant tension amplitudes obtained for these points, for both "head" and "beam" seas.

F.4 FATIGUE ANALYSIS

Figures F-2 and F-3 illustrate the logical process involved in the fatigue-life computations for the mooring lines. The first diagram illustrates the data manipulation used in the final calculations. The BARGE and ANCHOR LINE sections are addressed in the discussion on COMMON AREAS. The ENVIRONMENT section begins with a wave height frequency distribution table (Ref. F-4)

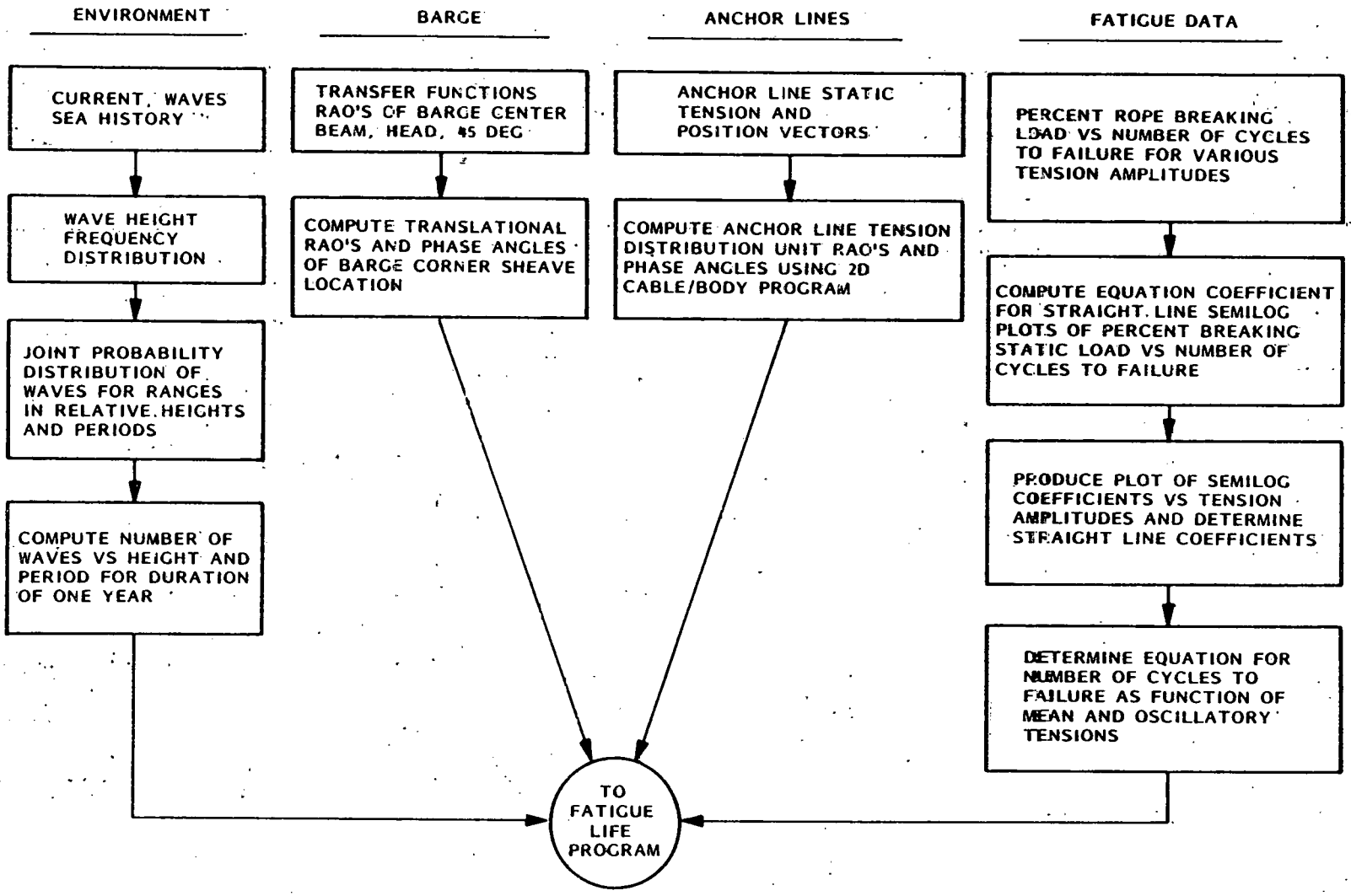

Fig. F-2 Fatigue Analysis Flow Diagram

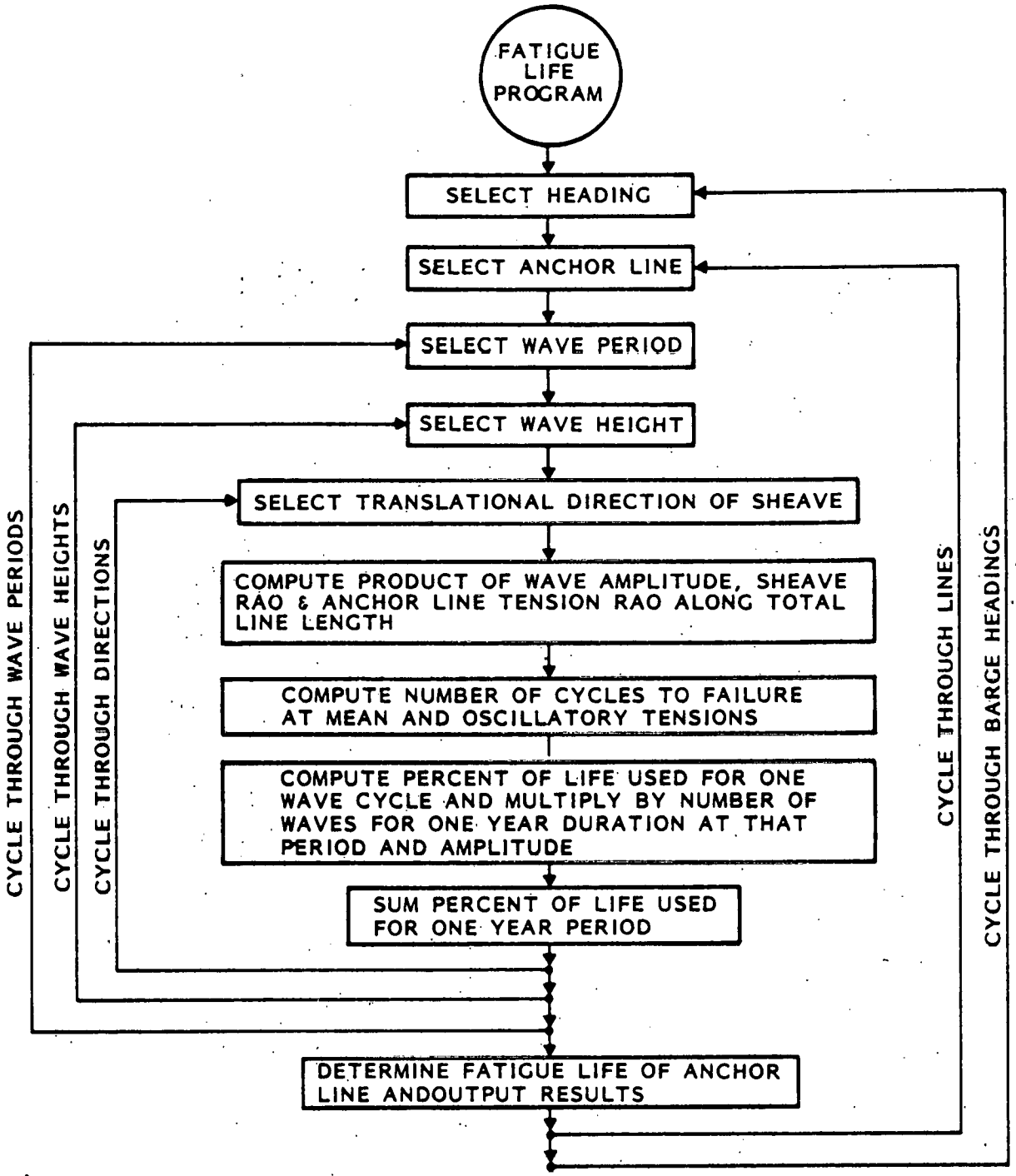

Fig. F-3 Fatigue Life Program

which is a sea history of observations for one year (Table F-1). The table shows the hours-per-month specific ranges of significant wave heights occur over the 12 month period. The totals at the bottom indicate the percent of total time these ranges occur. Table F-2 (Ref. F-5) shows the number of waves versus relative modal period, and relative significant height, for a total of 1,000 waves. The module period, T_o, is approximated as 0.93 times the significant period, T_s or $T_o = 0.93\ T_s$ for a Rayleigh distribution. The significant period, T_o, sec, is approximately related to significant wave height, H_s, ft, by

$$T_s = \sqrt{H_s/0.222}$$

Therefore

$$T_o = 0.93\ \sqrt{H_s/0.222}$$

This converts the relative period ratio to

$$T/(0.93\ \sqrt{H_s/0.222})$$

so that the histogram of wave frequency of occurrence is related to one variable, H_s.

Combining Tables F-1 and F-2, and converting the number of waves to relative duration of occurrence, Table F-3 is generated. This is a purely numerical procedure which does not account for the fact that some of these waves break, since the height to length ratio of 1/7 is exceeded. A more reasonable time histogram was then considered wherein the times allocated to the breaking waves are moved to heights where breaking waves occur. This modified histogram is shown in Table F-4. This time-histogram converted back to number of wave occurrences versus height, and period for one year, is shown in Table F-5.

Table F-1 WAVE HEIGHT FREQUENCY DISTRIBUTION

$H_{1/3}$ (ft)	(Hours/Month)										
	< 1	1-2	3-4	5-6	7	8-9	10-11	12	13-16	17-19	20-22
January	40	170	269	151	74	28	9	2	2	0	0
February	27	157	296	112	46	22	9	2	2	0	0
March	33	246	283	118	47	10	4	1	3	0	0
April	50	230	277	106	40	9	5	0	2	0	0
May	23	217	279	151	47	18	6	2	2	0	0
June	10	145	310	162	57	23	10	2	2	0	0
July	8	97	263	212	105	38	12	1	2	0	1
August	16	118	320	177	73	20	13	1	5	0	0
September	51	225	269	142	51	25	7	2	0	0	0
October	61	226	293	121	30	11	2	1	0	0	0
November	60	198	265	129	45	11	6	2	2	1	0
December	33	210	262	140	75	16	7	1	0	0	0
Annual	412	2,225	3,373	1,706	681	227	87	23	24	1	1
Cumulative	412	2,637	6,010	7,716	8,397	8,624	8,711	8,734	8,758	8,759	8,760

Table F-2

JOINT PROBABILITY DISTRIBUTION OF WAVE HEIGHT AND PERIOD (FOR ZERO CORRELATION) (AUG. 1978)

NUMBER OF WAVES PER 1000 CONSECUTIVE WAVES FOR RANGES IN RELATIVE HEIGHTS AND PERIODS

Range in Relative Height $\eta=H/H_s$	RANGES IN RELATIVE PERIOD $\tau = T/T_o$											Sum	Cumulative
	0-0.1	0.1-0.3	0.3-0.5	0.5-0.7	0.7-0.9	0.9-1.1	1.1-1.3	1.3-1.5	1.5-1.7	1.7-1.9	1.9-2.0		
0-0-0.2	.01	0.46	3.06	9.15	17.21	21.36	16.61	7.30	1.58	.14	0	76.88	76.88
0.2-0.4	.02	1.18	7.83	23.44	44.09	54.73	42.56	18.71	4.05	.36	.01	196.98	273.86
0.4-0.6	.02	1.43	9.51	28.49	53.59	66.51	51.73	22.74	4.92	.44	.02	239.40	513.26
0.6-0.8	.02	1.25	8.29	24.84	46.72	57.99	45.10	19.82	4.29	.39	.01	208.72	721.98
0.8-1.0	.01	0.85	5.67	16.98	31.94	39.65	30.84	13.55	2.93	.26	.01	142.69	864.67
1.0-1.2	.01	0.47	3.15	9.42	17.73	22.01	17.12	7.52	1.63	.15	-	79.21	943.88
1.2-1.4	-	0.22	1.44	4.32	8.12	10.08	7.84	3.45	.75	.07	-	36.29	980.17
1.4-1.6	-	0.08	0.55	1.65	3.10	3.85	3.00	1.32	.28	.03	-	13.86	994.03
1.6-1.8	-	0.03	0.18	.53	.99	1.23	.96	.42	.09	.01	-	4.44	998.47
1.8-2.0	-	0.01	0.05	.14	.27	.33	.26	.11	.03	-	-	1.20	999.67
2.0-2.2	-	-	0.01	.03	.06	.08	.06	.03	.01	-	-	0.28	999.95
2.2-2.4	-	-	-	.01	.01	.01	.01	-	-	-	-	0.04	999.99
Sum	.09	5.98	39.74	119.00	223.83	277.83	216.09	94.97	20.56	1.85	.05	999.99	
Cumulative	.09	6.07	45.81	164.81	388.64	666.47	882.56	977.53	998.09	999.94	999.99		

Table F-3 WAVE DISTRIBUTION - HEIGHT AND PERIOD

RELATIVE TIMES WITH BREAKING WAVES

HGT/PER	1	3	5	7	9	11	13	15	17	19	21	23	25	27	29
1	1.52	178.	169.	20.0	.383	.000	.000	.000	.000	.000	.000	.000	.000	.000	.000
3	2.16	379.	838.	279.	36.4	1.88	.210-01	.000	.000	.000	.000	.000	.000	.000	.000
5	1.31	104.	701.	343.	50.4	4.67	.365	.116-01	.450-03	.000	.000	.000	.000	.000	.000
7	.254	20.8	148.	129.	38.9	5.33	.755	.164-01	.426-03	.000	.000	.000	.000	.000	.000
9	.144	12.7	88.2	110.	36.3	4.54	.157	.136-01	.116-02	.357-04	.000	.000	.000	.000	.000
11	.211-01	2.42	20.9	26.8	18.9	3.23	.862	.172-01	.853-03	.000	.000	.000	.000	.000	.000
13	.201-02	.530	5.02	12.3	7.84	3.41	.804	.234-01	.111-02	.344-04	.000	.000	.000	.000	.000
15	.651-04	.185	1.27	4.00	2.69	1.23	.109	.729-02	.733-03	.370-04	.000	.000	.000	.000	.000
17	.230-04	.691-01	.688	2.23	1.97	1.36	.539	.159-01	.103-02	.172-04	.000	.000	.000	.000	.000
19	.185-05	.191-01	.114	.479	.342	.211	.793-01	.635-02	.650-03	.185-04	.000	.000	.000	.000	.000
21	.222-04	.121-01	.198	.590	.660	.561	.298	.979-02	.403-03	.172-04	.000	.000	.000	.000	.000
23	.179-05	.400-02	.840-01	.238	.300	.201	.190	.927-02	.666-03	.185-04	.000	.000	.000	.000	.000
25	.000	.653-03	.267-02	.181-01	.103-01	.739-02	.000	.000	.000	.000	.000	.000	.000	.000	.000
27	.926-06	.537-03	.282-01	.694-01	.106	.106	.819-01	.460-02	.358-03	.000	.000	.000	.000	.000	.000
29	.000	.254-03	.123-01	.310-01	.494-01	.519-01	.438-01	.267-02	.245-03	.000	.000	.000	.000	.000	.000

BREAKING WAVE REGION

Table F-4 WAVE DISTRIBUTION - HEIGHT AND PERIOD WITHOUT BREAKING WAVES

RELATIVE TIMES WITHOUT SREAKING WAVES.

HGT/PER	1	3	5	7	9	11	13	15	17	19	21	23	25	27	29
1	5.41	178.	169.	20.0	.383	.000	.000	.000	.000	.000	.000	.000	.000	.000	.000
3	.000	520.	838.	279.	36.4	1.88	.210-01	.000	.000	.000	.000	.000	.000	.000	.000
5	.000	.000	701.	343.	50.4	4.67	.365	.116-01	.450-03	.000	.000	.000	.000	.000	.000
7	.000	.000	265.	129.	38.9	5.33	.755	.164-01	.426-03	.000	.000	.000	.000	.000	.000
9	.000	.000	.000	110.	35.3	4.54	.157	.136-01	.116-02	.357-04	.000	.000	.000	.000	.000
11	.000	.000	.000	26.8	18.9	3.23	.862	.172-01	.853-03	.000	.000	.000	.000	.000	.000
13	.000	.000	.000	19.9	7.84	3.41	.804	.234-01	.111-02	.344-04	.000	.000	.000	.000	.000
15	.000	.000	.000	.000	2.69	1.23	.109	.729-02	.733-03	.370-04	.000	.000	.000	.000	.000
17	.000	.000	.000	.000	1.97	1.36	.539	.159-01	.103-02	.172-04	.000	.000	.000	.000	.000
19	.000	.000	.000	.000	1.47	.211	.793-01	.635-02	.650-03	.185-04	.000	.000	.000	.000	.000
21	.000	.000	.000	.000	.000	.561	.298	.979-02	.403-03	.172-04	.000	.000	.000	.000	.000
23	.000	.000	.000	.000	.000	.281	.190	.927-02	.666-03	.185-04	.000	.000	.000	.000	.000
25	.000	.000	.000	.000	.000	.739-02	.000	.000	.000	.000	.000	.000	.000	.000	.000
27	.000	.000	.000	.000	.000	.106	.819-01	.400-02	.358-03	.000	.000	.000	.000	.000	.000
29	.000	.000	.000	.000	.000	.519-01	.438-01	.267-02	.245-03	.000	.000	.000	.000	.000	.000

Table F-5 WAVE HEIGHT AND PERIOD ANNUAL OCCURRENCE DISTRIBUTION

NUMBER OF WAVES FOR VARIOUS PERIODS & HEIGHTS FOR 1 YEAR

HGT/PER	1	3	5	7	9	11	13	15	17	19	21	23	25	27	29
1	.446+05	.487+06	.278+06	.236+05	350.	.000	.000	.000	.000	.000	.000	.000	.000	.000	.000
3	.000	.143+07	.138+07	.328+06	.333+05	.141+04	13.3	.000	.000	.000	.000	.000	.000	.000	.000
5	.000	.000	.115+07	.403+06	.461+05	.350+04	232.	6.34	.218	.000	.000	.000	.000	.000	.000
7	.000	.000	.436+06	.152+06	.356+05	.399+04	478.	9.02	.207	.000	.000	.000	.000	.000	.000
9	.000	.000	.000	.129+06	.332+05	.340+04	99.6	7.46	.561	.155-01	.000	.000	.000	.000	.000
11	.000	.000	.000	.315+05	.173+05	.242+04	546.	9.46	.413	.000	.000	.000	.000	.000	.000
13	.000	.000	.000	.234+05	.718+04	.255+04	509.	12.8	.537	.149-01	.000	.000	.000	.000	.000
15	.000	.000	.000	.000	.246+04	922.	69.3	4.00	.355	.160-01	.000	.000	.000	.000	.000
17	.000	.000	.000	.000	.180+04	.102+04	341.	8.72	.499	.746-02	.000	.000	.000	.000	.000
19	.000	.000	.000	.000	.134+04	158.	50.2	3.49	.315	.802-02	.000	.000	.000	.000	.000
21	.000	.000	.000	.000	.000	420.	189.	5.37	.195	.746-02	.000	.000	.000	.000	.000
23	.000	.000	.000	.000	.000	210.	120.	5.09	.322	.802-02	.000	.000	.000	.000	.000
25	.000	.000	.000	.000	.000	5.53	.000	.000	.000	.000	.000	.000	.000	.000	.000
27	.000	.000	.000	.000	.000	79.5	51.9	2.52	.174	.000	.000	.000	.000	.000	.000
29	.000	.000	.000	.000	.000	38.8	27.7	1.46	.119	.000	.000	.000	.000	.000	.000

The rope tension fatigue data, supplied by British Rope, is contained in Fig. F-4. These data show straight line semi-log plots for various tension amplitudes of oscillation in terms of percent of minimum breaking load. The ordinate is linear and consists of mean load expressed in terms of percent of breaking load. The ordinate is linear, and consists of mean load expressed as a percent of breaking load; the abscissa is a logarithmic scale showing the fatigue life or cycles to failure. The equation for each of the straight lines on the plot is Mean Load (Percent Breaking Load) = A + B $\log_{10}$ (N cycles to failure). The coefficients A & B are determined for each of the straight line oscillatory amplitude family of curves and are given in Table F-6. The coefficients are plotted in Fig. F-5 versus oscillatory amplitude and are formed to approach a straight line. The equations which parameterize A & B as a function of percentage of breaking load, P, are also given in the plot. The equation for number of cycles to failure, N, is then derived and given as a function of mean load, ML, and oscillatory load, also in the figure.

The fatigue life program illustrated in Fig. F-3 is self-explanatory and illustrates five nested loops. Results from both the extreme condition "STORM" and fatigue life "FATIGUE" programs are discussed in Section 2.2.3.

The ship RAOs are shown in Fig. F-6 for beam seas and Fig. F-7 for head seas (Ref. F-1). The sheave joint translational RAOs and phase angles, generated using the method of conversion described in Ref. F-2, are shown in Figs. F-8 and F-9 for beam and head seas, respectively.

The transfer functions for all 20 points (pt. 1 is at the leg bottom) along the cable for 15 separate unit horizontal top motions with periods of (1, 3, 5, ... 27, 29 sec) are shown in Table F-7. These results are generated with the "FREQCABLE" method described in Ref. F-3. The transfer functions together with the corresponding phase angles, expressed in complex form and coupled with the sheave point RAOs (Figs. F-8 and F-9) are then used to generate tension unit response amplitude operators (lb/ft wave ampl.). This is shown in Table F-5 for all 20 points along the cable and 15 wave periods. The

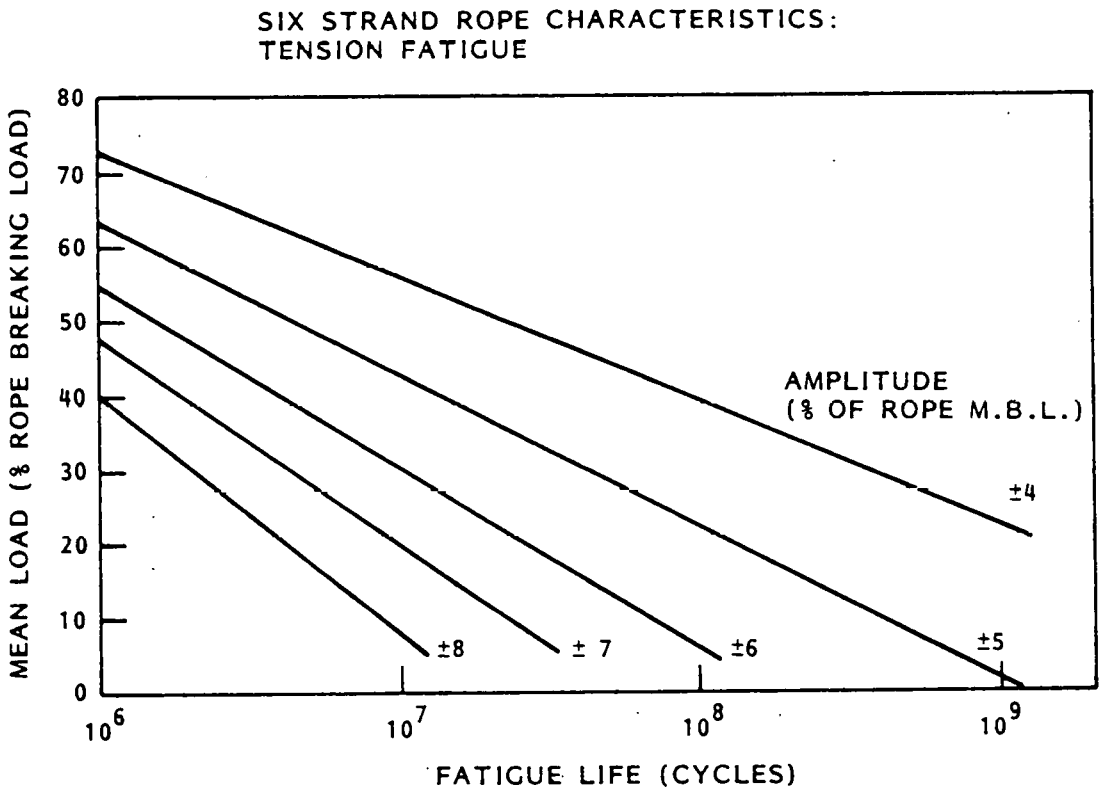

Fig. F-4 Fatigue Life Versus Mean Loads

Table F-6 COEFFICIENTS A & B FOR SIX STRAND ROPE TENSION FATIGUE CURVES - MEAN LOAD

Oscillatory Amplitude (% of Rope Minimum Breaking Load)(a)	A	B
± 4	174	-16.83
± 5	185	-20.33
± 6	202	-24.5
± 7	215.5	-28.0
± 8	232	-32.0

(a) Percent Breaking Load = $(A + B) \log_{10}$ (N cycles to failure)

$$N = 10^{\left(\frac{ML - A}{B}\right)}$$

$$N = 10^{\left[\frac{(ML - 113.75 - 14.625P)}{(-0.875 - 3.812P)}\right]}$$

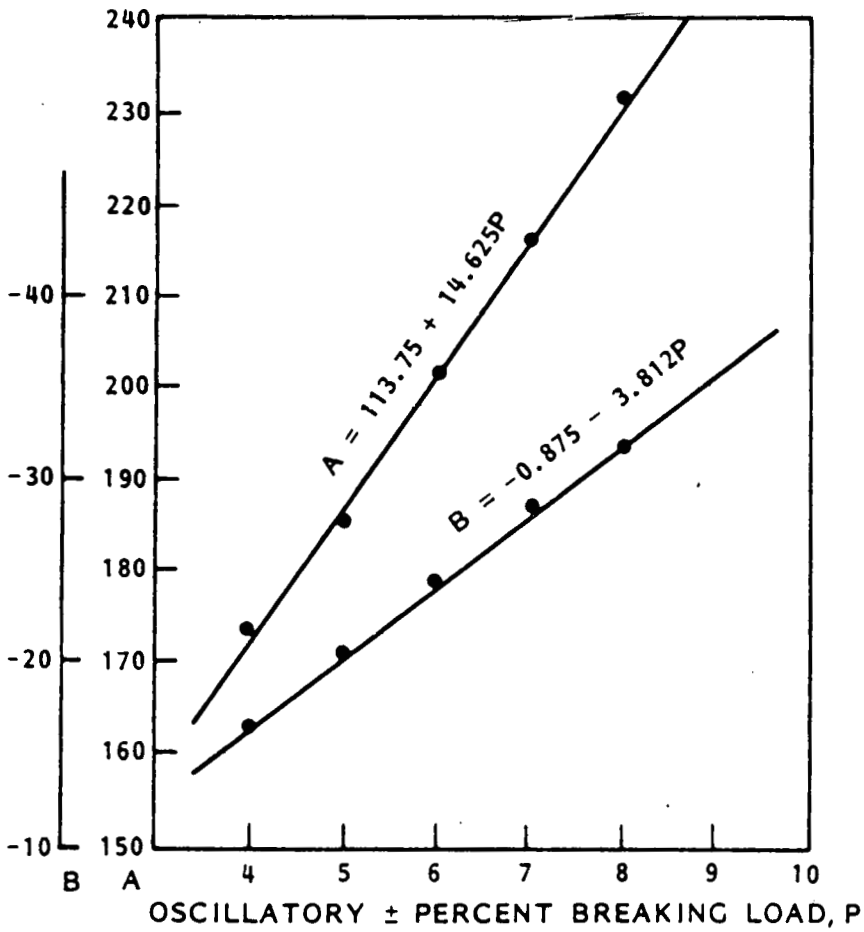

Fig. F-5 Plot of Coefficients A & B Used in Fatigue Curves

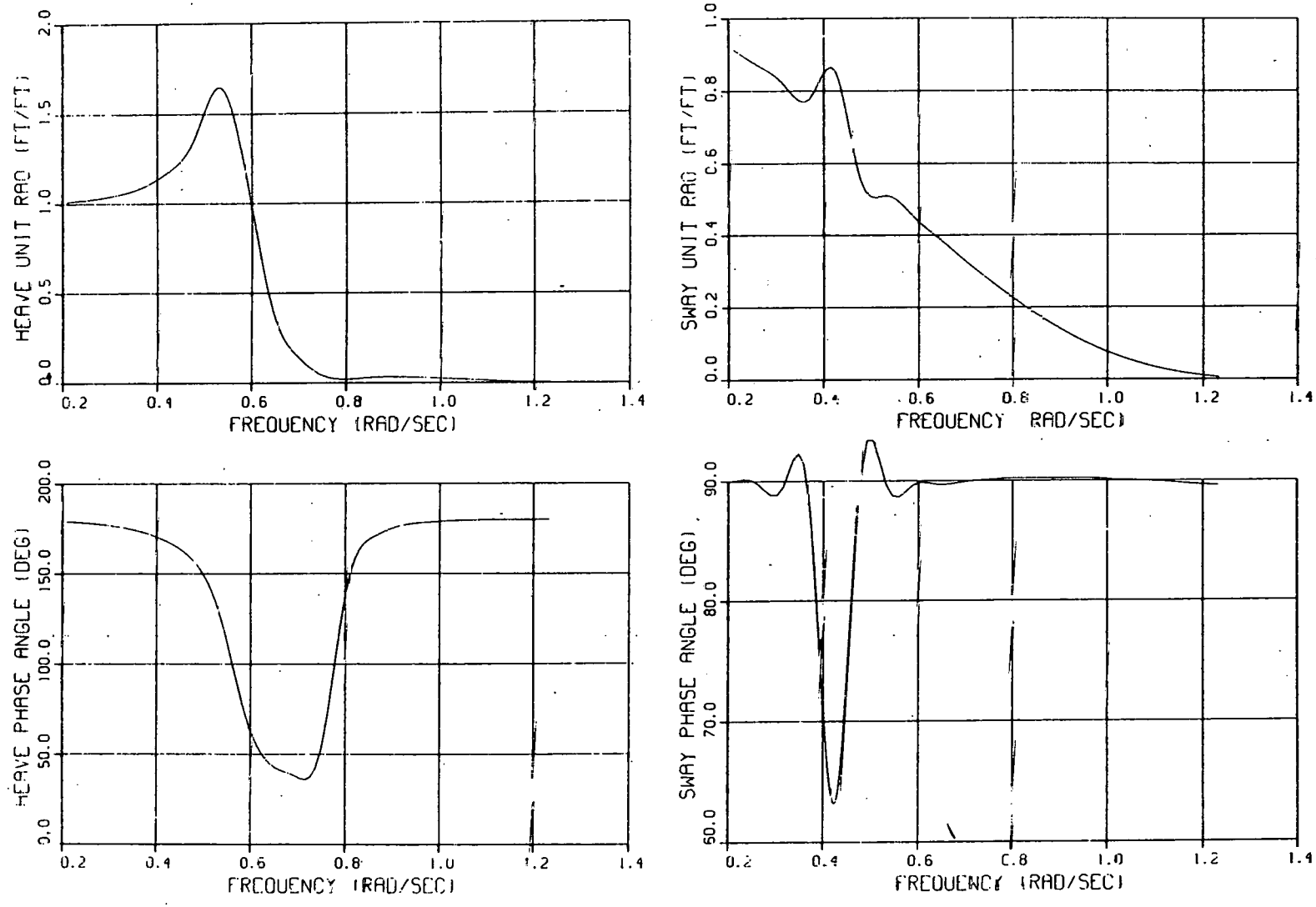

Fig. F-6 Beam Sea RAOs and Phases - OTEC Pilot Plant Ship

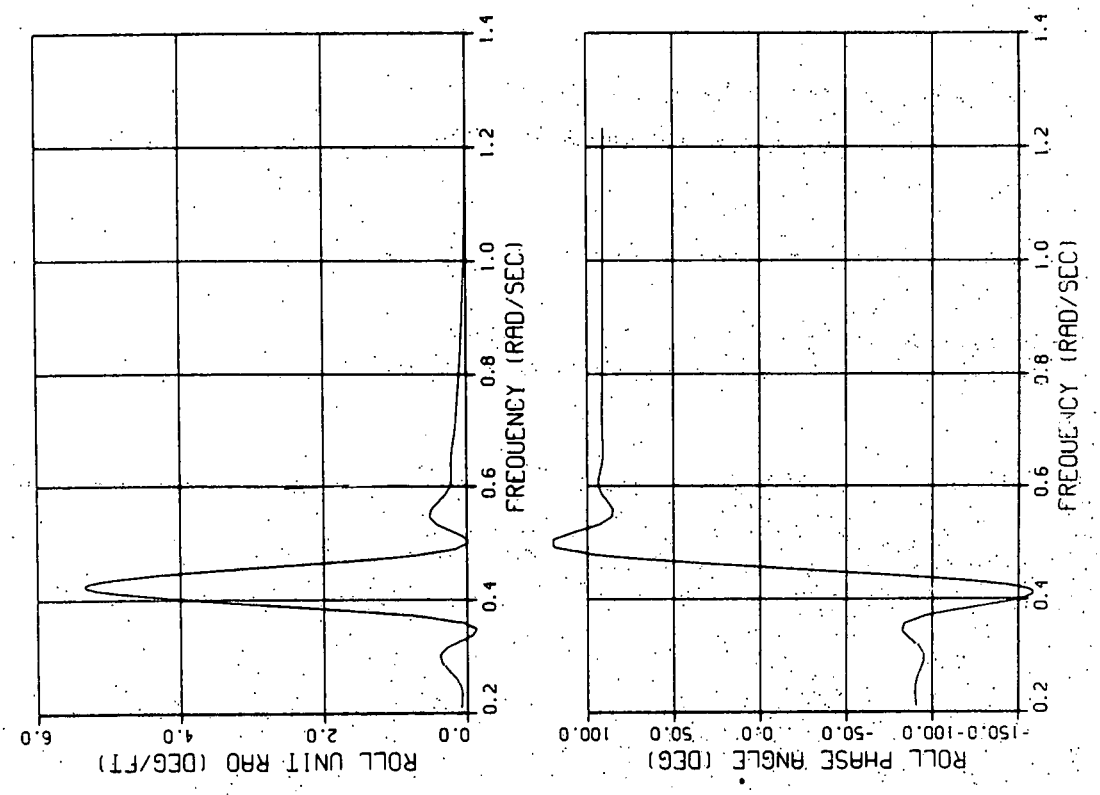
ROLL UNIT RAO (DEG/FT)
0.0
2.0
4.0
6.0
0.2
0.4
0.6
0.8
1.0
1.2
1.4
FREQUENCY (RAD/SEC)
ROLL PHASE ANGLE (DEG)
100.0
50.0
0.0
-50.0
-100.0
-150.0
FREQUENCY (RAD/SEC)

Fig. F-6 (Cont.)

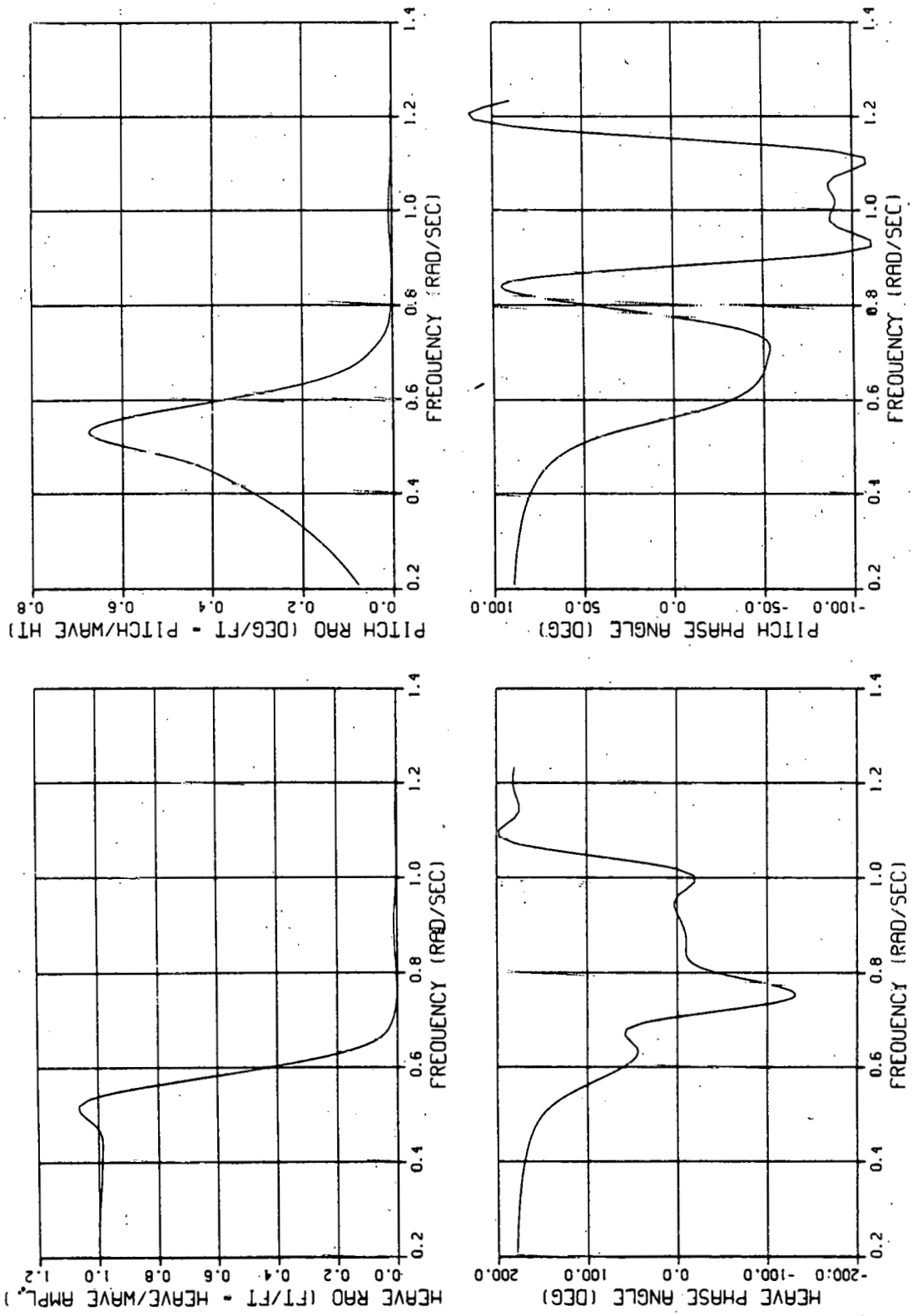

Fig. F-7 Head Sea Unit Amplitude Operators and Phases (RAOs) - OTEC Pilot Plant Ship

FREQUENCY (RAD/SEC)	AMPLITUDES X	Y (FT/FT)	Z (FT/FT)	PHASE ANGLES φ_X	φ_Y (DEG)	φ_Z (DEG)
.208000	.000000	.824361	1.01605	.000000	90.0871	-175.442
.262000	.000000	.706280	1.03805	.000000	90.0753	-172.411
.316000	.000000	.525500	1.08708	.000000	90.6143	-167.384
.370000	.000000	.145351	1.26675	.000000	106.249	-155.282
.424000	.000000	4.77235	6.51161	.000000	-151.007	-153.469
.478000	.000000	1.29172	1.83708	.000000	93.1711	135.969
.532000	.000000	.951584	2.02921	.000000	91.1388	121.832
.586000	.000000	.760595	1.49276	.000000	90.4859	78.1675
.640000	.000000	.621576	.631017	.000000	90.3198	60.3952
.694000	.000000	.510269	.301355	.000000	90.3455	66.4600
.748000	.000000	.413536	.175257	.000000	90.4605	81.9096
.802000	.000000	.328318	.121063	.000000	90.4849	98.4898
.856000	.000000	.253873	.908617-01	.000000	90.4153	110.153
.910000	.000000	.190202	.690605-01	.000000	90.3801	118.594
.964000	.000000	.136821	.511680-01	.000000	90.3764	124.751
1.01800	.000000	.937881-01	.360632-01	.000000	90.2439	129.193
1.07200	.000000	.604710-01	.239021-01	.000000	90.1694	132.617
1.12600	.000000	.357984-01	.145388-01	.000000	90.0676	135.053
1.18000	.000000	.185071-01	.770109-02	.000000	89.8932	137.051
1.23400	.000000	.715482-02	.305906-02	.000000	89.7913	139.055

Fig. F-8 Beam Sea Sheave Point RAOs

FREQUENCY (RAD/SEC)	AMPLITUDES X (FT/FT)	Y	Z (FT/FT)	PHASE ANGLES φ_X (DEG)	φ_Y	φ_Z (DEG)
.208000	.920870	.000000	1.03479	92.3261	.000000	-166.213
.262000	.863889	.000000	1.08367	92.7299	.000000	-159.210
.316000	.734111	.000000	1.17047	93.7087	.000000	-152.031
.370000	.336153	.000000	1.31383	99.4016	.000000	-145.799
.424000	.542153	.000000	1.54642	102.247	.000000	-142.581
.478000	.424869	.000000	1.96506	125.086	.000000	-145.992
.532000	.687821	.000000	2.57404	151.420	.000000	-170.415
.586000	.882110	.000000	1.70194	121.258	.000000	139.288
.640000	.576052	.000000	.603527	102.369	.000000	119.850
.694000	.317455	.000000	.192578	94.5945	.000000	121.472
.748000	.152744	.000000	.438396-01	170.826	.000000	144.121
.802000	.353833-01	.000000	.135925-01	-65.1899	.000000	-112.356
.856000	.114460	.000000	.103927-01	-76.3946	.000000	-40.0125
.910000	.145791	.000000	.147196-01	-87.7386	.000000	43.5159
.964000	.105518	.000000	.224797-01	-90.7522	.000000	71.3385
1.01800	.683818-01	.000000	.221720-01	-94.0364	.000000	85.4338
1.07200	.371796-01	.000000	.145629-01	-101.488	.000000	100.399
1.12600	.481597-01	.000000	.563740-02	-153.589	.000000	136.078
1.18000	.553362-01	.000000	.522283-02	156.806	.000000	-127.901
1.23400	.608391-01	.000000	.732213-02	104.032	.000000	-99.4465

Fig. F-9 Head Sea Sheave Point RAOs

Table F-7 TENSION AMPLITUDE TRANSFER FUNCTIONS FOR ALL CABLE POINTS AND FREQUENCIES
(UNIT HORIZONTAL MOTION AT TOP)

CABLE POINT/PER	1	3	5	7	9	11	13	15	17	19	21	23	25	27	29
1	.390+07	.228+04	.203+04	.181+04	.169+04	.185+04	.202+04	.206+04	.207+04	.210+04	.214+04	.216+04	.219+04	.215+04	.206+04
2	.214+07	.228+04	.202+04	.177+04	.161+04	.178+04	.199+04	.206+04	.209+04	.213+04	.219+04	.222+04	.223+04	.219+04	.210+04
3	.105+07	.226+04	.203+04	.183+04	.173+04	.187+04	.202+04	.205+04	.208+04	.212+04	.217+04	.222+04	.223+04	.220+04	.212+04
4	.339+07	.227+04	.212+04	.205+04	.210+04	.221+04	.217+04	.208+04	.204+04	.205+04	.210+04	.216+04	.218+04	.216+04	.209+04
5	.299+07	.234+04	.231+04	.242+04	.269+04	.279+04	.249+04	.216+04	.202+04	.198+04	.200+04	.205+04	.209+04	.209+04	.203+04
6	.175+06	.249+04	.256+04	.285+04	.333+04	.347+04	.295+04	.241+04	.208+04	.193+04	.190+04	.193+04	.197+04	.198+04	.195+04
7	.278+07	.256+04	.282+04	.324+04	.392+04	.412+04	.345+04	.271+04	.222+04	.194+04	.183+04	.182+04	.185+04	.186+04	.184+04
8	.350+07	.282+04	.302+04	.354+04	.436+04	.464+04	.399+04	.303+04	.240+04	.201+04	.180+04	.173+04	.173+04	.174+04	.173+04
9	.139+07	.292+04	.316+04	.375+04	.467+04	.503+04	.425+04	.330+04	.259+04	.211+04	.182+04	.168+04	.164+04	.163+04	.163+04
10	.184+07	.299+04	.325+04	.389+04	.490+04	.532+04	.452+04	.353+04	.277+04	.222+04	.186+04	.166+04	.157+04	.154+04	.153+04
11	.378+07	.315+04	.339+04	.404+04	.513+04	.560+04	.492+04	.389+04	.305+04	.241+04	.193+04	.162+04	.146+04	.141+04	.141+04
12	.175+07	.309+04	.328+04	.393+04	.511+04	.583+04	.518+04	.416+04	.328+04	.257+04	.201+04	.160+04	.136+04	.127+04	.128+04
13	.143+07	.253+04	.268+04	.334+04	.460+04	.549+04	.500+04	.407+04	.323+04	.253+04	.195+04	.152+04	.125+04	.115+04	.116+04
14	.345+07	.217+04	.219+04	.277+04	.410+04	.516+04	.485+04	.401+04	.321+04	.251+04	.192+04	.146+04	.116+04	.103+04	.104+04
15	.270+07	.217+04	.193+04	.230+04	.364+04	.488+04	.475+04	.400+04	.323+04	.254+04	.194+04	.144+04	.109+04	918.	917.
16	.243+06	.251+04	.200+04	.202+04	.327+04	.467+04	.472+04	.405+04	.331+04	.262+04	.199+04	.146+04	.105+04	826.	800.
17	.297+07	.308+04	.237+04	.199+04	.301+04	.455+04	.476+04	.417+04	.345+04	.275+04	.210+04	.152+04	.106+04	761.	689.
18	.332+07	.377+04	.292+04	.222+04	.289+04	.451+04	.486+04	.434+04	.363+04	.292+04	.225+04	.163+04	.111+04	735.	591.
19	.992+06	.452+04	.355+04	.263+04	.292+04	.455+04	.502+04	.456+04	.386+04	.313+04	.243+04	.178+04	.120+04	753.	515.
20	.214+07	.530+04	.424+04	.315+04	.309+04	.466+04	.523+04	.481+04	.411+04	.337+04	.264+04	.195+04	.133+04	814.	475.

horizontal and vertical RAOs of the sheave for a specific frequency are represented by

$$\text{Horizontal:} \quad A_H e^{i\phi_H}$$

$$\text{Vertical:} \quad A_V e^{i\phi_V}$$

where A is amplitude and ϕ are phase angles. The tension transfer function for a specific point on the cable at a specific frequency is

$$\text{Horizontal:} \quad T_H e^{i\psi_H}$$

$$\text{Vertical:} \quad T_V e^{i\psi_V}$$

where T is tension amplitude and ψ are phase angles.

Multiplying and adding, we get the tension RAO or the amplitude of tension that occurs at that point on the cable when a wave of unit amplitude at the specified frequency passes by.

$$T_{RAO} e^{i\gamma} = A_H T_H e^{i(\phi_H+\psi_H)} + A_V T_V e^{i(\phi_V+\psi_V)}$$

With the histogram of number of waves versus wave heights and periods, Table F-5 and the tension RAOs, Table F-8, the number of cycles to failure for a single point on the cable at a specific wave period and height is determined. The tension amplitude is:

$$T_{AMP} = T_{RAD} \times H_{WAVE/2}$$

Table F-8 TENSION AMPLITUDE RAOs (LB/FT OF WAVE AMPLITUDE)

ANG/PER	1	3	5	7	9	11	13	15	17	19	21	23	25	27	29
1	.154+05	23.1	35.0	367.	833.	.150+04	.262+04	.902+04	390.	921.	.129+04	.150+04	.163+04	.168+04	.169+04
2	.437+04	23.1	34.7	360.	796.	.145+04	.257+04	.902+04	392.	936.	.131+04	.153+04	.166+04	.171+04	.172+04
3	.215+04	22.9	35.0	371.	851.	.151+04	.261+04	.901+04	391.	930.	.131+04	.152+04	.167+04	.172+04	.174+04
4	.143+05	23.0	36.5	415.	.103+04	.174+04	.282+04	.913+04	391.	802.	.127+04	.148+04	.163+04	.169+04	.171+04
5	.736+04	23.8	39.8	409.	.132+04	.213+04	.324+04	.960+04	405.	868.	.120+04	.140+04	.155+04	.162+04	.166+04
6	.337+04	25.4	44.2	576.	.163+04	.260+04	.362+04	.105+05	443.	853.	.113+04	.131+04	.145+04	.154+04	.159+04
7	.112+05	27.2	48.5	655.	.191+04	.304+04	.444+04	.118+05	501.	871.	.109+04	.122+04	.135+04	.143+04	.150+04
8	.101+05	28.7	51.9	715.	.213+04	.341+04	.500+04	.131+05	566.	918.	.107+04	.115+04	.125+04	.133+04	.141+04
9	.561+04	29.8	54.3	756.	.228+04	.369+04	.545+04	.142+05	627.	980.	.109+04	.111+04	.117+04	.123+04	.131+04
10	.652+04	30.5	55.9	785.	.239+04	.390+04	.580+04	.152+05	678.	.104+04	.112+04	.109+04	.110+04	.115+04	.123+04
11	.125+05	32.1	58.4	815.	.250+04	.416+04	.632+04	.166+05	779.	.116+04	.113+04	.107+04	.101+04	.103+04	.111+04
12	.521+04	31.3	56.4	792.	.248+04	.423+04	.663+04	.176+05	864.	.127+04	.126+04	.107+04	937.	908.	995.
13	.368+04	25.3	45.7	669.	.222+04	.392+04	.633+04	.170+05	852.	.127+04	.125+04	.104+04	866.	812.	898.
14	.132+05	21.6	36.9	552.	.197+04	.363+04	.605+04	.166+05	838.	.127+04	.125+04	.102+04	809.	722.	800.
15	.615+04	21.5	32.1	455.	.175+04	.337+04	.583+04	.163+05	627.	.128+04	.126+04	.102+04	771.	641.	703.
16	.384+04	25.2	33.3	396.	.157+04	.318+04	.570+04	.164+05	822.	.131+04	.130+04	.104+04	760.	575.	609.
17	.121+05	31.2	40.0	392.	.145+04	.305+04	.565+04	.167+05	824.	.136+04	.137+04	.110+04	780.	534.	520.
18	.792+04	38.4	49.6	442.	.141+04	.301+04	.569+04	.173+05	836.	.142+04	.145+04	.118+04	831.	525.	441.
19	.756+04	46.2	60.8	528.	.144+04	.304+04	.582+04	.180+05	860.	.151+04	.156+04	.128+04	911.	553.	390.
20	.109+05	54.3	72.8	636.	.154+04	.314+04	.602+04	.190+05	897.	.161+04	.168+04	.140+04	.101+04	615.	349.

The percent of breaking strength is then obtained.

$$P = T_{AMP}/B.S. \times 100$$

The mean tension,

$$T_{MEAN} = T_{STATIC}$$

is converted to percent of breaking load,

$$ML = T_{MEAN}/B.S. \times 100$$

Substituting these values into the equation shown in Fig. F-4. The number of cycles to failure is obtained as:

$$N = 10 \cdot \exp\left[\frac{(ML - 113.75 - 14.625P)}{(-0.875 - 3.812P)}\right]$$

This process is performed for all the heights and periods for each cable point, a sample of which is shown in Table F-9. Since the exponent in the above equation becomes very large for small P values, a cut off of 15 was selected for the maximum exponent which explains why most of the values in Table F-9 are 1×10^{15}. Applying the Palmgren-Miner cumulative damage theory (Refs. F-6 and F-7), the number of loading cycles for 1 year histogram, Table F-5 is divided by the number of cycles to failure, Table F-9, and then summed for all periods and wave heights to obtain the fraction of life consumed in one year for the cable point in question. The inverse of this value gives the life expectancy (years) of that cable point. Table F-10 lists the fractions of life consumed for all 20 cable points for a beam sea condition and the minimum life expectancy.

Table F-9 NUMBER OF CYCLES TO FAILURE FOR SINGLE CABLE POINT

HGT/PER	1	3	5	7	9	11	13	15	17	19	21	23	25	27	29
1	.100+16	.100+16	.100+16	.100+16	.100+16	.100+16	.100+16	.100+16	.100+16	.100+16	.100+16	.100+16	.100+16	.100+16	.100+16
3	.693+13	.100+16	.100+16	.100+16	.100+16	.100+16	.100+16	.100+16	.100+16	.100+16	.100+16	.100+16	.100+16	.100+16	.100+16
5	.275+10	.100+16	.100+16	.100+16	.100+16	.100+16	.100+16	.100+16	.100+16	.100+16	.100+16	.100+16	.100+16	.100+16	.100+16
7	.799+08	.100+16	.100+16	.100+16	.100+16	.100+16	.100+16	.100+16	.100+16	.100+16	.100+16	.100+16	.100+16	.100+16	.100+16
9	.107+08	.100+16	.100+16	.100+16	.100+16	.100+16	.100+16	.100+16	.100+16	.100+16	.100+16	.100+16	.100+16	.100+16	.100+16
11	.290+07	.100+16	.100+16	.100+16	.100+16	.100+16	.100+16	.100+16	.100+16	.100+16	.100+16	.100+16	.100+16	.100+16	.100+16
13	.117+07	.100+16	.100+16	.100+16	.100+16	.100+16	.100+16	.100+16	.100+16	.100+16	.100+16	.100+16	.100+16	.100+16	.100+16
15	.596+06	.100+16	.100+16	.100+16	.100+16	.100+16	.100+16	.100+16	.100+16	.100+16	.100+16	.100+16	.100+16	.100+16	.100+16
17	.356+06	.100+16	.100+16	.100+16	.100+16	.100+16	.100+16	.100+16	.100+16	.100+16	.100+16	.100+16	.100+16	.100+16	.100+16
19	.236+06	.100+16	.100+16	.100+16	.100+16	.100+16	.501+15	.100+16	.100+16	.100+16	.100+16	.100+16	.100+16	.100+16	.100+16
21	.170+06	.100+16	.100+16	.100+16	.100+16	.100+16	.585+14	.100+16	.100+16	.100+16	.100+16	.100+16	.100+16	.100+16	.100+16
23	.129+06	.100+16	.100+16	.100+16	.100+16	.100+16	.959+13	.654+15	.100+16	.100+16	.100+16	.100+16	.100+16	.100+16	.100+16
25	.102+06	.100+16	.100+16	.100+16	.100+16	.641+15	.205+13	.106+15	.100+16	.100+16	.100+16	.100+16	.100+16	.100+16	.100+16
27	.838+05	.100+16	.100+16	.100+16	.100+16	.119+15	.540+12	.220+14	.100+16	.100+16	.100+16	.100+16	.100+16	.100+16	.100+16
29	.706+05	.100+16	.100+16	.100+16	.100+16	.274+14	.169+12	.555+13	.475+15	.100+16	.100+16	.100+16	.100+16	.100+16	.100+16

Table F-10 FRACTION OF LIFE CONSUMED IN ONE YEAR ALONG CABLE

.650281-08	.650331-08	.650425-08	.650683-08	.651622-08	.655744-08	.675231-08	.759910-08	.106561-07	.716500-08
.530350-07	.759159-07	.527281-07	.380558-07	.296163-07	.254856-07	.245009-07	.263945-07	.682371-08	.677806-08

MINIMUM LIFE OF ANCHORR LEG .131725+08

The long fatigue life is a result, in part, of small amplitude tension oscillations. The data presented in Fig. F-4 are extrapolated from tests in air. The manufacturer recommends that these data be used until data for fatigue life of wire rope in seawater is obtained. There are, however, many references which show a great reduction in fatigue strength of steels in salt water. One program involving axial fatigue testing of bright wire rope under accelerated loading provides data which indicates a significant reduction in cycles to failure in water as compared to in-air conditions (Ref. F-8). The high frequency of loading, relatively high load range, and ungalvanized condition bring in question the applicability of these results to SKSS fatigue analysis. Fatigue tests of large diameter wire rope in seawater are recommended in the Task IV report.

The assumptions and limitations of this analysis are summarized as follows:

- o Line dynamics do not affect short term barge response to waves
- o Small perturbation theory for mooring line response is valid
- o Salt water immersion does not affect wire rope cyclic fatigue strength
- o Straight line, semi-log extrapolation of fatigue data is valid
- o Linearization applies
- o Vortex shedding effects not included
- o Mooring line dynamic program has only two dimensional capability
- o Waves are all in same direction
- o Orientation of barge remains constant throughout fatigue life duration

F.5 REFERENCES

F-1 L. R. Glosten and Associates, Comprehensive Seakeeping Report for the OTEC Pilot Plant Ship Phase III, 811 First Ave., Seattle, Washington, Sep 78

F-2 Lockheed Missiles & Space Company, Inc., Mathematical Modeling of Marine Riser Systems, by R. Cowan, Sunnyvale, Calif., Sep 78

F-3 -----, Dynamics of Planar Cable-Body Systems, by J. V. Rattaya, Sunnyvale, Calif., Apr 73

F-4 -----, OTEC SKSS Task I Design Requirements, Sunnyvale, Calif., Jun 79

F-5 Department of Energy, OTEC Demonstration Plant Environmental Package, Washington, D.C., Dec 78

F-6 A. Palmgren, "Die Lebensdaur von Kugellagern," Zeitschrift des Vereins Deutscher Ingenieure, Vol. 68, Nr. 14, Apr 1924

F-7 M. A. Miner, "Cumulative Damage in Fatigue" J. Applied Mechanics, ASME Vol. 12, No. 3, Sep 45

F-8 F. Matango, Jr., "Axial Fatigue Testing of Wire Rope," Marine Technology Society Journal, Vol. 6, No. 6, Nov-Dec 1972

☆U.S. GOVERNMENT PRINTING OFFICE: 1980-640-258 308